IntechOpen

Mass Spectrometry

Edited by Mahmood Aliofkhazraei

MASS SPECTROMETRY

Edited by **Mahmood Aliofkhazraei**

Mass Spectrometry
http://dx.doi.org/10.5772/65165
Edited by Mahmood Aliofkhazraei

Contributors

David Friedecký, Fabiana Aparecida Lobo, Aline Souza, Isabela Cristina Matos Cunha, Júnior Olair Chagas, Karla Moreira Vieira, Elisandra Bárbara Pontes Carlos, Luana Lacerda Santos, Thamires Ráfaga Campus E Figueredo, Vanessa Moreira Osório, Lucília Alves Linhares Machado, Zhixun Luo, Anneleen Imelda Decloedt, Anita Van Landschoot, Lynn Vanhaecke, Renata Raina-Fulton, Teodor Octavian Octavian Nicolescu, Tore Vehus, David Johnson, Ana Claudia Fernandes Amaral, Aline De Souza Ramos, Jefferson Rocha De Andrade Silva, José Luiz Pinto Ferreira, Adélia Viviane Mello De Luna, Marcelo Henrique Cunha Chaves, Vinicius Vaz Cabral Nery, Jefferson Diocesano Da Cruz, Iasmim Castro De Lima, Arith Ramos Dos Santos

© **The Editor(s) and the Author(s) 2017**
The moral rights of the and the author(s) have been asserted.
All rights to the book as a whole are reserved by INTECH. The book as a whole (compilation) cannot be reproduced, distributed or used for commercial or non-commercial purposes without INTECH's written permission.
Enquiries concerning the use of the book should be directed to INTECH rights and permissions department (permissions@intechopen.com).
Violations are liable to prosecution under the governing Copyright Law.

Individual chapters of this publication are distributed under the terms of the Creative Commons Attribution 3.0 Unported License which permits commercial use, distribution and reproduction of the individual chapters, provided the original author(s) and source publication are appropriately acknowledged. If so indicated, certain images may not be included under the Creative Commons license. In such cases users will need to obtain permission from the license holder to reproduce the material. More details and guidelines concerning content reuse and adaptation can be foundat http://www.intechopen.com/copyright-policy.html.

Notice

Statements and opinions expressed in the chapters are these of the individual contributors and not necessarily those of the editors or publisher. No responsibility is accepted for the accuracy of information contained in the published chapters. The publisher assumes no responsibility for any damage or injury to persons or property arising out of the use of any materials, instructions, methods or ideas contained in the book.

First published in Croatia, 2017 by INTECH d.o.o.
eBook (PDF) Published by IN TECH d.o.o.
Place and year of publication of eBook (PDF): Rijeka, 2019. IntechOpen is the global imprint of IN TECH d.o.o.
Printed in Croatia

Legal deposit, Croatia: National and University Library in Zagreb

Additional hard and PDF copies can be obtained from orders@intechopen.com

Mass Spectrometry
Edited by Mahmood Aliofkhazraei
p. cm.
Print ISBN 978-953-51-3223-3
Online ISBN 978-953-51-3224-0
eBook (PDF) ISBN 978-953-51-4805-0

We are IntechOpen, the world's leading publisher of Open Access books

Built by scientists, for scientists

3,500+
Open access books available

111,000+
International authors and editors

115M+
Downloads

Our authors are among the

151
Countries delivered to

Top 1%
most cited scientists

12.2%
Contributors from top 500 universities

WEB OF SCIENCE™

Selection of our books indexed in the Book Citation Index in Web of Science™ Core Collection (BKCI)

Interested in publishing with us?
Contact book.department@intechopen.com

Numbers displayed above are based on latest data collected.
For more information visit www.intechopen.com

Meet the editor

Dr. Mahmood Aliofkhazraei works in the corrosion and surface engineering group at the Tarbiat Modares University. He is the head of Aliofkhazraei research group (www.aliofkhazraei.com). Dr. Aliofkhazraei has received several honors, including the Khwarizmi award and the best young nanotechnologist award of Iran. He is a member of the National Association of Surface Sciences, Iranian Corrosion Association, and National Elite Foundation of Iran. His research focuses on materials science, nanotechnology and its use in surface and corrosion science.

Contents

Preface

Mass spectrometry is an analytical technique that can be used for the structural characterization and quantification of a wide range of molecules. The technique is extensively used by chemists for the analysis of small and volatile organic compounds. It is highly sensitive and can be used to determine substances present at low concentrations, as in the case of doping, food control, environmental contamination, and many other areas of application. Mass spectrometry has long been an important technique for the identification of materials ranging from pure compounds to complex mixtures. Mass spectrometry can be used to determine molecular weight of compounds or using different ionization conditions, can provide more structural details through the analysis of fragmentation patterns. This level of detail can be attained for pure compounds and some mixtures. Mass spectrometry can also be combined with separation techniques such as gas chromatography or liquid chromatography to allow more complex mixtures to be examined. These hyphenated techniques provide a range of options for the characterization of complex materials.

This book collects new developments about mass spectrometry and its applications. I would like to appreciate all contributors to this book and thank them for their high-quality manuscripts. I wish the open access publishing of this book helps all researchers to benefit from this collection.

Dr. Mahmood Aliofkhazraei
Tarbiat Modares University
Iran

Section 1

Methods

Chapter 1

Deep Ultraviolet Single-Photon Ionization Mass Spectrometry

Zhixun Luo

Additional information is available at the end of the chapter

http://dx.doi.org/10.5772/68072

Abstract

The requirement of accurate analysis for organic chemicals has stimulated uprising research interest of single-photon ionization mass spectrometry (SPI-MS). Considering that ~90% compounds bear absorption in the deep ultraviolet (DUV) region, it is crucial for SPI-MS applications to employ effective DUV light sources. Here, we summarize the advances of SPI-MS by utilizing deep ultraviolet lamps and lasers, including the combination with quadrupole mass spectrometer (QMS), ion-rap mass spectrometer (ITMS), and time-of-flight mass spectrometer (TOFMS) systems. We then emphasize on the newly developed SPI-MS instrument coupled with an all-solid-state deep ultraviolet (DUV) laser at 177.3-nm wavelength. The advantages of SPI-MS instruments have been illustrated on several organic compounds, where the capability of low fragmentation enables to identify chemicals from unknown mixtures.

Keywords: deep ultraviolet (DUV), single-photon ionization (SPI), time-of-flight mass spectrometry (TOFMS), all-solid-state DUV laser, low-fragmentation

1. Introduction

Simply by measuring the ions abundance relating to their mass-to-charge ratios, mass spectrometry is known as the most powerful tool for identifying the quantity and type of chemicals present in a sample. According to the ionization strategies, mass spectrometry can be classified into hard ionization techniques (typically by direct electron impact, i.e., EI method) [1] and soft ionization techniques which usually include photoionization (PI) [2–8], chemical ionization (CI) [9, 10], matrix-assisted laser desorption/ionization (MALDI) [11], and electrospray ionization

INTECH
open science | open minds

© 2017 The Author(s). Licensee InTech. This chapter is distributed under the terms of the Creative Commons Attribution License (http://creativecommons.org/licenses/by/3.0), which permits unrestricted use, distribution, and reproduction in any medium, provided the original work is properly cited. CC BY

(ESI) [12]. Comparing with the EI technique which readily brings rigorous fragmentation for organic compounds, soft ionization techniques find their own advantages of maximal ionization efficiency without using high-energy electron impact. History keeps moving forward. The requirement for precise chemistry and fragmentation-free identification of mixed complexes has brought new opportunity and challenge to mass spectrometry.

Single-photon ionization mass spectrometry (SPI-MS) is known as an attractive soft-ionization technique resulting in simple mass identification neither utilizing matrix assistance nor rendering interference of multiple-charge ions [13–26]. Reasonable research interest has been attracted to SPI-MS due to the interference-free and fragmentation-free mass spectra, which is especially helpful for complex contaminant detection and mixed sample identification [7], for example, gasoline and diesel, cigarette smoke, and volatile organic compounds (VOCs) [27–48]. The accurate measurements of molecular weight also enable promising applications in conformational analysis [49, 50], real-time process monitoring [51], online characterization of aerosols [52, 53], and pyrolysis and combustion chemistry [54]. It is notable that ~90% of all organic compounds have absorption in the deep ultraviolet (DUV) region (λ<200 nm), and thus, the development of better DUV light sources becomes crucial for SPI-MS applications.

In general, DUV sources are obtained using nonlinear frequency conversion of the radiation of DUV lamps [13, 55], gas discharges [56], lasers [57], and electron synchrotrons [54, 58]. **Table 1** lists the present typical DUV light sources for SPI-MS investigations, where a coverage of 117–200 nm illustrates the applicability of SPI-MS for a variety of molecule systems with different ionization energies. Among them, the newly developed technique of all-solid-state DUV laser (177.3-nm) by second harmonic generation of 355-nm laser, in help of a KBBF-CaF_2 prism-coupled device [57, 59], has shown several advantages in photon flux, bandwidth,

Source of DUV	Generation	Medium	Center Wavelength (nm)
Laser-based DUV light	SHG of 355 nm Nd:YAG laser [59, 60]	KBBF crystal	177.3
	THG of 355 nm Nd:YAG laser [64, 65]	Xe-Ar gas	118
	Four-wave mixing [53]	Xe gas	122–168
	F_2 laser [66]	F_2 gas	157
	H_2 laser [67]	H_2 gas	160
Gas discharged DUV lamps	Excimer DUV lamp [56]	dense rare gases	120–200
	Krypton discharge lamps [68]	Kr gas	117
	Microwave discharge lamps [51]	He/H_2 gas	121.5
Synchrotron light	Monochromatizing the beam line [58]	Electromagnetic field	tunable

Table 1. Typical DUV light sources for single-photon ionization mass spectrometry.

beam quality, and coherence [59–61], giving rise to largely improved sensitivity/resolution of SPI-TOFMS [62, 63]. Here, we summarize the advances of DUV-SPI mass spectrometry, emphasizing on the SPI-MS techniques based on two typical ionization strategies, that is, VUV lamps and radiation of lasers.

2. VUV Lamps for SPI-MS

2.1. VUV Lamps for SPI-ITMS

Regarding to typical DUV light sources available for SPI-MS investigations (as listed in **Table 1**), low-pressure discharge lamps filled with rare gases (e.g., Kr and Xe/Ar) have been widely utilized in previously published studies such as the online monitoring of organic compounds [69]. Combining with thermogravimetric (TG) device, evolved gas analysis was demonstrated as the most straightforward way for gas-phase reactions. A typical set up in Zimmermann group (**Figure 1**) [69] employs sample matrix of evolved-off gas coupled with a single-photon ionization (SPI) ion-rap mass spectrometer system (ITMS). This set up has been utilized to provide distinct substance identification for evolved gas from roast and ground coffee powder, etc.

2.2. VUV Lamps for SPI-QMS

A similar VUV lamp apparatus relates to quadrupole mass spectrometry (QMS) which was designed to study free radical-molecule kinetics of molecular beam from a Knudsen flow

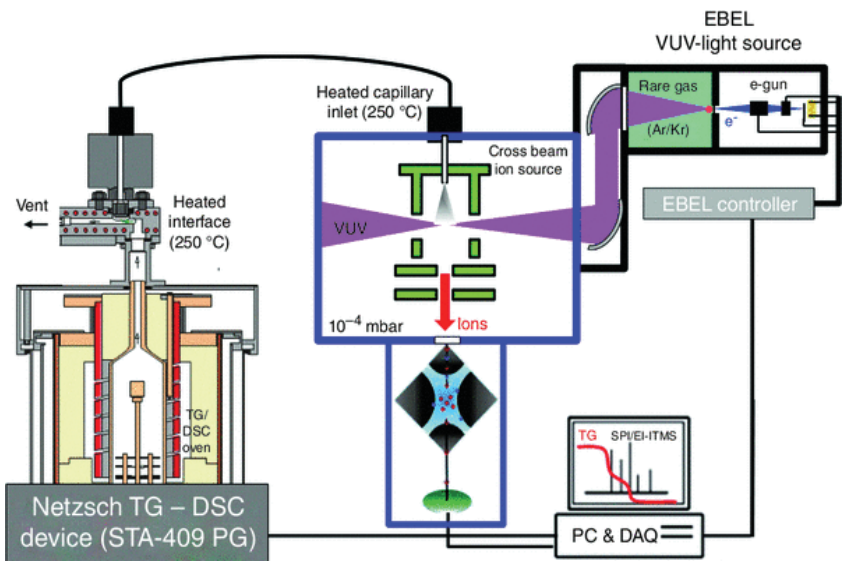

Figure 1. A scheme of the experimental TG–SPI–ITMS setup. The TG is depicted on the left side; the enlarged ionization manifold with ITMS is shown in the middle, and the electron beam pumped rare gas excimer light source (EBEL) for SPI with double parabolic mirror optics is sketched on the right side. Reproduced with permission from Ref. [69].

reactor (**Figure 2**) [70], where the propagating molecular beam and VUV photons meet in a crossed-beam ion source. From such a SPI-MS set up, an interesting study found steady-state exit flow of $C_2H_5^{\bullet}$ (ethyl) and t-$C_4H_9^{\bullet}$ (t-butyl) free radicals indicating the advantages of VUV-lamps for SPI-QMS analysis toward volatile organic compounds (VOCs).

2.3. VUV Lamps for SPI-TOFMS

The VUV lamp with SPI capability has also been developed for time-of-flight mass spectrometry (TOFMS). Utilizing a 10.6 eV krypton discharge lamp (a photon flux up to ~10^{11} photons per second), the coupling of SPI with TOFMS (SPI-TOFMS) takes the advantages of rapid detection speed and also simple spectral analysis. SPI-TOFMS has been recognized as a powerful technique for monitoring various fast processes in gas phase, for instance, to real-time monitor the catalytic olefin synthetic reactions [71], to help assign the double bond position in linear olefins, and to verify rapid chemical derivatization such as ozonolysis. **Figure 3** shows a typical SPI-TOFMS instrument in H. Li group [13], where the ion source includes a commercial VUV krypton discharge lamp and an ionization cavity that is made of six steel electrodes. Oxygen gas flow (e.g., olefin and olefin ozonolysis products) can be introduced into the ionization cavity by a fused-silica capillary. They found that relatively high pressure (0.3 mbar) of the ion source is helpful to extend the photoionization length (e.g., ~36 mm) and hence to improve ionization efficiency. As a result, toluene, benzene, and *p*-xylene were found to attain

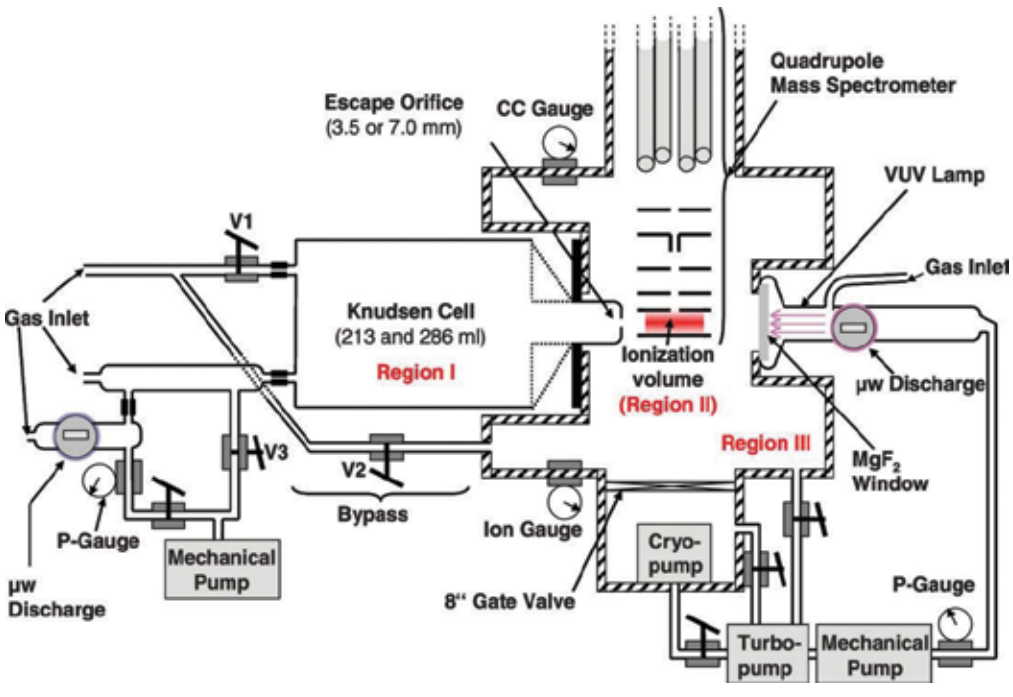

Figure 2. A schematic showing of the VUV-SPIMS for free radical detection by using an external free radical source based on microwave discharge (2.46 GHz) to create H or Cl atoms. Three PTFE capillary inserts of 1–2 mm diameter and 10–20 mm length are displayed on the free radical source (left). Reproduced with permission from Ref. [70].

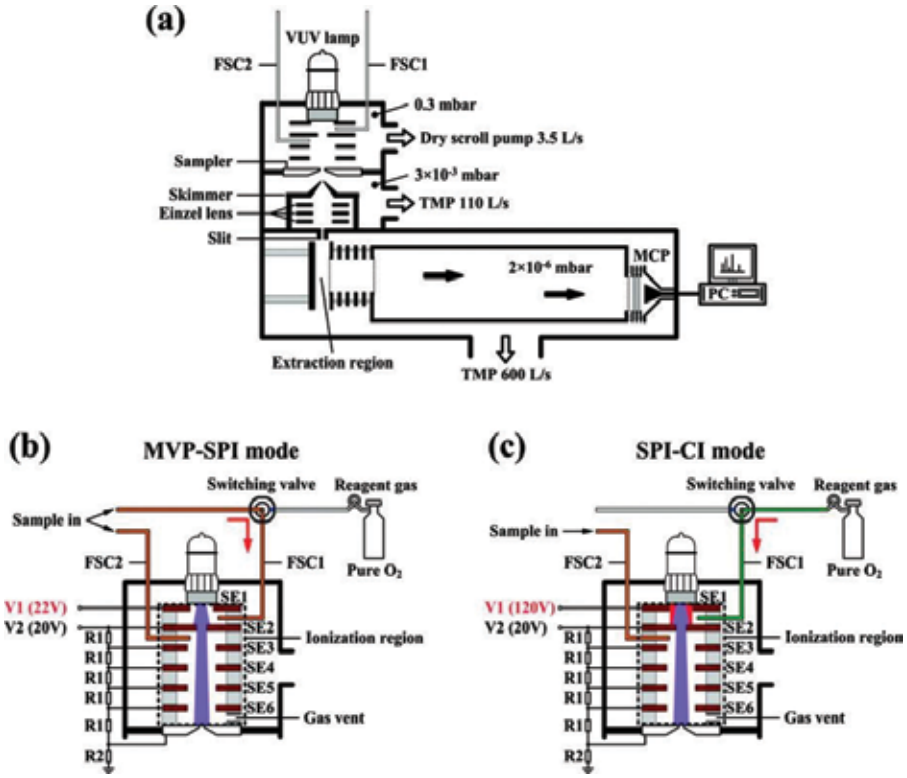

Figure 3. (a) Schematic diagram of a home-built mass spectrometer combining SPI and CI ion sources (a), and its operation in MVP-SPI mode (b), and in SPI-CI mode (c) respectively. Reproduced with permission from Ref. [13].

a limit of detection (LOD) down to 3, 4, and 6 ppbv. Within such SPI-TOFMS strategy, toluene and chloroform also showed LODs values of 8 and 10 ppbv [13]. The capability of SPI-TOFMS method with online ozonolysis has been found operative to quantitatively identify isomeric olefin mixtures [71]. Interestingly, the applicability of SPI-TOFMS for evolved gas analysis of coffee has also been demonstrated in the previously reported study, where kahweol was used as a tracer compound enabling to discriminate arabica coffee from robusta species [72].

Figure 4 presents the SPI mass spectra of linear 1-, 2-, 3- octenes, 1-, 2-, 5- decenes, and their corresponding ozonolysis products. It is notable that some ions which are absent in the SPI mass spectra become dominant in the spectra of corresponding ozonolysis products, such as *m*/*z* 96/97 and 113/114 ions for 1-octene, assigned to deprotonation (or protonation) of aldehyde dehydrated ions and aldehyde molecular ions. This was proven to result from ion-molecule reactions between aldehyde products and olefins. Also found from the SPI-MS was the appearance of two new ions corresponding to $[M + 12]^+$ due to "$-H_2O + CH_2O$" and $[M + 18]^+$ due to "$-C_2H_4 + O_3$", seen at *m*/*z* 126 and 132 for 1-octene, also at *m*/*z* 154 and 160 for 1-decene, which were found to be only formed for the terminal olefins. At this point, such SPI-TOFMS identification along with corresponding ozonolysis products could be used to distinguish isomers of linear terminal olefins.

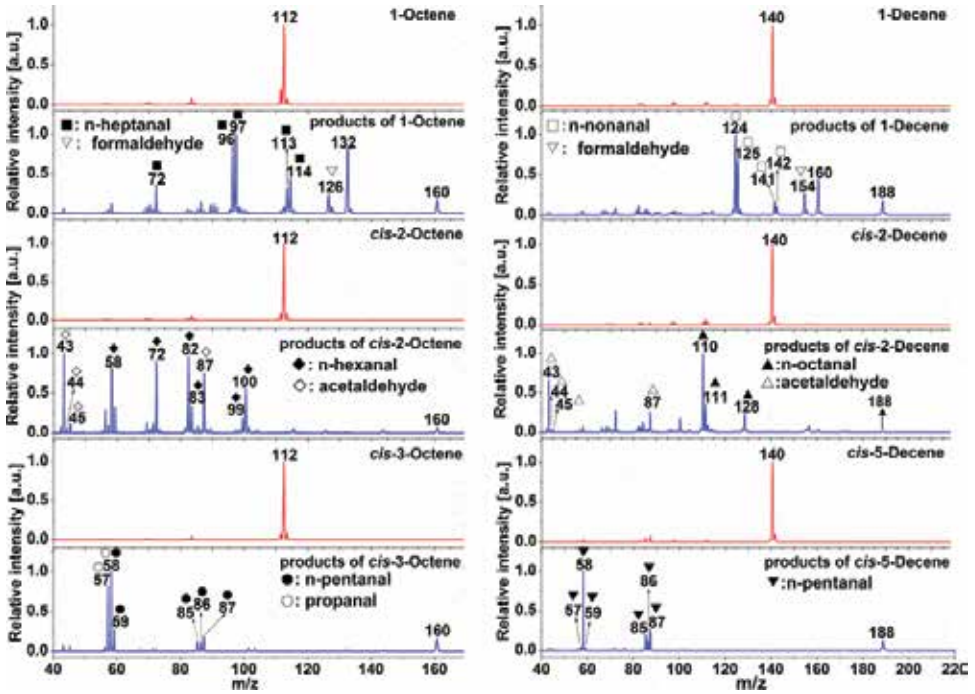

Figure 4. SPI mass spectra of linear octenes, decenes, and corresponding ozonolysis products. Reproduced with permission from Ref. [13].

Figure 5 presents an application of SPI-MS combined with a custom-made smoking machine system. Analogous to the above, the innovative EBEL source filled with argon provides ~9.8 eV single-photon energy of the VUV light. The investigated analytes include carbon nitride, acetone, acetaldehyde, acrolein, butadiene, propanal, butanal, 2-butanone, isoprene,

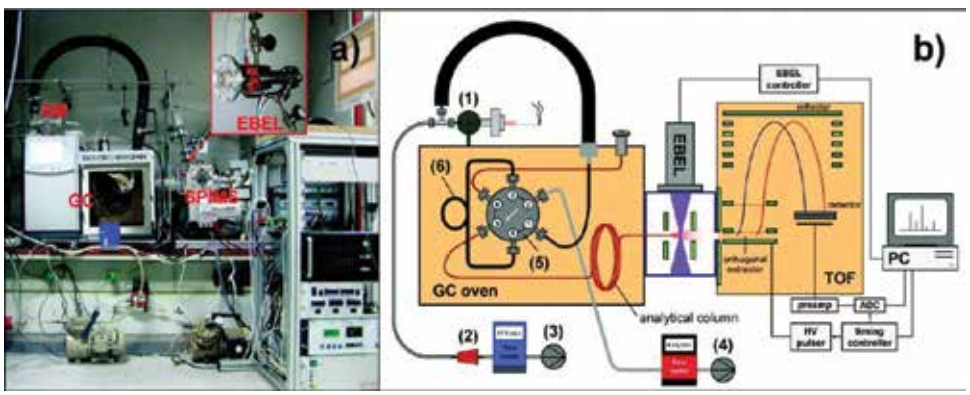

Figure 5. (a) A photo of the two-dimensional smoke analysis system consisting of a home-built smoking machine, a gas chromatograph, and a single-photon ionization mass spectrometer (SPI-MS). (b) Schematic representation of the smoke analyzer: (1) Borgwaldt smoking valve; (2) particle filter; (3) smoking pump; (4) sampling pump; (5) six-port, two-position valve; (6) sample loop. Reproduced with permission from Ref. [73].

furan, isobutanal, crotonaldehyde, benzene, toluene, etc [73]. From such SPI-MS analysis, the determined amounts of these compounds find well consistence with the empirical values. This is another important application of SPI-MS.

Among others, magnetic-field enhanced sources have also been coupled with SPI-MS instruments. Typically, a radio-frequency powered VUV lamp could be used, and the photoelectrons (generated by photoelectric effect) were accelerated to induce ionization, strengthened by a strong magnetic field (~800 G) with a permanent annular magnet. Compared to a nonmagnetic field SPI source, the signal could be enlarged two orders with photoelectron energy of ~20 eV, with soft-ionization characteristics remained. The advantages of this source are ascribed to the increased electron moving path and the improved electron transmission under magnetic field [74].

3. Laser radiation for SPI-TOF MS

3.1. THG of 355 nm laser in Xe-Ar gas cell

It is well known that a synchrotron source and four-wave mixing techniques have the ability to generate tunable DUV light, but the bulky and complicated devices confine their applications for SPI-MS [2]. Alternatively, there is an important finding that 118-nm laser can be generated through high harmonic generation (HHG) of 355-nm laser in a few noble gases such as a Xe-Ar mixture (e.g., 1:10) [64, 65]. By allowing the 355-nm laser penetrating through a convenient noble gas cell, the 118-nm DUV lasers have been widely applied for SPI-MS investigations. **Figure 6** shows such a method for analyzing organoselenium

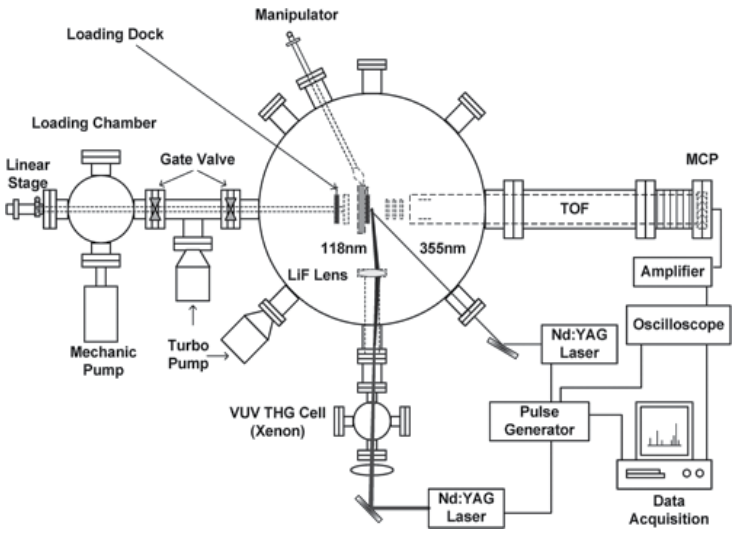

Figure 6. A sketch drawing of the laser desorption single-photon-ionization mass spectrometer consisting of an ultrahigh vacuum chamber equipped with a linear transfer antechamber, where a sample holder with an XYZ controller mounted on a 360° rotation stage, a THG cell, and a home-built linear TOF mass spectrometer. The neutrals were photoionized by a vacuum ultraviolet (118 nm) laser. Reproduced with permission from Ref. [32].

and organic acid metabolites [32], where the laser desorption was included from graphite surfaces coupled with a typical SPI-MS system. High sensitivity (up to fmol) allows quantitative detection of chemicals in complex biological samples such as from human/animal urine, where the accurate detection of biological metabolites is very helpful for medical diagnosis [32].

The application of such laser beam for SPI-TOFMS has also been demonstrated to be highly effective for the rapid detection of the nitro-containing explosives and the related compounds, such as nitrobenzene, *o*-nitrotoluene, 1,3-dinitrobenzene, 2,4-dinitrotoluene, and 2,4,6-trinitrotoluene, as shown in **Figure 7**. In addition to the direct identification capability, the limits of detection using such SPI-MS were found to be as low as ~40 ppb [75]. It is worth mentioning that, although ion mobility-based detection [3–5] is widely used for nitro-containing explosives, as known of a screening tool at airports, the conventional technology is not applicable to all explosive-related chemicals; also, any false negative and positive detection rates may be problematic. In this point, SPI-MS could be one of the most promising techniques for trace detection and identification of explosives.

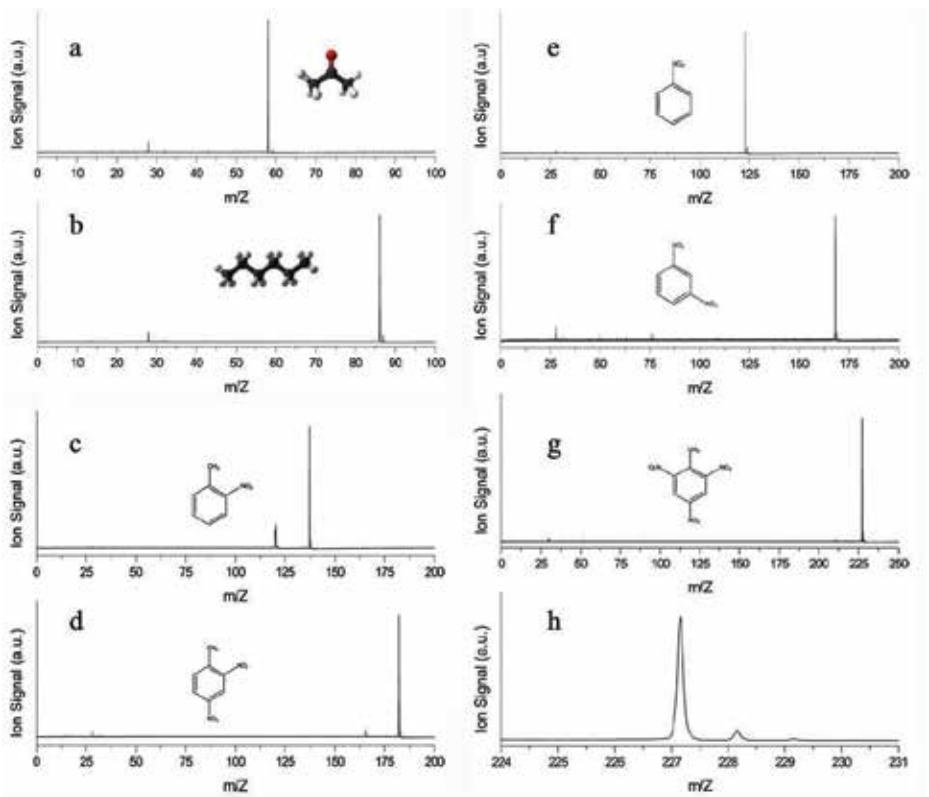

Figure 7. (a) Single-photon ionization mass spectrum of acetone (a), hexane (b), nitrobenzene (c), 1,3-dinitrobenzene (d), *o*-nitrotoluene (e), 2,4-dinitrotoluene (f), and 2,4,6-Trinitrotoluene (g/h). Reproduced with permission from Ref. [75].

3.2. All-solid-state DUV laser for SPI-MS: SHG of 355 nm

Figure 8 shows a sketch of the all-solid-state 177.3-nm DUV laser system for SPI-MS in Luo's group [76], where a picosecond 355-nm laser was chosen as the pump. The 355-nm laser comes from the third harmonic generation of 1064-nm Nd:YAG laser with a pulse duration of ~16 ps (a repetition rate of 10 Hz). The 355-nm pump laser was then well modulated at proper height and incident direction prior to the KBBF-PCT device for frequency doubling. The KBBF-PCT device was set on a mobile optics stage allowing rotation and XYZ translation in order to adjust the phase-matching angle and laser beam position. All the reflection mirrors (M4, M5, M6) are motor controlled from outside the chamber. A coated CaF_2 lens (800-mm focus length) was used to focus the DUV laser beam before it was introduced into the vacuum-connected TOFMS chamber. The power of the DUV laser source can be measured by two power meters with plug-in probes via ultrahigh vacuum feedthroughs to evaluate the transfer efficiency in the DUV laser chamber. The DUV optical chamber and the TOFMS chamber were separated by a CaF_2 window which maintains 95% transmittance of the 177 nm DUV laser.

Figure 9 sketches the customized Re-TOFMS system which is made up of two vacuum chambers along with relating pumping system, respectively. Two sampling systems were designed allowing different samples to be analyzed, that is, a pulsed buffer gas contained source and a thermal evaporation molecular beam source. The two sources share a same sampling chamber, and the thermal evaporation source is located downstream crossing the ionization region, allowing the sample vapor to expand upward entering the half-cylinder section through a nozzle and then a skimmer until arriving the ionization zone of Re-TOF chamber. Photo-

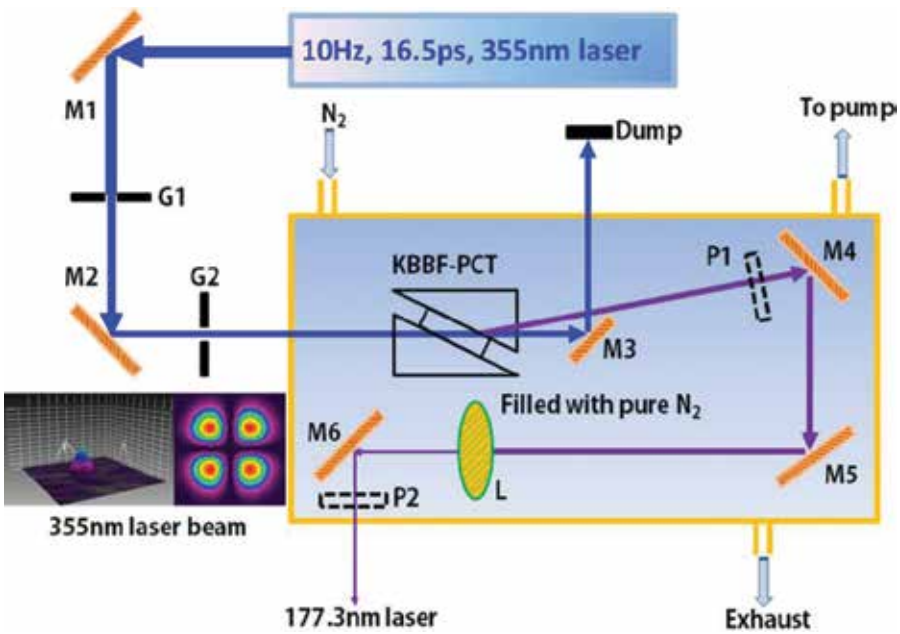

Figure 8. A schematic layout of the all-solid-state 177.3nm DUV laser optical system.

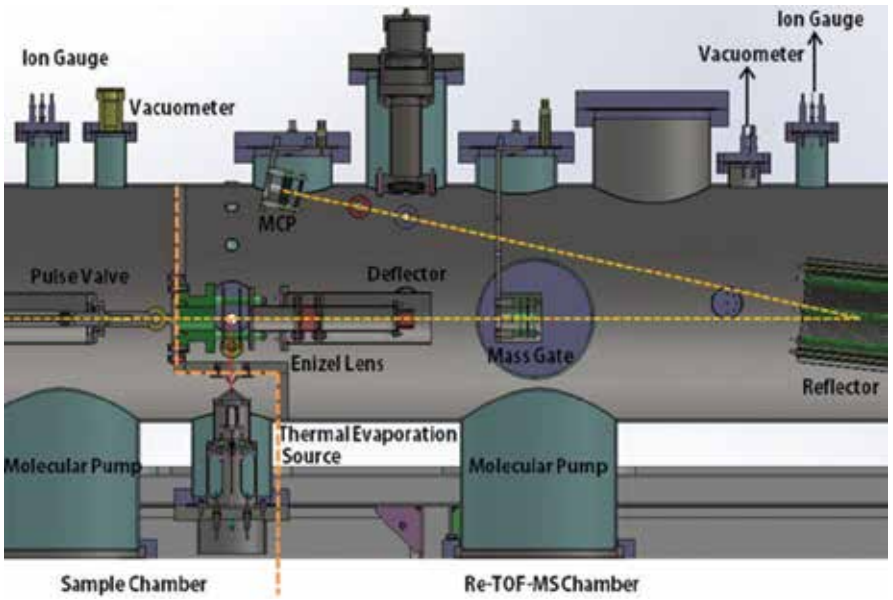

Figure 9. Schematic diagram of the customized mass spectrometer with two DUV-SPI sources.

ionized molecule beam will then horizontally or vertically go into the ionization region and accelerate along the electric field. An einzel lens was designed to focus the ions thus convert the initial energy dispersion of ions enabling to improve the ions collection and mass resolution capability of the TOF mass analyzer. Four electrostatic deflectors were designed to direct ions on the way to the reflector and finally MCP detector. For a maximum transmission efficiency of ions, typical voltages (U_1 and U_2) on the acceleration pole plates were set at 1.6 KV and 1.2 KV, respectively. The pulse valve and laser are synchronized using a DG 535 digital delay generator. A digital storage oscilloscope was employed to record the signal collected by MCP for which a voltage at −2100 V was used.

Based on this DUV-SPI-TOFMS system, several typical molecules have been tested, such as N,N-dimethyl-p-toluidine (DPT, $C_9H_{13}N$), p-phenylenediamine (PPD, $C_6H_8N_2$), 1,5-diaminonaphthalene (DAN, $C_{10}H_{10}N_2$), and porphyrins, as partly shown in **Figure 10**. From the mass spectra of them ionized with a 177.3-nm laser respectively, there are rare fragmentation peaks, which is in sharp contrast to that obtained by 355-nm laser ionization. Specifically for DPT sample, a predominant peak at m/z=135 points to DPT molecular ion, where a brother peak at m/z=134 is due to a hydrogen atom loss indicating the activation of C–H bond. Also a comparison of the ionization of PPD by 355-nm and 177.3-nm laser reveals that the mass spectrum obtained from DUV ionization shows a dominant peak at m/z = 108 identical to the molecular weight of PPD, verifying that the 177.3-nm DUV laser undergoes an excellent SPI process. In sharp contrast, the mass spectrum acquired from 355-nm laser ionization shows a weak parent peak but numerous fragments corresponding to the aromatic amines fragmentation. Several other unpublished DUV-SPI results have also been attained suggesting that the picosecond DUV laser is really an ideal choice for effective SPI-MS. Note that, the mass spectra obtained

http://dx.doi.org/10.5772/68072

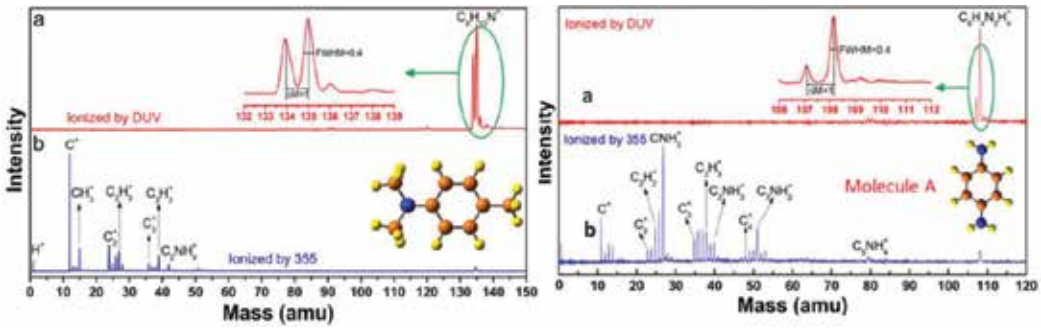

Figure 10. (Left) Mass spectra of N, N-dimethyl-p-toluidine ionized by 177.3 nm (a) and 355 nm laser (b). (Right) Mass spectra of p-phenylenediamine ionized by 177.3 nm (a) and 355 nm laser (b).

by the 177-nm DUV-SPI ionization display smaller full width at half maximum (FWHM) than that by 355-nm laser, indicating improved overall resolution associated with the all-solid-state DUV laser and ionization source.

To further reveal the DUV-SPI-MS ability to identify multicomponents, a sample by mixing the two solid samples PPD and DAN together has been tested, as shown in **Figure 11**. The mixture sample was prepared with a mass ratio of 1:1 of PPD and DAN by grinding method. As results, the parent peaks of PPD and DAN are solely observed in the 177.3-nm SPI-MS spectrum, which is in sharp contrast to the unjustifiable fruitful fragment peaks when ionized with 355-nm laser. The overlapped fragment peaks of organic chemicals make the 355-nm multiphoton ionization difficult to identify molecules from an unknown complex; however, the interference-free and fragmentation-free mass spectra by DUV-SPI-MS bear important

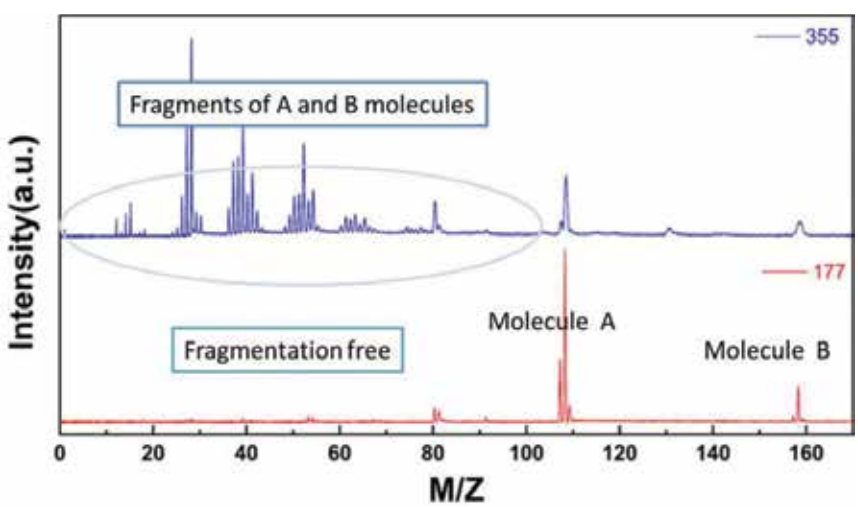

Figure 11. Mass spectra of the mixture of p-phenylenediamine (as named Molecule A) and 1,5-diaminonaphthalene (as named Molecule B) ionized by 355 and 177.3-nm DUV laser.

advantages to identify molecules from an unknown mixture. Further development of SPI-MS is desirable so as to identify intact atomic/molecular clusters & aggregates of strong/weak interactions, as involved in many chemical and biochemical processes [77, 78].

4. Conclusion

Single-photon ionization mass spectrometry (SPI-MS) is recognized a powerful technique for accurate molecular weight measurements with promising applications in a wide range of research fields, including conformational analysis, contaminant detection, real-time process monitoring, pyrolysis, combustion chemistry studies, and online characterization of aerosols. Considering that 90% compounds have light absorption in the DUV region, convenient DUV light sources are crucial for SPI-MS applications. The instrument development and technical research relating to DUV-SPI-MS demonstrate fragmentation-free and matrix-free advantages of over other mass spectrometers. DUV-SPI-MS is favorable for real-time and online detection of volatile organic compounds involved in environmental air and industrial waste.

Author details

Zhixun Luo

Address all correspondence to: zxluo@iccas.ac.cn

Institute of Chemistry, Chinese Academy of Sciences, Beijing, China

References

[1] Yang, S.; Brereton, S. M.; Wheeler, M. D.; Ellis, A. M. Soft or hard ionization of molecules in helium nanodroplets? An electron impact investigation of alcohols and ethers; *Phys. Chem. Chem. Phys.* **2005**, *7*, 4082–4088.

[2] Hanley, L.; Zimmermann, R. Light and molecular ions: the emergence of vacuum UV single-photon ionization in MS; *Anal. Chem.* **2009**, *81*, 4174–4182.

[3] Kauppila, T. J.; Syage, J. A.; Benter, T. Recent developments in atmospheric pressure photoionization-mass spectrometry; *Mass Spectrom. Rev.* **2015**, *103*, 377–378.

[4] Zimmerman, J. A.; O'Malley, R. M. Multiphoton ionization of aniline, aniline-15 N and aniline-2, 3, 4, 5, 6-d 5: ionization and fragmentation mechanisms; *Int. J. Mass Spectrom. Ion Processes* **1990**, *99*, 169–190.

[5] Schröder, D.; Loos, J.; Thissen, R.; Dutuit, O.; Mourgues, P.; Audier, H. E.; Lifshitz, C.; Schwarz, H. Barrier height titration by tunable photoionization combined with

chemical monitoring: Unimolecular keto/enol tautomerization of the acetamide cation radical; *Angew. Chem. Int. Ed.* **2002**, *41*, 2748–2751.

[6] Hamachi, A.; Okuno, T.; Imasaka, T.; Kida, Y.; Imasaka, T. Resonant and Nonresonant Multiphoton Ionization Processes in the Mass Spectrometry of Explosives; *Anal. Chem.* **2015**, *87*, 3027–3031.

[7] Liu, P.; Hu, Y.; Zhu, G.; Yang, Q.; Tao, Y. Direct and fast detection of chlorothalonil in soil samples using laser desorption VUV single photon post-ionization mass spectrometry; *Anal. Methods* **2015**, *7*, 6890–6895.

[8] Salpin, J. Y.; Scuderi, D. Structure of protonated thymidine characterized by infrared multiple photon dissociation and quantum calculations; *Rapid Commun. Mass Spectrom.* **2015**, *29*, 1898–1904.

[9] Munson, M. S. B.; Field, F. H. Chemical Ionization Mass Spectrometry. I. General Introduction; *J. Am. Chem. Soc.* **1966**, *88*, 2621–2630.

[10] Richter, W. J.; Schwarz, H. Chemical ionization—a mass-spectrometric analytical procedure of rapidly increasing importance; *Angew. Chem. Int. Ed.* **1978**, *17*, 424–439.

[11] Claydon, M. A.; Davey, S. N.; Edwards-Jones, V.; Gordon, D. B. The rapid identification of intact microorganisms using mass spectrometry; *Nat. Biotechnol.* **1996**, *14*, 1584–1586.

[12] Fenn, J. B.; Mann, M.; Meng, C. K.; Wong, S. F.; Whitehouse, C. M. Electrospray ionization for mass spectrometry of large biomolecules; *Science* **1989**, *246*, 64–71.

[13] Hua, L.; Wu, Q.; Hou, K.; Cui, H.; Chen, P.; Wang, W.; Li, J.; Li, H. Single photon ionization and chemical ionization combined ion source based on a vacuum ultraviolet lamp for orthogonal acceleration time-of-flight mass spectrometry; *Anal. Chem.* **2011**, *83*, 5309–5316.

[14] Adam, T.; Baker, R. R.; Zimmermann, R. Investigation, by single photon ionisation (SPI)-time-of-flight mass spectrometry (TOFMS), of the effect of different cigarette-lighting devices on the chemical composition of the first cigarette puff; *Anal. Bioanal. Chem.* **2007**, *387*, 575–584.

[15] Adam, T.; Mitschke, S.; Streibel, T.; Baker, R. R.; Zimmermann, R. Puff-by-puff resolved characterisation of cigarette mainstream smoke by single photon ionisation (SPI)-time-of-flight mass spectrometry (TOFMS): Comparison of the 2R4F research cigarette and pure Burley, Virginia, Oriental and Maryland tobacco cigarettes; *Anal. Chim. Acta* **2006**, *572*, 219–229.

[16] Butcher, D. J.; Goeringer, D. E.; Hurst, G. B. Real-time determination of aromatics in automobile exhaust by single photon ionisation ion trap mass spectrometry; *Anal. Chem.* **1999**, *71*, 489–496.

[17] R. Laudient, R. Schultze, J. Wieser, "Fast detection of narcotics by single photon ionization mass spectrometry and laser ion mobility spectrometry." Security + Defence International Society for Optics and Photonics, **2010**:125–131.

[18] Lei, C.; Zimmermann, R.; Kettrup, A.; Wang, H. Z. Investigation of combustion/pyrolysis behavior of polyvinyl chloride materials by on-line single photon ionization/resonance enhanced multi-photon ionization-time of flight mass spectrometry; *Chinese J. Anal. Chem.* **2004**, *32*, 699–704.

[19] Li, A.; Sun, Y.; Cui, Z. Detection of Polycyclic Aromatic Hydrocarbons in Soil Sample by Thermal Desorption/Single Photon Ionization Mass Spectrometry; *J. Instrum. Anal.* **2014**, *33*, 465–470.

[20] Li, C.; Zhou, Y.-F.; Tan, G.-B.; Liu, Y.-L.; Gao, W.; Zhou, Z.; Chen, H.-W.; Ouyang, Y.-Z. Rapid Identification of True and Fake Wines Using Single Photon Ionization Mass Spectrometry; *Chinese J. Anal. Chem.* **2013**, *41*, 1359–1365.

[21] Li, F.-L.; Hou, K.-Y.; Chen, W.-D.; Chen, P.; Zhao, W.-D.; Cui, H.-P.; Hua, L.; Xie, Y.-Y.; Pei, K.-M.; Li, H.-Y. Single Photon Ionization/Photoelectron Ionization-Membrane Introduction Mass Spectrometry for On-line Analysis Ethers Gasoline Additive in Water; *Chinese J. Anal. Chem.* **2013**, *41*, 42–48.

[22] Lockyer, N. P.; Vickerman, J. C. Single photon ionisation mass spectrometry using laser-generated vacuum ultraviolet photons; *Laser Chem.* **1997**, *17*, 139–159.

[23] Saraji-Bozorgzad, M.; Geissler, R.; Streibel, T.; Sklorz, M.; Kaisersberger, E.; Denner, T.; Zimmermann, R. Hyphenation of a thermobalance to soft single photon ionisation mass spectrometry for evolved gas analysis in thermogravimetry (TG-EGA); *J. Therm. Anal. Calorim.* **2009**, *97*, 689–694.

[24] Streibel, T.; Geissler, R.; Saraji-Bozorgzad, M.; Sklorz, M.; Kaisersberger, E.; Denner, T.; Zimmermann, R. Evolved gas analysis (EGA) in TG and DSC with single photon ionisation mass spectrometry (SPI-MS): molecular organic signatures from pyrolysis of soft and hard wood, coal, crude oil and ABS polymer; *J. Therm. Anal. Calorim.* **2009**, *96*, 795–804.

[25] Xie, Y.; Hua, L.; Chen, P.; Hou, K.; Jiang, J.; Wang, Y.; Li, H. Coupling of gas chromatography with single photon ionization time-of-flight mass spectrometry and its application to characterization of compounds in diesel; *Se pu = Chinese J. Chromatography* **2015**, *33*, 188–194.

[26] Xie, Y.-Y.; Hua, L.; Hou, K.-Y.; Chen, P.; Cui, H.-P.; Zhao, W.-D.; Chen, W.-D.; Li, J.-H.; Li, H.-Y. On-line Analysis of Flavor Compounds in Toothpastes by Single Photon Ionization Mass Spectrometry; *Chinese J. Anal. Chem.* **2012**, *40*, 1883–1889.

[27] Adam, T.; Baker, R. R.; Zimmermann, R. Characterization of puff-by-puff resolved cigarette mainstream smoke by single photon ionization-time-of-flight mass spectrometry and principal component analysis; *J. Agric. Food Chem.* **2007**, *55*, 2055–2061.

[28] Brown, A. L.; Dayton, D. C.; Nimlos, M. R.; Daily, J. W. Characterization of biomass pyrolysis vapors with molecular beam, single photon ionization time-of-flight mass spectrometry; *Chemosphere* **2001**, *42*, 663–669.

[29] Cao, L.; Muhlberger, F.; Adam, T.; Streibel, T.; Wang, H. Z.; Kettrup, A.; Zimmermann, R. Resonance-enhanced multiphoton ionization and VUV-single photon ionization as soft and selective laser ionization methods for on-line time-of-flight mass spectrometry: Investigation of the pyrolysis of typical organic contaminants in the steel recycling process; *Anal. Chem.* **2003**, *75*, 5639–5645.

[30] Chen, Y.; Aleksandrov, A.; Orlando, T. M. Probing low-energy electron induced DNA damage using single photon ionization mass spectrometry; *Int. J. Mass Spectrom.* **2008**, *277*, 314–320.

[31] Chen, Y.; Santai, C.; Hud, N. V.; Orlando, T. Investigating low-energy electron-induced DNA damage using single photon ionization mass spectrometry; *Abstr. Pap. Am. Chem. Soc.* **2006**, *231*, 6-ANYL.

[32] Chen, Y.; Sullards, M. C.; Hoang, T. T.; May, S. W.; Orlando, T. M. Analysis of organoselenium and organic acid metabolites by laser desorption single photon ionization mass spectrometry; *Anal. Chem.* **2006**, *78*, 8386–8394.

[33] Cui, H.; Hua, L.; Hou, K.; Wu, J.; Chen, P.; Xie, Y.; Wang, W.; Li, J.; Li, H. Coupling of stir bar sorptive extraction with single photon ionization mass spectrometry for determination of volatile organic compounds in water; *Analyst* **2012**, *137*, 513–518.

[34] Ehlert, S.; Hoelzer, J.; Rittgen, J.; Puetz, M.; Schulte-Ladbeck, R.; Zimmermann, R. Rapid on-site detection of explosives on surfaces by ambient pressure laser desorption and direct inlet single photon ionization or chemical ionization mass spectrometry; *Anal. Bioanal. Chem.* **2013**, *405*, 6979–6993.

[35] Fischer, M.; Wohlfahrt, S.; Varga, J.; Saraji-Bozorgzad, M.; Matuschek, G.; Denner, T.; Zimmermann, R. Evolved gas analysis by single photon ionization-mass spectrometry; *J. Therm. Anal. Calorim.* **2014**, *116*, 1461–1469.

[36] Geissler, R.; Saraji-Bozorgzad, M. R.; Groeger, T.; Fendt, A.; Streibel, T.; Sklorz, M.; Krooss, B. M.; Fuhrer, K.; Gonin, M.; Kaisersberger, E.; Denner, T.; Zimmermann, R. Single Photon Ionization Orthogonal Acceleration Time-of-Flight Mass Spectrometry and Resonance Enhanced Multiphoton Ionization Time-of-Flight Mass Spectrometry for Evolved Gas Analysis in Thermogravimetry: Comparative Analysis of Crude Oils; *Anal. Chem.* **2009**, *81*, 6038–6048.

[37] Hou, K.; Li, F.; Chen, W.; Chen, P.; Xie, Y.; Zhao, W.; Hua, L.; Pei, K.; Li, H. An in-source stretched membrane inlet for on-line analysis of VOCs in water with single photon ionization TOFMS; *Analyst* **2013**, *138*, 5826–5831.

[38] Kambe, Y.; Yamamoto, Y.; Yamada, H.; Tonokura, K. Measurement of gas- and particle-phase organic species in diesel exhaust using vacuum ultraviolet single photon ionization time-of-flight mass spectrometry; *Chem. Lett.* **2012**, *41*, 292–294.

[39] Muhlberger, F.; Streibel, T.; Wieser, J.; Ulrich, A.; Zimmermann, R. Single photon ionization time-of-flight mass spectrometry with a pulsed electron beam pumped excimer

VUV lamp for on-line gas analysis: Setup and first results on cigarette smoke and human breath; *Anal. Chem.* **2005**, *77*, 7408–7414.

[40] Saraj-Bozorgzad, M.; Geissler, R.; Streibel, T.; Muhlberger, F.; Sklorz, M.; Kaisersberger, E.; Denner, T.; Zimmermann, R. Thermogravimetry coupled to single photon ionization quadrupole mass spectrometry: A tool to investigate the chemical signature of thermal decomposition of polymeric materials; *Anal. Chem.* **2008**, *80*, 3393–3403.

[41] Saraji-Bozorgzad, M. R.; Eschner, M.; Groeger, T. M.; Streibel, T.; Geissler, R.; Kaisersbeiger, E.; Denner, T.; Zimmermann, R. Highly resolved online organic-chemical speciation of evolved gases from thermal analysis devices by cryogenically modulated fast gas chromatography coupled to single photon ionization mass spectrometry; *Anal. Chem.* **2010**, *82*, 9644–9653.

[42] Schlappi, B.; Litman, J. H.; Ferreiro, J. J.; Stapfer, D.; Signorell, R. A pulsed uniform Laval expansion coupled with single photon ionization and mass spectrometric detection for the study of large molecular aggregates; *Phys. Chem. Chem. Phys.* **2015**, *17*, 25761–25771.

[43] Schramm, E.; Hoelzer, J.; Puetz, M.; Schulte-Ladbeck, R.; Schultze, R.; Sklorz, M.; Ulrich, A.; Wieser, J.; Zimmermann, R. Real-time trace detection of security-relevant compounds in complex sample matrices by thermal desorption-single photon ionization-ion trap mass spectrometry (TD-SPI-ITMS) Spectrometry (TD-SPI-ITMS); *Anal. Bioanal. Chem.* **2009**, *395*, 1795–1807.

[44] Schramm, E.; Muehlberger, F.; Mitschke, S.; Reichardt, G.; Schulte-Ladbeck, R.; Puetz, M.; Zimmermann, R. Determination of the ionization potentials of security-relevant substances with single photon ionization mass spectrometry using synchrotron radiation; *Appl. Spectrosc.* **2008**, *62*, 238–247.

[45] Steenvoorden, R.; Kistemaker, P. G.; Devries, A. E.; Michalak, L.; Nibbering, N. M. M. Laser single photon ionization mass-spectrometry of linear, branched and cyclic hexanes; *Int. J. Mass Spectrom. Ion Processes* **1991**, *107*, 475–489.

[46] Wang, B. G.; Gu, Y. G.; Zhou, L.; Wang, H.; Gao, W.; Zhou, Z. Determination of dimethyl sulfide in gas samples by single photon ionization time of flight mass spectrometry; *Anal. Lett.* **2014**, *47*, 2003–2011.

[47] Wohlfahrt, S.; Fischer, M.; Saraji-Bozorgzad, M.; Matuschek, G.; Streibel, T.; Post, E.; Denner, T.; Zimmermann, R. Rapid comprehensive characterization of crude oils by thermogravimetry coupled to fast modulated gas chromatography-single photon ionization time-of-flight mass spectrometry; *Anal. Bioanal. Chem.* **2013**, *405*, 7107–7116.

[48] Wu, Q.; Hua, L.; Hou, K.; Cui, H.; Chen, P.; Wang, W.; Li, J.; Li, H. A combined single photon ionization and photoelectron ionization source for orthogonal acceleration time-of-flight mass spectrometer; *Int. J. Mass Spectrom.* **2010**, *295*, 60–64.

[49] Zhang, L.; Pan, Y.; Guo, H.; Zhang, T.; Sheng, L.; Qi, F.; Lo, P.-K.; Lau, K.-C. Conformation-specific pathways of β-alanine: A vacuum ultraviolet photoionization and theoretical study; *J. Phys. Chem. A* **2009**, *113*, 5838–5845.

[50] Stearns, J. A.; Mercier, S.; Seaiby, C.; Guidi, M.; Boyarkin, O. V.; Rizzo, T. R. Conformation-specific spectroscopy and photodissociation of cold, protonated tyrosine and phenylalanine; *J. Am. Chem. Soc.* **2007**, *129*, 11814–11820.

[51] Kuribayashi, S.; Yamakoshi, H.; Danno, M.; Sakai, S.; Tsuruga, S.; Futami, H.; Morii, S. VUV single-photon ionization ion trap time-of-flight mass spectrometer for on-line, real-time monitoring of chlorinated organic compounds in waste incineration flue gas; *Anal. Chem.* **2005**, *77*, 1007–1012.

[52] Shu, J.; Wilson, K. R.; Ahmed, M.; Leone, S. R. Coupling a versatile aerosol apparatus to a synchrotron: Vacuum ultraviolet light scattering, photoelectron imaging, and fragment free mass spectrometry; *Rev. Sci. Instrum.* **2006**, *77*, 043106.

[53] Hanna, S.; Campuzano-Jost, P.; Simpson, E.; Robb, D.; Burak, I.; Blades, M.; Hepburn, J.; Bertram, A. A new broadly tunable (7.4–10.2 eV) laser based VUV light source and its first application to aerosol mass spectrometry; *Int. J. Mass Spectrom.* **2009**, *279*, 134–146.

[54] Li, Y.; Qi, F. Recent applications of synchrotron VUV photoionization mass spectrometry: Insight into combustion chemistry; *Acc. Chem. Res.* **2009**, *43*, 68–78.

[55] Zhu, Z.; Wang, J.; Qiu, K.; Liu, C.; Qi, F.; Pan, Y. Note: a novel vacuum ultraviolet light source assembly with aluminum-coated electrodes for enhancing the ionization efficiency of photoionization mass spectrometry; *Rev. Sci. Instrum.* **2014**, *85*, 046110.

[56] Mühlberger, F.; Wieser, J.; Morozov, A.; Ulrich, A.; Zimmermann, R. Single-photon ionization quadrupole mass spectrometry with an electron beam pumped excimer light source; *Anal. Chem.* **2005**, *77*, 2218–2226.

[57] Chen, C.; Lin, Z.; Wang, Z. The development of new borate-based UV nonlinear optical crystals; *Applied Physics B* **2005**, *80*, 1–25.

[58] Guo, H.; Zhang, L.; Deng, L.; Jia, L.; Pan, Y.; Qi, F. Vacuum ultraviolet photofragmentation of sarcosine: photoionization mass spectrometric and theoretical insights; *J. Phys. Chem. A* **2010**, *114*, 3411–3417.

[59] Liu, G.; Wang, G.; Zhu, Y.; Zhang, H.; Zhang, G.; Wang, X.; Zhou, Y.; Zhang, W.; Liu, H.; Zhao, L. Development of a vacuum ultraviolet laser-based angle-resolved photoemission system with a superhigh energy resolution better than 1meV; *Rev. Sci. Instrum.* **2008**, *79*, 023105.

[60] Jin, S.; Fan, F.; Guo, M.; Zhang, Y.; Feng, Z.; Li, C. Note: deep ultraviolet Raman spectrograph with the laser excitation line down to 177.3 nm and its application; *Rev. Sci. Instrum.* **2014**, *85*, 046105.

[61] Gao, L.; Ren, W.; Xu, H.; Jin, L.; Wang, Z.; Ma, T.; Ma, L.-P.; Zhang, Z.; Fu, Q.; Peng, L.-M. Repeated growth and bubbling transfer of graphene with millimetre-size single-crystal grains using platinum; *Nat. commun.* **2012**, *3*, 699.

[62] Jin, S.; Guo, M.; Fan, F.; Yang, J.; Zhang, Y.; Huang, B.; Feng, Z.; Li, C. Deep UV resonance Raman spectroscopic study of C_nF_{2n+2} molecules: the excitation of C–C σ bond; *J. Raman Spectrosc.* **2013**, *44*, 266–269.

[63] Meng, J.; Liu, G.; Zhang, W.; Zhao, L.; Liu, H.; Jia, X.; Mu, D.; Liu, S.; Dong, X.; Zhang, J. Coexistence of Fermi arcs and Fermi pockets in a high-Tc copper oxide superconductor; *Nature* **2009**, *462*, 335–338.

[64] Fu, H.; Hu, Y.; Bernstein, E. IR+ vacuum ultraviolet (118 nm) nonresonant ionization spectroscopy of methanol monomers and clusters: neutral cluster distribution and size-specific detection of the OH stretch vibrations; *J. Chem. Phys.* **2006**, *124*, 024302.

[65] Hu, Y.; Guan, J.; Bernstein, E. R. Mass-selected IR-VUV (118 nm) spectroscopic studies of radicals, aliphatic molecules, and their clusters; *Mass Spectrom. Rev.* **2013**, *32*, 484–501.

[66] Putter, M.; von Helden, G.; Meijer, G. Mass selective infrared spectroscopy using a free electron laser; *Chem. Phys. Lett.* **1996**, *258*, 118–122.

[67] Finch, J. W.; Toerne, K. A.; Schram, K. H.; Denton, M. B. Evaluation of a hydrogen laser vacuum ultraviolet source for photoionization mass spectrometry of pharmaceuticals; *Rapid Commun. Mass Spectrom.* **2005**, *19*, 15–22.

[68] Hua, L.; Hou, K.; Chen, P.; Xie, Y.; Jiang, J.; Wang, Y.; Wang, W.; Li, H. Realization of in-source collision-induced dissociation in single-photon ionization time-of-flight mass spectrometry and its application for differentiation of isobaric compounds; *Anal. Chem.* **2015**, *87*, 2427–2433.

[69] Holzer, J.; Fischer, M.; Groger, T.; Streibel, T.; Saraji-Bozorgzad, M.; Wohlfahrt, S.; Matuschek, G.; Zimmermann, R. Hyphenation of thermogravimetry and soft single photon ionization-ion trap mass spectrometry (TG-SPI-ITMS) for evolved gas analysis; *J. Therm. Anal. Calorim.* **2014**, *116*, 1471–1479.

[70] Leplat, N.; Rossi, M. J. Effusive molecular beam-sampled Knudsen flow reactor coupled to vacuum ultraviolet single photon ionization mass spectrometry using an external free radical source; *Rev. Sci. Instrum.* **2013**, *84*, 114104.

[71] Xie, Y.; Chen, P.; Hua, L.; Hou, K.; Wang, Y.; Wang, H.; Li, H. Rapid identification and quantification of linear olefin isomers by online ozonolysis-single photon ionization time-of-flight mass spectrometry; *J. Am. Soc. Mass Spectrom.* **2016**, *27*, 144–152.

[72] Schramm, E.; Kuerten, A.; Hoelzer, J.; Mitschke, S.; Muehlberger, F.; Sklorz, M.; Wieser, J.; Ulrich, A.; Puetz, M.; Schulte-Ladbeck, R.; Schultze, R.; Curtius, J.; Borrmann, S.; Zimmermann, R. Trace detection of organic compounds in complex sample matrixes by single photon ionization ion trap mass spectrometry: real-time detection of security-relevant compounds and online analysis of the coffee-roasting process; *Anal. Chem.* **2009**, *81*, 4456–4467.

[73] Eschner, M. S.; Selmani, I.; Groeger, T. M.; Zimmermann, R. Online comprehensive two-dimensional characterization of puff-by-puff resolved cigarette smoke by hyphenation of fast gas chromatography to single-photon ionization time-of-flight mass spectrometry: quantification of hazardous volatile organic compounds; *Anal. Chem.* **2011**, *83*, 6619–6627.

[74] Wu, Q.; Fua, L.; Hou, K.; Cui, H.; Chen, W.; Chen, P.; Wang, W.; Li, J.; Li, H. Vacuum ultraviolet lamp based magnetic field enhanced photoelectron ionization and single photon ionization source for online time-of-flight mass spectrometry; *Anal. Chem.* **2011**, *83*, 8992–8998.

[75] Mullen, C.; Irwin, A.; Pond, B. V.; Huestis, D. L.; Coggiola, M. J.; Oser, H. Detection of explosives and explosives-related compounds by single photon laser ionization time-of-flight mass spectrometry; *Anal. Chem.* **2006**, *78*, 3807–3814.

[76] Yuan, C.; Liu, X.; Zeng, C.; Zhang, H.; Jia, M.; Wu, Y.; Luo, Z.; Fu, H.; Yao, J. All-solid-state deep ultraviolet laser for single-photon ionization mass spectrometry; *Rev. Sci. Instrum.* **2016**, *87*, 024102.

[77] Luo, Z.; Castleman, A. W., Jr.; Khanna, S. N. Reactivity of metal clusters; *Chem. Rev. (Washington, DC, U. S.)* **2016**, *116*, 14456–14492.

[78] Luo, Z.; Castleman, A. W., Jr. Special and general superatoms; *Acc. Chem. Res.* **2014**, *47*, 2931–2940.

Chapter 2

Interpretation of Mass Spectra

Teodor Octavian Nicolescu

Additional information is available at the end of the chapter

http://dx.doi.org/10.5772/intechopen.68595

Abstract

The chapter includes an introduction to the main ionisation techniques in mass spectrometry and the way the resulting fragments can be analysed. First, the fundamental notions of mass spectrometry are explained, so that the reader can easily cover this chapter (graphs, main pick, molecular ion, illogical pick, nitrogen rule, etc.). Isotopic percentage and nominal mass calculation are also explained along with fragmentation mechanism. A paragraph emphasises the ionisation energy issues, the basics of ionisation voltage, the developing potential and the energy balance. A frame time of the main theoretical milestones in both theory and experimental mass spectrometry is highlighted here. In the second part of the chapter, the molecular fragmentation for alkanes, iso-alkanes, cycloalkanes, halogen, alcohols, phenols, ethers, carbonyl compounds, carboxylic acids and functional derivatives, nitrogen compounds (amines, nitro compounds), sulphur compounds, heterocycles and biomolecules (amino acids, steroids, triglycerides) is explained. Fragmentation schemes are followed by the simplified spectra, which help the understanding of such complex phenomena. At the end of the chapter, acquisition of mass spectrum is discussed. The chapter presented here is an introduction to mass spectrometry, which, we think, helps the understanding of the mechanism of fragmentation corroborating spectral data and molecular structures.

Keywords: mass spectra, ionisation techniques, detectors, fragmentation, organic molecules

1. Introduction

Mass spectrometry is a destructive method used to measure molecular weight and provide data on molecular structure; it differs from the other methods in that the sample is ionised and not subject to electromagnetic radiation. Ionised compounds are excited, which induces fragmentation. Analysis of such fragments provides information on the structure of molecules. Each fragment is characterised by the mass-to-charge ratio, m/z, and devices are able to separate and detect such ions. Mass spectrometers consist of three distinct parts (**Figure 1**):

INTECH
open science | open minds

© 2017 The Author(s). Licensee InTech. This chapter is distributed under the terms of the Creative Commons Attribution License (http://creativecommons.org/licenses/by/3.0), which permits unrestricted use, distribution, and reproduction in any medium, provided the original work is properly cited. CC BY

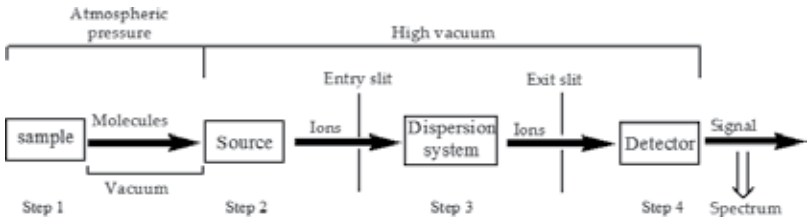

Figure 1. Schematics of a mass spectrometer [1].

- The source where ionisation of molecules and ion fragmentation occurs
- The dispersion system, the analyser, which ensures ion separation by mass/charge ratio
- The detector measuring the relative abundance of each ion

Traditionally limited to the study of classical small organic molecules ($M < 2000$), the scope of mass spectrometry has been recently also extended to the study of macromolecules ($M > 100{,}000$), polypeptides in particular.

The devices may be either used with a system for direct sample introduction (pure substances) or coupled with a chromatographic system. There are also devices (the MS-MS tandem) allowing for analysis of mixtures without prior chromatography. The first MS stage serves for selection of an ion, whereas the second analyses of ions result from fragmentation of the ion separated in the first stage [1, 2].

The first mass spectral measurements were undertaken by J.J. Thomson, in 1912, and, in 1918, F.L. Arnot and J.C. Milligan introduced the method of ionisation and pass through a magnetic sector. In 1946, W.E. Stephens assembled a time-of-flight (TOF) device, and, in 1953–1958, W. Paul used a quadrupole analyser. F.H. Field applied chemical ionisation in 1966, which was followed by the 'thermospray' method, introduced by the C.R. Blackley team in 1968. Coupling with gas chromatography was performed by C. Gohlke and F. McLafferty, the latter further introducing coupling with liquid chromatography in 1973. Since then, mass spectrometry techniques are continually improving (**Table 1**).

1.1. Ionisation methods

1.1.1. Electron impact (EI)

Electron impact ionisation occurs in a stainless steel chamber (**Figure 2**) at a pressure of less than 6×10^{-7} mmHg (i.e. vacuum conditions) achieved by means of a diffusion oil pump or a turbo-molecular pump. At 2000°C by thermoelectronic effect, electrons emitted by a rhenium filament are accelerated to the anode by a 5–100-V potential difference [1, 14].

To increase the electron-molecule impact probability, a magnetic field is applied, with the same direction as that of the electric field. The magnetic field induces a circular course to electrons,

The scientific term *spectrograph* starts being part of the scientific vocabulary (**1884**) [1, 3]

E. Goldstein studied 'canal rays' composed of positive ions. His work opened the gate to mass spectrometry (**1886**) [1, 3]

Wilhelm Wien showed that the mass-to-charge ratio of the positive ions (canal rays) has opposite polarity that of the electron (**1898**) [1, 3]

Francis William Aston and J. J. Thomson were the first to use mass spectrometry (**1897–1898**) [1, 3, 4]

F. W. Aston and A. J. Dempster introduced 'modern techniques' of mass spectrometry (**1918–1919**) [1, 3, 5, 6]

W. Kaufmann measured the relativistic mass increase of electrons using a mass spectrometer (**1901**) [1, 3]

J. J. Thomson separated the ^{20}Ne and the ^{22}Ne isotopes and assigned the m/z 11 signal to the doubly charged ^{22}Ne particle (**1913**) [1, 3, 4]

Construction of the first focusing mass spectrograph with a resolution of 130 (**1919**) [1, 3]

Nobel Prize in Chemistry (F. W. Aston)—mass spectrograph of isotopes for non-radioactive elements of the whole number rule (**1922**)

Double-focusing mass spectrograph developed by J. Mattauch and R. Herzog (**1934**)

A. J. Dempster—spark ionisation source (**1936**)

F. W. Aston—mass spectrograph with a resolution of 2000 (**1937**)

Westinghouse—new method for accurate gas analysis—a mass spectrometer (**1943**) [1]

W. Stephens introduces the time-of-flight (TOF) mass spectrometer (**1946**)

Nobel Prize in Physics for W. Paul—the quadrupole and quadrupole ion trap (**1953**)

The hydrogen transfer reaction or the 'McLafferty rearrangement'—A. J. C. Nicholson (**1954**)

Mass Spectrometric Analysis. Molecular Rearrangements by F. W. McLafferty (**1959**) [7]

Gas chromatograph coupled to a mass spectrometer the GS-MS technique introduced at Dow Chemical (**1959**)

World's first mass spectrometry society—British Mass Spectrometry Society (**1964**) [1, 3]

Chemical ionisation introduced by F. H. Field and M. S. B. Munson (**1966**) [8]

Electrospray ionisation (ESI)—M. Dole (**1968**)

Field desorption—H. D. Beckey (**1969**) [9]

Fourier transform ion cyclotron resonance mass spectrometry—M. B. Comisarow and A. Marshall (**1974**) [10]

Atmospheric pressure chemical ionisation (APCI) based on gas chromatography (GC)—Horning (**1974**) [11]

Plasma desorption mass spectrometry—R. MacFarlane (**1976**)

M. L. Vestal and C. R. Blakely's work with heating a liquid stream became known as thermospray. It became a harbinger of today's commercially applicable instruments (**1983**)

Electrospray ionisation, the technique for large molecules and liquid chromatography, coupled with mass spectrometry—J. B. Fenn Nobel Prize in Chemistry 2002 (**1984**) [12]

The term matrix-assisted laser desorption/ionisation (MALDI)—F. Hillenkamp and M. Karas (**1985**) [13]

The development of the ion trap technique—H. Dehmelt and W. Paul Nobel Prize in Physics (**1989**)

API III—the first commercial dedicated to LC-MS/MS for the pharmaceutical industry (**1989**)

The first low-cost high-performance MS/MS system—TurboIonSpray (**1997**)

Orbitrap mass spectrometer—A. Makarov (**1999**)

Development of electrospray ionisation (ESI) and soft laser desorption (SLD): mass spectrometric analyses of biological macromolecules (i.e. proteins)—J. B. Fenn and K. Tanaka Nobel Prize in Chemistry. Large-molecule laser desorption ionisation (**2002**)
SCIEX Corporation—Single platform: quantitative and qualitative capabilities associated with triple quadrupoles and, respectively, with high-resolution accurate-mass system MS experiments for a broad spectrum of applications (**2010**)
Waters Corporation—'quadrupole/time-of-flight' a hybrid mass spectrometer (**2016**)

Table 1. A timeline in spectrometric measurement.

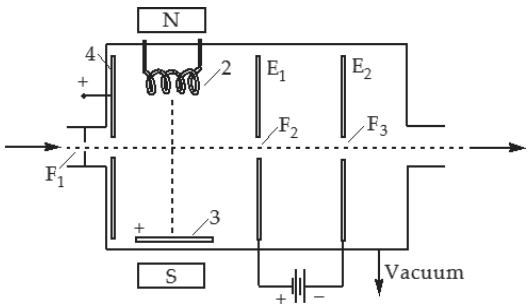

Figure 2. Schematics of an electron impact ionisation chamber (F1, entrance slit; F2, filament; F3, anode; F4,positive ion repeller; F2 and F3, slits; E1 and E2, electronic lenses) [1].

perpendicular to magnetic induction. The combination of the accelerated uniform rectilinear motion and the circular motion in the perpendicular plane lends electrons a helical movement of longer trajectory, thus increasing the likelihood of impact with the molecules. This results in ionisation with 0.01% yield, acceptable for an electron impact source [1, 15, 16].

The electron kinetic energy generates the pulling out of an electron, resulting in a positive molecular ion, also provided with a single electron:

$$M + e^- \rightarrow M^{+\bullet} + 2e^- \quad (1)$$

The molecular ion has the same empirical formula as the respective neutral molecule. The difference comes from one or several electrons. The molecular ion may be positive or negative.

The masses of these ions are equal with the sum of masses of abundant isotopes of the various atoms making up the molecule.

The symbol $M^{\bullet}$ *(or* $M^{+\bullet}$*) does not refer to an added electron but to a post-ionisation unpaired electron. Addition of an electron (electron capture) to the neutral molecule yields a negative radical ion* M^{-} [1, 17–19].

The ease of electron removal from the molecule depends on its nature, $n > \pi > \sigma$.

Molecule ionisation energy ranges from 8 to 12 eV; for electrons, the commonly used one is 70 eV, providing maximum ionisation efficiency.

In case of too much fragmentation, resulting in significant decrease of the M^+ molecular ion peak, electron energy may be reduced.

After crossing the source volume, electrons are trapped on a cathode (hatch), and impact-generated ions are expelled from the source by means of a plate (4) with a certain same-sign potential. Next, such electrons are accelerated at the source-analyser interface by a V_0 potential difference.

The positive plate (4) (**Figure 2**) is also meant to attract negative ions produced on sample projectile electron impact, such electrons being evacuated together with the other neutral particles after neutralisation of the negative electric charge [1, 20–22].

The excess energy is collected as internal energy by the molecular ion (from 12 to 70 eV). The molecular ion breaks into ion fragments, with sufficient internal energy to further break themselves, and the process continues.

A plasma ion is thereby obtained in the ionisation chamber, of which H^+ is the lightest and $M^{+\bullet}$ is the weightiest. All respective ions have a very short life span (milliseconds only), which requires their removal from the source as soon as possible, for analysis purposes.

Positive ions attracted to electrode E_1 enter through a slit in the area between E_1 and E_2, where an 8 kV accelerating magnetic field operates 1, 23].

- **Sample feed-in**

Solid, liquid or gaseous organic compounds can be analysed; however, inside the ionisation chamber, samples need to be in the gas phase.

The sample amount weighs microliters or micrograms and may be reduced to picograms when coupled with gas chromatography.

High-boiling solids and liquids are introduced into a quartz crucible (5 mm long/1 mm diameter) and transferred directly into the ionisation chamber, where they sublimate slowly depending on temperature.

Very volatile liquids are first vaporised and then introduced into the ionisation chamber. Gases are introduced with an accuracy valve [24–28].

1.1.2. Chemical ionisation (CI)

A reactant gas is introduced into the ionisation chamber, whose molecules become ionised on collision with a beam of electrons accelerated by a 400-V potential difference. Plasma formed is driven to the centre of the source by electrostatic lenses.

Positive chemical ionisation occurs when methane (or isobutane as a reactant gas) is used. For instance, ionised species may be generated where methane is used, such as

$$CH_4 + e^- \longrightarrow CH_4^{+\bullet},\ CH_3^+,\ CH_2^{+\bullet},\ CH^+,\ C^{+\bullet},\ H^+ \qquad (2)$$

which may react with neutral methane molecules, e.g.

$$\begin{aligned} CH_3^+ + CH_4 &\longrightarrow C_2H_5^+ + H_2 \\ CH_4^+ + CH_4 &\longrightarrow CH_5^+ + CH_3^\cdot \end{aligned} \quad (3)$$

The CH_5^+ ion, the plasma majority, is an acid (i.e. an electrophile) able to protonate most organic molecules by an exothermic reaction:

$$CH_5^+ + M \longrightarrow MH^+ + CH_4 \quad (4)$$

The MH^+ ion is a pseudo-molecular ion (peak at M+1), with weak internal energy and little potential for fragmentation. Therefore, molecular weight is easily determined, and its fragments provide information on the molecular structure. Isobutane is a 'milder' ionising agent than methane. The reactive entity is the emergent *tert*-butyl ion, $C_4H_9^+$:

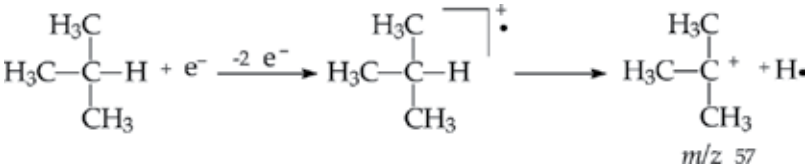

(5)

In chemical ionisations with isobutene, a molecule M yields the pseudo-molecular ion MH^+ (peak at M+1) and isobutene:

$$C_4H_9^+ + M \longrightarrow MH^+ + C_4H_8 \quad (6)$$

However, the M+57 ion also frequently emerges:

$$C_4H_9^+ + M \longrightarrow M - C_4H_9^+ \quad (7)$$

The reaction of the $C_4H_9^+$-M molecular ion (peak at M+57) is less exothermic than for methane, resulting in almost no MH^+ ions.

Positive ionisation also occurs in the case of ammonia which at 20 Pa yields plasma mostly consisting of NH_4^+ ammonium ions of average acidity. Depending on the M basic (nucleophilic) nature, the result is either MH^+ ions (peak at M+1) or one MNH_4^+ ion (peak at M+18) [1, 29]:

$$\begin{aligned} NH_4^+ + M &\longrightarrow MH^+ + NH_3 \\ NH_4^+ + M &\longrightarrow M\text{-}NH_4^+ \end{aligned} \quad (8)$$

Less nucleophilic compounds such as hydrocarbons do not undergo ionisation.

Negative chemical ionisation occurs by bombarding the reaction gas, nitrogen, butane, or isobutene, with high-energy (240 eV) primary electrons, resulting in low-energy electrons, easy to capture by sample molecules. Capture may be non-dissociative or dissociative:

$$\begin{aligned} MX + e^- &\longrightarrow MX^- \\ MX + e^- &\longrightarrow M + X^- \end{aligned} \quad (9)$$

For compounds with an affinity for electrons, negative chemical ionisation is about three orders of magnitude more sensitive than positive chemical ionisation [30–32].

As highly dependent on experimental conditions (source temperature, pressure in the ionisation chamber, reactant gas purity), mass spectra resulting from chemical ionisation are less reproducible than those obtained by electron impact [1, 24].

1.1.3. 'Mild' electrospray ionisation (ESI)

The solution of macromolecular compounds such as polypeptides is introduced under pressure of a gas, N_2, into a capillary tube (50 μm, diameter), exiting in mist form (spray), further subjected to action of a powerful (4 kV) electric field (**Figure 3**).

Contrary to the other methods, ionisation occurs at atmospheric pressure and room temperature, the 'mildest' conditions possible. Methanol and water solutions (50%:50%) are used, as well as acetonitrile and water, in the same proportions [33–35].

The resulted mist is subjected to the electric field, and, after solvent removal in a nitrogen stream, ions with multiple charges remain, to be analysed next in a dispersive system of the spectrometer (**Figure 3**) [36–39].

1.1.4. Fast atom bombardment ionisation

Fast atom/ion bombardment (FAB) requires dissolution of the sample in a liquid, low-vapour-pressure matrix, able to yield protons, such as glycerol, thioglycerol and *m*-nitrobenzyl alcohol. Atoms accelerated to 10 keV (Xe, Ar, Kr) bombard the sample solution, and ionisation occurs at room temperature, producing an abundance of positive $(M+H)^+$ and negative $(M+H)^-$ pseudo-molecular ions [1].

1.1.5. Field desorption ionisation

The sample solution is deposited on a rhenium/tungsten filament covered with carbon needles, in a very high electric field of up to 10^8 volts/cm. The filament is heated to the sample melting point, and the ions migrate, accumulating at the end of the needles, finally desorbing and thus engaging sample molecules with molecular $M^{+\bullet}$ ions.

Field desorption ionisation is used for high molecular mass compounds and unstable or little volatile polar compounds such as carboxylic acids and sugars [1].

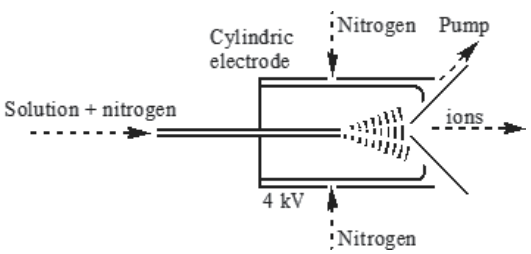

Figure 3. Schematics of an electrospray source where ions separate by the *m*/*z* ratio (z ≥ 1). Ions detected are of the MH_n^{n+} type, where n ≥ 1 [1].

1.1.6. MALDI 'mild' ionisation

MALDI is the abbreviation of matrix-assisted laser desorption/ionisation. The method uses a solid aromatic matrix, e.g. acids such as α-cyanocinnamic acid, sinapinic acid (3,5-dimethoxy-4-hydroxycinnamic acid), picolinic acid, 3-aminopicolinic acid, etc., where the sample is dispersed in a definite proportion: one sample molecule per 10^4 matrix molecules, both in crystalline state and at room temperature and atmospheric pressure, in dry nitrogen atmosphere. By means of a microscope, a 3–10-ns-pulse UV laser irradiation is focused on a small matrix spot, 0.05–0.2 mm in diameter (**Figure 4**). An electronic and thermal excitation of molecules in the sample matrix occurs, able to yield protons causing ionisation. The matrix serves as an energy vector between the laser beam and the molecules of the analysed compound. Ionisation of organic molecules is 'mild', resulting in pseudo-molecular ions [40].

Ion and neutral molecule desorption occurs after laser irradiation, as a supersonic expansion jet. Desorbed ions are transferred to the analyser under vacuum by means of an interface. MALDI is the most used analytical method in modern biochemistry and polymer science [1, 41–43].

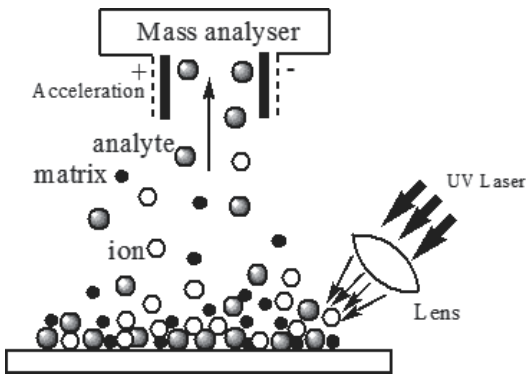

Figure 4. Schematics of the MALDI process [1].

2. Mass spectra

2.1. Mass spectral description: rules

Mass spectrum is the two-dimensional representation of signal intensity (peak) on the vertical axis versus the *m*/*z* ratio on the horizontal axis. Peak intensity directly reflects ionic species abundance with the respective *m*/*z* ratio [1].

The *m*/*z* ratio is dimension-free because it derives from the ion *m* mass number and the *z* number of elementary charges, which is equal to 1. Therefore, values on the horizontal axis are a direct reflection of *m* [1].

Data acquisition and processing are performed by a computer, in line with the diagram below:

http://dx.doi.org/10.5772/intechopen.68595

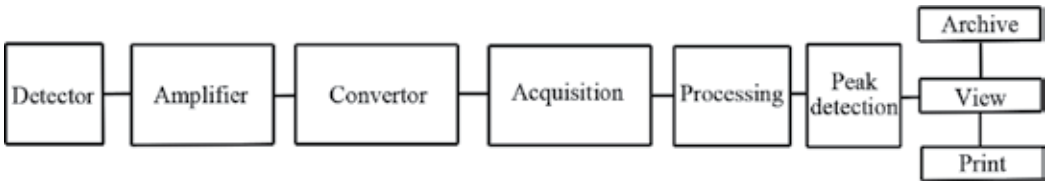

Figure 5 shows the spectrum of 2-methylimidazole. We may notice that the peak corresponds to the molecular ion (*m*/*z* 81.48), i.e. the *base peak* represents the greatest relative abundance (100%). Other peaks correspond to ion fragments.

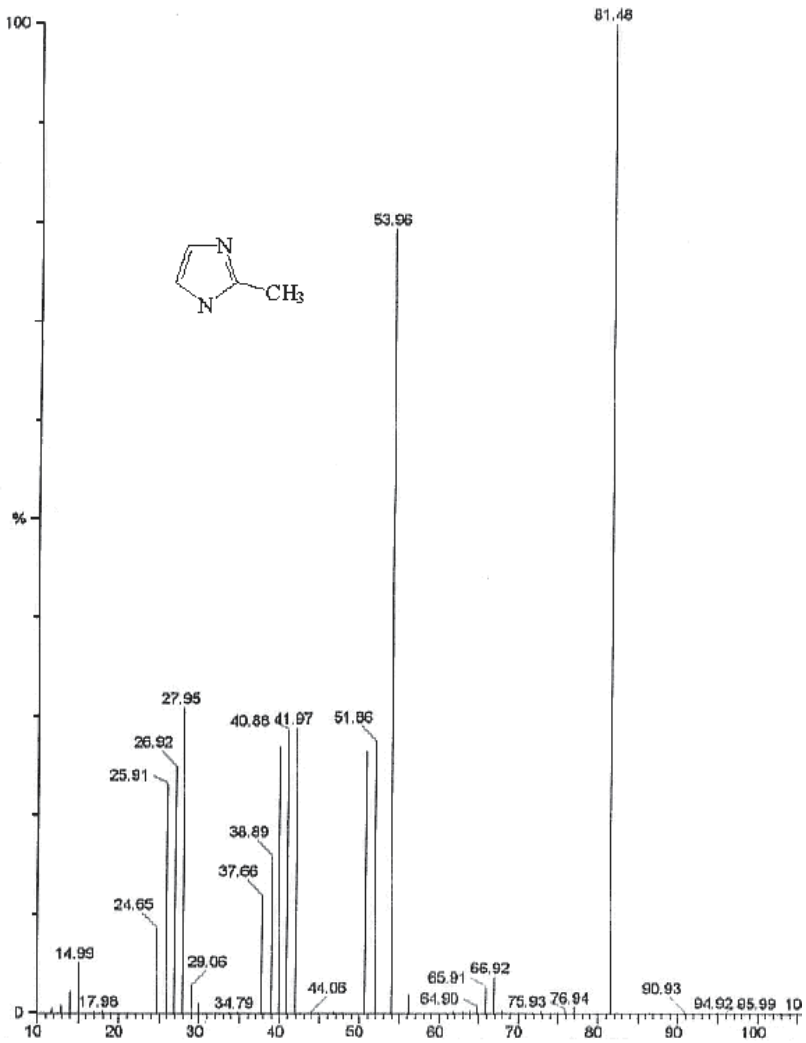

Figure 5. Mass spectrum for 2-methylimidazole [1].

The base peak results from spectrum *normalisation* consisting in selection of the most intense signal, which is assigned the 100% value. In relation to it, percent intensity is assigned to each signal, which represents the relative percent abundance of each ion fragment [1, 44, 45].

The molecular peak, the parent peak, corresponds to the $M^{+\bullet}$ molecular ion in pure compounds. This is the one that has the largest, easily identifiable *m*/*z* ratio. The existence of the molecular ion in the spectrum allows accurate determination of molecular mass. In certain compounds, the molecular ion is not present because it is very unstable and molecular mass cannot be determined [1, 44, 45].

Electron pair cations, resulting from fragmentation of the molecular ion, are usually more stable than the molecular ion and have hence greater abundance.

The nitrogen rule. *Molecular mass of organic compounds are even, except for those containing an odd number of nitrogen atoms.* When a compound is nitrogen-free, but an odd mass corresponds to the last peak, this is definitely not the molecular peak. The rule may be extended to fragmentation ions as well.

The nitrogen rule may be explained by the fact that elements contained in organic compounds have either even valence and atomic mass (O, C, S) or odd valence and atomic mass (H (halogen)) and by the fact that make the compounds containing only C, H, O, S and halogen show an even molecular mass only.

Illogical peaks. The difference between the predicted molecular mass and the immediately following fragment mass must correspond to the elimination of a hydrogen atom (mass 1) or one CH_3 group (mass 15). There are no fragments of masses between 3–14 and 21–25 mass units (*mu*). A smaller difference between those limits indicates that either the sample is impure or that greater mass peak is not the molecular peak [1, 44, 45].

2.1.1. Isotopes

An isotope is an element that has the same number of electrons in the electronic layer but a different number of neutrons in the nucleus. Therefore, isotopes have the same chemical properties and only differ in their mass. All elements have several natural-state isotopes [46–49].

Table 2 presents natural isotopes of the most common elements encountered in organic chemistry. One may note that the lightest isotope also has the greatest abundance [1, 50–52].

2.1.2. Molecular peaks of bromide compounds

When the molecule displays several isotopes such as those of bromine, of relatively close abundance, the dibromo-molecular ion, Br_2, has three peaks (**Figure 6**):

- One ^{79}Br–^{79}Br species of mass M = 158
- One ^{79}Br–^{81}Br species of mass M = 160
- One ^{81}Br–^{81}Br species of mass M = 162

Assuming for simplicity reasons that mass 79 and 81 isotopes have the same relative abundance, the likelihood of a mixed dibromo-^{79}Br–^{81}Br is two times higher than that of homogeneous

Element	Isotopes/relative abundance					
Hydrogen	^{1}H	100	^{2}H	0.0151		
Carbon	^{12}C	100	^{13}C	1.112		
Nitrogen	^{14}N	100	^{15}N	0.37		
Fluorine	^{19}F	100				
Silica	^{28}Si	100	^{29}Si	5.10	^{30}Si	3.35
Phosphorus	^{31}P	100				
Chlorine	^{35}Cl	100	^{37}Cl	31.98		
Bromine	^{79}Br	100	^{81}Br	97.28		
Iodine	^{127}I	100				
Oxygen	^{16}O	100	^{17}O	0.04	^{18}O	0.20

Abundances are calculated by assigning the 100 values to the prominent isotope [1, 3].

Table 2. Natural isotope abundance of common elements.

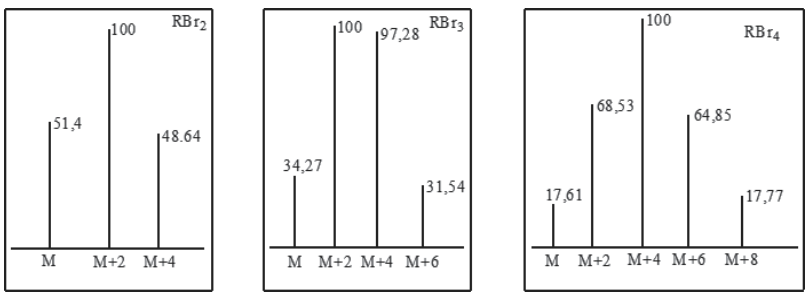

Figure 6. Molecular peaks of bromide compounds [1].

dibromo-^{79}Br–^{79}Br or ^{81}Br–^{81}Br. The molecular peak of the bromine molecule (Br_2) occurs in the form of a triplet of 1:2:1 intensities (**Figure 7**).

The abundance of these species corresponds to the binomial $(a+b)^n$ coefficient, where a is the relative abundance of the first isotope, b that of the second isotope and n the number of elements [3].

The exact calculation of peaks for brominated compounds is given in **Figure 6**. A similar calculation is possible for chlorinated compounds as well. Fluorine and iodine are isotopically pure. In halogenated compounds, carbon, hydrogen and oxygen isotopes are a minority. The ^{13}C isotopic contribution is 68 times higher than that of ^{2}H deuterium and 27 times higher than that of ^{17}O [1, 3].

Figure 8 represents the spectrum of bromo-chloromethane, with three prominent peaks for molecular ions. One may note that, the same as in all compounds with two bromine atoms, two chlorine atoms or one chlorine atom and one bromine atom in the molecule, the M+4 peak also appears in the spectrum.

High-resolution mass spectrometry is widely used to determine molecular formulas of certain unknown compounds. Spectrometers have a software that compares exact masses with those of various possible formulas [1, 3].

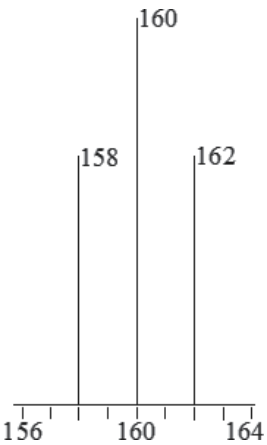

Figure 7. Simplified dibromo mass spectrum. [1].

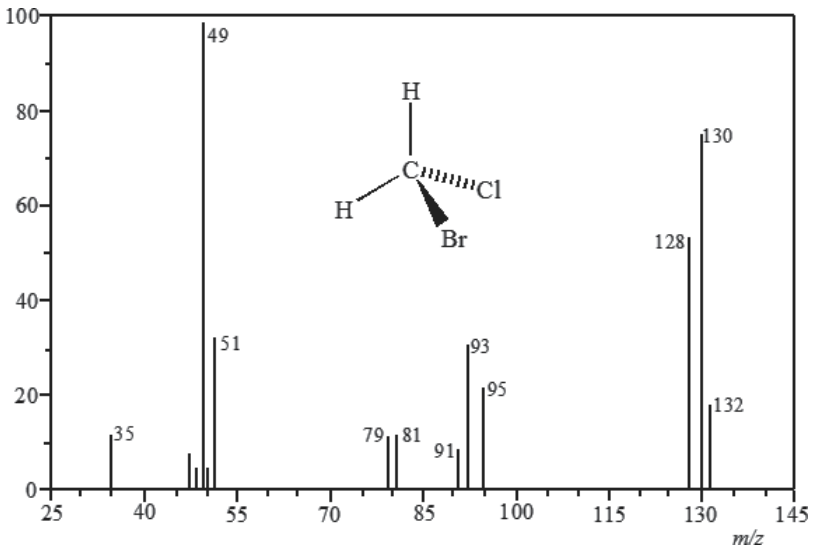

Figure 8. Simplified bromo-chloromethane mass spectrum [1].

2.1.3. Molecular formula

The molecular formula may often be obtained by high-resolution spectrometer measurements, because atomic weights are not integers. For example, a distinction among CO, N_2, CH_2N and C_2H_4 is possible for nominal weight[1] 28:

[1]*Nominal mass* corresponds to an integer which is the sum of the number of protons and neutrons contained in the atom. For example, ^{12}C contains six protons and six neutrons, and therefore its nominal weight is 12. The nominal molecular weight of ethene, CH_2=CH_2, is 28 Da (dalton). This mass is rendered by low-resolution spectrometers.

^{12}C 12.0000	$^{14}N_2$ 28.0062	^{12}C 12.0000	$^{12}C_2$ 24.0000
^{16}O 15.9949		$^{1}H_2$ 2.0116	$^{1}H_4$ 4.0312
27.9949		^{14}N 14.0031	28.0312
		28.0187	

Molecular mass observed for the CO molecular ion is the sum of exact masses of the most abundant carbon and oxygen isotope, which sum differs from the CO molecular mass based on atomic masses averaging the masses of all natural isotopes of an element (e.g. C = 12.01; O = 15.999).

Table 3 includes exact masses of isotopes of ordinary elements in organic compounds.

There are tables including formulas corresponding to molecules or fragments with their exact masses, obtained by addition of exact masses of the most abundant isotopes of each element.

Element	Atomic mass	Nucleus	Exact mass
Hydrogen	1.00794	^{1}H	1.00783
		^{2}H	2.01410
Carbon	12.01115	^{12}C	12.00000
		^{13}C	13.00336
Nitrogen	14.0067	^{14}N	14.0031
		^{15}N	15.0001
Oxygen	15.9994	^{16}O	15.9949
		^{17}O	16.9991
		^{18}O	17.9992
Fluorine	18.9984	^{19}F	18.9984
Silica	28.0855	^{28}Si	27.9769
		^{29}Si	28.9765
		^{30}Si	29.9738
Phosphorus	30.9738	^{31}P	30.9738
Sulphur	32.066	^{32}S	31.9721
		^{33}S	32.9715
		^{34}S	33.9679
Chlorine	35.4527	^{35}Cl	34.9689
		^{37}Cl	36.9659
Bromine	79.9094	^{79}Br	78.9183
		^{81}Br	80.9163
Iodine	126.9045	^{127}I	126.9045

Table 3. Exact masses of certain isotopes [1, 3].

The mass of the molecular ion is the sum of the most abundant isotope (^{12}C, ^{1}H, ^{16}O, etc.) in the molecule [1, 3].

In the case of methane, the molecular ion occurs by *m/z* 16 corresponding to the formula $^{12}C^{1}H_4$. However, there are also molecular species containing less abundant isotopes: $^{13}C^{1}H_4$ (*m/z* 17, peak M+1), $^{12}C^{2}H^{1}H_3$ (*m/z* 17, peak M+1), $^{13}C^{2}H^{1}H_3$ (*m/z* 18, peak M+2) and so on [1, 3].

In the spectrum of methane presented below in tabular form, the M+1 peak represents 1.14% of the M (basic) peak, and the M+2 peak is negligible:

m/z	1	2	12	13	14	15	16	17
Relative abundance	3.4	0.2	2.8	8.0	16.0	86.0	100	1.14

Intensity of isotope peaks is lower than the molecular M peak, except for cases when chlorine or bromine is present (**Figure 8**).

2.2. Fragmentation: mechanism

The impact of a very energetic electron with a molecule turns the latter into a cation radical, with loss of an electron. A range of rearrangements or fragmentations follow, which depend on the molecule nature and structure [1, 3]:

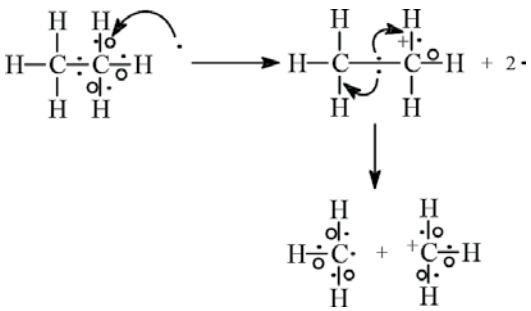

(10)

Straight-chain or branched hydrocarbon fragmentation occurs, resulting in formation of more stable carbocations; their stability increases in the order:

$$^{+}CH_3 < RCH_2^{+} < R_2CH^{+} < R_3C^{+} < CH_2{=}CH{-}CH_2^{+} < C_6H_5{-}CH_2^{+}$$

2.3. Energy aspects

In ionisation chambers, about one molecule in 10,000 is ionised. This requires 8–12 eV, i.e. 800–1200 KJ mol^{-1}. This energy is known as *ionisation potential (IP) (M).*

http://dx.doi.org/10.5772/intechopen.68595

Depending on electron impact conditions, molecular ions have internal energy, E_{int}, ranging from 0 to 10 eV. In the case of too weak internal energy, the $M^{+\bullet}$ molecular ion does not undergo breakdown, generating the molecular peak; for energies over 1 eV, the $M^{+\bullet}$ ion undergoes breakdown, resulting in formation of primary ion fragments [53]:

$$M^{+\bullet} \rightarrow A^{+} + B^{\bullet} \tag{11}$$

The difference in enthalpy required to produce the A^+ ion is known as the A^+ *potential occurrence*, i.e. *PO* (A^+).

In cases of high internal energy, $M^{+\bullet}$ decomposes, in formation of both primary and secondary fragments;

$$M^{+\bullet} \longrightarrow A^{+} + B^{\bullet}, \quad A^{+} \longrightarrow C^{+} + D^{\bullet} \text{ ..... etc.} \tag{12}$$

At one point, *the balance of all fragments from ions of different internal energies is the mass spectrum* achieved by electron impact at 70 eV.

In line with the diagram in **Figure 9**,

$$IP(M) = \Delta fH^{0}(M^{+}) - \Delta fH^{0}(M) \tag{13}$$

Considering that the energy of the reverse reaction is close to 0, the (E_a) activation energy is

$$E_a = \Delta fH^{0}(A^{+}) + \Delta fH^{0}(B\cdot) - \Delta fH^{0}(M^{+}) \tag{14}$$

Therefore, the potential of A^+ is equal to

$$PO(A^{+}) = IP(M) + E_a \tag{15}$$

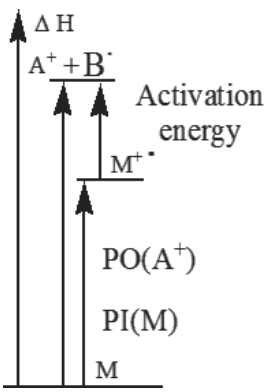

Figure 9. Energy diagram of a fragmentation [1].

$$PO(A^+) = \Delta fH^0(A^+) + \Delta fH^0(B\cdot) - \Delta fH^0(M) \tag{16}$$

ΔfH^0 is the standard enthalpy for formation in the gas phase.

Mass spectrum is the balance of a series of competing and consecutive reactions [54–56].

2.4. Processes under electronic ionisation conditions

The following types of ions are produced during electronic ionisation: molecular ions, fragmentation ions, multiple charge ions, metastable ions, rearrangement ions and pair ions [1, 3, 57, 58]:

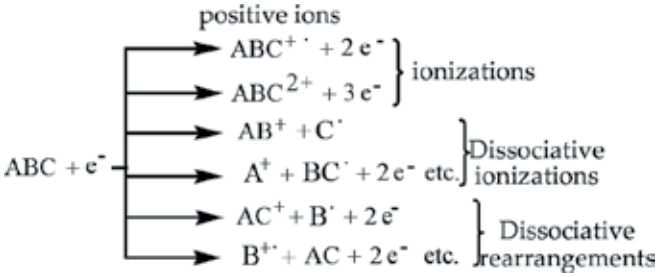

(17)

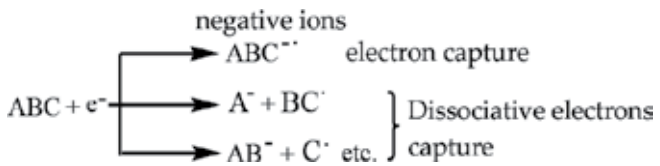

(18)

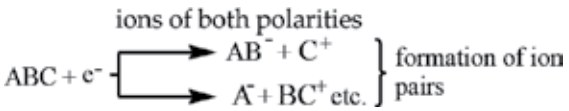

(19)

Most processes are very rapid, occurring within a few nano- or microseconds. Fragmentation of a molecular ion $M^{+\bullet}$ may be performed by homo- or heterolytic cleavage of a single bond. In homolytic cleavage, each electron moves independently. One fragment is an even-electron cation and another free radical with an unpaired electron [1, 3, 54]:

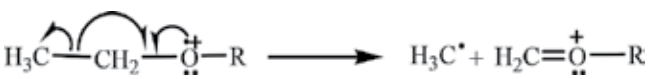

(20)

In heterolytic cleavage, an electron pair moves together to the charged atom. Once again, fragments are an even-electron cation and a radical. The charge is placed on the alkyl group:

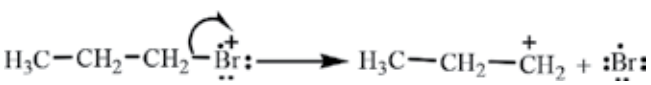

(21)

Further fragmentation of such a cation generally results in another even-electron cation and a fragment or even-electron molecule:

http://dx.doi.org/10.5772/intechopen.68595

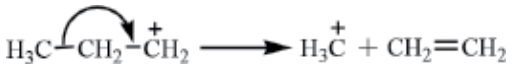

(22)

Multiple bond consecutive or simultaneous fragmentations may occur when an energy advantage exists, deriving from formation of a very stable cation and/or a stable radical or a neutral molecule.

Fragmentation of a certain bond is related to bond strength, to the possibility of low-energy transition and to the stability of arising fragments.

Given the greatly reduced pressure of a spectrometer, the likelihood of collisions is low, and therefore unimolecular breakdowns occur [57–59].

The following general rules have been established to predict prominent peaks in electronic impact mass spectra:

- The relative height of molecular ion peaks is greater for straight-chain ions and smaller than that of branched-chain ones.
- Generally, the relative height of the molecular ion peak decreases with increase of the molecular mass in a homologous series. Fatty ethers may be an exception.
- Due to an increased stability of tertiary carbocations as compared to secondary and primary ones, likelihood of cleavage increases as the carbon atom is more substituted.

$$^{+}CH_3 < RCH_2^{+} < R_2CH^{+} < R_3C^{+}$$

The longest chain may be eliminated as a radical, because such a radical may be stabilised by stabilisation of the lone pair ion:

- Double bonds and cyclic structures, particularly aromatic ones, stabilise the molecular ion and increase its likelihood.
- Double bonds favour allylic cleavage, resulting in formation of resonance-stabilised allylic cations:

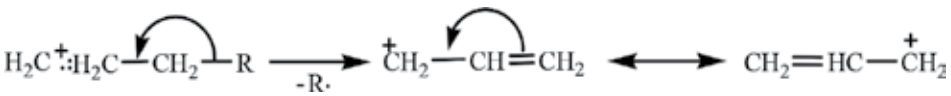

(23)

- Cyclic alkanes with side chains cleave at α, and the positive charge tends to remain on the cyclic fragment:

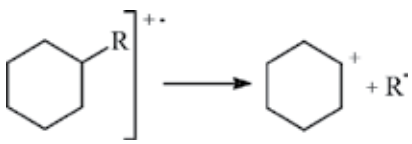

(24)

Unsaturated rings may undergo a retro-Diels-Alder reaction:

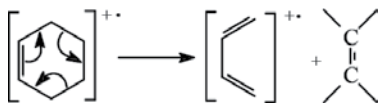

(25)

- Alkyl arenes cleave at the β to the aromatic ring and give rise to a resonance-stabilised benzyl ion or a tropylium ion.
- Heteroatom-containing compounds cleave at the C–C bond next to the heteroatom, passing the charge over to the heteroatom-containing fragment:

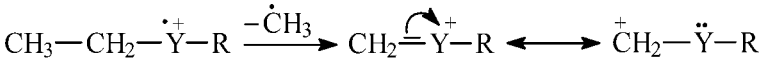

(Y = O, NH, S) (26)

- Cleavage often associates with the elimination of small, neutral, stable molecules such as CO, H_2O, NH_3, H_2S, HCN, olefines, mercaptans, ketone or alcohols [60–62].

2.5. Derivatisation

In the case of difficult-to-volatilise compounds or compounds whose molecular peak cannot be determined, a derivative which can be prepared that is more volatile, has a predictable cleavage pattern, a simplified fragmentation pattern and a better stability of the molecular ion. A low-volatility polar group of compounds such as carbohydrates, dicarboxylic acids and peptides become volatile and able to render characteristic peaks by acylation of the –OH or $–NH_2$ groups or methylation of the –COOH groups.

Trimethylsilylating of the same groups allows passage of corresponding compounds through the chromatographic column (GC).

Reducing ketones to hydrocarbons allows elucidation of their carbonate skeletons. Reducing polypeptides to more volatile poly-amino alcohols also allows prediction of the fragmentation pattern [1, 28].

2.6. Qualitative and quantitative analysis

Mass spectrometry is particularly important to organic chemistry because it allows acquisition of information about the composition and particularly about the structure of molecular compounds. Mass spectra provide data for structural assessments, fragmentation being performed by semi-empirical rules serving to the study of unknown compounds.

The identified molecular ion must correspond to spectrum ions produced by loss of fragments.

High intensity of the molecular ion indicates stable molecular structure.

A multiplet in the molecular ion area indicates the presence of a specific isotopic structure heteroatom, such as silica, sulphur, chlorine and bromine.

Proportionality of the intensity of the signal with the analyte amount allows the use of mass spectrometry in quantitative assays. For this purpose internal standard methods are used. As standard a compound similar to the analyte is employed provided that the ionisation produces easily to monitor ions different from those of the analyte. As analyte similar chemical compound,

http://dx.doi.org/10.5772/intechopen.68595

such as a deuterated isotope or analogue whose ionisation produces easily to monitor ions, different from those of the analyte can be employed [1, 3, 63].

2.7. Mass spectra of the main classes of organic compounds

2.7.1. Alkanes

Hydrocarbon mass spectra are easy to interpret because hydrocarbons have C–C and H–H bonds only. Taking into account molecule dissociation enthalpies, one finds that C–C bonds are the easiest to break:

Bond	C–C	C–H	C=C
Δ in kJ	340	420	660

In straight-chain alkanes, fragmentation occurs through loss of a methyl, leading to fragments of *m*/*z* = molecular mass 15. For instance,

$$\underset{m/z\ 58}{CH_3\text{-}CH_2\text{-}CH_2\text{-}CH_3}\Big]^{+\cdot} \longrightarrow \underset{m/z\ 43}{CH_3\text{-}CH_2\text{-}CH_3}^{+} + \underset{m\ 15}{CH_3}^{\cdot} \tag{27}$$

In general, fragments correspond to *m*/*z* 29, 43, 57, 71, 85, 99, etc., i.e. to molecular mass −15 and −14 × n or C_nH_{2n+1} ions separated by 14 mass units. Ethene neutral molecules may also form:

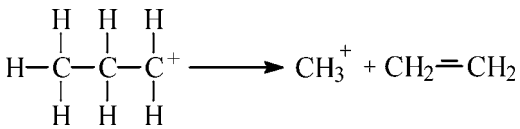

$$\longrightarrow CH_3^{+} + CH_2{=}CH_2 \tag{28}$$

Ions 43 and 57 are among the most stable of the spectrum (with the highest peaks), consistent with their standard formation enthalpy. Unlike higher mass ions, they do not undergo secondary fragmentation [3]:

R^+ ion	CH_3^+	$CH_3–CH_2^+$	$CH_3–CH_2–CH_2^+$	$C_3H_7–CH_2^+$
m/*z*	15	29	43	57
ΔfH^0 in kJ/mol	1086	915	873	911

Compounds with more than eight carbon atoms show similar spectra (**Figure 10**). Their identification depends on the molecular ion peak.

Branched alkane spectra are largely similar to those of straight-chain alkanes, but fragment abundance does not decrease evenly. Fragmentation preferentially occurs at branching points [64].

For example, in the case of 4-methylheptane, the same fragment with *m*/*z* 71 as in the case of *n*-octane is produced, but the relative abundance of that resulting from the fragmentation of 4-methylheptane is higher. So you can distinguish the *n*-alkanes from branched alkanes [1, 3].

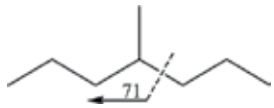

Cyclohexane undergoes complex fragmentation requiring much energy on cycle break. The mass spectrum (**Figure 11**) shows a more intense molecular ion than those of acyclic compounds,

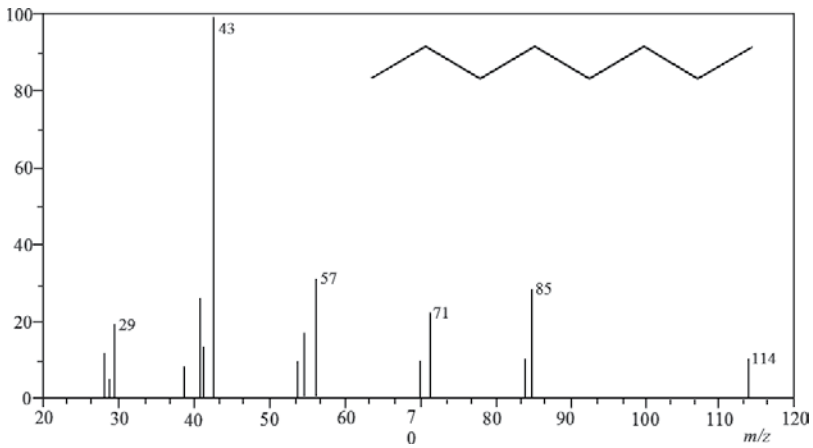

Figure 10. *n*-Octane-simplified mass spectrum [1].

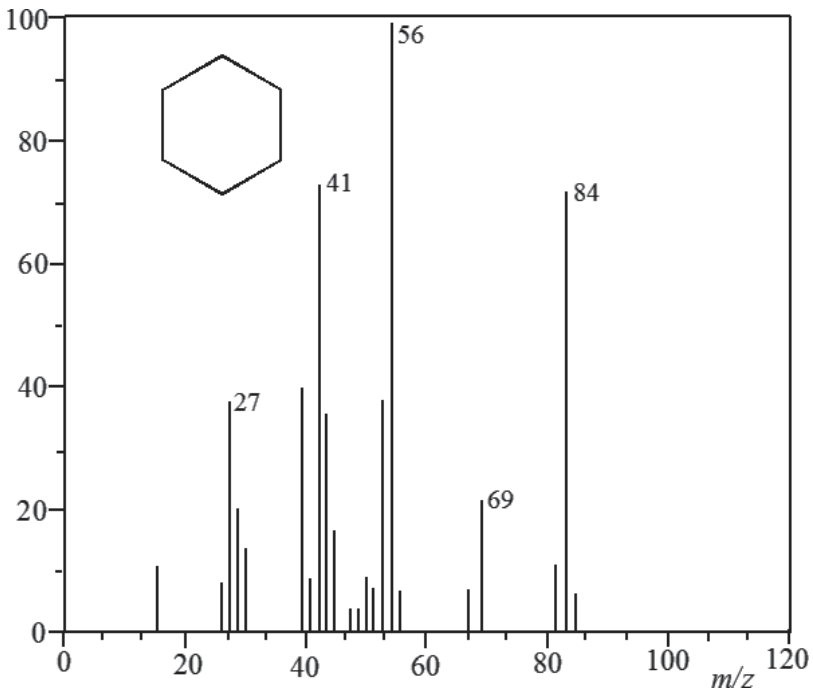

Figure 11. Cyclohexane mass spectrum [1].

http://dx.doi.org/10.5772/intechopen.68595

because fragmentation involves a break of two C–C bonds. The base peak is at *m/z* 56, following ethene elimination [54]:

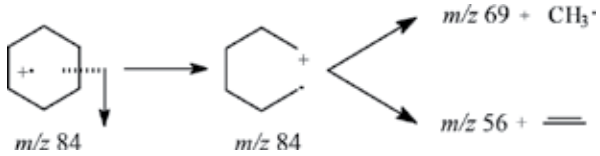

(29)

2.7.2. Alkenes

By ionisation and fragmentation, alkenes produce a fragment *m/z* 41, corresponding to the allyl carbocation:

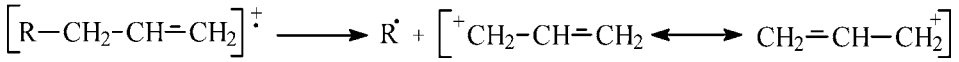

(30)

The molecular ion peak is visible in alkenes. It is difficult to locate the double bond in acyclic alkenes since it easily migrates from one fragment to the other. Location of the double bond in cyclic alkenes results from the tendency to allylic cleavage without double-bond migration. Limonene shows a unique, retro-Diels-Alder cleavage pattern:

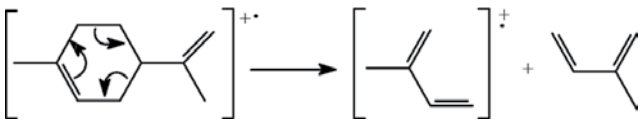

(31)

Similar to saturated hydrocarbons, acyclic alkenes are characterised by a number of peaks separated by 14 unit intervals. Among them, C_nH_{2n-1} and C_nH_{2n} peaks are more intense than C_nH_{2n+1} peaks [1, 3, 54].

2.7.3. Arenes

These compounds render easy-to-interpret spectra. The molecular peak is intense because the aromatic ring is very stable (**Figure 12**). Accurate measures can be performed for peaks M+1 and M+2.

Although reduced, molecular ion fragmentation can produce characteristic ions: *m/z* 77 $(M-H)^+$, *m/z* 51 ($C_4H_3^+$), *m/z* 91–26 (HC≡CH) and *m/z* 39 ($C_3H_3^+$) aromatic ions. The alkyl radical substituted benzene undergoes cleavage at β to the aromatic ring, the so-called benzyl fragmentation, leading to formation of peak *m/z* 91, C_6H_5–CH_2^+, often the base peak. Toluene also converts to the *m/z* 91 ion, known as the *tropylium ion*, isolated at low temperatures where its NMR spectrum was recorded [1, 3]:

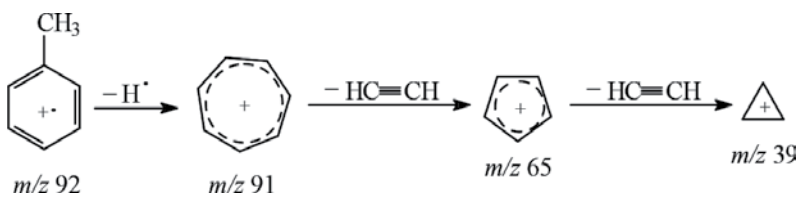

(32)

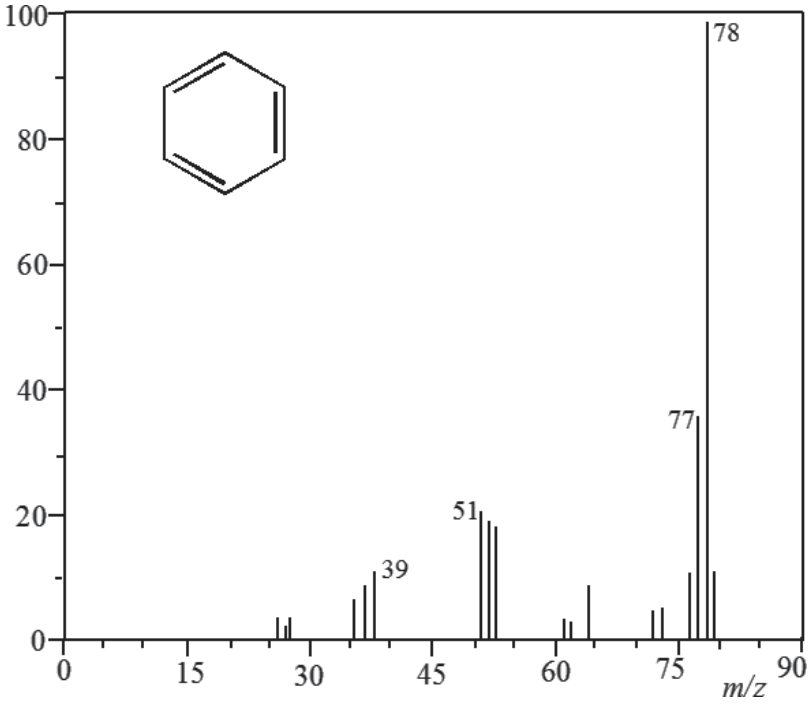

Figure 12. Benzene-simplified mass spectrum [1].

In xylenes, a methyl group is lost to reach the very stable tropylium ion:

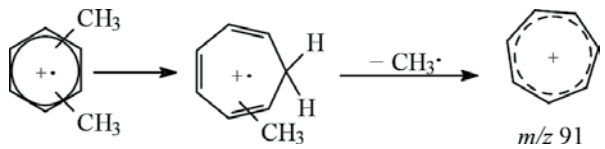

(33)

By elimination of an acetylene molecule, the tropylium ion converts to *m/z* 65, which in turn loses an acetylene molecule, converting to the 'aromatic ion' *m/z* 39 [54].

2.7.4. Halogenated compounds

Bromine and chlorine compounds are mainly distinguishable by appearance of molecular peak of their natural isotopes. Based on dissociation energies of their molecule bonds, fragmentation patterns of molecular ions can be predicted:

Bond	C–C	C–H	C–F	C–Cl	C–Br	C–I
ΔH_0 in kJ/mol	340	420	456	334	268	230

Characteristic fragmentation of brominated and iodised compounds consists of cleavage of the C–Br and C–I bonds at low dissociation energy. Two patterns of fragmentation are then possible:

http://dx.doi.org/10.5772/intechopen.68595

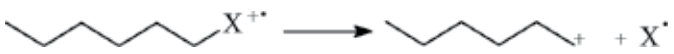

(34)

accompanied by the rearrangement of hydrogen at β, observed particularly in chlorinated compounds:

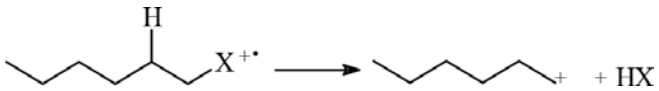

(35)

Low-molecular-mass monochlorinated alkanes show a detectable molecular peak. Although the chlorine atom does occur in fragmentation of the molecular ion, its intervention is much smaller than in oxygen-, nitrogen- or sulphur-containing compounds. Cleavage at adjacent C–C in a monochlorinated chain results in a small peak *m/z* 49 as well as in the isotope peak *m/z* 51 [1, 3, 54, 65]:

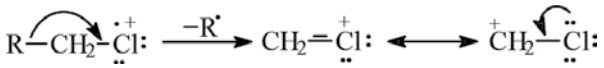

(36)

Cleavage of the C–Cl bond results in a small Cl^+ peak and an R^+ peak, dominant in low-molecular-mass halogens but very weak when the chain is greater than C_5.

Here, the chain > C_5-chlorinated compounds render $C_3H_6Cl^+$, $C_4H_8Cl^+$ and C_5HCl^+ ions, of which $C_4H_8Cl^+$ shows the most intense peak (the base peak sometimes, because of its cyclic structure):

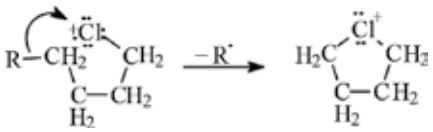

(37)

HCl elimination occurs probably at 1,3 position, resulting in formation of a weak peak (on average) M–36. Conduct of brominated compounds is similar to that of chlorinated ones [65]:

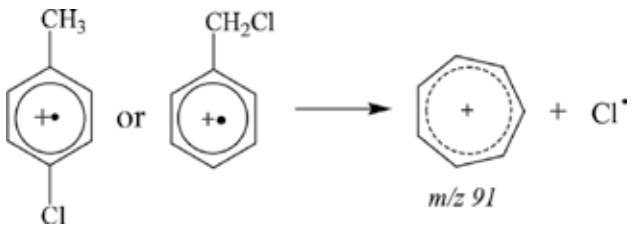

(38)

Halogenated aromatic compounds have a prominent peak M–X when X is directly related to the cycle. When possible, the tropylium ion is easily formed [1, 3, 60].

2.7.5. Hydroxy compounds

Alcohols easily losing one water molecule, their molecular ion, are almost non-existent. Water loss may occur under the influence of heat even before fragmentation. Therefore, in this case, the spectrum resembles that of an alkene.

Generally, the break occurs in the bond next to the oxygen atom. Primary alcohols mainly show a predominant peak due to the CH_2=OH+ (*m*/*z* 31). Secondary and tertiary alcohols cleave with formation of ions:

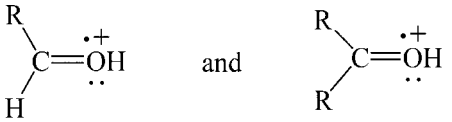

(*m*/*z* 45, 59. 73 ...) (*m*/*z* 59, 73, 87 ...) , respectively (39)

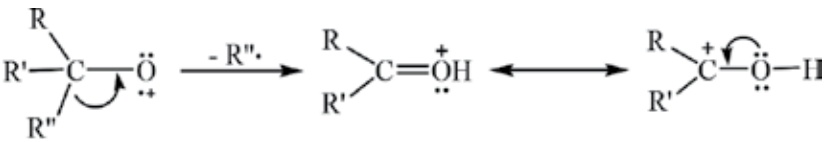

(R''>R') (40)

When R and/or R′=H, a peak may show at M−1. Analysis of branched alcohols is more difficult [3]:

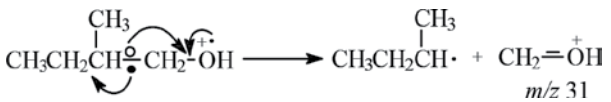

(41)

The mass spectrum of 2-methyl-1-butanol also renders the peak at *m*/*z* 57 (**Figure 13**) corresponding to the $CH_3CH_2^+CHCH_3$ fragment, whose rise is difficult to explain [66].

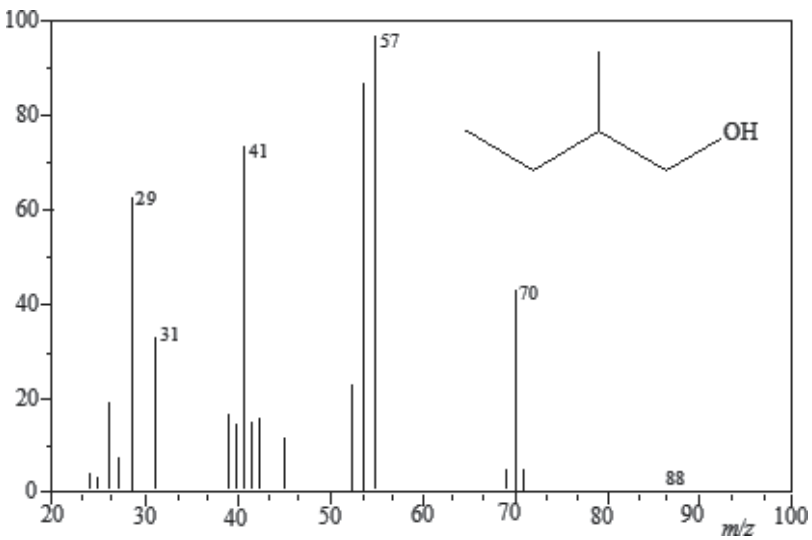

Figure 13. 2-Methyl-1-butanol-simplified mass spectrum. The *m*/*z* 88 molecular peak cannot be observed.

http://dx.doi.org/10.5772/intechopen.68595

The peak at m/z 70 corresponds to a dehydration (M−18), which is supposed to occur according to the following mechanism:

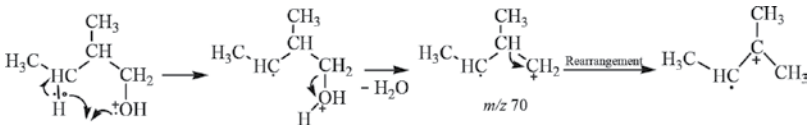

(42)

In over C_6-chain primary alcohols, the break of C–C bonds results in spectra similar to those of alkenes. Concomitant elimination of water and an alkene gives rise to a peak M–(alkene + water) [3]:

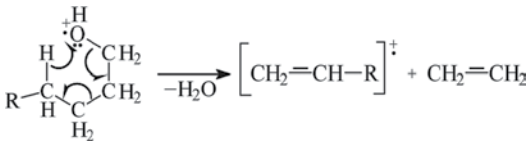

(43)

The alkene ion undergoes breakdown by successive elimination of ethylene.

Cycloalkanes undergo complex fragmentation. Cyclohexanol (M^+ = *m/z* 100), by elimination of one hydrogen at α, forms the $C_6H_{11}O^+$ ion, by elimination of water forms the $C_6H_{10}^+$ ion and by complex cycle cleavage results in the $C_3H_5O^+$ ion.

Benzyl alcohol and substitution counterparts form a prominent parent peak. Following a cycle cleavage at β, an average abundance peak (M–OH) is also present [60]:

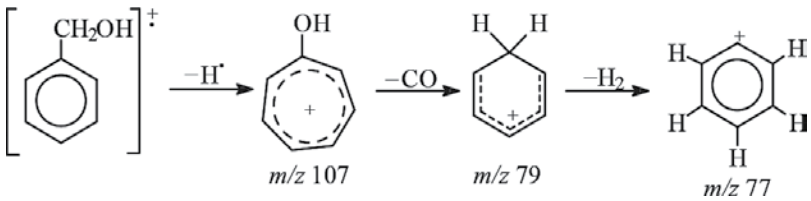

(44)

The sequence of M−1, M−2 and M−3 peaks should be noted. Also, the $C_6H_7^+$ ion is formed by the elimination of CO, as well as the $C_6H_5^+$ ion, by elimination of hydrogen.

Phenols are characterised by abundant molecular peak as well as by the M–CO (M−28) fragment arising from formation of a cyclohexadienyl intermediate:

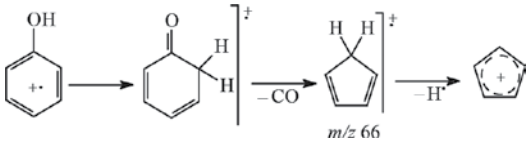

(45)

The molecular ion peak in ordinary phenol is the base peak, and the M−1 peak is weak. In cresols, as a result of a slight benzylic C–H cleavage, the M−1 peak is more prominent than the molecular ion peak.

Fragmentation of alkylphenols is similar to that of alkylbenzenes, which further cleave in the same way as un-alkylated phenols [61, 62]:

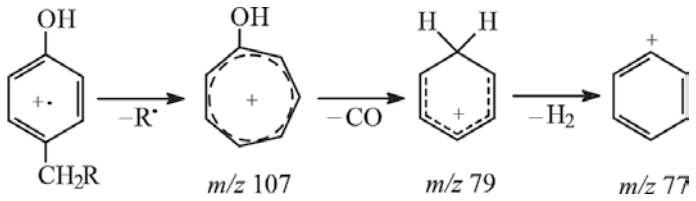

(46)

2.7.5.1. Ethers

The molecular ion peak is weak in *aliphatic ethers* (**Figure 14**) and intense in aromatic ones. The M+1 peak (resulted on H· collision with the molecular ion) is more visible.

The presence of a hydrogen atom can be inferred from the presence of prominent peaks by m/z 31, 45, 59, 73, etc., representing RO^+ and $ROCH_2^+$ fragments [3].

Compared to alcohols, ethers do not support fragmentation with water elimination.

Ethers are characterised by fragmentation of the C–C bond at β to oxygen [67–71]:

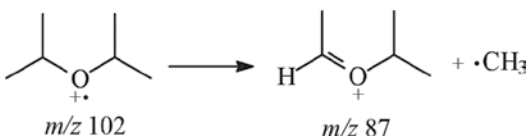

(47)

For a possible H at β to O^+, secondary fragmentation then follows:

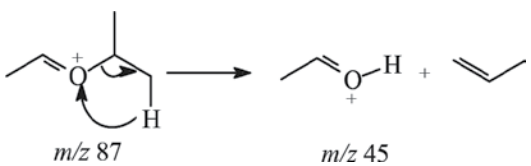

(48)

Cleavage of the simple C–O bond, sometimes observed in simple ethers, gives rise to branched ions:

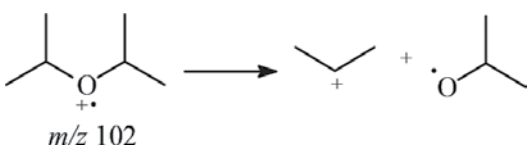

(49)

The molecular peak is predominant in *alkyl aryl ethers*. The bond at β to the cycle is the first to break, followed by further breakdown of the resulting fragment. Anisole with M^+ by *m/z* 108 converts to *m/z* 93, *m/z* 65 and *m/z* 39 ions [1, 3, 67–71]:

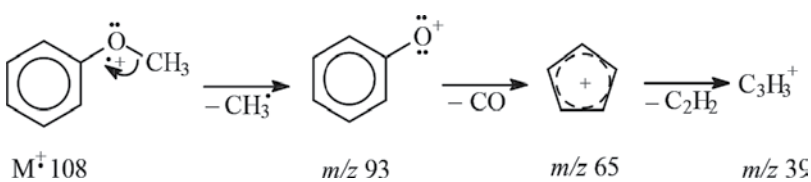

(50)

http://dx.doi.org/10.5772/intechopen.68595

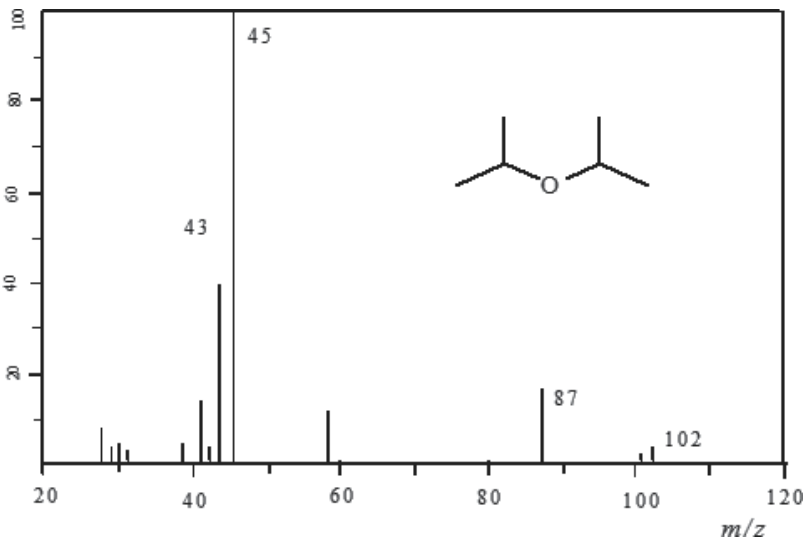

Figure 14. Di-isopropyl ether-simplified mass spectrum [1].

Concomitant loss of formaldehyde results in formation of *m*/*z* 78, m/z 77 and *m*/*z* 51 ions (**Figure 15**):

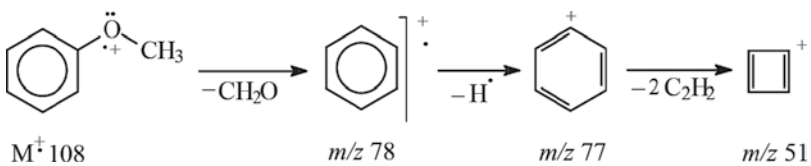

(51)

Due to complex rearrangements, *diphenyl ethers* display peaks at M–H, M–CO and M–CHO.

2.7.6. Carbonyl compounds

2.7.6.1. Aldehydes

Generally, the aldehyde molecular peak may be identified. Break of the C–H and C–C bonds next to the oxygen atom renders an M−1 peak and an M–R peak (*m*/*z* 29, CHO^+). The M−1 peak is characteristic even for long-chain aldehydes, but the *m*/*z* 29 peak in > C_4 aldehydes may also result from the $C_2H_5^+$ hydrocarbon ion [1, 3, 72].

McLafferty fragmentation of the C–C α,β bond occurs in these aldehydes, resulting in formation of a prominent peak by *m*/*z* 44, 58 or 72, etc., depending on substituents in α position (**Figure 16**). This resonance-stabilised ion arises in cyclic transition state. Based on pentanal as reference, there are four fragmentation patterns:

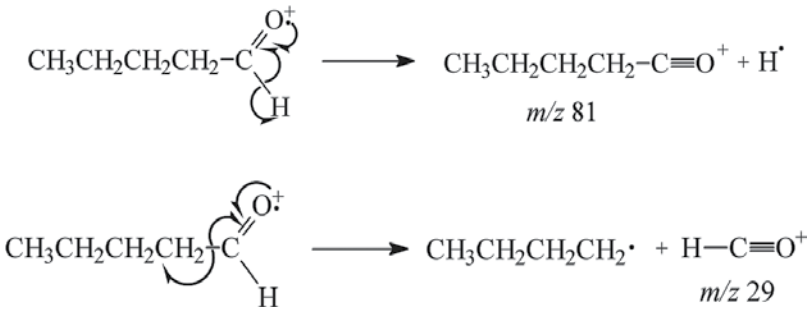

(52)

Cleavage of the bond in β position:

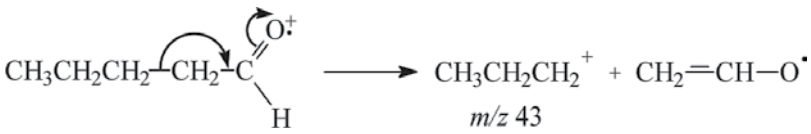

(53)

Cleavage of the bond in α position:

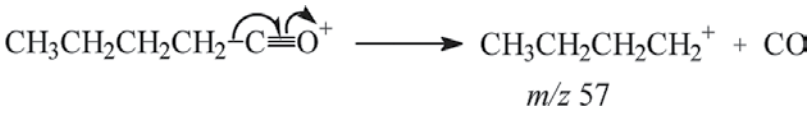

(54)

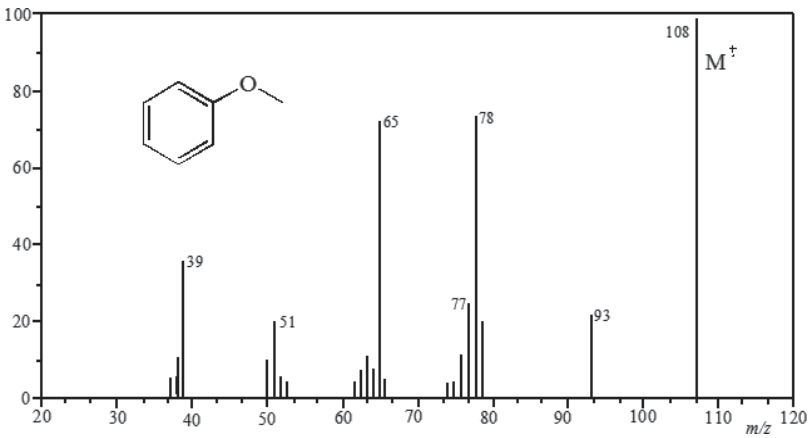

Figure 15. Anisole-simplified mass spectrum with intense peak [M–CH_2O] by *m*/*z* 78 [1].

http://dx.doi.org/10.5772/intechopen.68595

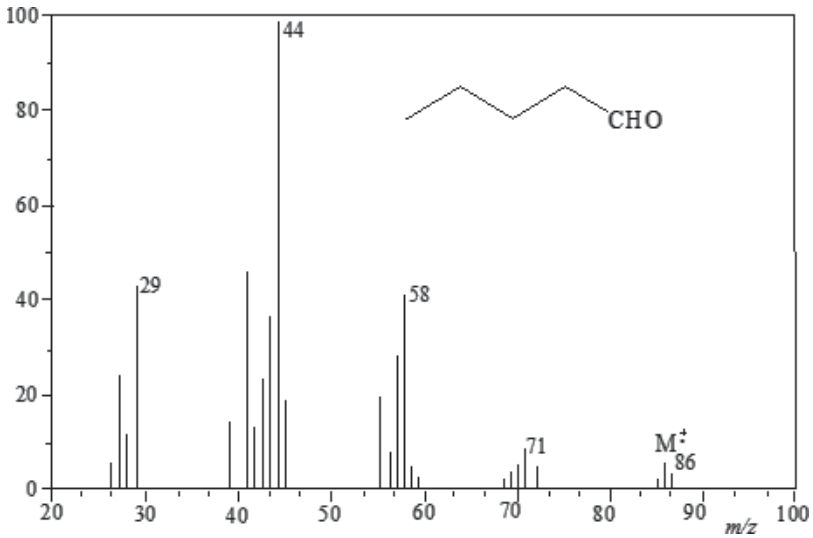

Figure 16. Simplified mass spectrum of pentanal [1].

McLafferty rearrangement:

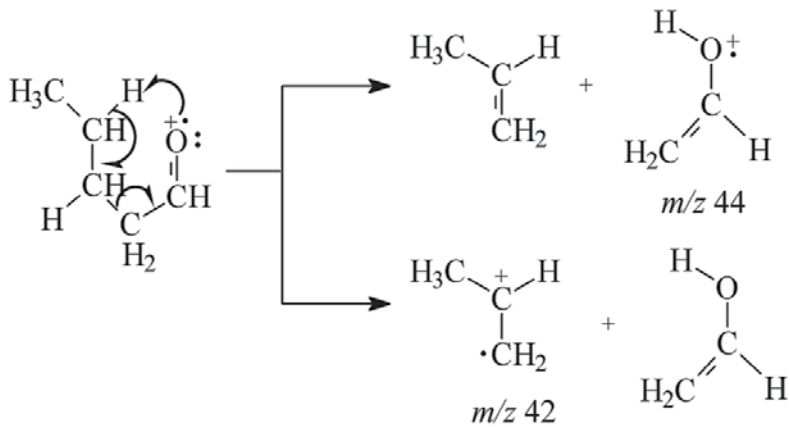

(55)

Spectra of straight-chain aldehydes show other characteristic peaks as well, e.g. M−18 (water loss), M−28 (ethene loss) and M−43 (loss of CH_2=CH–OH). The hydrocarbon-fragmentation-like pattern becomes more prominent with an increase in the chain [3].

Aromatic aldehydes lose one hydrogen and convert to the benzoyl ion, peak by M−1, further converting to the phenyl cation by CO elimination:

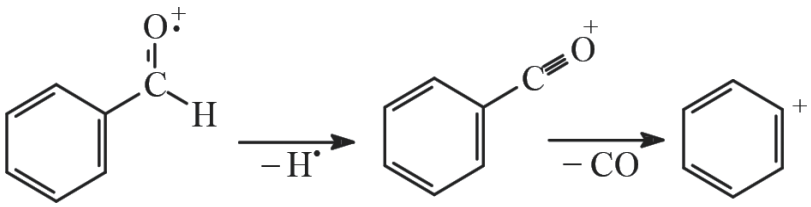

(56)

2.7.6.2. Ketones

Ketone molecular ion peak is generally sufficiently prominent. One exception is that of the 3-methyl-2-pentanone, whose spectrum does not display the molecular ion peak by *m*/*z* 100 (**Figure 17**). The most frequent R′–CO–R ketone fragmentation pattern results in formation of resonance-stabilised $R'–CO^+$ or $R–CO^+$ acylium ions [1, 3, 73]:

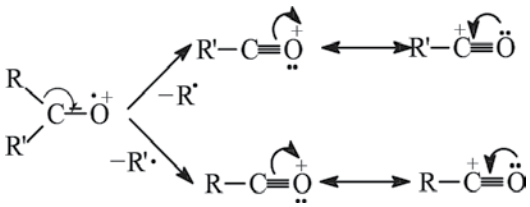

(57)

Fragmentation generates the peaks by *m*/*z* 43, 57 or 71. The base peak commonly results by loss of the most important alkyl group.

For an alkyl chain bound to the CO group with three or more carbon atoms, cleavage of the C–C bond at α–β occurs, accompanied by hydrogen migration and formation of a prominent peak [60–62].

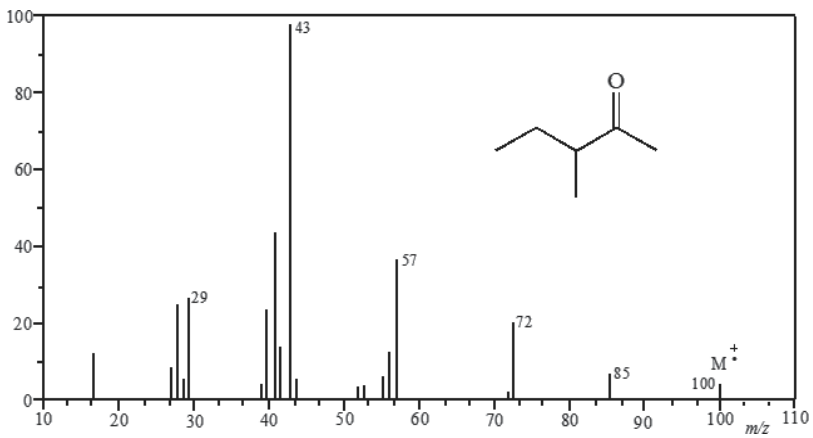

Figure 17. 3-Methyl-2-pentanone-simplified mass spectrum [1].

http://dx.doi.org/10.5772/intechopen.68595

McLafferty rearrangement occurs:

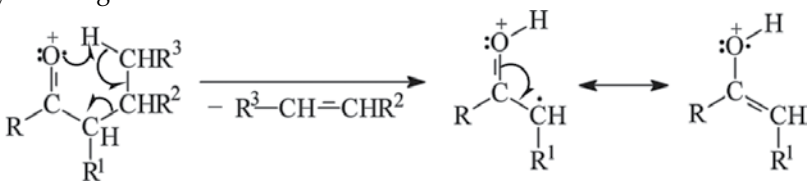

(58)

Cleavage of the α–β bond does not occur because an unstable ion would otherwise result, with two adjacent positive cores:

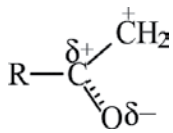

(59)

Unless high-resolution techniques are used, in long-chain ketones, hydrocarbonated peaks may not be distinguished from acylated ones because the mass of one C=O unit (28) equals that of two CH_2 units.

The molecular ion of *cyclic ketones* is predominant. Similar to aliphatic ketones, the first fragmentation occurs at the bond adjacent to the carbonyl group [53]:

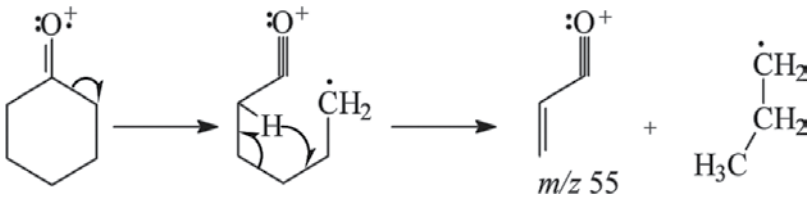

(60)

The resulting ion by *m/z* 55 is the base peak. The same ion results in cyclopentanone as well, on elimination of an ethyl radical (instead of a propyl radical, the same as in cyclohexanone) [53].

Distinctive peaks by *m/z* 42 and 43 in the cyclohexanone spectrum arise from the following fragmentations:

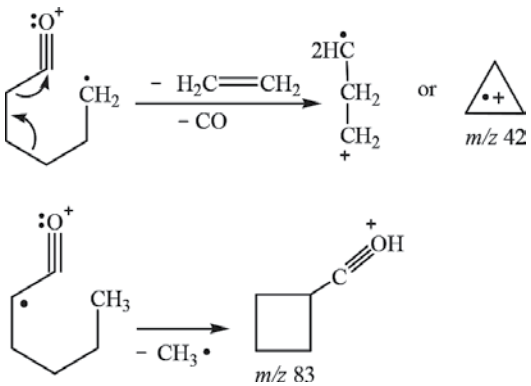

(61)

The molecular ion peak is predominant in *aromatic ketones*. Fragmentation of alkyl aryl ketones occurs at the bond at β to the cycle, resulting in formation of the benzoyl Ar–C≡O^+ cation, usually the base peak. This may lose CO, resulting in formation of one aryl ion (*m/z* 77 for acetophenone) [1, 53, 73]:

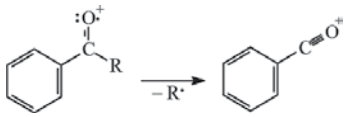

(62)

In the case of R with one hydrogen at γ, a McLafferty rearrangement occurs, similar to aliphatic ketones, resulting in formation of one ion by *m/z* 120 [3, 53, 73].

2.7.7. Carboxylic acids

In *straight-chain monocarboxylic acids*, although weak, the molecular peak can generally be observed. The *m/z* 60 peak is characteristic and sometimes the base peak, due to the McLafferty rearrangement [53, 73]:

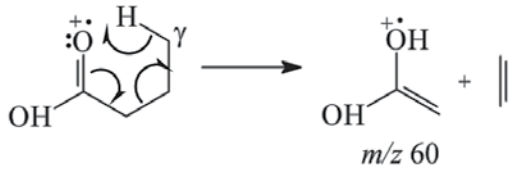

(63)

Short-chain acids display predominant peaks by M–OH and M–COOH. The $COOH^+$ ion by *m/z* 45 is low in intensity, and M–OH^+, by *m/z* M–17, may only rarely be observed:

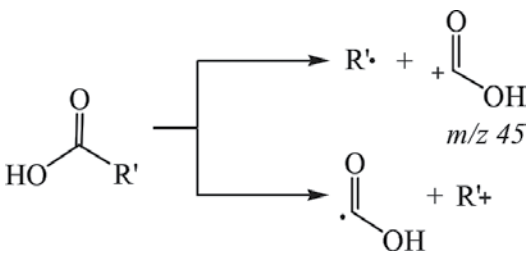

(64)

Long-chain acids display spectra (**Figure 18**) with two peak series resulting from cleavage of each C–C bond whose charge is either on the oxygen fragment (*m/z* 45, 59, 73, 87, etc.) or the alkyl fragment (by *m/z* 27, 28, 41, 42, 55, 56, 69, 70, etc.) [3, 53, 73]:

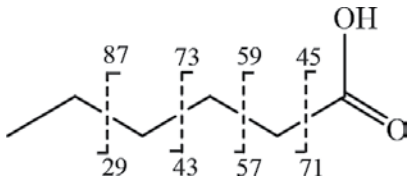

(65)

Dicarboxylic acids are termed into esters to increase their volatility. Trimethylsilyl esters[2] are very suitable.

---

[2]Similar to trimethylsilyl ethers, trimethylsilyl esters are used for volatilisation of carboxylic acids or alcohols in electronic impact MS (EI-MS) or GC-MS. In EI-MS, a clear peak, $[M–CH_3]^+$and often $[Si(CH_3)_3]^+$ results by *m/z* 73, as base peak.

http://dx.doi.org/10.5772/intechopen.68595

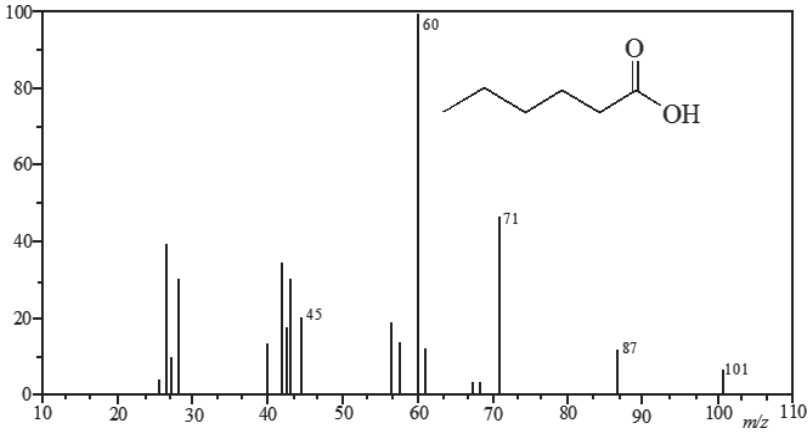

Figure 18. Hexanoic acid-simplified mass spectrum [1].

Aromatic acids display easily noticeable molecular peaks. Other peaks result by OH loss (M−17) and COOH loss (M−45). Water loss (M−18) occurs if there exists one in orthohydrogen or a hydrogen group.

One instance of *ortho-effect* is that of *o*-methylbenzoic (*o*-toluic) acid [1, 3, 53]:

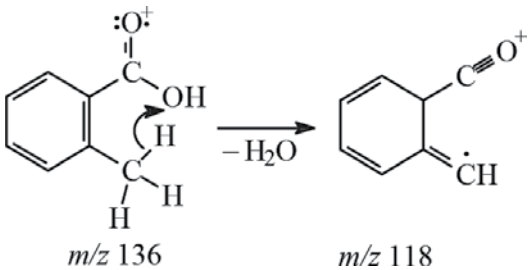

(66)

2.7.8. Carboxylic esters

Esters of aliphatic acids, even soaps, usually display one noticeable molecular peak. The following ions may result by break of the bonds at α to the carbonyl group:

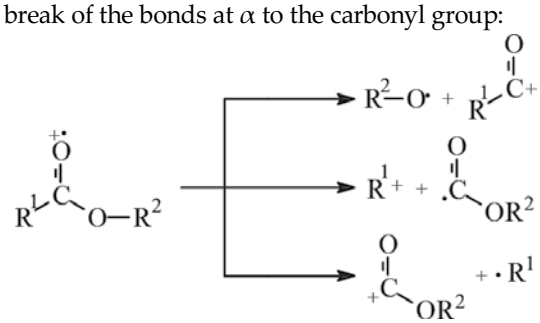

(67)

In a $R^1CO–OR^2$ ester, simple fragmentations in the α position of the carbonyl group give rise to several ions: R^{1+}, R^1CO^+ and $COOR^{2+}$.

The characteristic peak occurs due to common McLafferty rearrangement, with cleavage of a bond not directly adjacent to the carbonyl group.

In case of multiple rearrangement possibilities, there is a tendency to favour that of the 'acid' part as compared to the 'alcohol' part [1, 3]:

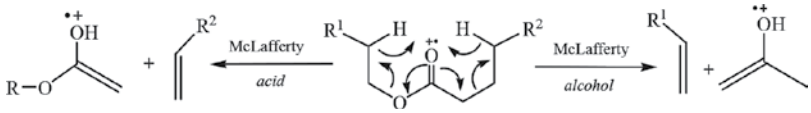

(68)

The McLafferty rearrangement of the *alcohol* part does not occur unless there is a competition with rearrangement of the *acid* part or the arising ion is stabilised, e.g. by an aromatic substituent. Instead, rearrangement of the *alcohol* part to acetals often occurs, where the $[M-60]^+$ ion is important, whereas the ion by *m/z* 60 $[C_2H_4O_2]^+$ is virtually non-existent [3]:

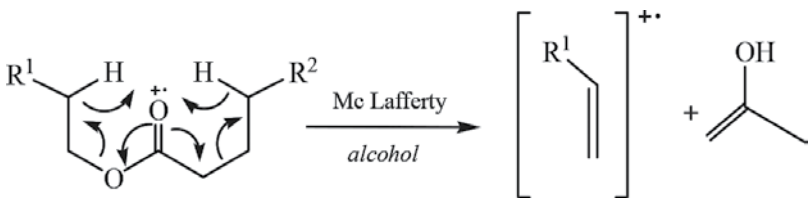

(69)

$R^1CO–OR^2$ esters, where R^2 has more than two carbon atoms, also produce an $R^1C(OH)_2^+$ ion originating from a double rearrangement of the alcohol part.

In $R^1CO–OR^2$ esters, there are characteristic ionic series, allowing for unambiguous determination of the 'acid' part (**Table 4**) and the 'alcohol' part.

For example, the ethyl propanoate spectrum (**Figure 19**) includes R^{1+} ions (where R^1 is ethyl) by *m/z* 29, R^1CO^+ by *m/z* 57 and $R^1C(OH)_2^+$ by *m/z* 75 [3, 53].

Esters of aromatic acids display a predominant molecular peak. Alkyl benzoates eliminate alcohol by *ortho-effect*, similarly to aromatic acids. For example, in the spectrum of methyl salicylate, the base peak ion is that of the ion by *m/z* 120. The ion *m/z* 92 results by CO elimination:

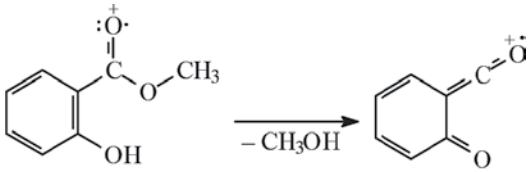

m/z 152 *m/z* 120

(70)

In phthalic esters, widely used as plasticisers, there is a prominent peak by *m/z* 149, likely resulted from fragmentation of two ester groups and finally of a water molecule [74]:

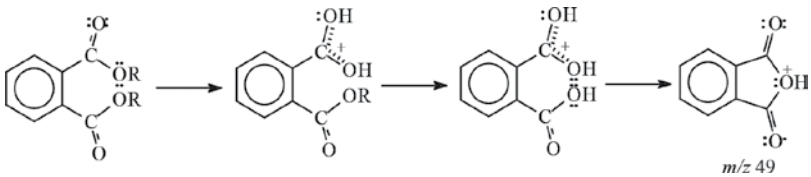

(71)

R^1 'acid' part	**CH_3**	**C_2H_5**	**C_3H_7**	**C_4H_9**	**C_5H_{11}**
m/z R^{1+}	15	29	43	57	71
m/z R^1CO^+	43	57	71	85	99
$R^1C(OH)_2^+$	61	75	89	103	117
R^2 'alcohol' part	**CH_3**	**C_2H_5**	**C_3H_7**	**C_4H_9**	
m/z R^2OCO^+	59	73	87	101	
m/z McLafferty	74	88	102	116	

Table 4. Ion characteristic to the ester 'acid' and 'alcohol' parts, respectively [1, 3].

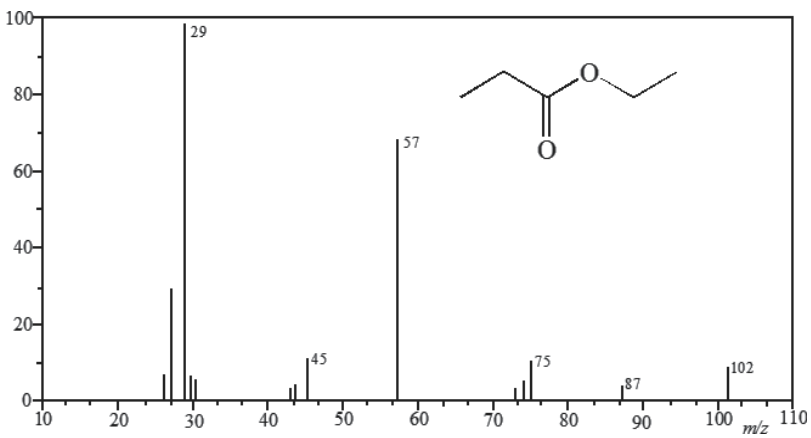

Figure 19. Ethyl propanoate-simplified mass spectrum [1].

2.7.9. Amines

The molecular ion peak of *aliphatic amines* is odd, generally weak, unnoticeable even in long chain or strongly branched amines. The base peak results from a C–C (α,β) fragmentation next to the nitrogen atom.

Mass spectra reveal the presence of *iminium* ions due to nitrogen, which is a very good stabiliser of adjacent ions.

Primary amines undergo break of the β bond to the NH_2 group [1, 3]:

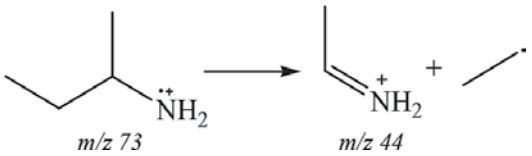

(72)

For instance, 2-phenylethylamine, found in chocolate, red wine, cheese and also involved in migraine, provides a molecular ion of relatively low abundance on electron impact, which undergoes fragmentation in the β position resulting in formation of two carbocations:

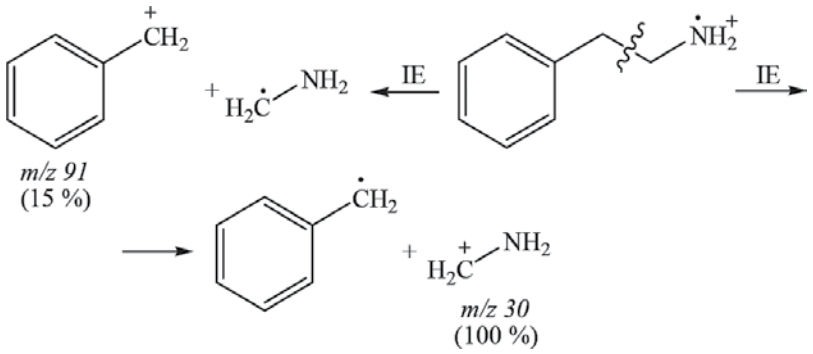

(73)

Secondary amines have the same degradation pathway as esters (**Figure 20**). Fragmentation of the C–C bond at β to nitrogen occurs [1, 3, 75]:

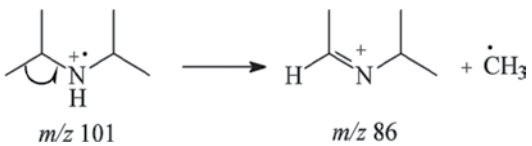

(74)

In case of one H^+ at C at β, ion rearrangement occurs:

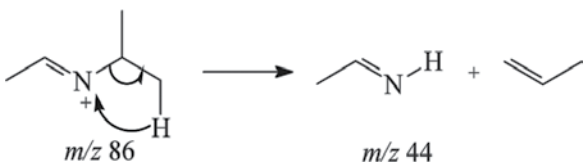

(75)

The *m*/*z* 44 ion is the base peak in the *di*-isopropylamine spectrum.

Tertiary amines lose an alkyl radical, resulting in formation of a resonance-stabilised iminium radical. For instance, the base peak of *m*/*z* 101 molecular peak triethylamine is by *m*/*z* 86 [1, 3]:

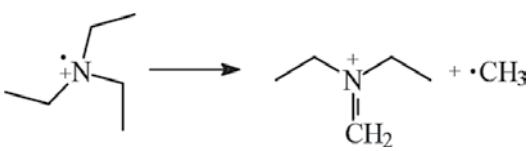

(76)

http://dx.doi.org/10.5772/intechopen.68595

Amino acids may undergo fragmentation in two C–C bonds next to nitrogen, favouring the one arising from loss of the carboxyl group. The aliphatic amine-containing fragment undergoes breakdown, resulting in a peak by *m/z* 30 [76]:

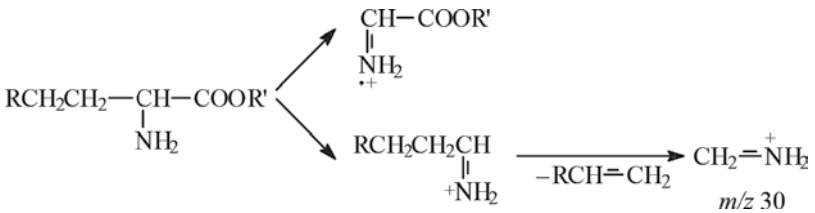

(77)

Unlike acyclic amines, *cyclic amines* have intense molecular peaks. The first cleavage occurs at either the carbon at α with loss of a hydrogen atom, resulting in formation of a prominent peak M−1, or by cycle opening, followed by ethene elimination (for pyrrolidine) to form $CH_2N^+H{=}CH_2$ (*m/z* 43, the base peak). Further, $CH_2{=}N^+{=}CH_2$ (*m/z* 42) results by loss of a hydrogen atom.

Monomolecular *aromatic amines* (with odd number of nitrogen atoms) display an intense molecular ion [76]:

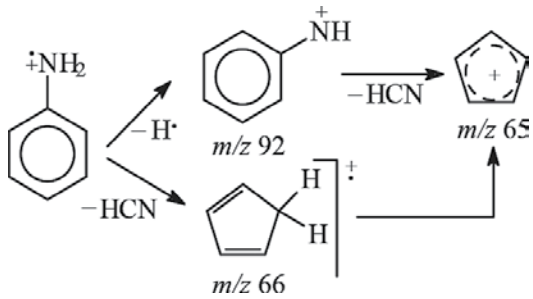

(78)

By loss of a proton of the amino group, aniline converts into an M−1 peak ion, which, by subsequent loss of one HCN molecule, renders the predominant peak by *m/z* 65 (the *cyclopentadienyl ion*).

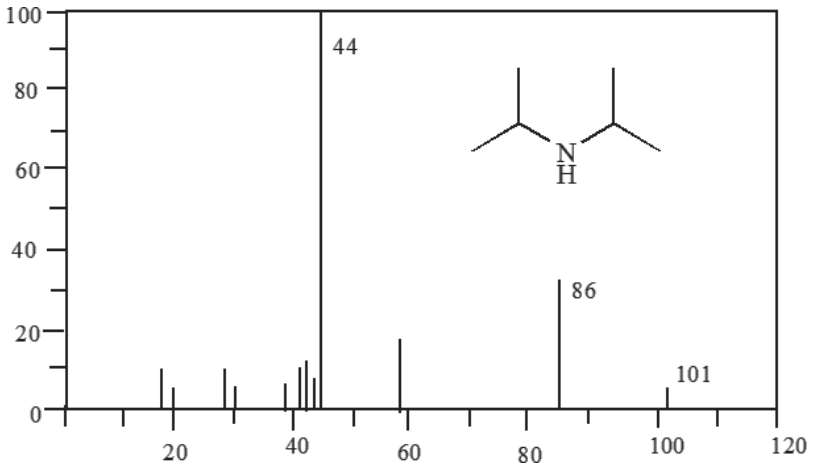

Figure 20. Di-isopropylamine-simplified mass spectrum [1].

Alkyl anilines undergo tropylic cleavage, resulting in formation of amino-tropylium ion, peaking by *m/z* 106 [76]:

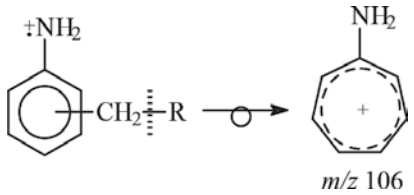

(79)

2.7.10. Amides

In *aliphatic amides*, the molecular ion of a monoamide is generally identifiable. Dominant fragmentation patterns depend on chain length as well as on the number and length of nitrogen-bound alkyl groups [76].

Simple fragmentations at α to the carbonyl result in the following ions:

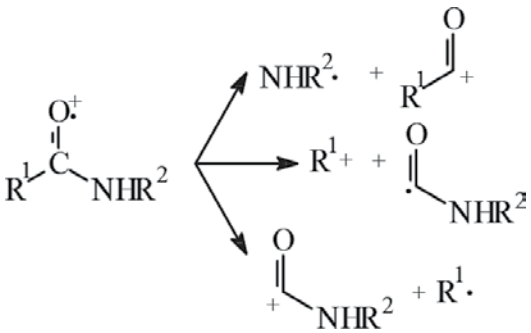

(80)

The base peak of primary amides with straight chain longer than that of propionamide results from McLafferty rearrangement [1, 3, 54, 77]:

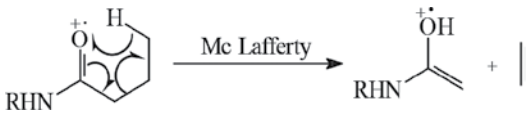

(81)

Secondary and tertiary amides with one hydrogen at γ of the acyl part and methyl groups at the nitrogen atom undergo McLafferty rearrangement, producing a dominant peak.

Aromatic amides are typically represented by benzamide (**Figure 21**). The molecular ion loses NH_2, resulting in a resonance-stabilised benzoyl cation which then undergoes fragmentation, leading to the phenyl cation [1, 3, 77]:

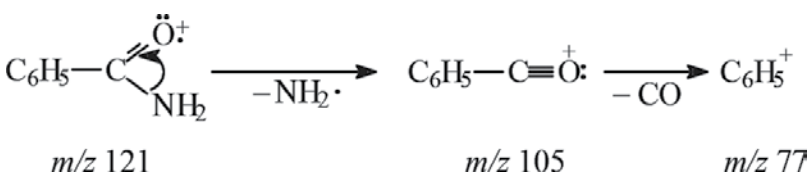

(82)

http://dx.doi.org/10.5772/intechopen.68595

2.7.11. Nitriles

Except for acetonitrile and propionitrile, molecular peaks of aliphatic nitriles are weak. They are often accompanied by M+1 or M−1 peaks.

In C_4–C_9 straight-chain nitriles, rearrangement to transition status with a six-atom cycle results in ion *m/z* 41, the base peak [1, 3]:

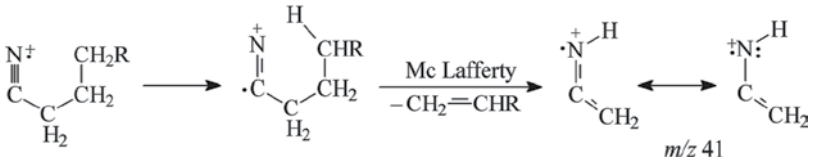

(83)

This peak is no certain indication because of the presence of another peak $C_3H_5^+$ (*m/z* 41), in all aliphatic chain hydrocarbons.

Following McLafferty rearrangement, straight-chain nitriles of more than seven carbon atoms render a characteristic peak by *m/z* 97:

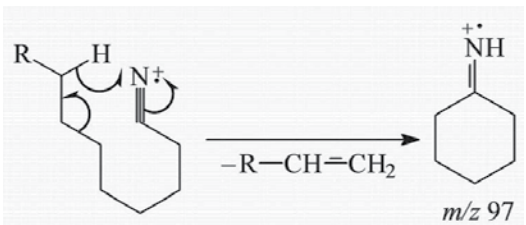

(84)

Simple fragmentation of the C–C bond, aside from the one next to nitrogen, renders a series of homologous peaks of even mass along the hydrocarbon chain by *m/z* 40, 54, 68 and 82, due to the $(CH_2)_nC{\equiv}N^+$ ions, similar to hydrocarbons [1, 3].

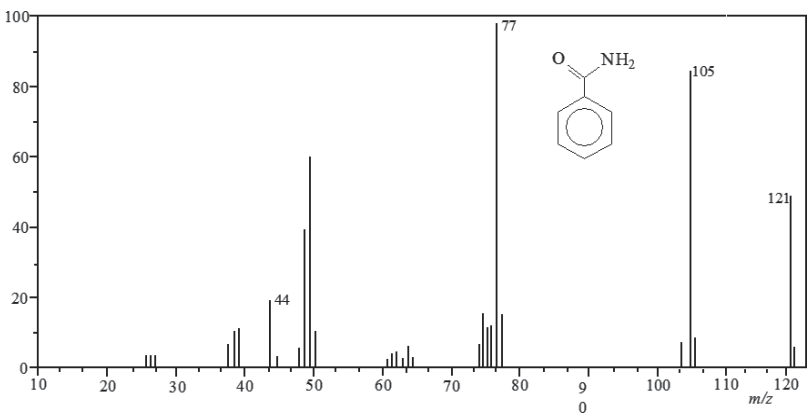

Figure 21. Benzamide-simplified mass spectrum [1].

2.7.12. Nitro compounds

Aliphatic nitro-derivatives have (odd) weak or absent molecular peaks. As the nitro group produces sharp polarisation of the C–N bond, the latter is broken, giving rise to hydrocarbon characteristic fragments:

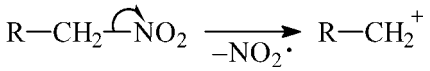

(85)

The presence of the NO_2 group is shown by a weak peak by *m/z* 46 (NO_2^+) and a sizeable one by *m/z* 30 (NO^+).

Aromatic nitro-derivatives have a prominent molecular peak. Predominant peaks result from elimination of an NO_2 radical (M−46) and a neutral NO molecule with rearrangement for formation of the phenoxy cation [1, 3].

2.7.13. Sulphur-containing compounds

Mercaptan and thio-ether compounds render more intense molecular ion peaks than corresponding oxygen compounds. *Mercaptan* fragmentation is similar to that of alcohols. Cleavage of the C–C bond (αβ) results in a characteristic ion:

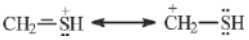

(86)

by *m/z* 47. Fragmentation of the β–γ bond gives rise to an average intensity peak by *m/z* 61 and γ–δ fragmentation results in a peak by *m/z* 75. Fragmentation at the δ–ε bond renders a more intense, cyclisation-stabilised peak by *m/z* 89 [1, 3, 54]:

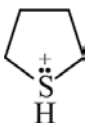

(87)

Similar to alcohols, primary mercaptans lose H_2S, resulting in a prominent peak by *m/z* 34.

Aliphatic *sulphides* render an intense peak by M+2. Fragmentations occur similarly to ethers. Cyclic sulphides fragment differently from cyclic ethers. For instance, similarly to tetrahydrofuran, in addition to hydrogen fragmentation at α and β, tetrahydrothiophene undergoes ethene fragmentation in different positions, resulting in formation of the *m/z* 60 ion, the base ion [75]:

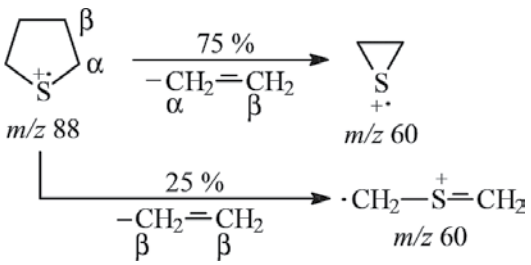

(88)

2.7.14. Heterocyclic compounds

Molecular ions of saturated heterocyclic compounds show a strong tendency to transannular rearrangement, often rendering the base peak.

http://dx.doi.org/10.5772/intechopen.68595

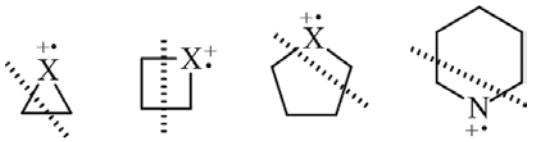

(89)

X=O, S, NH

Whether alkylated or not, *heteroaromatic compounds* render an intense molecular peak. Cleavage of the bond at β occurs as for alkylbenzenes. The charge of the molecular ion is mainly localised on the heteroatom and not on the aromatic ring. Five-atom aromatic heterocycles display similar fragmentation patterns. The first step consists in the cleavage of the carbon–heteroatom bond:

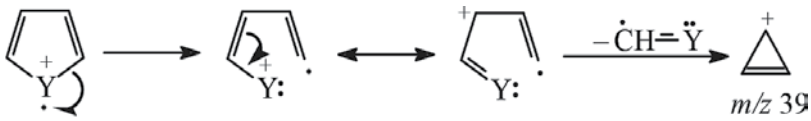

(90)

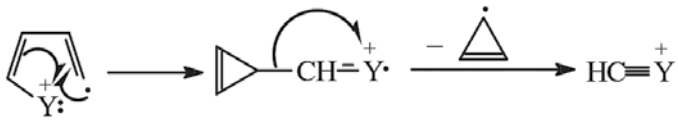

Y=O, S, NH

Furan displays two main peaks $C_3H_3^+$ (*m*/*z* 39) and $HC{\equiv}O^+$ (*m*/*z* 29). *Thiophene* shows three peaks: $C_3H_3^+$ (*m*/*z* 39), $HC{\equiv}S^+$ (*m*/*z* 45) and $C_2H_2S^{+\bullet}$ (*m*/*z* 58) [1, 3, 54, 78, 79].

Pyrrole displays three peaks as well: $C_3H_3^+$ (*m*/*z* 39), $HC{\equiv}NH^{+\bullet}$ (*m*/*z* 28) and $C_2H_2N^{+\bullet}H$ (*m*/*z* 41). It also eliminates one neutral HCN molecule, producing an intense peak by *m*/*z* 40. *Indole* as well eliminates hydrocyanic acid, and the ion fragment *m*/*z* 90 is stabilised by hydrogen elimination, resulting in formation of a dehydrotropylium ion:

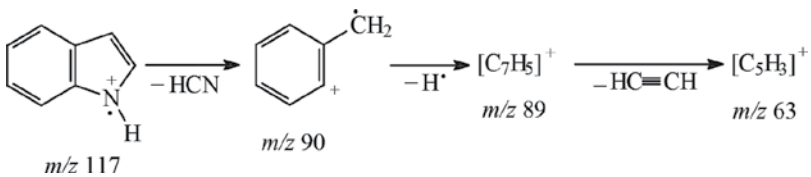

(91)

The pentatomic poly-heterocycles such as oxazoles, imidazoles, pyrazoles, etc. fragment more easily. In the case of an N heteroatom, elimination of HCN is preferred. For three or more directly bonded carbon atoms, the characteristic peak arises—$C_3H_3^+$ (*m*/*z* 39). Unsubstituted pyridines eliminate HCN, resulting in a base peak by *m*/*z* 52. Similarly to toluene, β- and γ-picolines also render intense peaks by M–HCN, *m*/*z* 66, and l M−1, *m*/*z* 78.

Substituted pyridines with large alkyl groups undergo fragmentation at β, γ, δ as well as McLafferty rearrangements, resulting in a peak by *m*/*z* 93 [1, 3]:

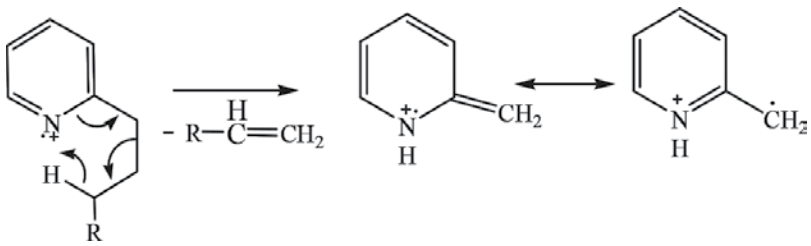

(92)

Ease of rearrangement depends on substituent position, decreasing in the order 2 > 4 > 3. Pyrazines undergo similar fragmentations because all substituents are in ortho to nitrogen atoms [1, 3].

2.7.15. Natural compounds

2.7.15.1. Amino acids

As amino acids are zwitterionic compounds, often non-volatile, their methyl esters are studied instead. The spectra produced by electron impact ionisation display weak or non-existent molecular peaks, because of amino acid capacity to easily lose their carboxyl group and of their esters to easily lose their carboalkoxyl group on electronic impact [76, 77]:

(93)

Esters of amino acids basically have two fragmenting patterns:

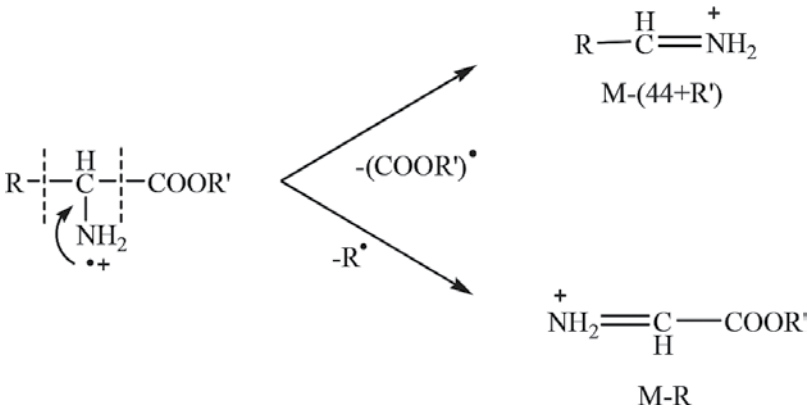

(94)

There is an average or high peak intensity of iminium ions, $RCH{=}N^{+}H_2$, as well as of the $N^{+}H_2{=}CHCO_2R'$ ion. The [M–R] ester group ion may undergo McLafferty rearrangement:

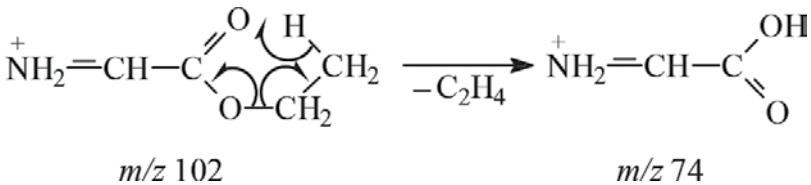

(95)

http://dx.doi.org/10.5772/intechopen.68595

If field desorption (FD) ionisation is used, as for leucine, for instance, spectra show the MH^+ *m/z* 132 ion, which eliminates a carboxyl group to convert to the *m/z* 87 ion, which in turn eliminates a hydrogen atom, resulting in formation of the *m/z* 86 ion [76, 77]:

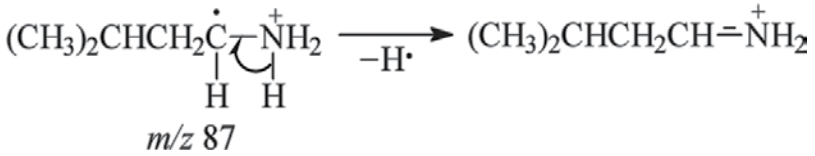

(96)

2.7.15.2. Triacylglycerols

Triglyceride molecular ions convert to characteristic ions [M–O_2CR] formed by stabilising the positive charge of the neighbouring oxygen:

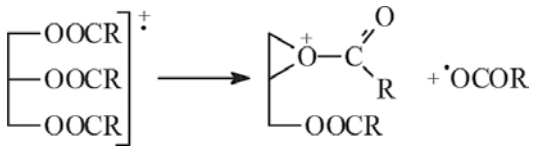

(97)

The OCOR fragment converts to the $[RCO_2H + H]^+$ fragment, allowing for identification of fatty acids. By the electron impact ionisation technique and by chemical ionisation, high-molecular-mass and low-volatility glycerides render weak or non-existent molecular peaks (MH^+) [1, 3, 77].

2.7.15.3. Steroids

Cholestane is a typical representative of steroids [80]. The intense peak molecular ion undergoes four fragmentation patterns:

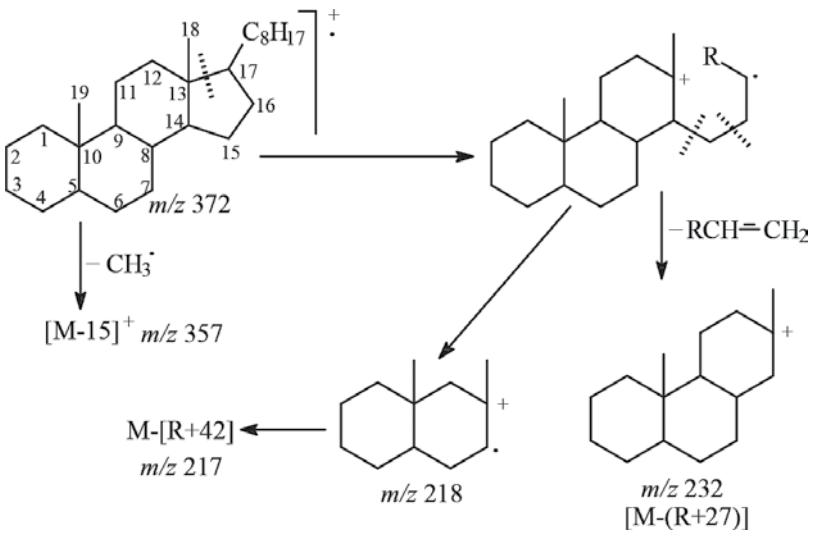

(98)

a. Fragmentation of an angular methyl resulting in formation of the *m/z* 357 peak fragment [31, 32].

b. Fragmentation of the C_{13}–C_{18} bond, favoured by C_{13} being tertiary, resulting in formation of the intermediary ion which is able to fragment in various ways. Fragmentation of the C_{15}–C_{16} bond, with elimination of an olefine and formation of the *m*/*z* 232 ion of mass M–(C_8H_{17}+27).

Cleavage of the C_{14}–C_{15} bond with formation of the resonance-stabilised *m*/*z* 217 ion followed by elimination of a hydrogen atom gives rise to the m/z 217 peak ion the most intense of the spectrum.

c. Fragmentation of the C_9–C_{10} bond, resulting in formation of a cation radical undergoing fragmentation of the C_5–C_6 or C_6–C_7 bonds and transfer of one hydrogen atom with generation of stable ions by *m*/*z* 95 and *m*/*z* 109 [80]:

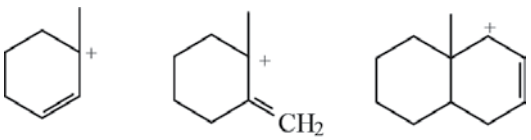

m/z 95 *m/z* 109 *m/z* 149 (99)

d. Fragmentation of C_8–C_{14} and C_9–C_{11} bonds, followed by transfer of a hydrogen atom to form the ion peak at *m*/*z* 149.

Polyhydroxylated steroids such as cholesterol have spectra with weak or non-existent molecular peaks. Dehydrations occur on heating. Chemical ionisation cannot be used, and the protonated molecular ion dehydrates quickly. Spectra obtained by field desorption (FD) mass spectrometry does not show dehydrations, and the molecular peak is present [1, 3, 81].

2.8. Recommendations for a mass spectrum analysis

Identification of the molecular ion is the first stage for mass spectrum interpretation because the molecular ion is the source of information on molecular composition.

If the electron impact ionisation-rendered spectrum does not allow identification of the molecular ion, other ionisation methods might be used.

Prominent peaks in a mass spectrum are generally those resulting from **primary fragmentations**. Secondary fragmentations may be used as aids for spectrum analysis. Fragment ions of higher mass close to that of the molecular ion are easy to identify because they correspond to formation of a small neutral entity such as CH_3, CH_2=CH_2, etc. Even if at low intensity, they have a key contribution to establishing the structure.

Mass differences between the molecular ion and the fragments must correspond to an actual chemical composition.

The molecular formula inferred must comply with the nitrogen rule.

Contrary to interpretation of NMR spectra, interpretation of all peaks in a mass spectrum is less interesting; only important characteristic peaks are considered. Small mass and low intensity ions are generally not significant.

Systematic spectrum interpretation requires compliance with the following *recommendations*:

- Gathering of basic information such as sample origin, alleged class of compounds, solubility, thermal stability and other spectrometric data.
- Writing down of *m*/*z* values for all relevant peaks and calculation of mass differences between prominent peaks.
- Consideration of the ionisation method used and examination of the general spectrum appearance. Other aspects to consider are whether there is an intense molecular ion (as in aromatic, heterocyclic, polycyclic compounds) or a weak molecular ion (as in aliphatic and multifunctional compounds) or the presence of impurities (solvents, lubricants, plasticisers) or occurrence of basic signals from residual air or wash fractions from chromatographic column.
- Investigation of the presence or absence of functional groups.
- Consultation of tables showing possible structures of different ions and potential structures of neutral fragments (**Tables 5** and **6**).
- Assignment of the unknown compound structure using known structures. Analyte structures can sometimes only arise partly from the known structure, or isomers cannot be determined.
- The proposed molecular structure is correlated with mass spectrum data [82–87].

2.9. Anomalies

Spectra may occur in mass spectrometry that are difficult to define, giving rise to confusion, which can only be avoided by appropriate preparation of samples or change of working conditions [1, 3].

2.9.1. The presence of impurities

Small amounts of impurities may produce peaks in the regions in which the MS spectrum should be white. Such peaks make it difficult to determine the *m*/*z* of the molecular ion. GC-MS impurities may result from residues of previous samples or degradation of the chromatography column. Small peaks may occur at values higher than *m*/*z* of the molecular mass. Sufficient time is necessary between injections into the chromatograph to evacuate previous samples. A background scan can be used to identify peaks due to residual material in the mass spectrometer [1, 3].

2.9.2. Metastable ions

Under normal conditions, the ion arising in the source is sufficiently stable to reach the detector and determine occurrence of a peak. If its life is less than a few μs, the ion is *metastable* and undergoes partial breakdown in its path, in line with a first-order kinetic [81, 87]:

Fragment (*m*/*z*)	Potential structure
15	CH_3^+
17	OH^+
18	H_2O^+; NH_4^+
19	F^+
26	CN^+
27	$C_2H_3^+$
28	$C_2H_4^{+\bullet}$; $CO^{+\bullet}$
29	$C_2H_5^+$; CHO^+
30	CH_4N^+ (amine)
31	CH_2OH^+ (alcohol, ether)
33	CH_2F^+
35	$^{35}Cl^+$ (together with $^{37}Cl^+$ by *m*/*z* 37)
39	$C_3H_3^+$ (aromatic)
41	$C_3H_5^+$; $C_2H_3N^{+\bullet}$ (nitrile)
42	$C_3H_6^{+\bullet}$
43	$C_3H_7^+$; CH_3CO^+ (carbonyl)
44	$C_2H_6N^+$ (amine); $C_2H_4O^{+\bullet}$ (McLafferty: aldehyde)
45	CH_3–CH–OH^+ (alcohol); CH_3–O–CH_2^+ (ether); $COOH^+$ (acid)
49	$CH_2{}^{35}Cl^+$
51	CHF_2^+; $C_4H_3^+$ (aromatic)
53	$C_4H_5^+$
54	NC–CH_2–CH_2^+ (nitrile); $C_4H_6^{+\bullet}$
55	$C_4H_7^+$; CH_2=CH–CO^+ (unsaturated ester, cyclic ketone)
56	$C_4H_8^{+\bullet}$ (cycle)
57	$C_4H_9^+$; C_2H_5–CO^+
58	$C_3H_6O^{+\bullet}$; (McLafferty); $C_3H_8N^+$ (amine)
59	$C_3H_7O^+$ (alcohol, ether); CH_3–OCO^+ (ester); $C_2H_5NO^{+\bullet}$ (amide)
60	$CH_3COOH^{+\bullet}$ (McLafferty: acetate)
61	$C_2H_5O_2^+$ (double rearrangement: acetate)
65	$C_5H_5^+$ (aromatic)
68	$C_5H_8^{+\bullet}$; $C_4H_6N^+$ (nitrile)
69	$C_5H_9^+$; CF_3^+; $C_4H_5O^+$
71	$C_5H_{11}^+$; C_3H_7–CO^+
72	$C_4H_8O^{+\bullet}$ (McLafferty); $C_4H_{10}N^+$ (amine), $C_3H_6NO^+$
73	$C_4H_9O^+$ (alcohol, ether); C_2H_5–OCO^+ (ester); $C_3H_7NO^{+\bullet}$
74	$C_3H_6O_2^{+\bullet}$ (McLafferty: ester, acid)

Fragment (*m*/*z*)	Potential structure
75	$C_3H_7O_2^+$ (double rearrangement: propionate)
77	$C_6H_5^+$ (aromatic)
79	$C_6H_7^+$ (aromatic); $^{79}Br^+$ (together with $^{81}Br^+$ by *m*/*z* 81)
80	$C_4H_3NHCH_2^+$ (pyrrole)
81	$C_4H_3O–CH_2^+$ (furan)
82	$C_6H_{11}^{+\bullet}$ (alkene, cyclane); $CH_2{}^{35}Cl_2^{+\bullet}$
85	$C_6H_{13}^+$; $C_4H_9–CO^+$
86	$C_5H_{10}O^{+\bullet}$; $C_5H_{12}N^+$
87	$C_5H_{11}O^+$ (alcohol, ether); $C_3H_7–OCO^+$ (esters); $C_4H_9NO^{+\bullet}$
88	$C_4H_8O_2$ (McLafferty: ester, acid)
89	$C_4H_9O_2^+$ (double rearrangement: butanoate)
91	$C_7H_7^+$ (aromatic)
92	$C_7H_8^{+\bullet}$ (McLafferty: aromatic)
93	$CH_2{}^{79}Br^+$; $C_6H_5O^+$ (phenol); $C_7H_9^+$ (terpene)
94	$C_6H_6O^+$ (Mc Lafferty: phenyl ether)
95	$C_4H_3O–CO^+$ (furan)
97	$C_7H_{13}^+$
98	$C_6H_{10}O^{+\bullet}$
99	$C_7H_{15}^+$; $C_6H_{11}O^+$
100	$C_6H_{14}N^+$
101	$C_4H_9–OCO^+$
103	$C_6H_5–CH=CH^+$; $C_5H_{10}O_2^+$
104	$C_6H_5–CH=CH_2^{+\bullet}$ (Mc Lafferty: ester and aromatic ketone)
105	$C_6H_5–C_2H_4^+$; $C_6H_5–CO^+$
107	$C_6H_5–OCH_2^+$; $C_6H_5–CH_2–O^+$
108	$C_6H_5–OCH_3^{+\bullet}$; $C_6H_5–CH_2–OH^{+\bullet}$ (benzyl ester)
117	$C_6H_5–C_3H_4^+$
119	$C_6H_5–C_3H_6^+$; $C_6H_5–C_2H_2O^+$
120	$C_7H_4O_2^{+\bullet}$
121	$C_7H_5O_2^{+\bullet}$; $C_8H_9O^+$; $C_9H_{13}^+$ (terpene)
127	I^+
131	$C_3F_5^+$; $C_6H_5–CH=CH–CO^+$
149	$C_8H_5O_3^+$ (phthalate)
152	$C_6H_4= C_6H_4^{+\bullet}$
154	$C_6H_5=C_6H_5^{+\bullet}$

Table 5. Ion fragments and potential structures [1, 3, 78, 79].

Fragment (*m*/*z*)	Potential structure
1	H•
15	CH_3•
17	•OH (small weight acid)
18	H_2O (alcohol, aldehyde, ketone)
19	F•
20	HF
26	HC≡CH; •CN
27	HCN
28	CH_2=CH_2; CO (aldehyde)
29	C_2H_5•; HCO•
30	NH_2CH_2•; CH_2=O; NO•
31	CH_3O•; •CH_2OH; NH_2CH_3
32	CH_3OH; S
33	CH_3• and H_2O (alcohol); SH•
34	H_2S
35	^{35}Cl• together with ^{37}Cl•
36	H^{35}Cl together with H^{37}Cl
40	CH_3C≡C–H
41	CH_2=CH–CH_2•
42	CH_2=C=O; CH_2=CH–CH_3
43	CH_3–CO•; C_3H_7•
44	CO_2; CH_2=CH–OH; N_2O; NH_2–CO•
45	•COOH; C_2H_5O•; $C_2H_5NH_2$
46	C_2H_5OH; •NO_2
49	•$CH_2{}^{35}$Cl
51	•CH_2F_2
54	CH_2=CH–CH=CH_2
55	CH_2=CH–CH_2–CH_2•
56	C_4H_8
57	C_4H_9•; C_2H_5–CO•
58	C_3H_6O
59	CH_3OCO•; CH_3COO•; CH_3CONH_2
60	CH_3COOH (acetate); C_3H_7OH
63	^{35}Cl–CH_2CH_2•
64	SO_2
68	C_5H_8

http://dx.doi.org/10.5772/intechopen.68595

Fragment (*m*/*z*)	Potential structure
69	CF_3•
70	C_5H_{10}
71	C_5H_{11}•; C_3H_7–CO•
73	CH_3CH_2–O–CO•
74	C_4H_9OH; CH_3CH_2COOH
77	C_6H_5•
78	C_6H_6
79	^{79}Br• together with ^{81}Br•
80	$H^{79}Br$
100	CF_2=CF_2
119	CF_3CF_2•
122	C_6H_5COOH
127	I•
128	HI

Table 6. Neutral fragments and potential structures [1, 3, 78, 79].

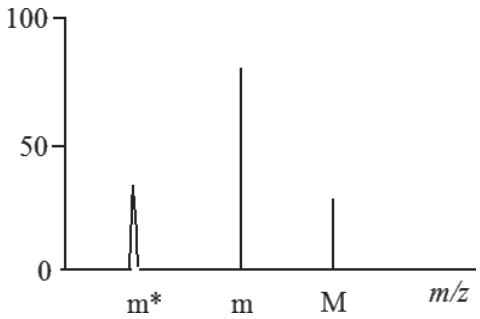

Figure 22. Three peaks of a metastable transition [1].

$$M^{\bullet +} \rightarrow m^{+} + m'^{\bullet} \quad (100)$$

In case the fin m^+ ion occurs in a dual-focus device before exiting the electrostatic sector, because of its insufficient kinetic energy, it is wasted on the walls of the device. Instead, if the breakdown occurs between the outlet of the electrostatic reactor and the entrance to the magnetic reactor, the trace of the m^+ ion can be observed at a pseudo-mass m^* not corresponding to an actual mass.

A metastable transition leads to occurrence of three peaks in the mass spectrum (**Figure 22**). The metastable peak, also known as the *diffuse peak*, is less definitely shaped, and its position

does not necessarily correspond to a mass close to an integer. Metastable ion peaks appear flattened, of low intensity and sometimes concealed by normal peaks. Metastable peak detection can be achieved inter alia by reducing the acceleration potential of ions for their longer maintenance in the ionisation chamber, with reduction of those fragmenting in flight [1, 3].

2.9.3. The absence of the molecular ion

Many compounds such as tertiary alcohols and alkyl halides fragment so easily that the molecular ion cannot be identified in the mass spectrum.

Tertiary alcohols dehydrate easily, and bromides and chlorides can easily lose halogens by fragmentation. Even without the molecular ion peak, the use of the spectra library may predict molecular structure [1, 75, 78].

2.9.4. Complex fragmentations

Mass spectra of pure compounds show difficult-to-interpret peaks. Corresponding fragments thereof may result from multiple-stage fragmentations or certain complex rearrangements (**Tables 5** and **6**). Such peaks should not be insisted upon [1, 3, 78, 79, 88].

3. Conclusion

Mass spectrometry is currently used both in research and development of new molecular structures in industry and other related fields. This method along with NMR, IR, XRD and UV-Vis has become indispensable to any research laboratory in the field of organic chemistry. It has many uses in pharmaceutical (drug design, combinatorial chemistry, pharmacokinetics, drug metabolism, etc.) in the clinical field (neonatal screening, haemoglobin analysis, drug abuse, doping), environmental protection (water quality, food contamination) in geology (oil composition) and of course in biotechnology (analysis of proteins, polypeptides, hormones, etc.).

Pharmacokinetics needs the use of mass spectrometry because of the complex nature of the matrix (often blood or urine). Pharmacokinetics deserves high sensitivity to observe low dose and long-time data point. Commonly used for this application is liquid chromatography-mass spectrometry (LC-MS) with a triple-quadrupole mass spectrometer. A specificity of the experiment is added by tandem mass spectrometry.

Mass spectrometry has utility both in quantitative and qualitative analysis. The method is used to identify the isotopic species and calculation of nominal weight in organic compounds. The development of detectors and ionisation techniques along with its coupling with chromatography greatly widened the scope of combinations including ionic compounds or macromolecules.

Mass spectrometry is also used in protein characterisation and sequencing. Methods for protein ionisation are electrospray ionisation (ESI) and matrix-assisted laser desorption/ionisation (MALDI). Here, two approaches are used for protein characterisation. First, intact proteins are ionised via two techniques, ESI and MALDI, followed by passing them to a mass spectrum analyser. This approach in protein analysis is commonly referred to as the 'top-down' strategy.

Mass spectrometry is also a complementary method to HPLC in glycan analysis. Intact glycan molecules is to be detected directly as single charged ions via MALDI or, after permethylation or peracetylation, via fast atom bombardment (FAB) mass spectrometry. Smaller glycans give good signals in electrospray ionisation mass spectrometry (ESI-MS).

The Universe has also been hit by mass spectrometry via the Viking programme as a standard method for analysis. A specialised GC-MS instrument aboard the Huygens probe entered the atmosphere of Titan in early 2005.

Author details

Teodor Octavian Nicolescu

Address all correspondence to: nicolescu.teodor@gmail.com

Organic Chemistry Department, Faculty of Pharmacy, "CAROL DAVILA" University of Medicine and Pharmacy, Bucharest, Romania

References

[1] Iovu M, Nicolescu TO. Chimie Organică. Metode Experimentale. 1st ed. Bucharest: Editura Universitară CAROL DAVILA; 2009. p. 652. DOI: ISBN 978-973-708-3494

[2] Balaban AT, Banciu M, Pogany I. Aplicații ale Metodelor Fizice în Chimia Organică. Bucharest: Editura Științifică și Enciclopedică; 1983

[3] Jürgen GH. Mass Spectrometry. A Textbook. 1st ed. Berlin: Heidelberg: Springer-Verlag; 2004. DOI: 10.1007/3-540-35756-X

[4] Griffiths IW. J.J. Thomson—The centenary of his discovery of the electron and of his invention of mass spectrometry. Rapid Communications in Mass Spectrometry. 1997;**11**: 1-16

[5] Dempster AJ. A new method of positive ray analysis. Physical Reviews. 1918;**11**:316-325

[6] Busch KL. Synergistic developments in MS. A 50-year journey from "Art" to science. Spectroscopy. 2000;**15**:30-39

[7] McLafferty FW. Mass spectrometric analysis. Molecular rearrangements. Analytical Chemistry. 1959;**31**(1):82-87. DOI: 10.1021/ac60145a015

[8] Field FH, Munson MSB. Chemical ionization mass spectrometry. I. General introduction. Journal of American Chemical Society. 1966;**88**(12):2621-2630. DOI: 10.1021/ja00964a001

[9] Grayson MA, editor. Measuring Mass—From Positive Rays to Proteins. Santa Fe and Philadelphia: ASMS and CHF; 2002

[10] Comisarow MB, Marshall A. Fourier transform ion cyclotron resonance detection: Principles and experimental configuration. International Journal of Mass Spectrometry. 2002;**215** (1–3):59-75

[11] Denoyer E, Van Grieken R, Adams F, Natusch DFS. Laser microprobe mass spectrometry. 1. Basic principles and performance characteristics. Analytical Chemistry. 1982;**54**(1):26-41. DOI: 10.1021/ac00238a001

[12] Robinson CV. John Fenn (1917–2010) chemist who enabled mass spectrometry to weight up biology. Nature. 2011;**469**(7330):300. DOI: 10.1038/469300a

[13] Hillenkamp F, Unsöld E, Kaufmann R, Nitsche R. A high-sensitivity laser microprobe mass analyzer. Applied Physics. 1975;**8**(4):341-348. DOI: 10.1007/BF00898368

[14] Baykut G, Franzen J. Mobile mass spectrometry; a decade of field applications. Trends in Analytical Chemistry. 1994;**13**:267-275

[15] Steger E. Strukturaufklärung-Spektroskopie und Röntgenbeugung. Leipzig: Deutscher Verlag fur Grundstoffindustrie; 1973

[16] Tănase GhI. Tehnici și Metode Spectrometrice de Analiză. Bucharest: Editura Ars Docendi; 2001

[17] Meyerson S. Reminiscences of the early days of MS in the petroleum industry. Organic Mass Spectrometry. 1986;**21**:197-208

[18] Quayle A. Recollections of MS of the fifties in a UK petroleum laboratory. Organic Mass Spectrometry. 1987;**22**:569-585

[19] Maccoll A. Organic mass spectrometry—The origins. Organic Mass Spectrometry. 1993;**28**: 1371-1372

[20] Meyerson S. Mass spectrometry in the news, 1949. Organic Mass Spectrometry. 1993;**28**: 1373-1374

[21] Meyerson S. From black magic to chemistry. The metamorphosis of organic MS. Analytical Chemistry. 1994;**66**:960A-964A

[22] Hoffman E De, Charette J, Strooband V. Mass Spectrometry: Principles and Application. New York: Wiley & Sons; 1996

[23] Lambert JB, Shurvell HF, Lightner D, Cooks RG. Introduction to Organic Spectroscopy. New York: Macmillan; 1987

[24] Watson JT. Introduction to Mass Spectrometry. 3rd ed. Philadelphia: Lippincott-Raven; 1997

[25] Rouessac F, Rouessac A. Analyse Chimique. Methodes et Techniques Instrumentales Modernes. 4th ed. Paris: Dunod; 1998

[26] Howe DH, Williams BRD. Mass Spectrometry. 2nd ed. Maidenhead: McGraw-Hill; 1981

[27] Karasek FW, Clement RE. Basic Gas Chromatography - Mass Spectrometry. Amsterdam: Elsevier; 1991

[28] Kitson FG, Larsen BS, McEwan CN. Gas Chromatography—Mass Spectrometry. London: Academic Press; 1996

[29] Harrison AG. Chemical Ionization Mass Spectrometry. 2nd ed. Boca Raton: CRC Press; 1992

[30] Nier AO. Some reflections on the early days of mass spectrometry at the University of Minnesota. International Journal of Mass Spectrometry and Ion Processes. 1990;**100**:1-13

[31] Price P. Standard definitions of terms relating to mass spectrometry. A report from the committee on measurements and standards of the ASMS. Journal of American Society of Mass Spectrometry. 1991;**2**:336-348

[32] Todd JFJ. Recommendations for nomenclature and symbolism for mass spectroscopy including an appendix of terms used in vacuum technology. International Journal of Mass Spectrometry Ion Processes. 1995;**142**:211-240

[33] De Graeve J, Berthon F, Prost M. Méthodes Chromatographiques coupplée à la Spectrométrie de Masse. Paris: Masson; 1986

[34] Constantin E, Schnell A. Spectrométrie de Masse, Principe et Applications. Paris: Lavoisier; 1986

[35] Cole RB. Electrospray Ionization Mass Spectrometry. New York: Wiley & Sons; 1997

[36] Fuerstenau SD, Benner WH. Molecular weight determination of megadalton DNA electrospray ions using charge detection time-of-flight-MS. Rapid Communication in Mass Spectrometry. 1995;**9**:1528-1538

[37] Felitsyn N, Peschke M, Kebarle P. Origin and number of charges observed on multiply-protonated native proteins produced by ESI. International Journal of Mass Spectrometry. 2002;**219**:39-62

[38] Kebarle P. A brief overview of the present status of the mechanisms involved in ESI-MS. Journal of Mass Spectrometry. 2000;**35**:804-817

[39] Straub RF, Voyksner RD. Negative ion formation in ESI-MS. Journal of American Society for Mass Spectrometry. 1993;**4**:578-587

[40] Beckey HD. Principles of Field Ionisation and Field Desorption Spectroscopy. Oxford: Pergamon Press; 1977. p. 335. DOI: 10.1002/bms.1200050710

[41] Bartolini WP, Johnston MV. Characterizing DNA photo-oxidation reactions by high resolution mass measurements with MALDI-TOF-MS. Journal of Mass Spectrometry. 2000;**35**:408-416

[42] Annar RS, Köchling HJ, Hill JA, Biemann K. Matrix-assisted laser desorption using a fast-atom bombardment ion source and a magnetic mass spectrometer. Rapid Communication for Mass Spectrometry. 1992;**6**:298-302

[43] Kühn G, Weidner S, Just U, Hohner S. Characterization of technical waxes. Comparison of chromatographic techniques and matrix-assisted laser-desorption/ionization-MS. Journal of Chromatography A. 1996;**732**:111-117

[44] Commission on Analytical Nomenclature of the Analytical Chemistry Division. Recommendation for nomenclature of mass spectrometry. Pure and Applied Chemistry. 1974;**37** (4):469-480

[45] Murray KK, Boyd RK, Eberlin MN, Langley GJ. Liang L, Yasuhide N. Definitions of terms relating to mass spectrometry (IUPAC Recommendations 2013). Pure and Applied Chemistry. 2013;**85**(7):1515-1609

[46] Yergey JA A general approach to calculating isotopic distributions for mass spectrometry. International Journal of Mass Spectrometry and Ion Physics. 1983;**52**:337-349

[47] Beynon JH. The compilation of a table of mass and abundance values. In: Mass Spectrometry and it's Applications to Organic Chemistry. 1st ed. Amsterdam: Elsevier; 1960. pp. 294-302

[48] McLafferty FW, Turecek F. Interpretation of Mass Spectra. 4th ed. Mill Valley: University Science Books; 1993

[49] Margrave JL, Polansky RB. Relative abundance calculations for isotopic molecular species. Journal of Chemical Education. 1962:335-337

[50] Brown DW, Floyd AJ, Sainsbury M. Organic Spectroscopy. New York: Wiley & Sons Inc; 1988. DOI: ISBN 10: 047191911X ISBN 13: 9780471919117

[51] Budzikiewicz H, Djerassi C, Williams DH. Mass Spectrometry of Organic Compounds. San Francisco: Holden-Day Inc; 1967. p. 690. DOI: 10.1002/jps.2600570236

[52] Chapman JR. Practical Organic Mass Spectrometry—A Guide for Chemical and Biochemical Analysis. 2nd ed. New York: John Wiley & Sons; 1993. p. 338. DOI: ISBN 047195831X 9780471958314

[53] McLafferty FW. Mass Spectrometry of Organic Ions. 2nd ed. New York: Academic Press, Elsevier; 1963

[54] McLafferty FW, Turecek F. Interpretation of Mass Spectra. 4th ed. Sansalito: University Science Books; 1993

[55] Schwarz H. The chemistry of naked molecules or the mass spectrometer as a laboratory. Chemie in Unserer Zeit. 1991;**25**:268-278

[56] Lorquet JC. Landmarks in the theory of mass spectra. International Journal of Mass Spectrometry. 2000;**200**:43-56

[57] Cappiello A, Famiglini G, Mangani F, Palma P. New trends in the application of electron ionization to liquid chromatography-mass spectrometry interfacing. Mass Spectrometry Reviews. 2001;**20**(2):88-104. DOI: 10.1002/mas.1004

[58] Koontz SL, Denton MB. A very high yield electron impact ion source for analytical mass spectrometry. International Journal of Mass Spectrometry and Ion Physics. 1981;**37**:227-239

[59] Pretsch E, Bühlmann P, Affolter C. Structure Determination of Organic Compounds. Tables of Spectral Data. 3rd ed. Berlin Heidelberg: Springer-Verlag; 2000. DOI: 10.1007/978-3-662-04201-4

[60] Schader S. Introductory Mass Spectrometry. Boston: Allyn and Bacon; 1971

[61] Schalley CA. Modern Mass Spectrometry. Berlin Heidelberg: Springer; 2003. DOI: 10.1007/3-540-36113-8

[62] Silverstein RM, Webster FX, Kiemle DJ. Spectrometric Identification of Organic Compounds. 7th ed. New York:Wiley; 2005. ISBN 10: 0471393622/ISBN 13: 9780471393627

[63] Stenhagen E, Abrahamson S, McLafferty FW. Register of Mass Spectral Data. New York: Wiley-Interscience; 1974

[64] Svec HJ, Junk GA. Electron-impact studies of substituted alkanes. Journal of American Chemical Society. 1967;**89**:790-796

[65] McLafferty FW. Mass spectrometric analysis. I. Aliphatic halogenated compounds. Analytical Chemistry. 1962;**34**:2-15

[66] Friedel RA, Shultz JL, Sharkey AG Jr. Mass spectra of alcohols. Analytical Chemistry. 1956;**28**:927-934

[67] Djerassi C, Fenselau C. Mass spectrometry in structural and stereochemical problems. LXXXIV. The nature of the cyclic transition state in hydrogen rearrangements of aliphatic ethers. Journal of American Chemical Society. 1965;**87**:5747-5762

[68] Sozzi G, Audier H E, Mourgues P, Milliet A. Alkyl phenyl ether radical cations in the gas phase: A reaction model. Organic Mass Spectrometry. 1987;**22**:746-747

[69] Morton TH. Ion-molecule complexes in unimolecular fragmentations of gaseous cations. Alkyl phenyl ether molecular ions. Journal of American Chemical Society. 1980;**102**:1596-1602

[70] Blanchette MC, Holmes JL, Lossing FP. The fragmentation of ionized alkyl phenyl ethers. Organic Mass Spectrometry. 1989;**24**:673-678

[71] Harnish D, Holmes JL. Ion-radical complexes in the gas phase: Structure and mechanism in the fragmentation of ionized alkyl phenyl ethers. Journal of American Chemical Society. 1991;**113**:9729-9734

[72] Liedtke RS, Djerassi C. Mass spectrometry in structural and stereochemical problems. CLXXXIII. A study of the electron impact induced fragmentation of aliphatic aldehydes. Journal of American Chemical Society. 1969;**91**:6814-6821

[73] Henion JD, Kingston DGI. Mass spectrometry of organic compounds IX. McLafferty rearrangements in some bicyclic ketones. Journal of American Chemical Society. 1974;**96**: 2532-2536

[74] Rădulescu V, Oprea E, Chiliment S. Isolation and Analysis Methods of Volatile Compounds from Flowers and Leaves in Floriculture, Ornamental and Plant Biotechnology: Advanced and Topical Issues. 1st ed. Teixeira da Silva JA, UK: Global Science Books; 2006

[75] Pfleger K, Maurer H, Weber A. Mass Spectra and GC Data of Drugs, Pesticides, Polluants and Their Metabolites, Part I-IV. New York: Wiley & Sons; 2000

[76] Lehmann WD, Bohne A, von der Lieth CW. The information encrypted in accurate peptide masses—Improved protein identification and assistance in glycopeptide identification and characterization. Journal of Mass Spectrometry. 2000;**35**:1335-1341

[77] Maux D, Enjalbal C, Martinez J,.Aubagnac. Ion mass spectrometry to monitor solid-phase peptide synthesis. Journal of the American Society for Mass Spectrometry. 2001;**12**:1099-1105

[78] McLafferty FW. Registry of Mass Spectral Data. 5th ed. New York: Wiley; 1989

[79] McLafferty FW, Stauffer DB. Wiley/NBS Registry of Mass Spectral Data. New York: Wiley; 1989. p. 7872. ISBN: 978-0-471-62886-6

[80] Reed RI. Electron impact and molecular dissociation. Part I. Some steroids and triterpenoids. Journal of Chemical Society. 1958:3432-3436

[81] Ionescu C, Țârcomnicu I, Ionescu MA, Nicolescu TO, Boda D, Nicolescu F. Identification and characterization of the methanolic extract of hellebrigenin 3-acetate from hellebori rhizomes. II. Mass spectrometry. Revista de Chimie., Vol.1, 2014;**65**(8):972-975

[82] Mouget Y, Bertrand M J. Graphical method for artefact peak interpretation and methods for their rejection, using double and triple sector magnetic mass spectrometers. Rapid Communication for Mass Spectrometry. 1995;**9**:387-396

[83] McLafferty FW, Stauffer DB, Loh SY. Comparative evaluations of mass spectral data bases. Journal of American Society for Mass Spectrometry. 1991;**2**:438-440

[84] Lebedev KS, Cabrol-Bass D. New computer aided methods for revealing structural features of unknown compounds using low resolution mass spectra. Journal of Chemical Information and Computer Science. 1998;**38**:410-419

[85] Stein SE. Estimating probabilities of correct identification from results of mass spectral library searches. Journal of American Society for Mass Spectrometry. 1994;**5**:316-323

[86] Smith RM, Busch KL. Understanding Mass Spectra—A Basic Approach. 1st ed. New York: John Wiley & Sons; 1999

[87] Porter CJ, Beynon JH, Ast T. The modern mass spectrometer. A complete chemical laboratory. Organic Mass Spectometry. 1981;**16**:101-114

[88] Oprean I. Spectrometria de Masă a Compușilor Organici. Cluj: Editura Dacia; 1974

Chapter 3

Performing Quantitative Determination of Low-Abundant Proteins by Targeted Mass Spectrometry Liquid Chromatography

Tore Vehus

Additional information is available at the end of the chapter

http://dx.doi.org/10.5772/intechopen.68713

Abstract

Mass spectrometry coupled to nanoliquid chromatography aims to be an alternative to antibody-based determination of low-abundant proteins. High-resolution mass spectrometers, plug-and-play systems and pumps have been developed for this purpose. Important aspects of approaches are limit of detection, specificity, variability and cost. In this chapter, the most recent literature (from 2008) has been reviewed and a checklist/workflow for targeted proteomics is presented with special focus on low-abundant proteins in complex matrices. The chapter is intended to serve as a starting point for low-abundant target determination and highlights some of the most central studies in this field.

Keywords: targeted mass spectrometry, nanoliquid chromatography, proteomics, tandem mass spectrometry

1. Introduction

The ~1,000,000 different proteins (including modifications) determine much of an organism function. The protein abundance range from 0.01 to 10,000 ppm [1] in humans, a major challenge when working in the low ppm-area.

Obtaining qualitative and quantitative information of proteins is of interest in biological systems, analysing samples such as cells [2, 3], tissue [4], blood [5] or extracellular vesicles [6, 7]. However, determinations of these are not that straightforward, although several 'routine-based' methods exist in industry, research laboratories and clinics (see **Table 1**) [8, 9].

INTECH
open science | open minds

© 2017 The Author(s). Licensee InTech. This chapter is distributed under the terms of the Creative Commons Attribution License (http://creativecommons.org/licenses/by/3.0), which permits unrestricted use, distribution, and reproduction in any medium, provided the original work is properly cited. CC BY

	Living organism	Timing*	Quantification	Quantification value	User demand
Immunofluorescence (IF)	+	1 day	++	Relative	+
ELISA	–	30 minutes–6 hours	++	Relative/absolute	+
SDS-PAGE + silver staining/ Coomassie blue	–	30 minutes–4 hours	+	Relative	+
Western blot (WB)	–	30 minutes–2 days	++	Relative	+
LC-MS/MS	–	4 hours–2 days	+++	Relative/absolute	+++

+, equals low user demand and cost; +++, equals high user demand and cost.
*Estimated duration from in-house experience

Table 1. Comparison of methods used to quantify proteins in biological samples.

Determination of proteins through targeted tandem mass spectrometry (tMSMS) with nanoliquid chromatography (nanoLC) has gained interest in the last 10 years; major reason is increased sensitivity through LC downscaling and more accurate and sensitive mass spectrometers [10–14]. This enhanced sensitivity enables digging deeper into a sample, which may provide the desired data, compared to attempting whole-proteome determination (comprehensive proteomics, demonstrated by Thakur et al. [15] and Pirmoradian et al. [16]).

This chapter provides a short introduction to the state of the art targeted nanoliquid chromatography-mass spectrometry (nanoLC-MS/MS), recent examples from literature and finally a workflow suitable for confident determination and quantification of proteins in complex matrices.

1.1. Proteomics by mass spectrometry

Proteomics is the large-scale measurement of proteins [10, 17]. Study of the proteome and set of proteins are nowadays often standard in cancer, studies of extracellular vesicles, blood analysis, etc. Proteomics by mass spectrometry can mainly be divided into two major approaches: comprehensive and targeted approach.

In comprehensive proteomics, the goal is to identify as many proteins as possible based on search algorithms (e.g. Mascot [18], SEQUEST [19], MSAmanda [20], Andromeda [21]). In targeted proteomics, the target protein(s) is known [22]. The latter is focused in this chapter. In addition to the two approaches, proteomics is often divided into whether proteins analysed intact (top-down proteomics) or in pieces (bottom-up proteomics). Bottom-up proteomics is mainly used, as the smaller pieces of proteins are easier to handle in liquid chromatography, easier to transfer to mass spectrometer and data analysis is also easier.

For over 10 years, the quest to implement quantitative proteomics for biomarker studies has been debated and attempted [4, 23–27]. Although LC-MS has been the standard approach to small molecule analysis, there is still a way to go before proteomics enters the clinic.

1.2. Targeted nanoLC-MS/MS, a rapid overview

In most targeted nanoLC-MS/MS approaches, peptides are used, due to their easy transfer through electrospray ionization (ESI), and favourable LC traits. In most cases, Trypsin and/or LysC are/is chosen to cleave the proteins, although other enzymes are also used [28]. A set of peptides containing a protein-specific sequence representing the target protein are selected; proteotypic/signature peptides. In the selection process, the UniProt database [29], Expasy [30], Skyline [31] and PeptideAtlas [32] can be helpful. After selection, the peptides are normally bought as synthetic labelled standards (i.e. Absolute quantification (AQUA) peptides [33]) as ideal internal standards, and subsequently chromatographed and detected on the nanoLC-MS/MS platform available.

The golden standard in nanoLC is usually a 75 μm inner diameter (ID) column packed with 2–3 μm diameter silica-particles functionalized with C18-phase. A solid-phase extraction (SPE) column is often connected on-line, to increase loading capacity [34].

The chromatographed peptides elute, ideally at different retention times and are transferred to the MS through ESI. In later years, quadrupole-Orbitraps (QOrbitrap) and quadrupole time-of-flight (QTOF) instruments have been introduced in targeted MS/MS, alongside triple quadrupoles (QqQ). The two first options provide higher resolution compared to traditional QqQ, and thus less interferences [35, 36]. Common for the instruments is that a parent mass-to-charge (*m*/*z*) is monitored in the first quadrupole and fragmented prior to the second mass analyser. In QqQ and QTOF instruments, collision induced dissociation (CID) is the most common, whereas in QOrbitrap instruments, higher energy collision induced dissociation is used (HCD). The main daughter ions in either dissociation are positive *b* and *y* ions. For QqQ, multiple-reaction monitoring (MRM) and selected reaction monitoring (SRM) are most common, whereas for the QOrbitrap and QTOF, a mode referred to as parallel reaction monitoring (PRM) is mostly used (**Figure 1**).

In SRM or MRM mode, both the parent and fragment *m*/*z* ratios have to be inserted into the method, whereas for the PRM mode, only the parent *m*/*z* ratio is inserted, and all fragment *m*/*z* ratios are recorded and can be isolated after data acquisition in the software of choice.

1.3. Peptide selection: considerations regarding proteotypic peptides

Peptides used for LC-MS/MS identification usually contains between 6 and 20 amino acids in sequence [37]. The proteotypic peptides should ideally not contain amino acids which are prone to modifications, either during sample preparation or in the biological system. Hence, methionine, tryptophane, tyrosine and cysteine are often not chosen when possible. Although, if no other proteotypic peptide exists, the normal rate of phosphorylation, for example, is less than 5%, which may be neglected. Methionine oxidation is one of the most common modifications in bottom-up proteomics, mainly due to sample handling. Hence, quantification based on a peptide containing methionine is not preferable, except when using labeled proteins as internal standards which can correct for this.

1.4. Quantification of proteins with tMSMS: labelled proteins versus labelled peptides

The major advantage of LC-MS/MS-based proteomics over Enzyme-linked immunosorbent assay (ELISA), WB or IF-based proteomics is the quantification quality [38]. Quantification in

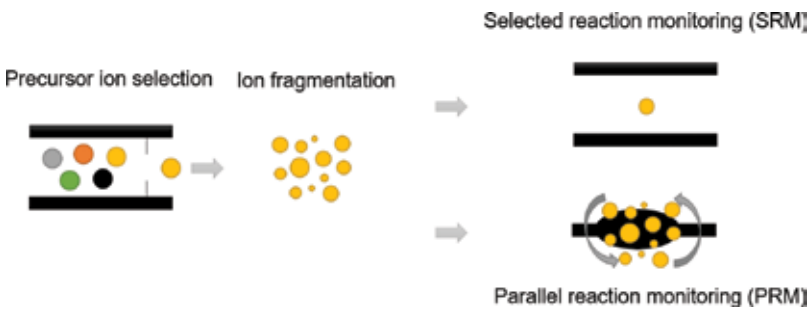

Figure 1. Selected reaction monitoring (SRM) where single ion transitions are monitored in contrast to parallel reaction monitoring (PRM) where a single ion is fragmented into several fragment ions and monitored.

tMSMS is mainly based on heavy labelled peptides (normally ^{15}N and/or ^{13}C isotopes of arginine and lysine) which are added to the sample as internal standard. In contrast antibodies, housekeeping proteins are usually used for standardization. In later years, the housekeeping protein method has been criticized, as these may change in experiments [39]. But there are also a pitfall using synthetic internal standard peptides, namely variation during cleavage of proteins to peptides [28, 40]. Up to 85% of the variation in bottom-up proteomics arises from enzymatic cleavage [40]. Hence, addition of synthetic heavy-labelled proteins as internal standards is a far better approach, but may prove to be more costly. As shown in **Figure 2**, using labelled proteins can correct for sample preparation as well as data analysis, whereas labelled peptides only correct for sample preparation on peptide level and not sample preparation on protein level which often is needed for low-abundant target isolation techniques.

Correction of all steps involved in analyses is important, with internal standards, software and manual inspection of data [26, 41–43].

1.5. Reducing sample complexity

Proteomics of low-abundant targets often requires specialized sample clean-up. Removal of high-abundant targets, direct target isolation and fractionation are among the most common approaches. In blood, a common approach is a removal of the most abundant targets by multi-affinity removal system (MARS), lowering the dynamic range of the sample. However, with this approach, the target(s) may also be lost due to protein-protein interactions, and quantification may be an issue. Yadav et al. claims that for a biomarker discovery, both depleted fractions and non-depleted fractions should be analysed [44]. Recently, oxytocin was shown to have a high degree of binding to blood proteins, which severely affects quantification [45]. An alternative approach is a direct target isolation aiming to isolate the protein(s) of interest [46]. This is also quite effective, but time-consuming and rather costly. Additionally, proper

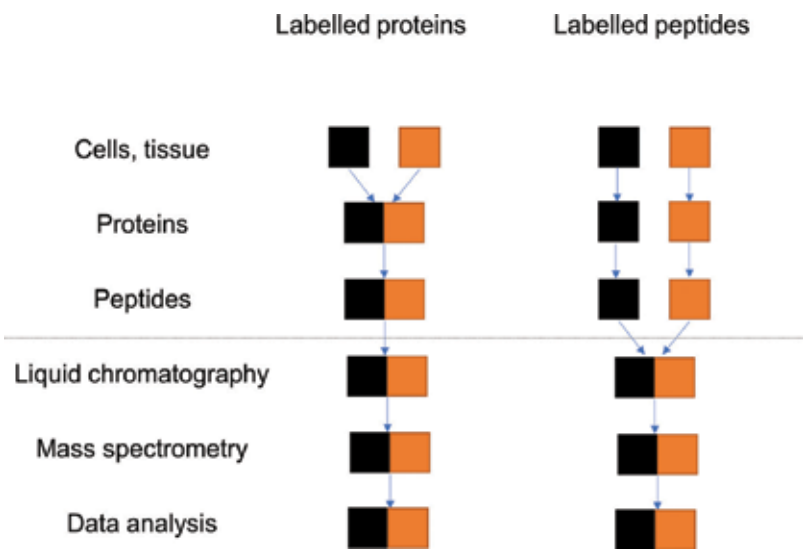

Figure 2. Labelled proteins compared to labelled peptides in bottom-up targeted proteomics.

control of isolation efficiency with proper protein internal standards is needed. The latter has been shown by Edfors et al. where protein targets were isolated with polyclonal antibodies in HeLa spiked with recombinant protein internal standards [47]. Fractionating proteins by LC and gel electrophoresis is also common for reducing sample complexity.

1.6. Downscaled LC systems: enhanced sensitivity with ESI-MS

In 2002, Shen et al. displayed a ~200-fold increase in sensitivity when downscaling LC columns from 75 to 15 μm when connected to ESI-MS [48]. Fifteen years later, proteomics in 75–50 μm format has become commercially available through the largest instrument manufacturers [34, 42], whereas more downscaled systems are used for even higher sensitivity. For peptides, the demonstrated sensitivity is in the attomolar-zeptomolar range. A major drawback with downscaled systems is that they traditionally are often low-capacity systems, i.e. sample capacity is lower on these systems compared to conventional larger ID systems. Hence, using strong cation exchange (SCX) columns on-line [49] or high capacity solid phase extraction columns (poly-styrene-octadecene-divinylbenzene, PS-OD-DVB [50]) often needed to take full advantage of the increased sensitivity of such downscaled systems [51].

1.7. Mass spectrometers: selectivity and sensitivity

Selectivity and sensitivity are among the two most important aspects of low-abundant target determination by mass spectrometry. Selectivity in this context is defined as the ability to differentiate between masses, and the mass spectrometers selectivity is often characterized by measuring full width at half maximum-value (FWHM), where a high value is better. Sensitivity at which the signal level is higher than the noise is often characterized by a signal-to-noise ratio. In **Table 2**, the resolution and mass accuracy are reported for the three most common mass analysers used in targeted mass spectrometry today.

The resolution for the QTOF and QOrbitrap instruments is up to 20 times as large as a typical QqQ-instrument. In MS/MS, interferences are common and Gallien et al. showed that high-resolution of a QOrbitrap instrument is superior in eliminating these, compared to QqQ-instruments [35]. Additionally, we have earlier showed that at least three transitions are needed (even with high-resolution QOrbitrap) to eliminate false positives [42].

A sketch of important technological developments (**Figure 3**) developing targeted proteomics by NanoLC-MS/MS highlights the importance of hardware developments, such as ESI, QOrbitrap instruments, sample preparation strategies, such as Stable isotope labeling by amino acids in cell culture (SILAC) and software/database developments (e.g. Skyline and UniProt).

Mass spectrometer	Resolution	Mass accuracy
Triple quadrupole	2000–10,000	100 ppm
QOrbitrap	140,000–240,000	2 ppm
QTOF	100,000	2–5 ppm

Table 2. Resolution and mass accuracy of common mass spectrometers used for targeted proteomics.

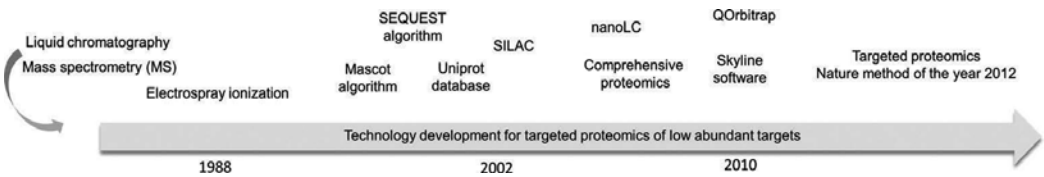

Figure 3. Selected technological developments aiding targeted proteomics by nanoLC-MS/MS.

2. Selected studies in targeted mass spectrometry

In the following subsections, a set of studies performing targeted mass spectrometry of proteins in various biological samples will be presented and discussed with emphasis on high-quality targeted proteomics results and lead to a protocol for targeted mass spectrometry of low-abundant targets.

In 2014, a study by Edfors et al. demonstrated use of recombinant manufactured proteins labelled with SILAC mixture as internal standard [47]. To approximately lysate from 1 million HeLa cells, 1 pmol of recombinant proteins were added and digested with trypsin. The resulting peptide mixture was then immunoprecipitated with protein antibodies applied on peptides, which is cheaper than ordering specific peptide-recognizing antibodies. With the lowered complexity and increased concentration, 57 of 127 proteins were identified by at least one peptide in data-dependent acquisition (i.e. not tMSMS). Even though this study is not used with tMSMS, it evaluates and presents a method for immunoprecipitation on peptide level with protein antibodies which enables easier access to targets. Additionally, it keeps quantification in mind with the use of protein internal standards. Additionally, reduction of complexity meant that the LC-MS analysis could be reduced from 3 hours to 15 minutes. The relative standard deviation in the study ranged from 10 to 40%, which for some targets is somewhat higher than the required 10–20% as set by the Food and Drug Administration and others [52, 53].

In contrast to the protein internal standard, peptide internal standards have also recently been used for quantitative proteomics in breast cancer cells [54]. 319 protein targets were monitored and from this selection, coefficients of variations for 79 of the protein targets presented. For each target a heavy labelled proteotypic peptide was added. A pool of breast cancer cells was lysed at one specific location and distributed to three sites, where sample preparation and analysis were conducted. The authors report a median variation within and between laboratories <10% for 95% of the monitored targets. The study shows a feasibility for tMSMS analysis of high-abundant targets, whenever extensive pre-fractionation is not needed and protocols are made carefully.

The dynamic range of proteins in blood/serum/plasma is far more demanding than cells [5]. Hence, searching for low-abundant proteins in this matrix often requires depletion strategies. But, other strategies can also be used to increase detection limits. Recently, a study showed that with internal standard triggered parallel reaction monitoring (IS-PRM), a lower

limit of quantification can be reached, compared to traditional SRM [55]. With the use of algorithms and synthetic internal standard AQUA peptides, data acquisition of endogenous peptides was triggered by detection of IS-peptides during chromatography (for comprehensive proteomics, this is known as data-independent acquisition (DIA)). For example, at a peptide amount of 50 amol using IS-PRM could use ~300 transitions, whereas SRM could use ~50 transitions. The reason could be attributed to a much higher resolution of the QOrbitrap compared to the QqQ instrument, and more dedicated use of the mass analyser with real-world triggered analysis, enabling high fill times.

Another study from 2011 used accurate inclusion mass screening (AIMS [56]), comprehensive proteomics and targeted proteomics to verify biomarkers in plasma [25]. Using depleted plasma and comprehensive proteomics, a selection of candidates for biomarker analysis was made and transferred to an SRM method with internal standard peptides. Of the 373 targets investigated in SRM, only 164 of these were identified with >3 transitions per peptide, which is attributed to the targets abundance. The study however makes a very important point regarding tMSMS-procedures. It must be made cost-effective compared to ELISA and Western blot (WB).

A highly promising tool, developed a few years back, compares the relative intensities between the ions in the internal standard and the endogenous target (**Figure 4** adapted from Ref. [43]).

The check, of course, could be performed manually, but for large datasets automation is desirable. The authors showed that the developed algorithm worked in 90–100% of the cases, and that specificity was above 80%.

The hunt for low-abundant targets can, as previously mentioned, be accomplished with fractionation. A study aimed for detection of prostate specific antigen (PSA) in serum samples in pg/mL-level by depletion and fractionation [57]. Specifically, serum samples were depleted of high-abundance proteins, digested with trypsin, spiked with internal standard peptide and

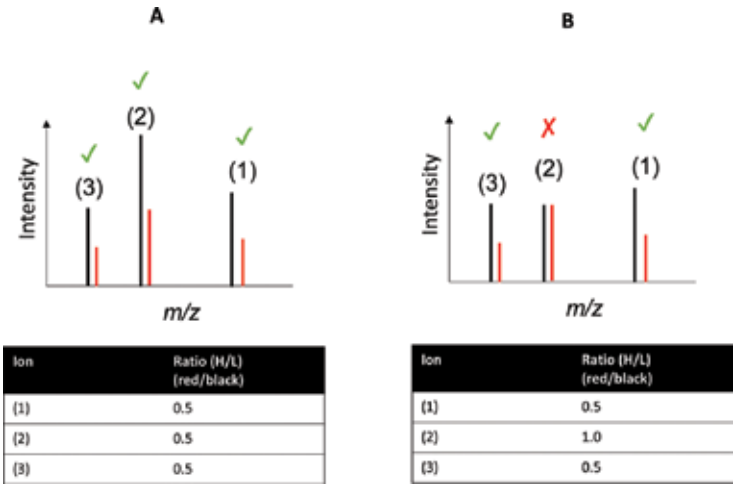

Ion	Ratio (H/L) (red/black)
(1)	0.5
(2)	0.5
(3)	0.5

Ion	Ratio (H/L) (red/black)
(1)	0.5
(2)	1.0
(3)	0.5

Figure 4. (A) Transitions and relative intensities for three ions (1–3) where the relative ratio is constant and target is verified. (B) Same as (A), but relative ratio of ion 2 is not equal to the ratio of ions 1 and 3 and target is discarded.

resulting peptides LC fractionated at high pH. Approximately 9% of the eluent were introduced directly onto an LC-MS system, and the remaining 91% was fractionated on 96 well plates. This allows for determining which of the fractions containing the target peptide and which subsequently could be pooled and analysed by LC-SRM. They reached correlation coefficients of >0.99, limits of quantifications of 50 pg/mL for PSA and CV of <<10%. As the authors discuss, the throughput is lower with fractionation, but for specialized applications fractionation may be necessary.

Some of the presented studies above have successfully used peptide internal standards for quality control during analysis and quantification. Alternatively, labelled proteins can be used and another approach that has gained interest in the later years is protein standard absolute quantification (PSAQ™ [58]). Proteins are made recombinantly in e.g. bacteria and labelled metabolically with heavy lysine and arginine. These are subsequently purified based on tags (e.g. His6X, glutathione S-transferase tag, etc.). Full-length or partial proteins can be made with this approach. As shown in **Figure 2**, these can be added directly after proteins have been extracted from the organism and used for normalization. However, as the authors describe, the necessary protein-tag affects the protein and it is not an ideal internal standard in that way, and hence must be evaluated. Nonetheless, this approach has recently been used for detection of toxins in food [59] and acute kidney injury biomarkers in urine [60].

3. Brief summary and possible areas of applications

Targeted mass spectrometry has increased in popularity with easier access to databases, LC-MS equipment, methods and software. **Table 3** lists a selection of the cited literature on which this chapter is based on and divided into appropriate sections for easier access.

High-sensitivity mass spectrometers and miniaturized liquid chromatography operating at 20–200 nL/minute in systems have been introduced, enabling low zeptomolar detection of peptides in various complex matrices. Specificity has increased with high-resolution mass spectrometers having >30,000 resolution. Variation is the main bottleneck for quantitative mass spectrometry entering clinical use, mainly due to the use of non-ideal internal standards. Costs are still high, but developments in easy transfer of methods and easy standard production have reduced the cost/benefit ratio.

Keyword	Some references
Databases	[29, 32]
Quantification	[25, 54, 55, 58, 60]
Liquid chromatography	[2, 3, 13, 42, 49, 51]
Mass spectrometry	[10, 11, 35, 56]
Data treatment	[18–21, 30, 31]

Table 3. A selection of studies referenced in the chapter focused on databases, quantification, liquid chromatography, mass spectrometry and data treatment.

Determination of proteins in extracellular vesicles has been proposed as a tool for early prognosis of cancer, and as the vesicles themselves are in low abundance, the protein amount found within them is also in extremely low abundance [61, 62]. Blood is also a very interesting sample matrix for targeted proteomics, as sample acquisition is relatively low-invasive (compared to tissue) and contains a vast majority of biomarkers for diseases, and where the low-abundant targets may give future information for early diagnosis of diseases. With highly sensitive systems, determination of important pathway proteins can be achieved [63], and with future development of robust quantification techniques for proteins such systems can be applied to tissue, cells and urine as well, and gain their way in clinical diagnostic applications together with DNA and metabolite screening.

4. Four-point workflow for bottom-up-based proteomics of low-abundant targets

Based on the few selected studies, a four-step guide to confident low-abundant protein identification is presented (**Figure 5**). The workflow can either be used for relative quantification or absolute quantification depending on knowledge about the protein internal standard.

4.1. Standard and internal standard preparation

Determine protein targets and use UniProt, PeptideATLAS, SRMAtlas and Skyline to find appropriate proteotypic peptides for your protein (minimum two peptides for each protein).

Based on the origin of your sample; prepare a metabolically labelled internal standard, e.g. SILAC labelled cell line for tissue/cells studies or recombinant with ^{15}N, ^{13}C isotopes. For absolute protein quantification, the target protein concentration in the internal standard is needed.

4.2. LC-MS/MS method development

Monitor LC retention time with AIMS platform and data-dependent proteomics with the labelled internal standard if possible and make sure that perform retention time is. For extra low-abundant proteins, acquire recombinant proteins which can be used to prepare stable peptides, or if not available buy recombinant peptides (not necessarily labelled).

For the LC-system in question: optimize chromatography with adjusting gradient slope, gradient time, column choice, etc.

If available, use a high-resolution mass spectrometer with mass resolution >30,000. Perform LC-MS/MS analysis of the peptides in question, optimize parameters to enable highest possible signal to noise (S/N) ratio and highest fragment ion intensities and finally determine ion intensity ratios.

4.3. Sample preparation

Acquire the sample(s) in question and add the protein internal standard in the process as early as possible. Choose the appropriate sample preparation strategy depending on the target abundance (MARS-depletion, immunoaffinity purification or similar)

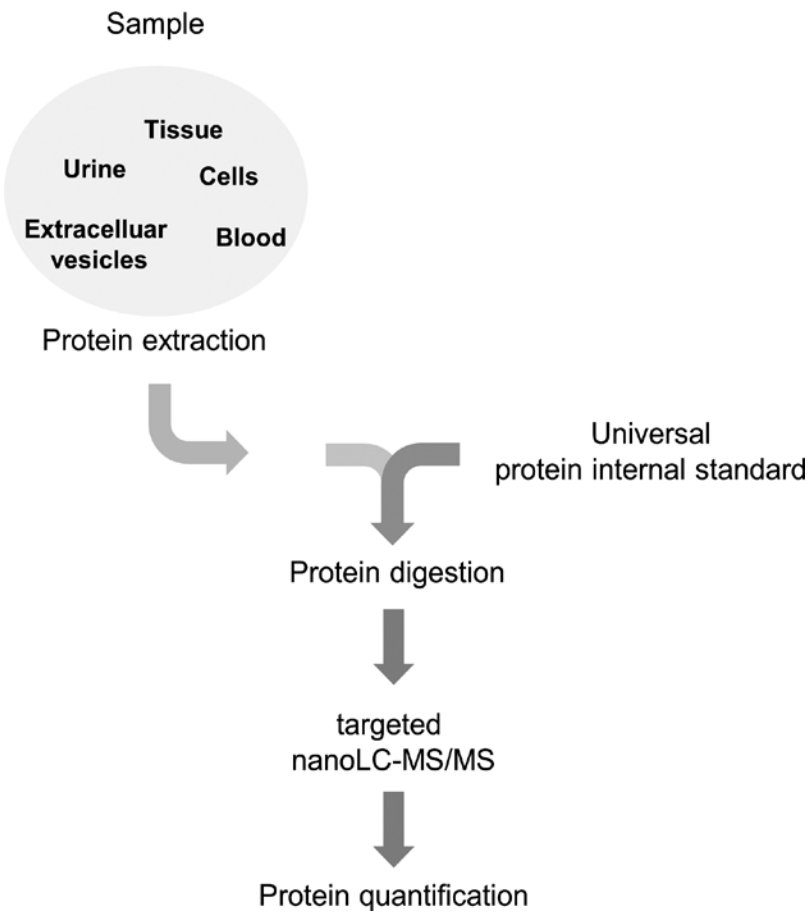

Figure 5. Schematic drawing of workflow for targeted nanoLC-MS/MS of low-abundant protein targets in cells, tissue, blood, extracellular vesicles and urine.

4.4. LC-MS/MS analysis

With the established method, analyse the sample and with the determined ion intensity ratios, retention time, etc. validate your targets either manually or with software (i.e. Skyline). Use target/internal standard ion ratio for complete method variation correction.

Author details

Tore Vehus

Address all correspondence to: tore.vehus@uia.no

1 Department of Engineering Sciences, University of Agder, Grimstad, Norway

2 Department of Chemistry, University of Oslo, Oslo, Norway

References

[1] Wang M, Weiss M, Simonovic M, Haertinger G, Schrimpf SP, Hengartner MO, et al. PaxDb, a database of protein abundance averages across all three domains of life. Molecular & Cellular Proteomics. 2012;**11**(8):492–500

[2] Olsen PA, Solberg NT, Lund K, Vehus T, Gelazauskaite M, Wilson SR, et al. Implications of targeted genomic disruption of β-catenin in BxPC-3 pancreatic adenocarcinoma cells. PLoS One. 2014;**9**(12):e115496

[3] Cohen AA, Geva-Zatorsky N, Eden E, Frenkel-Morgenstern M, Issaeva I, Sigal A, et al. Dynamic proteomics of individual cancer cells in response to a drug. Science (New York, NY). 2008;**322**(5907):1511–1516

[4] Liu NQ, Braakman RB, Stingl C, Luider TM, Martens JW, Foekens JA, et al. Proteomics pipeline for biomarker discovery of laser capture microdissected breast cancer tissue. Journal of Mammary Gland Biology and Neoplasia. 2012;**17**(2):155–164

[5] Anderson NL, Anderson NG. The human plasma proteome: History, character, and diagnostic prospects. Molecular & Cellular Proteomics: MCP. 2002;**1**(11):845–867

[6] Choi DS, Kim DK, Kim YK, Gho YS. Proteomics of extracellular vesicles: Exosomes and ectosomes. Mass Spectrometry Reviews. 2015;**34**(4):474–490

[7] Raposo G, Stoorvogel W. Extracellular vesicles: Exosomes, microvesicles, and friends. Journal of Cell Biology. 2013;**200**(4):373–383

[8] Yalow RS, Berson SA. Immunoassay of endogenous plasma insulin in man. The Journal of clinical investigation. 1960;**39**:1157–1175

[9] Towbin H, Staehelin T, Gordon J. Electrophoretic transfer of proteins from polyacrylamide gels to nitrocellulose sheets: Procedure and some applications. Proceedings of the National Academy of Sciences of the United States of America. 1979;**76**(9):4350–4354

[10] Aebersold R, Mann M. Mass spectrometry-based proteomics. Nature. 2003;**422**(6928):198–207

[11] Mann M. Origins of mass spectrometry-based proteomics. Nature Reviews Molecular Cell Biology. 2016;**17**(11):678

[12] Kocher T, Pichler P, Pra MD, Rieux L, Swart R, Mechtler K. Development and performance evaluation of an ultra-low flow nano liquid chromatography-tandem mass spectrometry set-up. Proteomics. 2014;**14**(17–18):1999–2007

[13] Rogeberg M, Vehus T, Grutle L, Greibrokk T, Wilson SR, Lundanes E. Separation optimization of long porous-layer open-tubular columns for nano-LC-MS of limited proteomic samples. Journal of Separation Science. 2013;**36**(17):2838–2847

[14] Bereman MS, Hsieh EJ, Corso TN, Van Pelt CK, Maccoss MJ. Development and characterization of a novel plug and play liquid chromatography-mass spectrometry (LC- MS)

source that automates connections between the capillary trap, column, and emitter. Molecular & Cellular Proteomics: MCP. 2013;**12**(6):1701–1708

[15] Thakur SS, Geiger T, Chatterjee B, Bandilla P, Fröhlich F, Cox J, et al. Deep and highly sensitive proteome coverage by LC-MS/MS without prefractionation. Molecular & Cellular Proteomics. Mol Cell Proteomics. 2011 Aug;**10**(8):M110.003699. doi: 10.1074/mcp.M110.003699.

[16] Pirmoradian M, Budamgunta H, Chingin K, Zhang B, Astorga-Wells J, Zubarev RA. Rapid and deep human proteome analysis by single-dimension shotgun proteomics. Molecular & Cellular Proteomics. 2013;**12**(11):3330–3338

[17] Anderson NL, Anderson NG. Proteome and proteomics: New technologies, new concepts, and new words. Electrophoresis. 1998;**19**(11):1853–1861

[18] Perkins DN, Pappin DJ, Creasy DM, Cottrell JS. Probability-based protein identification by searching sequence databases using mass spectrometry data. Electrophoresis. 1999;**20**(18):3551–3567

[19] Tabb DL. The SEQUEST family tree. Journal of the American Society for Mass Spectrometry. 2015;**26**(11):1814–1819

[20] Dorfer V, Pichler P, Stranzl T, Stadlmann J, Taus T, Winkler S, et al. MS Amanda, a universal identification algorithm optimized for high accuracy tandem mass spectra. Journal of Proteome Research. 2014;**13**(8):3679–3684

[21] Cox J, Neuhauser N, Michalski A, Scheltema RA, Olsen JV, Mann M. Andromeda: A peptide search engine integrated into the MaxQuant environment. Journal of Proteome Research. 2011;**10**(4):1794–1805

[22] Han X, Aslanian A, Yates JR. Mass spectrometry for proteomics. Current Opinion in Chemical Biology. 2008;**12**(5):483–490

[23] Rifai N, Gillette MA, Carr SA. Protein biomarker discovery and validation: the long and uncertain path to clinical utility. Nature Biotechnology. 2006;**24**(8):971–783

[24] Grebe SKG, Singh RJ. LC-MS/MS in the clinical laboratory—where to from here? The Clinical Biochemist Reviews. 2011;**32**(1):5–31

[25] Whiteaker JR, Lin C, Kennedy J, Hou L, Trute M, Sokal I, et al. A targeted proteomics-based pipeline for verification of biomarkers in plasma. Nature Biotechnology. 2011;**29**(7):625–634

[26] Addona TA, Abbatiello SE, Schilling B, Skates SJ, Mani DR, Bunk DM, et al. Multi-site assessment of the precision and reproducibility of multiple reaction monitoring-based measurements of proteins in plasma. Nature Biotechnology. 2009;**27**(7):633–641

[27] Hanash SM, Pitteri SJ, Faca VM. Mining the plasma proteome for cancer biomarkers. Nature. 2008;**452**(7187):571–579

[28] Tsiatsiani L, Heck AJR. Proteomics beyond trypsin. FEBS Journal. 2015;**282**(14):2612–2626

[29] Consortium U. The universal protein resource (UniProt). Nucleic Acids Research. 2008; **36**(suppl 1):D190-D195

[30] Gasteiger E, Gattiker A, Hoogland C, Ivanyi I, Appel RD, Bairoch A. ExPASy: The proteomics server for in-depth protein knowledge and analysis. Nucleic Acids Research. 2003;**31**(13):3784-3788

[31] MacLean B, Tomazela DM, Shulman N, Chambers M, Finney GL, Frewen B, et al. Skyline: An open source document editor for creating and analyzing targeted proteomics experiments. Bioinformatics. 2010;**26**(7):966–968

[32] Deutsch EW, Lam H, Aebersold R. PeptideAtlas: A resource for target selection for emerging targeted proteomics workflows. EMBO Reports. 2008;**9**(5):429–434

[33] Gerber SA, Rush J, Stemman O, Kirschner MW, Gygi SP. Absolute quantification of proteins and phosphoproteins from cell lysates by tandem MS. Proceedings of the National Academy of Sciences. 2003;**100**(12):6940–6945

[34] Wilson SR, Vehus T, Berg HS, Lundanes E. Nano-LC in proteomics: Recent advances and approaches. Bioanalysis. 2015;**7**(14):1799–1815

[35] Gallien S, Duriez E, Demeure K, Domon B. Selectivity of LC-MS/MS analysis: Implication for proteomics experiments. Journal of Proteomics. 2013;**81**:148–158

[36] Kiyonami R, Schoen A, Prakash A, Peterman S, Zabrouskov V, Picotti P, et al. Increased selectivity, analytical precision, and throughput in targeted proteomics. Molecular & Cellular Proteomics. Mol Cell Proteomics. 2011 Feb;**10**(2):M110.002931. doi: 10.1074/mcp.M110.002931

[37] Chiva C, Sabidó E. Peptide selection for targeted protein quantitation. Journal of Proteome Research. 2017

[38] Aebersold R, Burlingame AL, Bradshaw RA. Western blots versus selected reaction monitoring assays: Time to turn the tables? Molecular & Cellular Proteomics: MCP. 2013;**12**(9):2381–2382

[39] Ferguson RE, Carroll HP, Harris A, Maher ER, Selby PJ, Banks RE. Housekeeping proteins: A preliminary study illustrating some limitations as useful references in protein expression studies. Proteomics. 2005;**5**(2):566–571

[40] van den Broek I, Romijn FPHTM, Smit NPM, van der Laarse A, Drijfhout JW, van der Burgt YEM, et al. Quantifying protein measurands by peptide measurements: Where do errors arise? Journal of Proteome Research. 2015;**14**(2):928–942

[41] Addona TA, Shi X, Keshishian H, Mani DR, Burgess M, Gillette MA, et al. A pipeline that integrates the discovery and verification of plasma protein biomarkers reveals candidate markers for cardiovascular disease. Nature Biotechnology. 2011;**29**(7):635–643

[42] Vehus T, Seterdal KE, Krauss S, Lundanes E, Wilson SR. Comparison of commercial nanoliquid chromatography columns for fast, targeted mass spectrometry-based proteomics. Future Science OA. 2016

[43] Abbatiello SE, Mani DR, Keshishian H, Carr SA. Automated detection of inaccurate and imprecise transitions in peptide quantification by multiple reaction monitoring mass spectrometry. Clinical Chemistry. 2010;**56**(2):291–305

[44] Yadav AK, Bhardwaj G, Basak T, Kumar D, Ahmad S, Priyadarshini R, et al. A systematic analysis of eluted fraction of plasma post immunoaffinity depletion: Implications in biomarker discovery. PLoS One. 2011;**6**(9):e24442

[45] Brandtzaeg OK, Johnsen E, Roberg-Larsen H, Seip KF, MacLean EL, Gesquiere LR, et al. Proteomics tools reveal startlingly high amounts of oxytocin in plasma and serum. Scientific Reports. 2016;**6**:31693

[46] Schoenherr RM, Zhao L, Ivey RG, Voytovich UJ, Kennedy J, Yan P, et al. Commercially available antibodies can be applied in quantitative multiplexed peptide immunoaffinity enrichment targeted mass spectrometry assays. Proteomics. 2016;**16**(15–16):2141–2145

[47] Edfors F, Bostrom T, Forsstrom B, Zeiler M, Johansson H, Lundberg E, et al. Immunoproteomics using polyclonal antibodies and stable isotope-labeled affinity-purified recombinant proteins. Molecular & Cellular Proteomics: MCP. 2014;**13**(6):1611–1124

[48] Shen Y, Zhao R, Berger SJ, Anderson GA, Rodriguez N, Smith RD. High-Efficiency nanoscale liquid chromatography coupled On-Line with mass spectrometry using nanoelectrospray ionization for proteomics. Analytical Chemistry. 2002;**74**(16):4235–4249

[49] Luo Q, Gu Y, Wu SL, Rejtar T, Karger BL. Two-dimensional strong cation exchange/porous layer open tubular/mass spectrometry for ultratrace proteomic analysis using a 10 microm id poly(styrene-divinylbenzene) porous layer open tubular column with an on-line triphasic trapping column. Electrophoresis. 2008;**29**(8):1604–1611

[50] Gu C, Lin L, Chen X, Jia J, Ren J, Fang N. Fabrication of a poly (styrene–octadecene–divinylbenzene) monolithic column and its comparison with a poly (styrene–divinylbenzene) monolithic column for the separation of proteins. Journal of Separation Science. 2007;**30**(7):1005–1012

[51] Vehus T, Roberg-Larsen H, Waaler J, Aslaksen S, Krauss S, Wilson SR, et al. Versatile, sensitive liquid chromatography mass spectrometry—Implementation of 10 μm OT columns suitable for small molecules, peptides and proteins. Scientific Reports. 2016;**6**:37507

[52] Food, Administration D. Guidance for Industry: Bioanalytical Method Validation [Internet]. 2001. Available from: www.Fda.gov/downloads/drugs/guidancecomplianceregulatoryinformation/guidances/ucm368107.pdf. 2007

[53] Yang E, Welink J, Cape S, Woolf E, Sydor J, James C, et al. 2016 White Paper on recent issues in bioanalysis: focus on biomarker assay validation (BAV) (Part 1—small molecules, peptides and small molecule biomarkers by LCMS). Bioanalysis. 2016

[54] Kennedy JJ, Abbatiello SE, Kim K, Yan P, Whiteaker JR, Lin C, et al. Demonstrating the feasibility of large-scale development of standardized assays to quantify human proteins. Nature Methods. 2014;**11**(2):149–155

[55] Gallien S, Kim SY, Domon B. Large-scale targeted proteomics using internal standard triggered-parallel reaction monitoring (IS-PRM). Molecular & Cellular Proteomics. 2015; **14**(6):1630–1644

[56] Jaffe JD, Keshishian H, Chang B, Addona TA, Gillette MA, Carr SA. Accurate inclusion mass screening: A bridge from unbiased discovery to targeted assay development for biomarker verification. Molecular & Cellular Proteomics: MCP. 2008;**7**(10):1952–1962

[57] Shi T, Fillmore TL, Sun X, Zhao R, Schepmoes AA, Hossain M, et al. Antibody-free, targeted mass-spectrometric approach for quantification of proteins at low picogram per milliliter levels in human plasma/serum. Proceedings of the National Academy of Sciences of the United States of America. 2012;**109**(38):15395–15400

[58] Picard G, Lebert D, Louwagie M, Adrait A, Huillet C, Vandenesch F, et al. PSAQ™ standards for accurate MS-based quantification of proteins: From the concept to biomedical applications. Journal of Mass Spectrometry. 2012;**47**(10):1353–1363

[59] Gilquin B, Jaquinod M, Louwagie M, Kieffer-Jaquinod S, Kraut A, Ferro M, et al. A proteomics assay to detect eight CBRN-relevant toxins in food. Proteomics. 2017;**17**(1–2): 1600357

[60] Gilquin B, Louwagie M, Jaquinod M, Cez A, Picard G, El Kholy L, et al. Multiplex and accurate quantification of acute kidney injury biomarker candidates in urine using Protein Standard Absolute Quantification (PSAQ) and targeted proteomics. Talanta. 2017;**164**:77–84

[61] D'Asti E, Chennakrishnaiah S, Lee TH, Rak J. Extracellular Vesicles in brain tumor progression. Cellular and Molecular Neurobiology. 2016;**36**(3):383–407

[62] Sadovska L, Eglitis J, Line A. Extracellular vesicles as biomarkers and therapeutic targets in breast cancer. Anticancer Research. 2015;**35**(12):6379–6390

[63] Hustoft HK, Vehus T, Brandtzaeg OK, Krauss S, Greibrokk T, Wilson SR, et al. Open tubular lab-on-column/mass spectrometry for targeted proteomics of nanogram sample amounts. PLoS One. 2014;**9**(9):e106881

Chapter 4

Pesticides and Their Degradation Products Including Metabolites: Chromatography-Mass Spectrometry Methods

Renata Raina-Fulton, Nicole Dunn and Zhen Xie

Additional information is available at the end of the chapter

http://dx.doi.org/10.5772/68074

Abstract

This chapter reviews the selection of chromatography-mass spectrometry methods for the analysis of organophosphorus pesticides, pyrethroid insecticides, carbamates, and phenylureas. Options with different GC-MS, GC-MS/MS, and LC-MS/MS methods will be discussed for inclusion of the targeted pesticides. In addition, methods for the analysis of metabolites of these chemical classes of pesticides are investigated, including the feasibility of simultaneous analysis with parent pesticides. In some cases, a targeted approach is required for the analyses of metabolites. These methods apply to a wide variety of sample matrices including environmental (air, water, and soil), food (fruits, vegetation, or food products), and biological samples (urine and blood). The focus of the chapter is on MS detection approaches with consideration of the chromatographic separation conditions as required. A short discussion of multiresidue analysis methods and/or where feasible, other chemical classes or selected pesticides from these chemical classes can be analyzed in existing methods is included.

Keywords: gas chromatography-mass spectrometry (GC-MS), gas chromatography-tandem mass spectrometry (GC-MS/MS), liquid chromatography-tandem mass spectrometry (LC-MS/MS), carbamates, organophosphorus pesticides (OPs), phenylureas, pyrethroids, metabolites, degradation products

1. Introduction

Organophosphorus pesticides, pyrethroids, carbamates, and phenylureas remain important chemical classes of pesticides that require chemical analysis by gas chromatography-mass

INTECH
open science | open minds

© 2017 The Author(s). Licensee InTech. This chapter is distributed under the terms of the Creative Commons Attribution License (http://creativecommons.org/licenses/by/3.0), which permits unrestricted use, distribution, and reproduction in any medium, provided the original work is properly cited. CC BY

spectrometry (GC-MS), gas chromatography-tandem mass spectrometry (GC-MS/MS), or liquid chromatography-tandem mass spectrometry (LC-MS/MS) methods. The most diverse range of chromatography-mass spectrometry methods is available for these chemical classes of pesticides with method selection often based upon sensitivity and selectivity needs (see **Figure 1**). The chapter will discuss selection of methods for chemical analysis for each of these chemical classes of pesticides along with the feasibility of separate or simultaneous

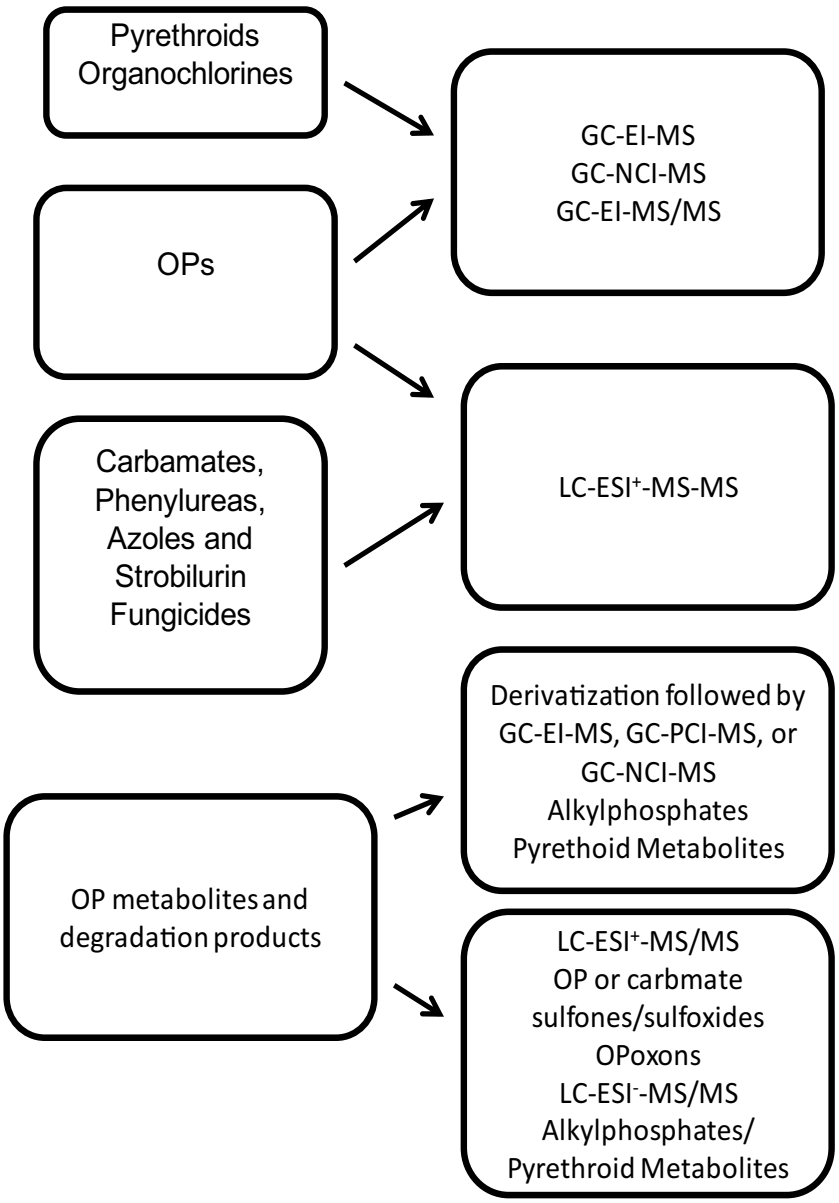

Figure 1. Options for the chromatography-mass spectrometric analysis of major chemical classes of pesticides and their metabolites or degradation products.

http://dx.doi.org/10.5772/68074

analysis of metabolites and degradation products of these parent pesticides. The focus of this chapter is on the chromatography-mass spectrometry aspects of the methods. Extraction and clean-up or pre-concentration procedures for the target analytes from sample matrices will also influence the magnitude of matrix enhancement or suppression in the MS detection and column choice (or separation conditions used) to minimize the influence of matrix peaks. Further discussion on sample preparation procedures has been recently reviewed [1, 2].

2. Organophosphorus pesticides and their degradation products or metabolites

Organophosphorus pesticides (OPs) include both organophosphates ($(RO)_3PO$) and organothio phosphates ($(R_1O)_3PS$, $R(R_1O)_2PS$, $RS(R_1O)_2PS$ with OR_1 typically methoxy or ethoxy group) as shown in **Figure 1**. Common organophosphates analyzed include bromofenvinphos, chlorfenvinphos, dichlorvos, mevinphos, and tetrachlorvinphos [3–6]. The majority of OPs analyzed (see **Table 1**) are organothiophosphates including aliphatic organothiophosphates (chlormephos, demephion-O and S, disulfoton, ethion, ethoprofos, malathion, phorate, and sulfotep) [3–10], aliphatic amide organothiophosphates (dimethoate, o-methoate) [4, 6, 9, 10], heterocyclic organothiophosphates (coumaphos, azinphos-methyl, azinphos-ethyl, phosmet, pyrazophos, chlorpyrifos-methyl, chlorpyrifos-ethyl, diazinon, pirimiphos) [3–10], phenyl organothiophosphates (bromophos-methyl, bromophos-ethyl, carbophenothion, dichlofenthion, fenchlorphos, fenitrothion, fenthion, parathion-methyl, parathion-ethyl, prothiofos, sulprofos) [3, 5–9] and phosphonothioates (fonofos, trichloronat, cyanofenphos, leptophos, fenamiphos, and acephate) [3, 4, 6, 7].

OP	Molecular formula	SIM *m/z* (quantitative, confirmation)	Ref.	SRM *m/z* (quantitative, confirmation)	Ref.
Acephate		136	[10]	136→42, 136→94	[3]
Aspon		211, 253	[1]	378→210, 378→115	[7]
Azinphos-methyl				160→105, 160→132	[3]
				132→104	[6]
Azinphos-ethyl				160→105, 160→132	[3]
				132→04	[6]
Bromfenvinphos-methyl				295→295	[5]
Bromfenvinphos-ethyl				267→159	[5]
Bromophos-ethyl				359→303, 359→331	[3, 6]
				359→303	[5]
Bromophos-methyl				331→286, 331→316	[3, 6]
				331→331	[5]
Carbofenothion		157, 342	[1]	342→157, 342→143	[7]

OP	Molecular formula	SIM *m*/*z* (quantitative, confirmation)	Ref.	SRM *m*/*z* (quantitative, confirmation)	Ref.
Chlormefos				234→121, 234→154	[3]
				243→121	[5]
				235→171, 235→199	[6]
Chlorphenvinphos				267→159, 323→267	[3]
				323→267	[5]
				267→159	[6]
Chlorpyrifos-methyl		286, 125	[1]	321→268, 321→208	[7]
		286	[10]	286→136, 286→241	[3]
		286, 288, 125	[17]	286→93	[5]
				286→208, 286→286	[6]
Chlorpyrifos-ethyl		97, 197	[1]	349→208, 349→40	[7]
		199	[10]	314→258, 314→286	[3, 6]
		97, 197	[11]	314→258	[5]
Coumaphos		362	[10]		
Cyanofenphos				185→157, 157→110	[3]
				157→139, 157→110	[6]
Demeton-o		88, 60	[11]		
Diazinon		137, 179	[1]	304→179, 304→137	[7]
		304	[10]	304→137, 304→179	[3]
		137, 304	[11]	304→179	[5, 6]
		287, 302, 288	[17]		
Diazinon-d_{10}		314	[1]	314→185	[7]
Dichlofenthion		223, 97	[1]	314→223, 319→81	[7]
				279→222, 279→251	[3]
				279→223	[5]
				279→223, 279→251	[6]
Dichlorvos		185	[10]	185→93	[5]
				221→141, 221→145	[6]
Dimethoate		125	[10]	230→199	[6]
		87, 125	[11]		
		87, 93, 125	[17]		
Disulfoton		88, 60	[11]	274→88	[5]

OP	Molecular formula	SIM *m*/*z* (quantitative, confirmation)	Ref.	SRM *m*/*z* (quantitative, confirmation)	Ref.
Dyfonate		109, 137	[1]	246→137, 246→109	[7]
Ethion		231, 97	[1]	384→231, 384→203	[7]
		231, 384	[11]	231→175, 231→203	[3]
Ethoprophos				158→97, 158→114	[3]
				158→97	[5]
				243→131, 243→173	[6]
Fenamiphos				303→154, 303→180	[3]
Fenchlorphos		125, 287	[1]	320→285, 320→204	[7]
				285→270	[5]
Fenitrothion		277, 125	[1]	277→260, 277→109	[7]
		109, 125	[11]	260→109, 260→125	[3]
				277→260	[5]
				260→125	[6]
Fenthion		278, 125	[11]	278→125, 278→245	[3]
				278→109	[5]
				278→135	[6]
Fonophos				246→109, 246→137	[3]
				246→137, 246→109	[6]
Leptophos		171, 377	[1]		
Malathion		173, 125	[1]	173→ 99	[5]
		173, 125, 93	[17]	173→127	[6]
		93, 125	[11]		
o-methoate		156	[10]		
Mevinphos		192	[10]	192→127, 192→164	[3]
				192→127	[5]
				193→127	[3]
Parathion ethyl		97, 291	[1]	291→109, 291→137	[12]
		291, 109	[11]	291→91, 291→109	[8]
				291→109	[3]
				291→263, 291→143	[18]
Parathion methyl		109, 125	[11]	263→79, 263→109	[8]
				263→109	[3]
				263→136, 263→246	[18]

OP	Molecular formula	SIM *m*/*z* (quantitative, confirmation)	Ref.	SRM *m*/*z* (quantitative, confirmation)	Ref.
Phorate		121, 75	[1]	260→75, 263→231	[12]
				231→129	[3]
Phosmet		160	[10]	160→77	[3]
Pirimiphos-ethyl				333→163, 333→168	[3]
				316→166	[5]
				318→182, 318→166, 318→246	[6]
Pirimiphos-methyl				290→125, 290→151	[3]
				290→125	[5]
				290→151	[6]
Prothiofos				309→221, 309→239	[3]
				162→63	[5]
				309→239, 309→281	[6]
Pyrazophos				265→138, 265→210	[3]
				221→93	[5]
				265→210	[6]
Quinalphos				298→156, 298→190	[3]
				146→91	[5]
				146→118	[11]
Sulfoprofos		140, 322	[1]	322→156, 322→97	[7]
				322→156, 322→139	[3]
Sulfotep		322, 202	[1]	322→202, 322→146	[7]
		322, 97	[11]	322→146, 322→266	[3]
				322→146	[5]
Tetrachlorvinphos				329→109	[3, 5]
				331→109	[6]
Tokuthion		113, 267	[1]	344→328, 344→73	[7]
Tolclophos methyl				265→220, 265→250	[3]
				265→250	[5]
				265→220, 265→215	[6]
Tributylphosphorotrithioite		169, 57	[1]	314→115, 314→113	[7]
Trichloronate		109, 297	[1]		

Table 1. Selected ion monitoring (SIM) or selected reaction monitoring (SRM) transitions for organophosphorus pesticides (OPs) by GC-EI-MS or GC-EI-MS/MS methods.

http://dx.doi.org/10.5772/68074

OPs are both GC-MS and LC-MS/MS amenable and the choice often depends upon instrument availability, what other pesticide chemical classes are analyzed for and whether there is a need to also analyze degradation products or metabolites of OPs [9, 12, 13]. In general, a greater diversity of OPs has been analyzed simultaneously by GC-MS or GC-MS/MS methods as compared to LC-MS/MS. For analysis of OPs by GC-MS methods, electron impact ionization (EI) remains the most widely used due to its ease of operation and ability to provide spectral library matches (see **Table 1**) [3–10]. Other pesticide classes that are most frequently analyzed with OPs by GC-MS include OCs, pyrethroids, and a few selected azole fungicides, strobilurin fungicides and carbamates [3, 5, 7, 9, 14].

Selection ion monitoring (SIM) with EI does not always meet sensitivity or selectivity needs or provide information on the molecular weight for some OPs due to the high amount of fragmentation in the EI source. OPs are prone to fragmentation in the EI source such that the molecular ion is often too low in abundance to monitor such that fragment ions are used for quantitation and confirmation analysis [3–7, 9, 10]. Positive or negative chemical ionization may be selected to obtain molecular weight confirmation, however, even with negative chemical ionization (NCI) significant amount of fragmentation of OPs may occur in the ion source although typically few fragment ions are observed in NCI as compared to EI [7, 10]. Electron capture in NCI can occur by dissociate electron capture and the structure of the OP may lead to more stable negatively charged fragment ions than the molecular ion. PCI is generally not selected for quantitative analysis as it does not provide significant improvements in selectivity over EI, while NCI is used for OPs, organochlorines (OCs), and pyrethroids when additional sensitivity or selectivity is required [7, 10]. OPs, organochlorines, and pyrethroids that contain halogen atoms or nitro groups often have lower detection limits with NCI than EI. For example, diazinon and malathion (see structures in **Figure 2**) have better sensitivity with GC-EI-MS than GC-NCI-MS, while chlorpyrifos-ethyl (chlorinated) and parathion-ethyl (contains a nitro group) have good sensitivity with GC-NCI-MS [7]. The ^{37}Cl or ^{81}Br isotopes of the molecular ion or fragment ions can be used for confirmation analysis with GC-EI-MS such as for chlorpyrifos methyl (m/z = 288); however, as there is a high degree of fragmentation of OPs with EI, generally more than two fragment ions of higher abundance than the isotope ions can be selected for quantitation and confirmation [3, 5–7, 9, 10].

Most halogenated OPs observed better sensitivity with GC-NCI-MS than GC-EI-MS or GC-EI-MS/MS [7]. To provide additional selectivity, GC-EI-MS/MS has been used; however, when the molecular ion is selected as the precursor ion for collision-induced dissociation (CID), the sensitivity is lower than when NCI in SIM mode is used [7]. If the OR_1 group is an ethoxy group, CID of the molecular ion may lead to loss of ethene (C_2H_4) from the ethoxy group and if the OP is halogenated, the loss of halogen radical (e.g., Cl radical) is also frequently observed [6]. For example, the SRM 349→286 of chlorpyrifos corresponds to CID of the molecular ion ($M^{+\bullet}$) to form fragment ion F^+ ($Cl_2NC_4HOPS(OC_2H_5)(OH)^+$) as a result of loss of C_2H_2 from an ethoxy group and Cl radical from the aromatic R group. Phorate observes loss of ethyl from the aliphatic R group (SRM: 260→231) to form ($^+SCH_2SPS(OC_2H_5)_2$) [5, 7]. As phorate has an aliphatic R group, fragmentation within the R group can result in a stable fragment ion $CH_3CH_2SCH_2^+$ at m/z = 75 (SRM: 260→75). The fragment ion at m/z = 231 can undergo further fragmentation through loss of two molecules of ethene from the two ethoxy groups

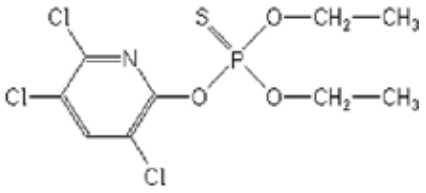

chlorpyrifos-ethyl

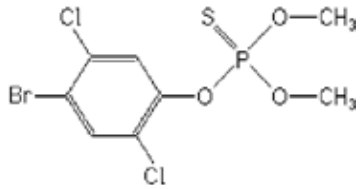

bromophos

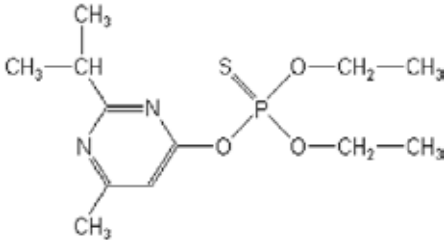

diazinon

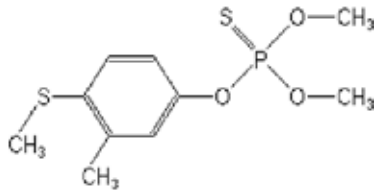

fenthion

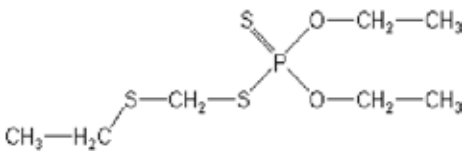

phorate

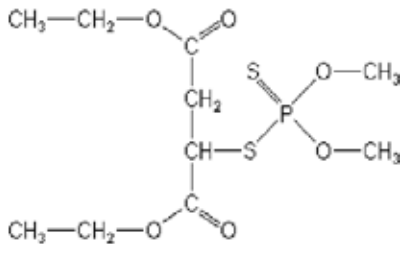

malathion

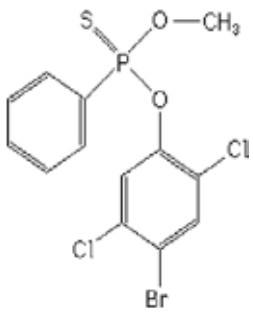

leptophos

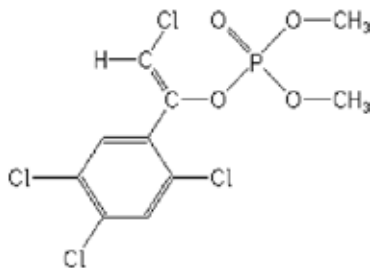

tetrachlorvinphos

Figure 2. Structures of common organophosphorus pesticides (OPs) from different subclasses. OP subclasses include organophosphates (tetrachlorvinphos), aliphatic organothiophosphates (malathion, phorate), heterocyclic organothiophosphates (chlorpyrifos ethyl and diazinon), phenyl organothiophosphates (bromophos), and phosphonothioates (leptophos).

and neutral loss of SCH_2 to form $SPS(OH)_2^+$ corresponding to ion at *m*/*z*=129 (SRM: 231→129 observed). For $(RO)PS(OR_1)_2$ where OR_1 is methoxy, CID of the molecular ion will either form $[PS(OR_1)_2]^+$ with loss of OR radical or a thiono-thiolo rearrangement may occur such that $[PO(OR_1)_2]^+$ is formed with loss of SR radical as observed for fenthion 278→125 and 278→109, respectively [3, 5]. Thiono-thiolo rearrangements have been proposed for fragmentation of diazinon in LC-MS/MS [15].

To improve the sensitivity of GC-EI-MS/MS, the precursor ion can be selected as an abundant fragment ion rather than the molecular ion (see **Table 1**). For bromophos-methyl (monoisotopic mass 364) and bromophos-ethyl (monoisotopic mass 392), the fragment ions at *m*/*z* = 331 and *m*/*z* = 359, respectively are selected for precursor ions (SRM 331→286 and 359→303, respectively; see **Table 1**) and correspond to the either the ^{37}Cl or ^{81}Br isotope of $[M\text{-}Cl]^+$[3, 6]. The R groups of OPs vary substantially and can play a significant role in the fragmentation pathway that dominates. For some OPs, the most abundant fragment ion available for CID is R+. For example, azinphos-methyl and azinphos-ethyl fragmentation at S-R bond of $RS(OR_1)_2PS$ to produce R^+ and ion at *m*/*z* = 160 is the dominant fragment ion formed by loss of the $S(OR_1)_2PS$ radical in the EI ion source. Both azinphos-ethyl and azinphos-methyl monitor the SRM transitions at *m*/*z* of 160→105, and 160→132 for quantitation and confirmation analysis [3, 6]. The *m*/*z* = 160 fragment ion undergoes collision-induced dissociation through loss of N_3CH or C_2H_2 to give fragment ions at 105 and 132, respectively.

Metabolite or degradation product analysis has become of increasing importance for biological monitoring studies (urine or blood) and environmental studies (atmosphere or surface water) [8, 14, 16–21]. Organophosphorus pesticides can be grouped into organophosphates and organothiophosphates with different R-group substituents. Alkylphosphates (dimethylphosphate and diethylphosphate) and alkylthiophosphates (dimethylthiophosphate, dimethylethylthiophosphate, dimethyldithiophosphate, and dimethyldithiophosphates) are formed from metabolism of OPs. They can be analyzed by GC-MS methods following a derivatization step with N-(*tert*-butyldimethylsilyl)-N-methyltrifluoroacetamide (MTBSTFA) to form *tert*-butyldimethylsilyl derivatives (GC-EI-MS); 2,3,4,5,6-pentafluorobenzylbromide (PFBBr) to form pentafluorobenzylbromide derivatives (GC-NCI-MS); and 1-chloro-3-iodropane (CIP) to form chloropropyl ethers (GC-PCI-MS) (see **Table 2**) [3, 14, 16, 17]. There has been a gradual shift from use of MTBSTFA derivatives that are analyzed by GC-EI-MS to PFBBr-derivatives that can be analyzed by negative chemical ionization for added sensitivity and selectivity, and CIP derivatives that are analyzed with positive chemical ionization.

The analysis of OPs by LC-ESI^+-MS/MS has grown [11, 22–39]. OPs that are amenable to electrospray ionization often have lower detection limits than with GC-MS methods particularly for those OPs most widely studied, including azinphos-methyl, chlorpyrifos, diazinon, and malathion [7, 8, 11]. Since electrospray ionization is a much softer ionization process than EI, the protonated molecular ion can be selected as the precursor ion for LC-ESI^+-MS/MS and generally two fragments of significant abundance are observed such that two SRM transitions are available for quantitative and confirmation analysis (see **Table 3**). Organochlorines have poor sensitivity with LC-ESI^+-MS/MS such that GC-MS methods are selected over LC-ESI^+-MS/MS if organochlorines (OCs) are targeted along with OPs in a multiclass method (see **Figure 1**). However, LC-ESI^+-MS/MS is also

OP degradation product, derivatization agent	Parent	SIM *m/z* (quantitative, confirmation) EI	Ref	SRM *m/z* (quantitative, confirmation)	Ref
Diazinon oxon (oxadiazinon)	diazinon			175→112, 258→112	[7]
Dibutylphosphate, PFBBr (IS)	OP	335, 279	[12, 13, 20]	209→79^{NCI}	[14]
2,4-Dichlorophenol, MTBSTFA	dichlofenthion	219, 221	[8]		
2,5-Dichlorophenol, MTBSTFA	p-dichlorobenzene	221, 219	[8]		
Diethyldithiophosphate, PFBBr	OP	366, 185	[18]	185→111, 185→157^{NCI}	[14]
Diethyldithiophosphate, CIP	OP	366, 185, 157	[12, 13, 20]	263→153, 265→153^{PCI}	[16, 17]
Diethylphosphate, MTBSTFA	OP	211, 155	[8]	153→79, 153→125	[14]
Diethylphosphate, PFBBr	OP	258, 334	[18]	231→127, 233→127^{PCI}	[16, 17]
Diethylphosphate, CIP	OP	334, 278, 258	[12, 13, 20]		
Diethylthiophosphate, MTBSTFA	OP	227, 199	[8]	169→95, 169→141^{NCI}	[14]
Diethylthiophosphate, PFBBr	OP	350, 274	[18]	247→191, 249→191^{PCI}	[16, 17]
Diethylthiophosphate, CIP	OP	350, 274, 169	[12, 13, 20]		
Diisopropylphosphate (IS), MTBSTFA	OP	155, 239	[8]		
Dimethyldithiophosphate, PFBBr	OP	338, 157	[12, 13, 20]	157→112, 157→142^{NCI}	[14]
Dimethyldithiophophate, CIP	OP			235→125, 235→125^{PCI}	[16, 17]
Dimethylphosphate, MTBSTFA	OP	183, 153	[18]	125→63, 125→79^{NCI}	[14]
Dimethylphosphate, PFBBr	OP	306, 110	[18]	203→127, 205→127^{PCI}	[16, 17]
Dimethylphosphate, CIP	OP	306, 307, 194	[12, 13, 20]		
Dimethylthiophosphate, MTBSTFA	OP	199, 169	[8]	141→126, 141→96^{NCI}	[14]
Dimethylthiophosphate, PFBBr	OP	322, 211, 110	[12, 13, 20]	219→143, 221→143^{PCI}	[16, 17]
Dimethylthiophosphate, CIP	OP				

http://dx.doi.org/10.5772/68074

OP degradation product, derivatization agent	Parent	SIM *m*/*z* (quantitative, confirmation) EI	Ref	SRM *m*/*z* (quantitative, confirmation)	Ref
Fenamiphos sulfone	fenamiphos			292→213, 320→292	[3]
Fenamiphos sulfoxide	fenamiphos			304→122, 304→196	[3]
2-Isopropyl-6-methyl-4-pyrimidinol, MTBSTFA	diazinon	209, 210	[19]		
3-Methyl-4-(methylthio)phenol, MTBSTFA	fenthion	268, 196	[14]		
6-Methyl-2-(1-methylethyl)4(1H)-pyrimidinone	diazinon	137, 152, 124	[19]		
3-Methyl-4-nitrophenol, MTBSTFA	fenitrothion	267, 210	[8]	152→122, 152→107^{NCI}	[14]
3-Methyl-4-nitrophenol, PFBBr	fenitrothion				
3,5,6-Trichloro-2-pyridinol, MTBSTFA	chlorpyrifos	254, 258	[8]	196→35, 198→35^{NCI}	[14]
3,5,6-Trichloro-2-pyridinol, PFBBr	chlorpyrifos	256, 254, 258	[21]		
Paraoxon methyl	parathion methyl			230→106, 230→136	[3]
Phosmet oxon	phosmet			160→77, 160→133	[3]

Electron ionization unless noted.

MTBSTFA, N-(*tert*-butyldimethylsilyl)-N-methyltrifluoroacetamide forms *tert*-butyldimethylsilyl derivatives; PFBBr, 2,3,4,5,6-pentafluorobenzylbromide forms pentafluorobenzylbromide derivatives; CIP, 1-chloro-3-iodropane forms chloropropyl ethers; NCI, negative chemical ionization; PCI, positive chemical ionization.

Table 2. Selected ion monitoring (SIM) or selected reaction monitoring (SRM) transitions for organophosphorus pesticides (OPs) degradation products including metabolites by GC/MS or GC/MS/MS methods.

OP	Organic modifier, additives in MP; column	SRM (quantitative, confirmation)	Ref
Acephate	MeOH, 10mM CH_3COONH_4; XTerra MS C18	182	[25]
	MeOH, 5 mM CH_3COONH_4; MAX RP, C-12	184→113, 184→95	[35]
	ACN, 0.1% HCOOH; C18	184→143	[4]
Azamethiphos	MeOH, 5 mM $HCOONH_4$; XDB-C18	325→183, 325→139	[23]
Azinphos-ethyl	MeOH, 0.1% HCOOH and 2 mM CH_3COONH_4; C_6phenyl	346→160, 346→132	[11]
Azinphos-methyl	MeOH, 0.1% HCOOH and 2 mM CH_3COONH_4; C_6phenyl	318→160, 318→132	[11]
	ACN, 0.1% HCOOH; C18	318→125, 318→132	[28]
	MeOH, 5 mM CH_3COONH_4; MAX RP, C-12	318→160, 318→132	[35]
	MeOH, 5 mM $HCOONH_4$; ODS-4	318→132, 318→160	[37]
Chlorpyrifos-ethyl	MeOH, 0.1% HCOOH and 2 mM CH_3COONH_4; C_6phenyl	352→97, 352→125	[11]
	MeOH, 5 mM $HCOONH_4$; XDB-C18	352→200, 352→97	[23]
	ACN, 0.1% HCOOH; C18	352→97, 352→200	[28]
	ACN, 20 mM CH_3COOH (pH 6.45-7.45); mixed mode RP/WAX	352→200, 352→115	[24]
	ACN, 0.025% HCOOH; Zorbax Extended C8	352→200	[29]
	ACN, 0.1% HCOOH; C18	350→198, 350→125, 352→200, 352→125	[30]
	ACN, 0.025% HCOOH; XDB-C8	352→200	[32]
	MeOH, 0.1% CH_3COOH; XSELECT™ CSH™C18	350→198, 352→200	[33]
	MeOH, 5 mM CH_3COONH_4; MAX RP, C-12	350→198, 350→97	[35]
	MeOH, 20 mM CH_3COONH_4; C18	350→198, 350→294	[36]
	MeOH, 5 mM $HCOONH_4$; ODS-4	350→198, 350→97	[37]
	MeOH, 2 mM CH_3COONH_4; C18	350→198, 352→200	[38]
	ACN, 20 mM CH_3COONH_4, RP18	350→125, 352→198	[39]
	ACN, 0.1% HCOOH; C18	352→198	[4]
Chlorpyrifos-methyl	MeOH, 0.1% HCOOH and 2 mM CH_3COONH_4; C_6phenyl	322→125, 324→125	[4]
	MeOH, 5 mM HCOONH4; XDB-C18	322→125, 322→290	[26]
	MeOH, 0.1% CH_3COOH; XSELECT™ CSH™C18	322→125, 324→125	[36]
	MeOH, 5 mM CH_3COONH_4; MAX RP, C-12	322→125, 322→290	[38]

OP	Organic modifier, additives in MP; column	SRM (quantitative, confirmation)	Ref
	MeOH, 5 mM $HCOONH_4$; ODS-4	322→125, 322→290	[40]
	ACN, 0.1% HCOOH; C18	322→290	[4]
Coumaphos	MeOH, 0.1% HCOOH and 2 mM CH_3COONH_4; C_6phenyl	363→227, 363→307	[6]
	MeOH, 0.1% HCOOH; Acquity UPLC™BEH C18	363→303, 363→289	[6]
	MeOH, 5 mM CH_3COONH_4; MAX RP, C-12	363→227, 363→307	[35]
Cyanophos	MeOH, 10mM CH_3COONH_4; XTerra MS C18	228	[25]
Demeton-S-methyl	MeOH, 0.1% HCOOH; Acquity UPLC™BEH C18	231→89, 231→61	[6]
	MeOH, 5 mM CH_3COONH_4; MAX RP, C-12	231→89, 231→61	[35]
Diazinon	MeOH, 0.1% HCOOH and 2 mM CH_3COONH_4; C_6phenyl	305→169, 305→153	[11]
	MeOH, 5 mM $HCOONH_4$; XDB-C18	305→169, 305→153	[23]
	MeOH, 5 mM CH_3COONH_4; MAX RP, C-12	305→169, 305→97	[35]
	MeOH, 5 mM $HCOONH_4$; ODS-4	305→169, 305→153	[37]
	MeOH, 2 mM CH_3COONH_4; C18	305→169, 305→153	[38]
	ACN, 20 mM CH_3COONH_4, RP18	305→169, 305→153	[39]
	ACN, 0.1% HCOOH; C18	322→290	[4]
	ACN, 0.1% HCOOH; XDB-C18	305.103, 277.077, 249.047, 169.077, 153.102*	[22]
	MeOH, 0.1 % HCOOH; X-Terra C18	305.1089→169.0799, 305.1089→153.1028*	[27]
Diazinon-d10 (IS)	MeOH, 0.1% HCOOH and 2 Mm CH_3COONH_4; C_6phenyl	315→170, 315→154	[11]
Dichlorvos	MeOH, 5 mM HCOONH4; XDB-C18	221→109, 221→127	[23]
	MeOH, 5 mM $HCOONH_4$; ODS-4	221→109, 221→127	[37]
	MeOH, 5 mM CH_3COONH_4; MAX RP, C-12	221→127, 221→109	[35]
	ACN, 0.1% HCOOH; C18	221→127	[4]
Dichlorvinphos	MeOH, 0.1% HCOOH; Acquity UPLC™BEH C18	238→112, 238→193	[6]
Dicrotophos	MeOH, 5 mM CH_3COONH_4; MAX RP, C-12	238→112, 238→127	[35]
Dimethoate	MeOH, 0.1% HCOOH and 2 Mm CH_3COONH_4; C_6phenyl	230→199, 230→125	[11]
	MeOH, 5 mM CH_3COONH_4; MAX RP, C-12	230→199, 230→125	[35]
	MeOH, 5 mM $HCOONH_4$; ODS-4	230→199, 230→125	[37]

OP	Organic modifier, additives in MP; column	SRM (quantitative, confirmation)	Ref
	MeOH, 2 mM CH_3COONH_4; C18	230→125, 230→143	[38]
	ACN, 0.1% HCOOH; C18	221→127	[4]
Disulfoton	MeOH, 5 mM CH_3COONH_4; MAX RP, C-12	275→89, 275→61	[35]
Ethion	MeOH, 5 mM CH_3COONH_4; MAX RP, C-12	385→199, 385→171	[35]
Ethoprofos	MeOH, 5 mM CH_3COONH_4; MAX RP, C-12	243→131, 243→97	[35]
	MeOH, 5 mM $HCOONH_4$; ODS-4	243→97, 243→131	[37]
Fenamiphos	MeOH, 5 mM CH_3COONH_4; MAX RP, C-12	304→217, 304→202	[35]
Fenchlorphos	MeOH, 0.1% HCOOH and 2 mM CH_3COONH_4; C_6phenyl	321→125, 321→109	[11]
Fenitrothion	MeOH, 10mM CH_3COONH_4; XTerra MS C18	262	[25]
	MeOH, 5 mM CH_3COONH_4; MAX RP, C-12	278→125, 278→109	[35]
Fensulfothion	MeOH, 0.1% HCOOH; Acquity UPLC™BEH C18	309→281, 309→157	[6]
Fenthion	MeOH, 5 mM CH_3COONH_4; MAX RP, C-12	279→169, 279→247	[35]
	MeOH, 5 mM $HCOONH_4$; ODS-4	279→169, 279→247	[37]
	MeOH, 2 mM CH_3COONH_4; C18	279→169, 279→105	[38]
Malathion	MeOH, 0.1% HCOOH and 2 mM CH_3COONH_4; C_6phenyl	331→127, 331→285	[11]
	MeOH, 10mM CH_3COONH_4; XTerra MS C18	315	[25]
	MeOH, 5 mM CH_3COONH_4; MAX RP, C-12	331→127, 331→99	[35]
	MeOH, 5 mM $HCOONH_4$; ODS-4	331→127, 331→99	[37]
	ACN, 20 mM CH_3COONH_4, RP18	331→127, 331→285	[39]
Mevinphos	MeOH, 5 mM CH_3COONH_4; MAX RP, C-12	225→127, 225→193	[35]
Methamidophos	MeOH, 5 mM HCOONH4; XDB-C18	142→94, 142→125	[23]
Monocrotophos	MeOH, 5 mM CH_3COONH_4; MAX RP, C-12	224→127, 224→98	[35]
	MeOH, 5 mM $HCOONH_4$; ODS-4	331→127, 331→99	[37]
Naled	MeOH, 5 mM CH_3COONH_4; MAX RP, C-12	398→127, 398→109	[35]
Parathion-ethyl	MeOH, 5 mM CH_3COONH_4; MAX RP, C-12	292→236, 292→97	[35]
Parathion-methyl	MeOH, 5 mM CH_3COONH_4; MAX RP, C-12	264→125, 264→232	[35]
	MeOH, 5 mM $HCOONH_4$; ODS-4	264→125, 264→109	[37]
Phorate	MeOH, 0.1% HCOOH and 2 mM CH_3COONH_4; C_6phenyl	261→75, 261→47	[11]
	MeOH, 5 mM CH_3COONH_4; MAX RP, C-12	261→75, 261→171	[35]

OP	Organic modifier, additives in MP; column	SRM (quantitative, confirmation)	Ref
Phosmet	MeOH, 5 mM CH_3COONH_4; MAX RP, C-12	318→160, 318→133	[35]
Pirimiphos methyl	MeOH, 5 mM HCOONH4; XDB-C18	306→164, 306→108	[23]
	MeOH, 5 mM CH_3COONH_4; MAX RP, C-12	306→164, 306→108	[35]
	MeOH, 5 mM $HCOONH_4$; ODS-4	306→164, 306→108	[37]
Prothiophos	MeOH, 5 mM CH_3COONH_4; MAX RP, C-12	345→241,345→133	[35]
	MeOH, 5 mM $HCOONH_4$; ODS-4	345→241,345→133	[37]
Pyrazophos	MeOH, 5 mM $HCOONH_4$; ODS-4	374→222, 374→194	[37]
Quinalphos	MeOH, 5 mM CH_3COONH_4; MAX RP, C-12	299→163, 299→147	[35]
Tebufos	MeOH, 0.1% HCOOH; Acquity UPLC™BEH C18	289→103, 289→57	[6]*
		289→57, 289→103	[35]
Temephos	ACN, CH_3COONH_4; C18	484, 523	[26]
Tetrachlorvinphos	MeOH, 5 mM CH_3COONH_4; MAX RP, C-12	367→127, 367→241	[35]
Triazophos	MeOH, 0.1% HCOOH; Acquity UPLC™BEH C18	314→162, 314→119	[6]
		314→162, 314→119	[35]
Trichlorfon	MeOH, 5 mM CH_3COONH_4; MAX RP, C-12	274→109, 274→221	[35]
	MeOH, 5 mM $HCOONH_4$; ODS-4	257→109, 257→221	[37]

*LC-ESI$^+$-QTOF-MS.

Table 3. Selected ion monitoring (SIM) or selected reaction monitoring (SRM) transitions for organophosphorus pesticides (OPs) products by LC-ESI$^+$-MS/MS methods.

more amenable to a wider range of other pesticides included in multiclass methods, including azole fungicides, carbamates, phenylureas, and strobilurin fungicides (see **Figure 1**). Either chemical class-specific or multiclass separations can be achieved on reversed-phase stationary phases including C8, C12, C18, C6phenyl. OPs, OPoxons, OPsulfoxides, and OPsulfones observed better sensitivity with methanol rather than acetonitrile as the organic modifier in the mobile phase. Generally, ammonium acetate or ammonium formate is selected as an additive and pending the target list of OPs and their degradation products, 0.1% formic acid may also be added to the mobile phase to improve sensitivity. Only a few OP sulfones, sulfoxides, and oxons have been analyzed by GC-EI-MS/MS methods (**Table 2**) often due to the poor sensitivity, poor peak shapes, or poor chromatographic separation of these analytes due to their more polar nature such that LC-ESI$^+$-MS/MS are preferred (see **Table 4**) [4, 6, 11, 19, 22–41].

An additional reason why LC-ESI$^+$-MS/MS is chosen over GC-MS methods for OPs is the ability to analyze OPs and OP sulfones, sulfoxides, and oxons simultaneously with often comparable sensitivities to their parent OPs [6, 11, 26, 28, 29, 32, 35]. Molecular weight confirmation is available as the protonated molecular ion is high in abundance and generally selected for the precursor ion

for LC-MS/MS (**Table 3**). Similar to the OPs, mobile phase containing methanol (and gradient elution) is often preferred for optimal sensitivity of OP degradation products. However, when OPs (or their degradation products) are included in multiclass methods, acetonitrile may be selected due to the sensitivity needs of other target chemical classes of pesticides and to reduce run times. Other degradation products including hydroxyl degrades of OPs and IMP can also be analyzed in positive ion mode by LC-ESI$^+$(or APCI$^+$)-MS/MS or LC-QTOF [11, 22, 27, 33, 40, 42].

Alkylphosphates and alkylthiophosphates can also be analyzed by LC-MS/MS but to achieve the required sensitivity LC-ESI$^-$-MS/MS is selected such that they are typically analyzed in a separate method from OPs (see **Table 4**) [11, 24, 27, 31, 33, 34, 39]. To provide the best sensitivity, acetonitrile rather than methanol is selected as the organic modifier in the mobile phase with either acetic or formic acid as a mobile phase additive. Chlorpyrifos degradation product 3,5,6-trichloro-2-pyridinol has been widely studied and can be included in LC-ESI$^+$-MS/MS methods with approximately a 50 times higher detection limit than OPoxons [11]. LC-ESI$^-$-MS/MS has also been widely used, however, collision-induced dissociation only produces the Cl^- fragment ion such that it is more common to monitor the ^{35}Cl and ^{37}Cl isotopes peaks of the deprotonated molecular ion at 196→196 or 198→198 if included in SRM methods when concentrations are lower [23, 29, 30, 32, 40, 41].

OP	Parent	Organic modifier, additives; column	SRM (quantitative, confirmation)	Ref
Azinphos methyl oxon	Azinphos methyl	MeOH, 0.1% HCOOH and 2 mM CH_3COONH_4; C_6phenyl	302→160, 302→132	[11]
		ACN, 0.1% HCOOH; C18	302→132, 302→245	[28]
Chlorpyrifos-methyl oxon	Chlorpyrifos-methyl	MeOH, 0.1% HCOOH and 2 mM CH_3COONH_4; C_6phenyl	308→109, 306→109	[11]
Chlorpyrifos-ethyl oxon	Chlorpyrifos-ethyl	MeOH, 0.1% HCOOH and 2 mM CH_3COONH_4; C_6phenyl	336→280, 336→200	[11]
		ACN, 0.1% HCOOH; C18	336→280, 336→308	[28]
		ACN, 0.025% HCOOH; Zorbax Extended C8	336→280	[29]
		ACN, 0.025% HCOOH; XDB-C8	336→280	[32]
Coumaphos oxon	coumaphos	MeOH, 0.1% HCOOH and 2 mM CH_3COONH_4; C_6phenyl	347→291, 347→211	[11]
Demeton-S-methyl sulfone	Demeton-S-methyl	MeOH, 0.1% HCOOH; Acquity UPLC™BEH C18	263→169, 263→121	[6]
		MeOH, 5 mM CH_3COONH_4; MAX RP, C-12	263→169, 263→108	[35]
Dibutylphosphate (IS)		ACN, 20 mM CH_3COOH (pH 6.45-7.45); mixed mode RP/WAX	209→79, 209→153^{ESI-}	[24]
Diethyl phosphate	OP	MeOH, 0.1% HCOOH and 2 mM CH_3COONH_4; C_6phenyl	155→99, 155→127	[11]

http://dx.doi.org/10.5772/68074

OP	Parent	Organic modifier, additives; column	SRM (quantitative, confirmation)	Ref
		ACN, 20 mM CH_3COOH (pH 6.45-7.45); mixed mode RP/WAX	153→79, 153→125^{ESI-}	[24]
		ACN, 0.1% HCOOH; MAXRP, RP12	153→125, 153→79^{ESI-}	[31]
		ACN, 1 mM tetrabutylammonium acetate; C18	153→79, 153→125, 153→63^{ESI-}	[34]
		MeOH, 0.1% HCOOH; X-Terra C18	153.0317→125.0004, 153.0317→78.9585^{ESI-*}	[27]
		MeOH, 0.1% CH_3COOH; XSELECT™ CSH™C18	153→79, 153→125^{ESI-}	[33]
Diethyldithiophosphate	OP	ACN, 1 mM tetrabutylammonium acetate; C18	185→111^{ESI-}	[31]
		ACN, 20 mM CH_3COONH_4, RP18	155→127, 155→99	[39]
Diethylthiophosphate	OP	ACN, 20 mM CH_3COOH (pH 6.45-7.45); RP/WAX	169→95, 169→141^{ESI-}	[24]
		ACN, 1 mM tetrabutylammonium acetate; C18	169→97, 169→141^{ESI-}	[31]
		MeOH, 0.1% CH_3COOH; XSELECT™ CSH™C18	169→95, 169→141^{ESI-}	[33]
		ACN, 0.1% HCOOH; MAXRP, C-12	169→95, 169→141, 169→63^{ESI-}	[34]
		MeOH, 0.1% HCOOH; X-Terra C18	169.0977→140.9775, 169.0977→94.9357^{ESI-*}	[27]
		ACN, 20 mM CH_3COONH_4, RP18	171→143, 171→115	[39]
Dimethylphosphate	OP	ACN, 1 mM tetrabutylammonium acetate; C18	125→63, 125→79^{ESI-}	[31]
		MeOH, 0.1% CH_3COOH; XSELECT™ CSH™C18	125→79, 125→63^{ESI-}	[33]
		ACN, 20 mM CH_3COONH_4, RP18	127→109, 129→95	[39]
Dimethylthiophoshate	OP	ACN, 1 mM tetrabutylammonium acetate; C18	141→126, 141→95^{ESI-}	[31]
		MeOH, 0.1% CH_3COOH; XSELECT™ CSH™C18	141→79, 141→63, 141→95^{ESI-}	[33]
		ACN, 20 mM CH_3COONH_4, RP18	143→125, 143→111	[39]

OP	Parent	Organic modifier, additives; column	SRM (quantitative, confirmation)	Ref
dimethyldithiophosphate	OP	ACN, 20 mM CH_3COONH_4, RP18	157→142, 157→112	[39]
Diazinon-oxon	diazinon	MeOH, 0.1% HCOOH and 2 mM CH_3COONH_4; C_6phenyl	289→153, 289→93	[11]
		MeOH, 0.1% HCOOH; X-Terra C18	289.1317→153.1028, 289.1317→261.1004*	[27]
Disulfoton sulfone	disulfoton	MeOH, 0.1% HCOOH; Acquity UPLC™BEH C18	307→97, 307→153	[6]
		MeOH, 5 mM CH_3COONH_4; MAX RP, C-12	307→153, 307→171	[35]
Disulfoton sulfoxide	disulfoton	MeOH, 0.1% HCOOH; Acquity UPLC™BEH C18	291→185, 291→97	[6]
		MeOH, 5 mM CH_3COONH_4; MAX RP, C-12	291→213, 291→185	[35]
Fenamiphos sulfone	fenamiphos	MeOH, 5 mM CH_3COONH_4; MAX RP, C-12	336→266, 336→308	[35]
Fenamiphos sulfoxide	fenamiphos	MeOH, 5 mM CH_3COONH_4; MAX RP, C-12	320→171, 320→251	[35]
Fenchlorphos oxon	fenchlorphos	MeOH, 0.1% HCOOH and 2 mM CH_3COONH_4; C_6phenyl	307→109, 305→109	[11]
Fenthion sulfone	fenthion	MeOH, 5 mM CH_3COONH_4; MAX RP, C-12	311→125, 311→279	[35]
Fenthion sulfoxide	fenthion	MeOH, 5 mM CH_3COONH_4; MAX RP, C-12	295→280, 295→127	[35]
5-hydroxydiazinon	diazinon	MeOH, 0.1% HCOOH; X-Terra C18	321.1038→293.0725, 321.1038→185.0749*	[27]
			319.0882→291.0568, 319.0882→229.0412^{ESI-*}	
7(1-hydroxy isopropyl diazinon	diazinon	MeOH, 0.1% HCOOH; X-Terra C18	321.1038→303.0932, 321.1038→275.0619*	[27]
4(1-hydroxyisopropyl diazoxon	diazinon	MeOH, 0.1% HCOOH; X-Terra C18	305.1266→287.1161, 305.1266→277.0953*	[27]
2-(1-hydroxy-1-methylethyl)-6-methyl-4(1H)-pyrimidinone	diazinon	MeOH, 0.1% HCOOH; Zorbax SB-CN	169→84	[19]
2-isopropyl-6-methyl-4-pyrimidinol	diazinon	ACN, 0.1% HCOOH; XDB-C18	153.1022, 84.0444, 70.0651*	[22]
		MeOH, 0.1% HCOOH; X-Terra C18	153.1028→137.0715, 153.1028→84.0575*, 151.0872→135.0558, 151.0872→123.0558^{ESI-*}	[27]
isomalathion	malathion	MeOH, 0.1% HCOOH and 2 mM CH_3COONH_4; C_6phenyl	331→99, 331→127	[11]

http://dx.doi.org/10.5772/68074

OP	Parent	Organic modifier, additives; column	SRM (quantitative, confirmation)	Ref
2-isopropyl-6-methyl-4-pyrimidinol (IMP)	diazinon	MeOH, 0.1% HCOOH and 2 mM CH_3COONH_4; C_6phenyl	153→84, 153→70	[11]
		MeOH, 0.1% CH_3COOH; XSELECT™ CSH™C18	153→84, 153→70	[33]
		MeOH, 1% CH_3COOH; C18	153→84, 153→70	[40]
		ACN, 0.1% HCOOH; XDB-C18	153.1022, 84.0444, 70.0651*	[22]
Malathion monocarboxylic acid	malathion	MeOH, 0.1% HCOOH and 2 mM CH_3COONH_4; C_6phenyl	303→127, 303→99	[11]
		MeOH, 0.1% CH_3COOH; XSELECT™ CSH™C18	301→142, 301→157	[33]
			301→126, 301→141	
Malathion dicarboxylic acid	malathion	MeOH, 0.1% CH_3COOH; XSELECT™ CSH™C18	273→141, 273→157	[33]
Malathion-oxon	malathion	MeOH, 0.1% HCOOH and 2 mM CH_3COONH_4; C_6phenyl	315→127, 315→99	[11]
o-methoate	dimethoate	MeOH, 0.1% HCOOH and 2 mM CH_3COONH_4; C_6phenyl	214→183, 214→125	[11]
		MeOH, 5 mM CH_3COONH_4; MAX RP, C-12	214→125, 214→109	[35]
		MeOH, 5 mM $HCOONH_4$; ODS-4	214→125, 214→183	[37]
			214→183	[4]
6-methyl-2-(1-methylethyl)4(1H)-pyrimidinone	diazinon	MeOH, 0.1% HCOOH; Zorbax SB-CN	153→84	[19]
3-methyl4-nitrophenol	fenitrothion	MeOH, 10mM CH_3COONH_4; XTerra MS C18	152	[25]
Parathion methyl oxon	Parathion methyl	MeOH, 5 mM CH_3COONH_4; MAX RP, C-12	248→202, 248→109	[35]
Phorate oxon	phorate	MeOH, 0.1% HCOOH and 2 mM CH_3COONH_4; C_6phenyl	245→75, 245→47	[11]
Phorate sulfone	phorate	MeOH, 5 mM CH_3COONH_4; MAX RP, C-12	293→171, 293→97	[35]
Phorate sulfoxide	phorate	MeOH, 5 mM CH_3COONH_4; MAX RP, C-12	277→199, 277→143	[35]
3,5,6-trichloro-2-pyridinol	chlorpyrifos	MeOH, 0.1% HCOOH and 2 mM CH_3COONH_4; C_6phenyl	198→107, 198→134	[11]
		ACN, 0.1% CH_3COOH; XDB-C18	198→198, 196→196^{ESI-}	[23]
		ACN, 20 mM CH3COOH (pH 6.45-7.45); RP/WAX	196→35, 198→35^{ESI-}	[24]

OP	Parent	Organic modifier, additives; column	SRM (quantitative, confirmation)	Ref
		ACN, 0.025% HCOOH; Zorbax Extended C8	198^{ESI-}	[29]
		ACN, 0.1% HCOOH; C18	196→196, 198→198, $200→200^{ESI-}$	[30]
		ACN, 0.025% HCOOH; XDB-C8	198→198	[32]
		MeOH, 0.1% CH_3COOH; XSELECT™ CSH™C18	198→37, 198→35, $196→35^{ESI-}$	[33]
		ACN, 0.1% HCOOH; MAXRP, RP12	196→35, 198→37, $198→35,^{ESI-}$	[34]
		MeOH, 1% CH_3COOH; C18	196→196, $198→198^{ESI-}$	[40]
		MeOH, 1% CH_3COOH; PhenylC6	196→196, $198→198^{ESI-}$	[41]
Temephos oxon	temephos	ACN, CH_3COONH_4; C18	468	[26]
Temephos sulfoxide	temephos	ACN, CH_3COONH_4; C18	482, 483, 500, 523	[26]
Terbufos sulfone	terbufos	MeOH, 5 mM CH_3COONH_4; MAX RP, C-12	321→115, 321→171	[35]
Terbufos sulfoxide	terbufos	MeOH, 5 mM CH_3COONH_4; MAX RP, C-12	305→131, 305→159	[35]

Table 4. Selected ion monitoring (SIM) or selected reaction monitoring (SRM) transitions for organophosphorus pesticides (OPs) metabolites or degradation products by LC-ESI^+-MS/MS methods.

3. Carbamates and phenylureas

LC-ESI^+-MS/MS can be used for the simultaneous analysis of carbamates (general structure $R_1OCONR_2R_3$), phenylureas, and selected degradation products (see **Table 5** for target list). Few carbamates are still analyzed directly by GC-EI-MS or GC-EI-MS/MS in multiclass methods (primarily carbaryl, carbofuran, carbosulfan, EPTC, isoprocarb, pirimicarb) [3, 9, 42, 43]. To improve sensitivity and extend the range of carbamates amenable to GC-EI-MS methods derivatized prior to analysis with 9-xanthydol, trimethylphenylammonium hydroxide and trimethylsulfonium hydroxide or sodium hydride has been used [43–45]. Metabolites of carbofuran and carbaryl have been analyzed after derivatization using trifluoroacetic acid with trimethylamine to produce volatile derivatives that can be analyzed by GC-EI-MS [46]. Photodegradation products (phenols and para-hydroxybenzamides) of carbamates were analyzed directly by GC-EI-MS/MS method [47].

LC-ESI^+-MS/MS is more frequently chosen than GC-MS methods for the analysis of carbamates and phenylureas in chemical class-specific or multiclass methods [39, 48–58]. OPs, carbamates, and phenylureas have a wide range of polarities so they can elute over similar

http://dx.doi.org/10.5772/68074

Carbamates

Compound (Parent compound) Molecular formula Molecular weight (g/mol)	**Structure**
Aldicarb $C_7H_{14}N_2O_2S$ 190.27	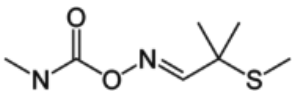
Aminocarb $C_{11}H_{16}N_2O_2$ 208.26	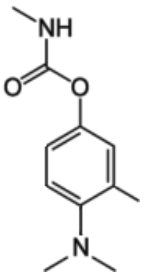
Carbaryl $C_{12}H_{11}NO_2$ 201.22	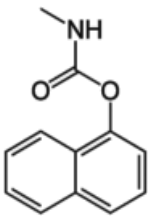
Carbofuran $C_{12}H_{15}NO_3$ 221.25	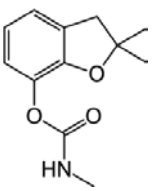
Carboxin $C_{12}H_{13}NO_2S$ 235.31	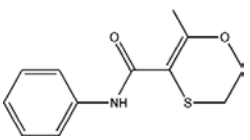
EPTC $C_9H_{19}NOS$ 189.32	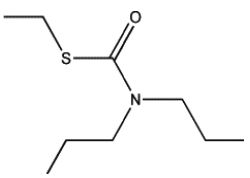
Methiocarb $C_{11}H_{15}NO_2S$ 225.31	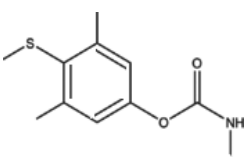

Carbamates	
Compound **(Parent compound)** **Molecular formula** **Molecular weight (g/mol)**	**Structure**
Methomyl $C_5H_{10}N_2O_2S$ 162.21	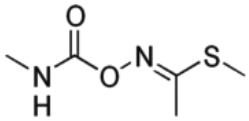
Oxamyl $C_7H_{13}N_3O_3S$ 219.36	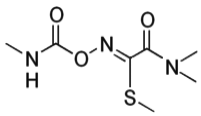
Pirimicarb $C_{11}H_{18}N_4O_2$ 238.29	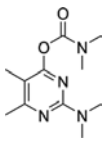
Propamocarb HCl $C_9H_{21}ClN_2O_2$ 224.73	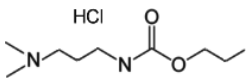
Thiodicarb $C_{10}H_{18}N_4O_4S_3$ 354.47	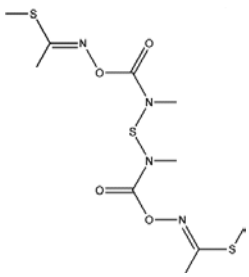
Degradation products	
Aldicarb sulfone (aldicarb) $C_7H_{14}N_2O_4S$ 222.26	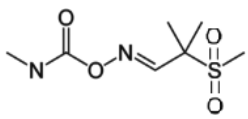
Aldicarb sulfoxide (aldicarb) $C_7H_{14}N_2O_3S$ 206.26	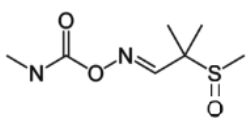
3-Hydroxycarbofuran (carbofuran) $C_{12}H_{15}NO_4$ 237.25	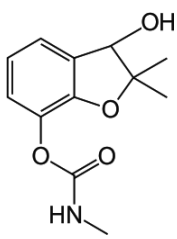

http://dx.doi.org/10.5772/68074

Carbamates	
Compound **(Parent compound)** **Molecular formula** **Molecular weight (g/mol)**	**Structure**
Methiocarb sulfone (methiocarb) $C_{11}H_{15}NO_4S$ 257.31	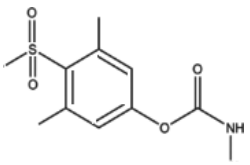
Methiocarb sulfoxide (methiocarb) $C_{11}H_{15}NO_3S$ 241.31	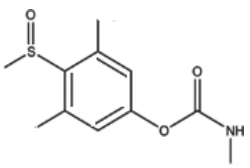
Methomyl-oxime (methomyl) C_3H_7NOS 105.16	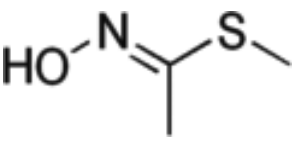
Oxamyl-oxime (oxamyl) $C_5H_{10}N_2O_2S$ 162.21	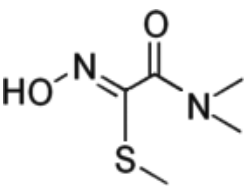
Phenylureas	
Diuron $C_9H_{10}Cl_2N_2O$ 233.10	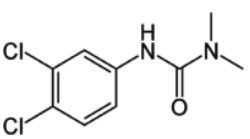
Linuron $C_9H_{10}Cl_2N_2O_2$ 249.09	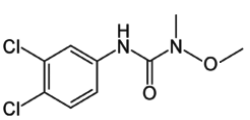
Neburon $C_{12}H_{16}Cl_2N_2O$ 275.18	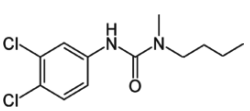
Siduron $C_{14}H_{20}N_2O$ 232.32	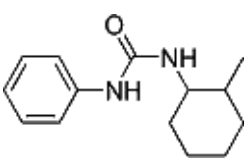

Table 5. Carbamates, selected degradation products, and phenylureas.

time periods when typical reversed-phase stationary phases are used; however, in general, phenylureas elute later than carbamates and within the time range for OPs and pyrethroid insecticides.

For LC-ESI$^+$-MS/MS the precursor ion is generally selected as the protonated molecular ion $[M+H]^+$ (see **Table 6**). Both methanol and acetonitrile have been used as the organic modifier in the mobile phase for the separation of carbamates and when both chemical classes are analyzed together; however, acetonitrile provides the best overall sensitivity. Sodium adducts of carbamates can also be observed with ESI$^+$ and have been attributed to impurities in methanolic mobile phases or sodium from metal tubing [51]. Both 0.1% formic acid and 5 mM ammonium acetate should be added to the mobile phase to improve sensitivity and to provide for ammonium adduct $[M+NH_4]^+$ formation for aldicarb, methiocarb sulfone, and oxamyl (see **Table 6**) [51, 53]. Ammonium acetate can also improve the peak shapes observed in the separation. Aldicarb sulfone and methiocarb sulfone observed both the protonated molecular ion and ammonium adduct under these conditions [53]. The addition of ammonium acetate to the mobile phase also minimizes sodium adduct formation which was observed in this work and others for aldicarb, aldicarb sulfone, aldicarb sulfoxide, 3-hydroxycarbofuran, siduron, and diuron [51]. The common, group-specific fragmentation pathway for *N*-methylcarbamates is the neutral loss of methyl isocyanate (CH_3-N=C=O), while for phenylureas, loss of the substituted aniline ring is common. For methomyl-oxime only one significant fragment ion was formed. The RSD of the ratio of areas SRM1/SRM2 was less than 20% for the majority of the compounds (see **Table 6**) and method detection limits are generally 1–5 μg/L. Methomyl-oxime and methiocarb sulfone are not as sensitive as other carbamates, with detection limits of 10 μg/L for the quantitative SRM transition. Siduron has two isomers which are partially resolved on the Fusion-RP column. Other carbamates and phenylureas that have been analyzed by LC-ESI$^+$-MS/MS include bendiocarb (224→167, 224→109 or 224→81 and 202→145), ethiofencarb (226→164, 253→126), ethiofencarb sulfone (258→107, 258→201), fenobucarb (208→152, 404→372), isoprocarb (194→137, 222→165), propoxur (210→110, 210→168), and other phenylureas include chlorotoluron (213→168, 213→140), desmethylisoproturon (193→151, 193→94), diflubenzuron (311→158, 311→141), isoproturon (207→165, 207→72), forchlorfenuron (248→129, 248→155), lufenuron (512→158, 512→141), metobromuron (259→148, 259→170), pencyuron (329→125, 329→218), teflubenzuron (381→158, 381→141), and triflumuron (359→156, 359→139) [6, 39, 49, 50, 53, 56].

Atmospheric pressure chemical ionization in positive and negative modes (APCI$^+$ or APCI$^-$) can give similar range of sensitivity and structural information as ESI$^+$ and can provide added selectivity for the LC-MS/MS analysis of carbamates [51]. Sodium adducts of the molecular ion do not form with APCI$^+$ and sensitivity is better in positive ion mode than in negative ion mode, partially due to greater fragmentation with to $[M\text{-}CONHCH_3]^-$ in the APCI$^-$ ion source [52, 59]. LC-APCI$^+$-MS has also been found to be more sensitive for some phenylureas [60].

Some of the main degradation products analyzed by LC-ESI$^+$-MS/MS are shown in **Table 6** and include carbamate sulfone or sulfoxides and hydroxyl derivative. Metabolites of carbofuran and carbosulfan have also been analyzed using LC-turboIonSpray-MS/MS, LC-APCI$^+$-MS and LC-QqTOF-MS/MS [61–66]. Other degradation products identified include 3-ketocarbofuran, 3-hydroxy-7-phenolcarbofuran, 3-keto-7-phenolcarbofuran, 7-phenolcarbofuran, and dibutyl amine.

http://dx.doi.org/10.5772/68074

Compound (molecular weight)	Transitions	Cone voltage (V)	Collision energy (eV)	Ratio SRM1/ SRM2 areas ± RSD	Retention time (min)
Aldicarb (190.27)	**208→89**	10	15	2.66 ± 12.5%	12.46
	208→116	10	15		
Aldicarb sulfone (222.26)	**223→76**	15	10	2.83 ± 35.9%	4.60
	240→86	15	20		
Aldicarb sulfoxide (206.26)	**207→89**	15	15	1.13 ± 17.7%	3.29
	207→132	10	5		
Aminocarb (208.26)	**209→152**	20	15	1.39 ± 4.72%	2.85
	209→137	20	20		
Carbaryl (201.22)	**202→145**	22	10	3.32 ± 14.2%	16.35
	202→127	20	25		
Carbofuran (221.25)	**222→123**	20	20	2.73 ± 34.5%	15.27
	222→165	20	20		
Carboxin (235.31)	**236→143**	25	15	3.08 ± 11.3%	16.35
	236→86	20	25		
EPTC (189.32)	**190→128**	20	10	1.70 ± 20.5%	19.99
	190→86	20	10		
3-Hydroxycarbofuran (237.25)	**238→163**	20	10	3.03 ± 10.6%	8.92
	238→220	20	10		
Methiocarb (225.31)	**226→121**	15	20	1.40 ± 11.4%	18.31
	226→169	15	10		
Methiocarb sulfone (257.31)	**275→122**	15	20	1.01 ± 2.10%	12.61
	258→122	25	15		
Methiocarb sulfoxide (241.31)	**242→122**	20	25	1.24 ± 9.46%	9.35
	242→170	20	25		
Methomyl (162.21)	**163→88**	10	10	1.63 ± 4.24%	5.48
	163→106	10	10		
Methomyl-oxime (105.16)	**106→58**	15	10	1.00 ± 7.02%	3.23
	106→106	20	0.010		
Oxamyl (219.36)	**237→72**	20	10	2.45 ± 35.9%	4.66
	237→90	20	10		
Oxamyl-oxime (162.21)	**163→72**	15	10	7.03 ± 27.7%	2.68
	163→90	15	20		
Pirimicarb (238.29)	**239→72**	25	20	2.51 ± 7.80%	8.35
	239→182	30	15		

Compound (molecular weight)	Transitions	Cone voltage (V)	Collision energy (eV)	Ratio SRM1/ SRM2 areas ± RSD	Retention time (min)
Propamocarb HCl (224.73)	**189→102**	30	10	7.49 ± 21.4%	2.90
	189→74	35	15		
Thiodicarb (354.47)	**355→163**	15	10	2.06 ± 29.5%	15.63
	355→108	15	15		
Diuron (233.10)	**233→72**	25	15	1.98 ± 23.1%	16.83
	235→72	25	15		
Linuron (249.09)	**251→162**	15	20	2.20 ± 30.5%	18.68
	251→184	20	15		
Neburon (275.18)	**276→88**	30	15	4.86 ± 15.0%	20.27
	276→114	35	15		
Siduron (232.32)	**233→94**	30	20	1.12 ± 6.70%	18.22
	233→137	30	17		
EPTC-d_{14} (203.4)	**204→50**	20	20	N/A	19.99
Diuron-d_6 (239.13)	**239→52**	20	20	N/A	16.83

Quantitative transitions, where applicable, are shown in bold.

LC-ESI$^+$-MS/MS conditions: Synergi™ Fusion-RP, 60 mm × 2.0 mm i.d., 2.5 μm column; mobile phase of water/acetonitrile with 5 mM ammonium acetate and 0.1% formic acid in aqueous and 0.1% formic acid in organic modifier at a flow rate of 0.15 mL/min with organic modifier starting at 25% v/v and undergoing a gradient to 35% v/v over 4 min, followed by a series of gradient steps as follows: to 80% v/v from 4 to 14.5 min, held for 8 min, to 100% v/v from 22.5 to 23.5 min, and held for 25 min with column temperature at 22°C.

Table 6. Selected reaction monitoring transitions, cone voltage, collision energy, and retention times for the selected carbamates, their degradation products, phenylureas.

LC-APCI $^+$-MS and LC-atmospheric pressure photoionization (APPI$^+$)-MS have also been used to analyze these metabolites as well as sulfoxides and sulfones of carbamates with the protonated molecular ion, ammonium adduct, and $[M+H-CH_3NCO]^+$ observed in the ion source [67–69].

4. Pyrethroid insecticides and their metabolites

Figure 3 shows the structures of the pyrethroid insecticides. They have been routinely analyzed with GC-EI/MS, GC-EI-MS/MS, or GC-NCI-MS methods (see **Table 7**) [3, 5, 6, 9, 10, 14, 42, 70–81]. For the diverse range of pyrethroids these methods are preferred over LC-MS/MS methods. Pyrethroid insecticides are also often analyzed simultaneously with OCs and OPs (either EI or NCI) and generally elute latter in the separation than OCs and OPs. Detection limits with GC-EI-MS for pyrethroids are often more than sufficient for routine analysis in the μg/L range [10].

http://dx.doi.org/10.5772/68074

Negative chemical ionization can provide higher MS selectivity for halogenated pyrethroids compared to GC-EI-MS [7, 10]. Some studies have shown that ammonia, rather than methane, as the reagent gas yields lower detection limits for pyrethroids analyzed by GC-NCI-MS [74], however, methane is still preferred for analysis of OCs and OPs [7, 10]. Pyrethroids also easily fragment in the EI source such that the molecular ion has low abundance and fragment ions are selected for quantitation and confirmation as shown in **Table 7**. For GC-EI-MS/MS the precursor ion is selected as a fragment ion in order to obtain sufficient sensitivity and used over GC-EI-MS when added selectivity is required for more difficult sample matrices.

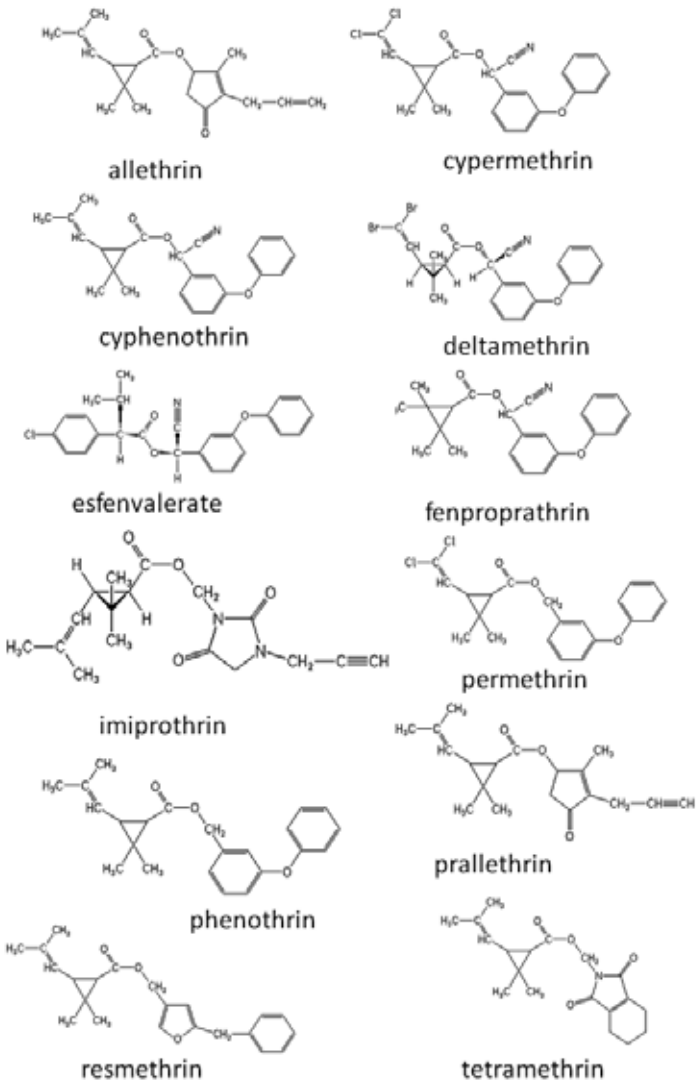

Figure 3: Structures of pyrethroid insecticides.

Analyte	SIM or SRM (*m/z*)	Ref
Pyrethroid insecticides		
Allethrin $C_{19}H_{26}O_3$	123, 136, 202	[70]
	167, 68$^{NCI, CH4}$	This work
Bifenthrin $C_{22}H_{22}ClF_3O_2$	181, 165	[5, 6]
	181, 105	[9]
	181→ 115, 181→165	[3]
	181, 165, 166	[79, 10]
	181→166, 181→165	[76]
	205, 241$^{NCI, CH4}$	[77], this work
	386, 387, 388$^{NCI, CH4}$	[10]
Cyfluthrin (4 peaks) $C_{22}H_{18}Cl_2FNO_3$	163, 226	[70]
	163, 127	[5]
	206, 150	[6]
	163→127, 226→206	[3]
	207, 209$^{NCI, CH4 or NH3}$	This work
λ-Cyhalothrin $C_{23}H_{19}ClF_3NO_3$	209, 181	[70]
	181, 127	[5]
	181, 152	[6]
	205→121, 241→205	[76]
	197→141, 197→161	[14]
	181→127, 197→161	[3]
	181→152, 197→141, 197→161	[80]
	205, 241$^{NCI, NH3 or CH4}$	[77], this work
Cypermethrin (4 peaks) $C_{22}H_{19}Cl_2NO_3$	163, 181	[70]
	181, 163, 209	[79]
	181, 127	[5]
	163, 127	[6]
	91, 163, 181	[42]
	163, 165, 181	[10]
	207, 171$^{NCI, NH3}$	[77]
	207, 209$^{NCI, CH4}$	This work
	207, 209, 171	[10]
	207→35, 209→35	[14]
	163→127, 181→127	[3]

http://dx.doi.org/10.5772/68074

Analyte	SIM or SRM (*m/z*)	Ref
	163→127, 165→127, 165→129	[80]
Deltamethrin (2 peaks)	253, 255	[70]
$C_{22}H_{19}Br_2NO_3$	253, 172	[14]
	93, 181, 253	[42]
	253, 172+174	[6]
	181, 253, 163, 165	[81]
	181, 253, 251	[10]
	172→93, 253→93	[3]
	253→172, 253→174	[80]
	79, 137$^{NCI, NH3}$	[77]
	79,81$^{NCI, CH4}$	This work
	297, 299, 79$^{NCI, CH4}$	[10]
Esfenvalerate (2 peaks) $C_{25}H_{22}ClNO_3$	419, 167, 181	[70]
	211, 167^{NCI}	[77]
	211, 213^{NCI}	This work
	225→119, 225→147	[3]
Fenpropathrin $C_{22}H_{23}NO_3$	181, 265	[70]
	141^{NCI}	[77], this work
Fenvalerate (2 peaks) $C_{22}H_{22}ClNO_3$	167, 125	[5]
	109, 127, 244	[42]
	211, 167^{NCI}	[77]
	211→167, 213→169	[14]
	225→119, 225→147	[3]
	167→125, 125→89, 125→99	[80]
τ-fluvalinate $C_{26}H_{22}ClF_3N_2O_3$	250, 55	[5]
	250, 206, 252	[79]
	250, 200+214	[6]
	294, 258^{NCI}	[77]
	294, 296^{NCI}	This work
	250→55, 250→200	[3]
Flucythrinate (2 peaks) $C_{26}H_{23}F_2NO_4$	199, 157	[5]
Imiprothrin	123, 318, 151	[70]
Cis/trans-permethrin (2 peaks) $C_{21}H_{20}Cl_2O_3$	183, 165	[6, 70, 78]
	183, 163	[5, 9]

Analyte	SIM or SRM (*m/z*)	Ref
	207, 171^{NCI}	[77]
	207, 209^{NCI}	This work
	207→35, 209→35	[14]
	163→127, 183→128	[3]
	163→127, 165→127	[80]
	165→129	
Phenothrin $C_{23}H_{26}O_3$	183, 163	[70]
	331, 167^{NCI}	[77]
Prallethrin $C_{19}H_{24}O_3$	123, 300	[70]
	167, 132, 168	This work
Resmethrin (two peak) $C_{22}H_{26}O_3$	171, 123, 338	[70]
	337, 167^{NCI}	[77]
Tefluthrin $C_{17}H_{14}ClF_7O_2$	205, 241^{NCI}	This work
Tetramethrin (two peak) $C_{19}H_{25}NO_4$	164, 123	[70]
	164, 107	[5]
	349, 167^{NCI}	[77]
Tralomethrin $C_{22}H_{19}Br_4NO_3$	181, 253, 163, 165	[81]
	79, 137^{NCI}	[77]
Transfluthrin $C_{15}H_{12}C_{l2}F_4O_2$	163→121, 163→117	[3]
Metabolites (derivatization reagent)		
CA (diazomethane)	182, 167, 123	[70]
CA (PFBBr)	295→79, 297→79	[14]
DBCA(diazomethane)	231, 233	[70]
DBCA (PFBBr)	312, 253, 231	[71]
DBCA (PFBBr)	295→79, 297→79	[14]
DBCA (MTBSTA)	355, 353, 357, 172	[73, 75]
DBCA (HFIP)	369	[74]
DCCA (diazomethane)	187, 189, 163	[70]
DCCA (PFBBr)	222, 187, 163	[71]
DCCA (PFBBr)	207→35, 209→35	[14]
DCCA (MTBSTA)	265, 267	[72, 75]
DCCA (MTBSTA)	265, 267, 128, 307	[73]
DCCA (HFIP)	323	[74]
3PBA (diazomethane)	197, 228	[70]
3PBA (PFBBr)	228, 197	[71]

Analyte	SIM or SRM (*m/z*)	Ref
3PBA (MTBSTFA)	271, 227, 197	[73, 75]
3PBA (HFIP)	364	[74]
4F3PBA (diazomethane)	246, 215	[70]
4F3PBA (PFBBr)	246, 215	[71]
4F3BA (MTBSTFA)	289, 245, 214	[73, 75]
FBAc(TMSI-TMCS)	251, 252	[72]
MCA(TMSI-TMCS)	211, 212	[72]
CH_3FBAc(TMSI-TMCS)	265, 266	[72]
FB-Al (TMSI-TMCS)	237, 238	[72]
CH3-FB-Al (TMSI-TMCS)	251, 252	[72]
CH_3OCH_2-FB-Al	281, 282	[72]
$HOCH_2$-FB-Al	339, 340	[72]

Electron ionization unless noted. Pentafluorobenzyl bromide, PFBBr; tert-butyldimethylsilyl derivatives of MTBSTFA; 1,1,1,3,3,3-hexafluoroisopropanol (HFIP); and N-trimethlsilylimidazole (TMSI)-trimethylchlorosilane (TMCS) for alcoholic metabolites.

Table 7. GC-MS or GC-MS/MS methods for pyrethroids and metabolites.

Metabolites of pyrethroids include the following: 3-(2,2-dimethylvinyl)-2,2-dimethylcyclopropane-1-carboxylic acid, CA (metabolite of allethrin, imiprothrin, phenothrin, prallethrin, resmethrin, and tetramethrin); 4-fluoro-3-phenoxybenzoic acid, 4-fluoro-3-phenoxybenzoic acid, 4FPBA (metabolite of cyfluthrin), cis- and trans-2,2-dichlorvinyl-2,2-dimethylcyclopropane-1-carboxylic acid, DCCA (metabolite of cyfluthrin, cypermethrin, and permethrin); and 3-phenoxybenzoic acid, 3-PBA (metabolite of cyhalothrin, cypermethrin, deltamethrin, esfenvalerate, fenpropathrin, phenothrin, and permethrin), cis-2,2-dibromovinyl-2,2-dimethyl-2,2-dimethylcyclopropane-1-carboxylic acid, DBCA (metabolite of deltamethrin). Additionally, both carboxylic acid and alcoholic derivatives can form fluoro-containing pyrethroids including the following: 2,3,5,6-tetrafluorobenzyl alcohol (FB-Al) and 2,3,5,6-tetraflurobenzoic acid (FB-Ac) (metabolites of transfluthrin); 2,3,5,6-tetrafluorobenzoic acid (CH_3-FB-Ac) and 4-methyl-2,3,5,6-tetrafluorobenzyl alcohol (CH_3-FB-Al) (metabolites of profluthrin); 4-methoxymethyl-2,3,5,6-tetrafluoro benzyl alcohol (CH_3OCH_2-FB-Al) (metabolite of metofluthrin); and 4-hydroxymethyl-2,3,5,6-tetrafluorobenzyl alcohol ($HOCH_2$-FB-Al) (metabolite of metofluthrin and profluthrin) [72]. Most studies include cis/trans-DCCA, DBCA, 4F3PBA, and 3PBA in their analysis of metabolites of pyrethroids (see **Table 7**). Analysis of metabolites by GC-EI-MS requires derivatization of the metabolites prior to analysis with pentafluorobenzyl bromide (PFBBr), tert-butyldimethylsilyl-N-methyltrifluoroacetamide (MTMSTFA). or 1,1,1,3,3,3-hexafluoroisopropanol (HFIP), and N-trimethlsilylimidazole (TMSI)-trimethylchlorosilane (TMCS) for alcoholic metabolites [14, 70–75]. GC-EI-MS/MS has not been widely used for analysis of the metabolites. Derivatization extends the range of metabolites that are amenable to GC-EI-MS above those commonly analyzed by LC-MS/MS. Some metabolites of pyrethroids including DBCA, DCCA, 4FPBA, and 3PBA can

be analyzed by LC-ESI$^-$-MS/MS (see **Table 8**) [33, 41, 82–84]. Pyrethroids that ionize in an electrospray ion source are more sensitive in positive ion mode with the ammonium adduct formed such that ammonium acetate at ~5 mM should be added to the mobile phase. For those pyrethroids that are more sensitive with LC-ESI$^-$-MS/MS (cyfluthrin and cyhalothrin), the deprotonated molecular ion forms in the ion source. The metabolites form the deprotonated molecular ion in the ESI ion source. In general, only a few pyrethroids have been included in LC-ESI$^+$-MS/MS multiclass methods.

Analyte (monoisotopic mass)	**SIM or SRM (*m/z*)**	**Reference**
Pyrethroids		
Bifenthrin (422.1)	440→182	[82]
Cyfluthrin (433.1)	451→191, 451→434	[39]
	435→191, 435→127	[84]
	432→405	[82]
Cyhalothrin (449.1)	448.2→402.8^{ESI-}	[82]
Cypermethrin (415.1)	433→191, 433→416	[35, 39, 84]
	433→191	[82]
Deltamethrin (502.0)	523→506, 523→281	[39]
	506→281, 506→253	[84]
	521→279	[82]
Permethrin (390.1)	408→355, 408→183	[84]
	408→183	[82]
Esfenvalerate (419)	437→167	[82]
Metabolites		
DBCA	343→81, 297→81^{ESI-}	[83]
	295→79^{ESI-}	[82]
	299→299	[84]
DCCA	207→207, 209→209^{ESI-}	[41, 84]
	207→207, 207→35^{ESI-}	[39]
	207→35, 209→35, 209→37^{ESI-}	[33]
	209→37, 207→35^{ESI-}	[83]
	207→35^{ESI-}	[82]
4-FPBA	231→93, 231→65^{ESI-}	[83]
	231→93^{ESI-}	[82]
3-PBA	213→93, 213→169^{ESI-}	[33, 41]
	213→93, 213→65^{ESI-}	[83]
	213→93^{ESI-}	[82]

Table 8. Pyrethroid insecticides and their metabolites by LC-MS/MS. Electrospray ionization in positive ion mode unless noted.

http://dx.doi.org/10.5772/68074

5. Other considerations

Generally, there is a larger diversity of azole fungicides and strobilurin fungicides that can be analyzed with LC-ESI$^+$-MS/MS methods as compared to those amenable to GC-MS methods [76, 79, 80, 85, 86]. For pesticides that are halogenated, GC-NCI-MS should be considered as an option to improve the sensitivity or selectivity of the analysis. Dissociative electron capture is often observed in negative chemical ionization for OPs, OCs, pyrethroids, azole fungicides, and strobilurin fungicides. GC-EI-MS/MS methods may also provide added selectivity; however, as many pesticides from these chemical classes fragment easily in an EI ion source, the precursor ion may need to be selected as a fragment ion which is capable of undergoing further collision-induced dissociation to achieve the required sensitivity. OP metabolites (OP oxons, sulfones, sulfoxides, and selected others) can be analyzed by LC-ESI$^+$-MS/MS, while alkylphosphates or alkylthiophosphates should be analyzed by LC-ESI $^-$-MS/MS or following derivatization by GC-MS. Pyrethroid metabolites are still commonly analyzed following derivatization with GC-EI-MS methods with a small selection of common pyrethroid metabolites also frequently analyzed by LC-MS/MS.

6. Conclusions

A larger number of OPs including organophosphates and organothiophosphates have been analyzed by GC-MS or GC-MS/MS methods as compared to LC-ESI$^+$-MS/MS. GC-EI-MS or GC-EI-MS/MS is most commonly selected for analysis of OPs, and GC-EI-MS provides excellent confirmation of identity of the OP through spectral library matches. When added selectivity is required, such as when matrix remains after sample clean-up, analysis of OPs by GC-NCI-MS or GC-EI-MS/MS should be selected. GC-NCI-MS analysis of halogenated (or nitro substituted) OPs generally provides better sensitivity than GC-EI-MS/MS, particularly when the precursor ion selected for CID is the molecular ion. Although NCI is a softer ionization process than EI, fragment ions are still often observed as a result of dissociative electron capture. Sensitivity of GC-EI-MS/MS can be improved by selection of an abundant fragment ion for the precursor ion rather than the molecular ion which may be too low in abundance. The number of applications using LC-ESI$^+$-MS/MS for the analysis of OPs has increased in the past ten years and for those OPs that can be ionized efficiently by ESI, the sensitivity may be better than with GC-MS methods (particularly for OPs that elute later in the GC separations). Another advantage of LC-ESI$^+$-MS/MS is that it is feasible to analyze OP degradation products (OP oxons, OP sulfones, or OP sulfoxides) simultaneously with parent OPs. Derivatization of alkylphosphates and alkylthiophosphates metabolites of OPs is required to achieve the desired sensitivity when analyzed by GC-MS or GC-MS/MS methods. Alkylphosphate metabolites can also be analyzed by LC-ESI$^-$-MS/MS.

Pyrethroids can be analyzed simultaneously with OCs and OPs using GC-EI-MS or GC-EI-MS/MS. A number of pyrethroids are halogenated and consequently they can be analyzed by GC-NCI-MS for added selectivity and sensitivity. Metabolites of pyrethroids are derivatized prior to the analysis by GC-EI-MS or GC-EI-MS/MS and this approach remains the method

of choice for their analysis. Analysis of pyrethroids by LC-MS/MS is more limited; however, metabolites of pyrethroids can be analyzed using LC-ESI$^-$-MS/MS.

Carbamates and phenylureas are commonly analyzed by LC-ESI$^+$-MS/MS. Selected carbamates can be analyzed by GC-MS methods, but a derivatization step is required prior to analysis. The main degradation products of carbamates including carbamate sulfone or sulfoxides can be analyzed by LC-ESI$^+$-MS/MS simultaneously with carbamates and phenylureas. APCI and APPI in positive ion mode have also been used to ionize metabolites of carbamates to achieve better sensitivity than ESI. APCI$^+$ is also not prone to sodium adduct formation. Mobile phase additives used for the LC-ESI$^+$-MS/MS separation of both OPs, carbamates and phenylureas include 0.1% formic acid and 5 mM ammonium acetate. Better sensitivity for OPs is obtained when methanol is used as the organic modifier for gradient elution, while acetonitrile is more commonly used for the separation of carbamates to obtain optimal sensitivity. Carbamates are prone to adduct formation (reduce sensitivity) in mobile phases containing methanol, and ammonium formate or ammonium acetate is generally used to reduce sodium adduct formation. Other pesticides that can be analyzed by LC-ESI$^+$-MS/MS include azole fungicides, neonicotinoid insecticides, and strobilurin fungicides. Pending the target list of pesticides, it is feasible to obtain simultaneous analysis of all these chemical classes; however, if optimal sensitivity is required then class-specific methods will achieve better results.

Acknowledgements

This work was financially supported by the Natural Sciences and Engineering Research Council (NSERC) of Canada and additional instrument support from Canadian Foundation for Innovation.

Author details

Renata Raina-Fulton*, Nicole Dunn and Zhen Xie

*Address all correspondence to: renata.raina@uregina.ca

Department of Chemistry & Biochemistry, Trace Analysis Facility, The University of Regina, Regina, SK, Canada

References

[1] Raina-Fulton, R.; Xie, Z. Intech submitted 2017, Chapter: Sample Preparation in Food and Beverage Analysis, Biological and Environment Matrices. Intech.

[2] Raina-Fulton, R. (2015). J. AOAC Int., 98, 1163–1170.

[3] Palenikova, A.; Martinez-Dominguez, G.; Arrebelo, F.J.; Romero-Gonzalez, R.; Hrouzkova, S.; Frenich, A.G. (2015). Food Chem., 173, 796–807.

[4] Lehotay, S.J.; Son, K.A.; Kwon, H.; Koesukwiwat, U.; Fu, W.; Mastovska, K.; Hoh, E.; Leepipatpiboon, N. (2010). J. Chromatogr. A, 1217, 2548–2560.

[5] Rasche, C.; Fournes, B.; Dirks, U.; Speer, K. (2015). J. Chromatogr. A, 1403, 21–31.

[6] Cazorla-Reyes, R.; Fernandez-Moreno, J.L.; Romerto-Gonzalez, R.; Frenich, A.G.; Martinez Vidal, J.L. (2011). Talanta, 85, 183–196.

[7] Raina, R.; Hall, P. (2008). Anal. Chem. Insights, 3, 111–125.

[8] Raina, R. (2011). Ch 5., Chemical Analysis of Pesticides using GC/MS, GC/MS/MS, and LC/MS/MS in Pesticides- Strategies for Pesticide Analysis, editor Margarita Stoytcheva. ISBN 978-953-307-460-3. Intech, Croatia - European Union

[9] Dos Anjos, J.P.; Andrade, J.B. (2014). Microchem. J., 112, 119–126.

[10] Huskova, R.; Matisova, E.; Hrouzkova, S.; Svorc, L. (2009). J. Chromatogr. A, 1216, 6326–6334.

[11] Raina, R.; Sun, L. (2008). J. Environ. Sci. Health, Part B, 43, 323–332.

[12] Hardt, J.; Angerer, J. (2000). J. Anal. Toxicol., 24, 678–684.

[13] Heudorf, U.; Angerer, J. (2001). Environ. Res. Sect. A, 86, 80–87.

[14] Hardy, E.M.; Duca, R.C.; Salquebre, G.; Appenzeller, B.M.R. (2015). Forensic Sci. Inter., 249, 6–19.

[15] Barr, J.D.; Bell, A.J.; Bird, M.; Mundy, J.L.; Murrell, J.; Timperley, C.M.; Watts, P.; Ferrante, F. (2005). J. Am. Soc. Mass Spectrom., 16, 515–523.

[16] Bravo, R.; Caltaiano, L.M.; Weerasekera, G.; Whitehead, R.D.; Fernandez, C.; Needham, L.L.; Bradman, A.; Barr, D.B. (2004). J. Expos. Anal. Environ. Epidemiol., 14, 249–259.

[17] Naeher, L,P.; Tulve, N.E.; Egeghy, P.P.; Barr, D.B.; Adetona, O.; Fortmann, R.C.; Needham, L.L.; Bozeman, E.; Hilliard, A.; Sheldon, L.S. (2010). Sci. Total Environ., 405, 1145–1153.

[18] Tsatsakis, A.M.; Barbounis, M.G.; Kavalakis, M.; Kokkinakis, M.; Terzi, I.; Tzatzarakis, M.N. (2010). J. Chromatogr. B, 878, 1246–1252.

[19] Yorkley, R.A.; Shen, N.; Cheung, M.W. (2000). J. AOAC Int., 83 (5), 1229–1238.

[20] Becker, K.; Seiwert, M.; Angerer, J.; Kolossa-Gehring, M.; Hoppe, H.; Ball, M.; Schulz, C.; Thumulla, J.; Seifert, B. (2006). Int. J. Hyg. Environ. Health, 209, 221–233.

[21] Koch, H.M.; Angerer, J. (2001). J. Chromatogr. B, 799, 43–49.

[22] Gomez-Ramos, M.; Perez-Parada, A.; Garcia-Reyes, J.F.; Fernandez-Alba, A.R.; Aguera, A. (2011). J. Chromatogr. A, 1218, 8002–8012.

[23] Garcia-Valcarcel, A.I.; Tadeo, J.L. (2009). Anal. Chim. Acta, 641, 117–123.

[24] Bicker, W.; Lammerhofer, M.; Lindner, W. (2005). J. Chromatogr. B, 822, 160–169.

[25] Inoue, S.; Saito, T.; Miyazawa, T.; Mase, H.; Inokuchi, S. (2009). Forensic. Toxicol., 27, 32–36.

[26] Lacorte, S.; Ehresmann, N.; Barcelo, D. (1996). Environ. Sci. Technol., 30, 917–923.

[27] Ibanez, M.; Sancho, J.V.; Pozo, O.J.; Hernandez, F. (2006). Anal. Bioanal. Chem., 384, 448–457.

[28] Armstrong, J.L.; Dills, R.L.; Yu, H.; Yost, M.G.; Fenske, R.A. (2014). J. Environ. Sci. Health, Part B, 49, 102–108.

[29] Williamson, L.N.; Bartlett, M.G.; Terry, A.V. (2007). J. Liquid Chromatogr. Related Technol., 30, 273–285.

[30] Sancho, J.V.; Pozo, O.J.; Hernandez, F. (2000). Rapid Commun. Mass Spectrom., 14, 1485–1490.

[31] Hernandez, F.; Sancho, J.V.; Pozo, O.J. (2002). Rapid Commun. Mass Spectrom., 16, 1766–1773.

[32] Williamson, L.N.; Terry, A.v.; Bartlett, M.G. (2006). Rapid Commun. Mass Spectrom., 20, 2689–2695.

[33] Rousis, N.I.; Zuccato, E.; Castiglioni, S. (2016). Sci. Total Environ., 571, 1349–1357.

[34] Bicker, W.; Lammerhofer, M.; Genser, D.; Kiss, H.; Lindner, W. (2005). Toxicol. Lett., 159, 235–251.

[35] Chung, S.W.C.; Chan, B.T.P. (2010). J. Chromatogr. A, 1217, 4815–4824.

[36] Liao, H.; Hsieh, C.; Chiang, S.; Lin, M.; Chen, P.; Wu, K. (2011). J. Chromatogr. A, 879, 1961–1966.

[37] Golger, O.; Kabak, B. (2015). Food Chem., 176, 319–332.

[38] Salm, P.; Taylor, P.J.; Roberts, D.; de Silva, J. (2009). J. Chromatogr. B, 877, 568–574.

[39] Berton, T.; Mayhoub, F.; Chardon, K.; Duca, R.; Lestremau, F.; Bach, V.; Tack, K. (2014). Environ. Res., 132, 311–320.

[40] Davis, M.D.; Wade, E.L.; Restrpo, P.R.; Roman-ESteva, W.; Bravo, R.; Kuklenyik, P.; Calafat, A.M. (2013). J. Chromatogr. B, 929, 18–26.

[41] Radford, S.A.; Panuwet, P.; Hunter, R.E.; Barr, D.B.; Ryan, P.B. (2016). J. Agric. Food Chem., 64, 4633–4638.

[42] Chowdhury, M.A.Z.; Fakhruddin, A.N.M.; Islam, N.; Moniruzzaman, M.; Gan, S.H.; Alam, K. (2013). Food Control, 34, 457–465.

[43] Chen, H.; Chen, R.; Li, S. (2010). J. Chromatogr. A, 1217, 1244–1248.

[44] Yang, E.; Shin, H. (2013). J. Chromatogr. A, 1305, 328–332.

[45] Zhang, J.; Lee, H.K. (2006). J. Chromatogr. A, 1117, 31–37.

[46] Crespo-Corral, E.; Santo-Delgado, M.J.; Polo-diez, L.M.; Sanz-Perucha, J. (2006). J. Chromatogr. A, 1132, 241–247.

[47] Petropoulou, S.E.; Gikas, E.; Tsarbopoulos, A.; Siskos, P.A. (2006). J. Chromatogr. A, 1108, 99–110.

[48] Climent, M.J.; Miranda, M.A. (1996). J. Chromatogr. A, 738, 225–231.

[49] Choi, S.; Kim, S.; Shin, J.Y.; Kim, M.; Kim, J. (2015). Food Chem., 173, 1236–1242.

[50] Nogueira, J.M.F.; Sandra, T.; Sandra, P. (2003). J. Chromatogr. A, 996, 133–140.

[51] Pirard, C.; Widart, J.; Nguyen, B.K.; Deleuze, C.; Heudt, L.; Haubruge, E.; De Pauw, E.; Focant, J.-F. (2007). J. Chromatogr. A, 1152, 116–123.

[52] Lee, S.J.; Park, S.; Choi, J.Y.; Shim, J.; Shin, E.; Choi, J.; Kim. S.T.; Abd El-Aty, A.M.; Jin, J.S.; Bae, D.W.; Shin, S.C. (2009). Biomed. Chromatogr., 23, 719–731.

[53] Wang, J.; Cheung, W.; Grant, D. (2005). J. Agric. Food Chem., 53, 528–537.

[54] Liu, M.; Hashi, Y.; Song, Y.; Lin, J. (2005). J. Chromatogr. A, 1097, 183–187.

[55] Aguilera-Luiz, M.M.; Plaza-Bolanos, P.; Romero-Gonzalez, R.; Martinez Vidal, J.L.; Garrido Frenich, A. (2011). Anal. Bioanal. Chem., 399, 2863–2875.

[56] Moreno-Gonalez, D.; Huertas-Perez, J.F.; Garcia-Campana, A.M.; Bosque-Sendra, J.M.; Gamiz-Gracia, L. (2013). J. Chromatogr. A, 1315, 1–7.

[57] Zainudin, B.H.; Salleh, S.; Mohamed, R.; Yap, K.C.; Muhamad, H. (2015), Food Chem., 172, 585–595.

[58] Shi, Z.; Hu, J.; Li, Q.; Zhang, S.; Liang, Y.; Zhang, H. (2014). J. Chromatgr. A, 1355, 219–227.

[59] Fernandez, M.; Pico, Y.; Manes, J. (2000). J. Chromatogr. A, 871, 43–56.

[60] Thurman, E.M.; Ferrer, I.; Barcelo, D. (2001). Anal. Chem., 73, 5441–5449.

[61] Soler, C.; Hamilton, B.; Furey, A.; James, K.J.; Manes, J.; Pico, Y. (2007). Anal. Chem., 79, 1492–1501.

[62] Soler, C.; Hamilton, B.; Furey, A.; James, K.J.; Manes, J.; Pico, Y. (2006). Anal. Chim. Acta, 571, 1–11.

[63] Totti, S.; Fernandez, M.; Ghini, S.; Pico, Y.; Fini, F.; Manes, J.; Girotti, S. (2006). Talanta, 69, 724–729.

[64] Abass, K.; Reponen, P.; Mattila, S.; Rautio, A.; Pelkonen, O. (2014). Toxicol. Lett., 224, 290–299.

[65] Soler, C.; Hamilton, B.; Furey, A.; James, K.J.; Manes, J.; Pico Y. (2006). Rapid Commun. Mass Spectrom., 20, 2151–2164.

[66] Detomaso, A.; Mascolo, G.; Lopez, A. (2005). Rapid Commun. Mass Spectrom., 19, 2193–2202.

[67] Takino, M.; Yamaguchi, K.; Nakahara, T. (2004). J. Agric. Food Chem., 52, 727–735.

[68] Nunes, G.S.; Alonso, R.M.; Ribeiro, M.L.; Barcelo, D. (2000). J. Chromatogr. A, 888, 113–120.

[69] Soler, C.; Manes, J.; Pico, Y. (2006). J. Chromatogr. A, 1109, 228–241.

[70] Starr, J.; Graham, S.; Stout, D.; Andrews, K.; Nishioka, M. (2008). Environ. Res., 108, 271–279.

[71] Angerer, J.; Ritter, A. (1997). J. Chromatogr. B, 695, 217–226.

[72] Yoshida, T. (2013). J. Chromatogr. B, 913, 77–83.

[73] Schettgen, T.; Koch, H.M.; Drexler, H.; Angerer, J. (2002). J. Chromatogr. B, 778, 121–130.

[74] Weilgomas, B.; Nahorski, W.; Czarnowski, W. (2013). Intern. J. Hyg. Environ. Health, 216, 295–300.

[75] Wei, B.; Mohan, K.R.; Weisel, C.P. (2012). Intern. J. Hyg. Environ. Health, 215, 465–473.

[76] Schummer, C.; Salquebre, G.; Briand, O.; Millet, M.; Appenzeller, B.M.R. (2012). Toxicol. Lett., 210, 203–210.

[77] Feo, M.L.; Elijarrat, E.; Barcelo, D. (2010). J. Chromatogr. A, 1217, 2248–2253.

[78] Pinheiro, A.S.; Rocha, G.O.; Andrade, J.B. (2011). Microchem. J., 99, 303–308.

[79] Tankiewicz, M.; Morrison, C.; Biziuk, M. (2013). Talanta, 107, 1–10.

[80] Salquebre, G.; Schummer, C.; Millet, M.; Briand, O.; Appenzeller, B.M.R. (2012). Anal. Chim. Acta, 710, 65–74.

[81] Valverde, A.; Aguilera, A.; Rodriguez, M.; Boulaid, M. (2001). J. Chromatog. A, 943, 101–111.

[82] Li, W.; Morgan, M.K.; Graham, S.E.; Starr, J.M. (2016). Talanta, 151, 42–50.

[83] Le Grand, R.; Dulaurent, S.; J.M. Gaulier, J.M.; Saint-Marcoux, F.; Moesch, C.; Lachatre, G. (2012). Toxicol. Lett., 210, 248–253.

[84] Meyer-Monath, M.; Chatellier, C.; Cabooter, D.; Rouget, F.; Morel, I.; Lestremau, F. (2015). Toxicol. Lett., 138, 231–239.

[85] Raina, R.; Smith, E. (2012). J. AOAC Int., 95, 1350–1356.

[86] Raina-Fulton, R. (2015). J. Agric. Food Chem., 63, 5152–5162.

Applications

Chapter 5

Mass Spectrometry for the Sensitive Analysis of Intracellular Nucleotides and Analogues

Kateřina Mičová, David Friedecký and Tomáš Adam

Additional information is available at the end of the chapter

http://dx.doi.org/10.5772/68073

Abstract

Nowadays, mass spectrometry is very important and widely applied tool in nucleotide analysis. As a result of technological advances in sample preparation, separation and mass spectrometry detection, the developed methods allow sensitive and selective measurement of polar compounds occurring in low levels in various biological matrices. This enables more potential uses in clinical field. Direct methods require no special sample pre-treatment before analysis in contrast to indirect methods, where fractionation, dephosphorylation and purification are needed. The use of ion-pairing agent, ion exchange chromatography with pH gradient, porous graphitic carbon columns and HILIC in liquid chromatography represents the most common methods of nucleotide analysis. High separation efficiency is also achieved with the use of CE with MS detection. Analysis of nucleotides was also described by the means of MALDI-TOF, but poor reproducibility and lack of applications make a limitation for this approach. The chapter summarizes different techniques and approaches for determination of endogenous nucleotides and its analogues in various clinical applications.

Keywords: nucleotides, nucleotide analogues, mass spectrometry, capillary electrophoresis, liquid chromatography, MALDI-TOF, HILIC-MS/MS, triple quadrupole, selected reaction monitoring

1. Introduction

Nucleotides and nucleosides, together with their deoxidized forms, are involved in several important cellular processes. The structure of the nucleoside molecule consists of a heterocyclic base (adenine, guanine, cytosine, uracil and thymine) joined to a molecule of pentose (ribose

INTECH
open science | open minds

© 2017 The Author(s). Licensee InTech. This chapter is distributed under the terms of the Creative Commons Attribution License (http://creativecommons.org/licenses/by/3.0), which permits unrestricted use, distribution, and reproduction in any medium, provided the original work is properly cited. CC BY

or deoxyribose) through a glycosidic bond. Nucleotides are formed by phosphorylation of nucleoside molecule. They represent a fundamental building block of the structure of nucleic acids formed by the polymerase-mediated synthesis of DNA and RNA from deoxynucleotides and nucleotides, respectively. All deoxynucleotides are synthesized from the corresponding nucleotides. Nucleotides play another important role in enzyme activation and metabolism. They are incorporated into important cofactors of enzymatic reactions such as transfer of various groups by coenzyme A (e.g. acetyl-CoA and succinyl-CoA) in many metabolic processes, NAD, NADP and FAD as coenzymes of oxidoreductases catalyses redox reactions in the cell. ATP and other nucleoside triphosphates are engaged as source energy providers. In the form of coenzymes, they transfer phosphate residues or nucleotide constituent and participate in the activation (e.g. uridine diphosphate glucose for pasting glucose units to polymeric saccharides or cytidine diphosphate-choline for phospholipid synthesis). Cyclic nucleotides act as secondary messengers in many signal transduction pathways. The most important nucleotide signal molecule is cyclic adenosine monophosphate (cAMP), which is an activator of protein kinases and participates in many metabolic pathways by transferring the effect of hormones into cells. Analogical molecule—cyclic guanosine monophosphate (cGMP)—also acts as a secondary messenger in the phototransduction process.

Nucleotide metabolism is one of the main therapeutic cellular targets. Synthetic analogues of these compounds have been widely applied in anti-cancer, anti-viral and immunosuppressive therapies [1–6]. Nucleoside analogues (e.g. cytarabine, gemcitabine and zidovudine) are modified at the base or sugar moiety. This 'prodrug' form requires intracellular activation by phosphorylation to mono, di or triphosphates. Related drugs are nucleobase analogues (6-mercaptopurine and thioguanine) without sugar-phosphate moiety and also fluoropyrimidines (fluorouracil, capecitabine and floxuridine). Its mechanism of action is based on the structural similarity to its natural endogenous precursor. Therefore, the analogues are called 'anti-metabolites' [4, 7].

Over 30 inherited disorders resulting from errors of purine and pyrimidine metabolism are known, and therefore the determination of the levels of nucleosides and nucleotides is used in their diagnosis and treatment monitoring. Disorders of purine and pyrimidine metabolism are clinically very diverse—manifestations include immunodeficiencies, urolithiases, mental defects and others. Adenosine deaminase deficiency, resulting in deoxyadenosine accumulation; purine nucleoside phosphorylase deficiency, characterized by elevated deoxyguanosine; hyperuricemia; hypoxanthine-guanine phosphoribosyl transferase deficiency, leading to high levels of uric acid, and phosphoribosylpyrophosphate synthetase overactivity, resulting in the overproduction of purine and uric acid. The most common pyrimidine metabolism disorder is orotic aciduria, where the defect of UMP-synthase causes the disease and leads to the excessive excretion of orotic acid in the urine [8].

Similarly, the determination of nucleotides and their intermediates is an important tool for understanding the metabolism of endogenous nucleotides and their synthetic analogues and also for the establishment of a diagnosis of disorders related to defects in the biosynthesis and degradation processes of purine/pyrimidine nucleotides [9]. The concentration of particular deoxy/nucleotides differs among various cell types and extracellular material

http://dx.doi.org/10.5772/68073

(plasma, urine—very low concentrations are physiologically present). Intracellular nucleotide analogue levels can also vary from patient to patient, which can result in under-treatment or toxicities [10]. In consequence of the often very low intracellular levels of nucleotide analogues in comparison to their natural variants, highly sensitive and selective analytical methods are necessary for the quantification [9–11].

Sample preparation is the major critical step in the determination of endogenous nucleotides and their analogues in biological material. The pre-analytical phase, including sampling, transport of material and sample preparation, plays an important role in the whole analytical process. The treatment of the sample is based on the material used for analysis, such as whole blood [12], erythrocytes [13–15], mononuclear cells [14, 16–24], cultured cells [25–35], plasma [12, 19, 20, 36, 37], urine [38], dry blood spots [15] and others [36, 39–47]. The enzymes involved in purine and pyrimidine metabolism can fundamentally change the nucleotide pool during the pre-analytical process and this should be stopped as soon as possible.

To date, many and various approaches using different analytical techniques have been developed for the determination of nucleotides and their analogues (in this chapter globally called nucleotides). Historically, the ATP concentration was measured by means of the luciferin-luciferase luminescence assay technique [48]. Radioimmunoassays were quite sensitive but had poor specificity as a result of cross-reactivity with structurally similar molecules [49, 50]. For separation of nucleotides, thin layer chromatography [51], capillary electrophoresis (CE) [52–56] and liquid chromatography [9, 12–15, 18, 19, 29, 30, 32, 36, 40, 42, 45, 46, 57–62] have been used. Because of the requirement of the simultaneous determination of several nucleotides and low-level deoxynucleotides occurring in complex matrices, separation techniques coupled predominantly to UV/DAD or mass spectrometry (MS) detection have become essential tool for analysis. Although UV detection has been widely applied for the detection of nucleotides in biological matrix [63–72], it suffers from very low sensitivity and specificity [9]. Sensitivity for adenosine nucleotides was significantly improved by fluorescence detection. However, analysis by means of this approach is time-consuming as a result of required derivatization step [73].

The first application of mass spectrometry to the analysis of amino acids and peptides was reported in 1958 [74]. With the advent of clinically useful mass spectrometers, this technology prevails for nucleotide detection in biological matrices. Because of the increasing requirements of clinical laboratories to analyse multiple analytes in a broad concentration range simultaneously, the high sensitivity and specificity of the technique and its growing price availability, it has become a prominent tool in most clinical research and routine practice.

Capillary electrophoresis (CE) can be used for the separation of mainly ionic and highly polar compounds with high resolution, which makes this technique suitable for nucleotide analysis. In combination with mass spectrometry, it has been used for nucleotide analysis in several applications [10, 52, 53, 55, 56, 75]. However, the most crucial problem in the coupling of CE to MS detection is the limited range of available and convenient interface techniques. Moreover, the electrophoresis run buffer has to be compatible with MS detection. Because of the practicality and wide possibilities of adjustment, presently liquid chromatography in

combination with mass spectrometry is the most frequently used separation technique for nucleotide determination in many biological materials.

Liquid chromatography has become an essential tool for the analysis of nucleotide in recent decades. The polarity of the nucleotides increases with the number of phosphate groups. Reversed-phase (RP) liquid chromatography is frequently used for the separation of nucleosides and also nucleoside monophosphates [14, 15, 22, 28, 30, 33, 36, 37, 58]. Because of their hydrophilicity, triphosphate nucleosides have very poor retention when separated on traditional reverse-phase high-performance liquid chromatography columns, and thus another chromatographic approach is required. The possibility is using ion-pairing [12, 16, 19–21, 23, 26, 31, 32, 41, 47] or anion exchange chromatography [13, 17, 18, 27, 42]. These approaches enhance the retention on RP columns, but they are, however, compromised by the high levels of additives in mobile phases (ammonium salts and alkylamines), which cause significant ion suppression, poor robustness and instability of the ion exchange columns, and also source pollution, which remains a major problem [10, 16, 60, 76]. The analysis of nucleotides on RP-HPLC is also possible by indirect methods based mainly on dephosphorylation using uric acid or alkaline phosphatase and subsequent analysis of particular nucleosides, the retention of which is significantly better on reverse-phase analytical columns compared to their triphosphate precursors [14, 15, 22, 33, 77, 78]. The indirect methods using fractionation and dephosphorylation simplify the final determination of significantly better ionizable nucleosides, but the overall complexity and time required for the use of the method rises and many errors could be introduced into the sample pre-treatment. Another possible way to measure nucleosides and their monophosphates (MP), diphosphates (DP) and triphosphates (TP) by liquid chromatography under MS-friendly conditions is using hydrophilic interaction liquid chromatography. Polar columns using mobile phase rich in organic solvent with increasing amount of water content during analytical run are suitable for coupling with MS [34, 39, 40, 43, 79].

In the last decade, many reviews on the analysis of endogenous nucleotides and low-level nucleotide analogues in biological matrices by various separation techniques but especially with liquid chromatography [9] and detection by mass spectrometry [10, 11] have been published. This chapter is focused on describing several approaches to the determination of endogenous nucleotides and low-level nucleotide analogues in biological matrices by means of various separation techniques in combination with mass spectrometry detection. In practical part, we are showing analysis of low-level of nucleotide analogues 5′-ethynyl-2′-deoxycytidine and 5′-ethynyl-2′-deoxyuridine, their mono-, di-, and triphosphates in the presence of the high levels of the physiological nucleotides by LC-MS/MS method.

2. Sample preparation

The sample preparation is probably the most critical step in separation methods. The mostly used mass spectrometers need a clean sample without salts and lipids causing ion suppression, signal response reduction and poor robustness of analytical methods. Gradual pollution

http://dx.doi.org/10.5772/68073

of the ion source and other parts of the instrument causes poor analytical quality and harms the long-term stability of the instrument. The pre-treatment of the sample and extraction of the nucleotides depend on the matrix sample types, such as peripheral blood mononuclear cells (PBMCs), cultured cells, tissue, plasma and so on, and also on the separation and detection mode. All matrices contain many active enzymes included in the biochemical pathways responsible for the conversions or transformations of nucleotides. Thus, cell lysis and inactivation of certain enzymes is the first required step. The extraction solution should therefore completely extract nucleotides and precipitate and inactivate proteins without compromising the stability of these analytes. The nucleotide structure contains phosphate groups and therefore the compounds have ionic character. It must be taken into account that during the preparation of the sample the organic agents used for each step of the sample preparation have enough polarity to prevent precipitation of the nucleotides. It is different for mono-, di-, and triphosphates, with triphosphates especially being sensitive to the choice of less polar solvents. In general, the sample preparation is initiated by the protein precipitation and extraction of the nucleotides, eventually purified from phospholipids by solid phase extraction (SPE) or liquid-liquid extraction (LLE), pre-concentrated by evaporating under the nitrogen flow or freeze drying and reconstituting in predominantly water solution.

Protein precipitation (PP) is usually performed with a strong acid such as perchloric acid (PCA) [17, 25, 36, 41, 62, 80] or trichloroacetic acid (TCA) [42, 75] and most often by organic solvents such as methanol (MetOH) [12, 18, 26–28, 39, 43, 55, 60, 81, 82] or ethanol (EtOH) [19] or acetonitrile (AcCN) [37]. Because of the instability of nucleotides at a low pH, a neutralization step after the PP with strong acid is required. Neutralization was performed using NaOH with a subsequent centrifugation step [80]. The PCA extracts were treated with KOH and the resulting $KClO_4$ precipitate was removed by centrifugation. The supernatant was directly stored at −20°C [25] or lyophilized [41] prior to the LC-MS analysis. The PP and extraction of the cyclic nucleotides by PCA was introduced in a study by Oeckl et al. and it was demonstrated on plasma and brain tissues. The materials were homogenized with 0.4 M PCA using sonication, and after centrifugation, the supernatant was filtered through cellulose membrane and stored at −80°C until analysis [36, 62].

PP with TCA is less frequently described because of its poor compatibility with MS detection; nevertheless Friedecký et al. used TCA for the deproteination of incubated cells followed by back-extraction into ether. This procedure provided an increased pH value and better stability of the nucleotides. Water phase extracts were used for the CE-MS analyses [75].

At present, precipitation by organic solvent is predominantly used. Derissen et al. described the usage of pure MetOH for the lysis of PBMC, and after mixing and centrifugation, the sample extract was stored at −70°C until analysis [18]. MetOH was used for the PP of the plasma samples designed for the determination of the nucleotides [12]. Soga et al. also used MetOH for cell lysis, but this procedure was followed by LLE based on the addition of chloroform and water to remove the phospholipids. After centrifugation, the resulting water-MetOH layer was lyophilized and dissolved in pure water before CE-ESI-MS analysis [55]. In a general metabolomic study covering 164 compounds including several nucleotides, 80% MetOH at the temperature of 75°C was used for three consecutive metabolite extractions [43]. Cell lysis,

PP and nucleotide extraction were also performed with ice-cold 70% MetOH [27, 39] followed by storage at −20°C [28, 82] or snap-frozen in liquid nitrogen [29]. A similar procedure can be performed with a 60% MetOH solution followed by incubation at −20°C for complete extraction and PP [26, 81] or frozen in liquid N_2 [60]. In a study of rat heart tissue, the extraction of the homogenate was performed with pre-cooled MetOH-water (1:1, v/v) and followed by centrifugation, and the supernatant was directly analysed [45]. Cyclic intracellular nucleotides were extracted by a mixture of AcCN/MetOH/water (2:2:1, v/v). The extract was heated to 95°C, cooled down, centrifuged, dried under flow of nitrogen and resuspended in water for analysis [30].

Several studies compared extraction procedures. Klawitter et al. compared four extraction agents [12% PCA, 70% AcCN, 70% MetOH and MetOH/chloroform (1:1, v/v)] applied to homogenized kidney tissue. The extracted homogenates were centrifuged, and the supernatant was collected, pellet was re-suspended in water and centrifuged and the supernatants were combined. In case of the PCA extraction, an additional neutralizing step (2 M KOH followed by 1 M $KHCO_3$) was performed. The resulting $KClO_4$ precipitate was removed and extracts were consequently lyophilized. The PCA extraction provided the best absolute recovery and best reproducibility among the four extraction procedures used in this study. The recovery varied from 75.6 to 89.1%, depending on the type of nucleotide [41]. Cordell et al. compared extraction solvents such as AcCN, ethanol (EtOH), MetOH, AcCN:water (8:2, v/v), EtOH:water (8:2, v/v), MetOH:water (8:2, v/v), 0.1 M formic acid, 0.5 M PCA and 0.1 M formic acid in MetOH using Chinese hamster ovary (CHO) cells. The authors also studied the effect of sonication on ice prior to the removal of the extraction fluid as well as the hexane addition in the case of methanol extraction. Methanol cooled to −20°C offered the most efficient extraction, with an average recovery of 53%. The addition of a hexane extraction step improves the sample clean-up and peak shapes and removes many problems attributed to the phospholipids [31]. Derissen et al. tested four extraction agents: MetOH, EtOH, AcCN and 1.35 M PCA at different volume ratios. Finally, 100 μL of methanol added to the 60 μL of the PBMC suspension, followed by extensive vortex mixing and direct centrifugation according to the extraction procedure 1 provided the most favourable results [18].

Sample pre-treatment by PP seems to be a suitable method for removing proteins and the extraction of nucleotides from biological samples. Since the concentration of some nucleotide analogues is often very low, and further clean-up procedures (ultrafiltration) and preconcentration [solid phase extraction (SPE), LLE] are needed. Cordell et al. showed that phospholipids can be removed from the sample by LLE by hexane [31]. A similar procedure was reported by Soga et al. using chloroform and water being added to a methanol extract of *Escherichia coli* culture to remove phospholipids liberated from the cell membranes [55]. An additional sample clean-up was used in the study of Crauste et al., where cell extracts were purified by a weak anion exchange (WAX) SPE column after PP by MetOH. The mean extraction recoveries were between 60 and 81%, depending on the analyte. The effect of ion suppression on the peaks before and after SPE was also compared and the results indicated that SPE extraction allows the matrix effect to be reduced [81]. An additional sample clean-up with WAX-SPE after PP was introduced in several studies [39, 42, 83]. Comparison of extraction efficiency in protein-precipitated samples with and without consequent WAX SPE clean-up

procedure was described by Kamčeva et al. Extraction recovery for the procedure without SPE was achieved in the range 59.2–91.9% and with SPE in the range from 94.2 to 121.8%. The lower recovery for the first method can be explained by higher ion suppression; however, the usage of isotope-labelled triphosphates (ATP, GTP, UTP, dATP, dCTP, dGTP, dTTP) as internal standards simplified the nucleotide extraction step. The analytes and their isotopically labelled standards are affected equally by the cell matrix and the interference originating from the cell matrix influencing the recovery is reduced. Thus, additional steps for sample clean-up such as time-consuming and expensive SPE were unnecessary [60]. Cell lysis, protein precipitation and nucleotides extraction can be also carried out by MetOH in combination with Tris-HCl buffer [16, 20]. Another cell sample treatment was introduced by Teleki et al. Biomasses of *E. coli* were quenched by liquid nitrogen, diluted to the defined extraction concentration, immediately pre-incubated at 100°C with short-time vortexing in a water bath for enzymatic inactivation and then chilled on ice water. The metabolite extracts were separated from the cell debris by centrifugation and stored at −70°C [40]. The analysis of the nucleotide content in red blood cells (RBC) is described in a study by Hofmann et al. RBC mixed with EDTA, dithiothreitol and IS were heated at 95°C in a water bath for protein denaturation. The samples were subsequently extracted by MetOH followed with dichloromethane. After centrifugation, the supernatant was used for LC-MS/MS analysis [13].

Another procedure for sample clean-up was reported. In a study of Klawitter et al. comparing four extraction procedures (see above), additional online desalting was applied. The final extracts were loaded onto a C18 cartridge desalting column and washed with dibutylammonium formate buffer/methanol (95:5). Thereafter, the valve was switched back onto the analytical column. This switching procedure led to better reproducibility of the HPLC retention times and significantly improved the stability of the electrospray (ESI) as a result of the lower amounts of salt precipitated in the spray chamber [41]. In a study by Wu et al., supernatant resulted from centrifugation after PP was additionally cleaned by ultrafiltration with a molecular weight cut-off of 3000 Da [32]. According to Becher et al., Tris-HCl/MetOH cell lysates were treated by immunoaffinity extraction [21].

Further study used ice-cold MetOH and subsequent cell lysis by fast heating or using of sonic dismembrator for the islets of Langerhans and *E. coli* cells in MALDI-TOF analysis. The samples were mixed with matrix (9-aminoacridine) and deposited onto a MALDI target plate using the dried-droplet method [44]. In a study by van Kampen of AZT-triphosphate and nucleotide triphosphates in PBMCs by the means of MALDI-TOF technique, the pre-treatment of the sample was also based on ice-cold MetOH extraction followed by overnight incubation at 4°C, centrifugation, freeze drying and reconstitution. Before analysis, the sample was pipetted onto an Anchor Chip target plate, onto which the matrix had previously been applied and dried [84].

For indirect methods, where parental nucleoside resulting from the dephosphorylation of nucleotides is detected, the preparation of the sample is based on PP and the extraction of nucleotides from the matrix and subsequent fractionation of the sample to MP, DP and TP, usually by means of a salt gradient applied to an anion exchange SPE cartridge. Particular fractions are exposed to dephosphorylation on parent nucleosides, mostly by means of an

acid or alkaline phosphatase, eventually desalted and pre-concentrated by additional SPE. Cells or other matrices were precipitated by the means of 70% aqueous MetOH and the extract was separated into MP, DP and TP fractions using strong anion exchange cartridge with a potassium chloride gradient. The resulted fractions were treated by acid [14, 22, 33, 59] or alkaline [15] phosphatase for dephosphorylation to parental nucleoside. After hydrolysis, samples were desalted and purified by SPE and analysed. Preparation of the sample for indirect analysis is time and material consuming. Even if the final nucleoside analysis is quite simple, each sample fraction must be analysed separately. Each step in an indirect method could be the cause of a definite error resulting in inaccurate determination of the nucleotides.

In summary, sample preparation is the most important and critical step in the analysis of nucleotides. The proper extraction and clean-up procedures depend on various matrices and separation and detection techniques and should be chosen carefully.

3. Capillary electrophoresis with mass spectrometry detection in analysis of nucleotides

Capillary electrophoresis (CE) is an analytical technique enabling the separation of compounds in a fused silica capillary using electrolyte solution (separation buffer) under an electrical field application. Ionized molecules migrate through an electrolyte solution (separation buffer) under an electrical field application. In CE, cations migrate towards the cathode, whereas anions move in the opposite direction. Molecules migrate to the detector at different velocities that are based on their electrophoretic mobilities. This depends on their charge and size, the pH buffer, ionic strength, buffer composition and viscosity. The next factor that significantly affects the electrophoretic migration and separation of analytes is the electro-osmotic flow (EOF). The silica capillary surface is negatively charged under the alkaline conditions resulting from the ionization of silanol groups. The EOF can be modified, inversed or deleted by covalent or dynamic capillary wall modifications using surfactants or neutral or ionized polymers.

Numerous modes in CE enable the separation of a wide spectrum of compounds and thanks to the different separation mechanisms that can provide complementary information. The most widely used is capillary zone electrophoresis (CZE), where the mobility of an analyte is a vector sum of its electrophoretic mobility and the electro-osmotic mobility of the buffer. Micellar electrokinetic chromatography (MEKC) can be used for the separation of charged as well as neutral less polar compounds. The running buffer is enriched by surfactants forming micelles that can interact with neutral less polar compounds in a chromatographic manner through both hydrophobic and electrostatic interactions. CE can also be used with a capillary filled with different phases, resulting in different separation modes. A capillary filled with gel buffer enables the separation of molecules according to their size (capillary gel electrophoresis, CGE) and is used mainly for macromolecules such as protein and DNA analysis. CE with a chromatographic stationary phase capillary filling, mixture of ampholytes creating a pH gradient in capillary and several running buffers with different conductivities is called

http://dx.doi.org/10.5772/68073

capillary electrochromatography (CEC), capillary isoelectric focusing (CIEF) and capillary isotachophoresis (ITP), respectively.

In the last three decades, CE represented the main technique for the direct determination of nucleotides. However, with the development of new stationary phases compatible with highly polar analytes, liquid chromatography plays a more important role in the analysis of nucleotides. Despite this fact, CE represents a valuable alternative to chromatographic techniques for nucleotide analysis. Separation is fast, with very high efficiency. Low solvent and sample consumption and low running costs represent other significant advantages in the application of the technique, especially in combination with mass spectrometry detection.

Several methods using CE-MS have been developed for the determination of nucleotide analogues in clinical applications. Cai et al. introduced a method for the simultaneous analysis of the nucleoside reverse transcriptase inhibitor (NRTI) Ziagen (Abacavir) and its phosphorylated metabolites such as carbovir monophosphate, carbovir diphosphate and carbovir triphosphate that is used for the treatment of human immunodeficiency virus (HIV) type 1. This method enables the separation and detection of positively charged nucleoside analogues and negatively charged nucleotides in a single electrophoretic run thanks to the application of a time-segment program. The linearity of the method was established in the range 2–100 μM and the limits of detection for all the analytes were less than 2 μM. The capability of the method was demonstrated on human PBMC extracts spiked with Ziagen and its phosphorylated metabolites at 20 μM levels. Some endogenous nucleotides, such as adenosine 5′-triphosphate (ATP), adenosine 5′-diphosphate (ADP) and adenosine 5′-monophosphate (AMP), were also detected in the cellular extracts [53].

Liu et al. used CE-ESI-MS for the determination of 14 compounds, including antiretroviral dideoxynucleosides (ddN), their nucleotides and a set of endogenous ribonucleosides and ribonucleotides. Separation by means of CE was performed on an untreated column using a volatile background electrolyte for ESI-MS. All the analytes were profiled within single 18 min CZE run. The method was applied to detect natural nucleotides, lamivudine and its mono-, di-, and triphosphates in the human hepatoma cell line Hep G2 [56].

The conversion of 5-amino-4-imidazolecarboxamide riboside (ZR) into mono-, di-, and triphosphates in human erythrocytes was demonstrated in a study by Friedecký et al. The erythrocytes were incubated with ZR in order to simulate the situation in the inherited metabolic disorder of the purine metabolism AICA-ribosiduria. Characteristic AICA-ribotides, together with the naturally occurring nucleotides AMP, ADP and ATP, were separated by means of capillary electrophoresis in an acetate buffer (20 mmol L^{-1}, pH 4.4) and identified online by mass spectrometry in negative mode [75].

Bezy et al. introduced the CE-ESI-MS/MS method for the simultaneous measurement of nucleoside 5′-triphosphate and 5′-monophosphate anabolites of the anti-HIV drugs, didanosine (ddATP, ddAMP) and stavudine (d4T-MP, d4T-TP), among a pool of 14 endogenous 5′-mono-, di- and triphosphate nucleosides in extracted PBMC. The running electrolyte consisted of an acetic acid/ammonia buffer with pH = 10 and ionic strength of 40 mM. Finally, the quantification of d4T-TP and ddATP was validated in this CE-MS/MS system [52].

The simultaneous analysis of naturally occurring nucleotides, nicotinamide-adenine dinucleotides and CoA compounds was introduced by Soga et al. using a pressure-assisted CE-MS. The method allowed simultaneous analysis of various compounds and offered sufficient sensitivity and selectivity, reproducibility, robustness and linearity. The required reproducibility of the system was achieved by exchanging the running electrolyte after every analysis using a buffer replenishment system. Under optimized conditions, 14 phosphorylated compounds were well determined in less than 20 min with detection limits between 0.5 and 1.7 μM. The usefulness of the method is demonstrated through the analysis of intracellular nucleotides and CoA compounds extracted from *E. coli* wild-type and pfkA and pfkB knockout mutants [55].

The combination of CE-enabling rapid analysis with efficient resolution and MS with excellent selectivity and sensitivity makes a very powerful technique for nucleotide analysis and a good alternative to the conventionally used LC-MS technique. Nevertheless, the development of the method for the separation of the nucleotides by means of CE coupled with MS detection still represents a big challenge. The hyphenation of CE with MS is technically demanding. Moreover, the commonly used electrophoresis running buffers are not compatible with MS detection as a result of the high concentration of electrolytes, which may create high background signals in ESI-MS analyses.

4. Liquid chromatography-mass spectrometry for the determination of nucleotides

Liquid chromatography (LC) is an analytical technique enabling very efficient and sensitive separation of compounds in complex sample matrices. The principle of the technique is based on the interactions and distribution of sample components between the stationary and mobile phase. The strength of the interaction determines the order of the elution of particular analytes. Because of the requirement for better efficiency of separation and shorter analysis time, high-performance liquid chromatography (HPLC) was investigated. The application of high pressure with a faster flow rate and separation columns with particles smaller than 2 μm offers highly efficient compound separation with a shorter analysis time in comparison to common column (low-pressure) chromatography. Currently, most applications for the analysis of nucleotides are based on liquid chromatography coupled with tandem mass spectrometry, and therefore descriptions of approaches involving these represent a major part of this chapter.

The majority of polar analytes are separated using reversed-phase high-performance liquid chromatography (RP-HPLC), where the stationary phase is usually non-polar [silica gel coated by octadecyl- (C18), octyl- (C8) or cyanogroup (CN)] and the mobile phase is composed of polar organic solvents (methanol or acetonitrile) in combination with a water buffer. The retention of compounds depends on hydrophobic interactions with the stationary phase. Using gradient elution, the polarity of the mobile phase is declined with a greater amount of organic solvent, resulting in the faster elution of non-polar analytes from the column. The

polarity of nucleotides increases with the number of phosphate groups. In contrast to nucleoside monophosphates (MP), nucleoside triphosphates (TP) and nucleoside diphosphates (DP) are therefore only minimally retained and are separated from other nucleotides on the commonly used reversed-phase HPLC columns under traditional conditions with a typical aqueous-organic mobile phase. In addition, many interferences from the matrix are poorly retained and the specificity and selectivity of the method is reduced even more. Introducing an ion-pairing (IP) reagent or anion exchange (AX) chromatography enabled the usage of RP-HPLC columns for the analysis of nucleotides. Although IP and AX chromatography are the most suitable methods for nucleotide analysis, high concentrations of a non-volatile ion-pairing reagent and/or a high salt concentration preclude the use of mass spectrometry for detection. Therefore, the type and concentration of the ion-pairing agent must be optimized. Moreover, the strong retention of ion-pairing agents inside the mass spectrometer makes it impossible to use instrumentation for other methods because of the interference of the IP agents with the compounds being analysed.

4.1. Reversed-phase liquid chromatography

As mentioned above, RP-HPLC-MS does not enable the analysis of nucleoside di- and triphosphates because of the low retention on the column. Therefore, RP-HPLC in a common setting is acceptable for the determination of nucleotides by indirect methods. The methods are usually based on the separation of the sample extract into MP, DP and TP fractions and subsequent dephosphorylation with alkaline or acid phosphatases on nucleoside forms. Consequently, nucleosides can be determined in a common RP-HPLC-MS setting.

Rodriguez et al. developed an indirect method for the quantification of the intracellular NRTIs zidovudine (ZDV) and lamivudine (3TC) triphosphates in patients with HIV infection. Extracted peripheral blood mononuclear cells (PBMCs) were separated into MP, DP and TP fractions using strong anion-exchange Sep-Pak plus (SAX-QMA) cartridges with a potassium chloride gradient. The cleavage of the phosphate groups was performed by acid phosphatase, the samples were desalted and the parental nucleosides ZDV, 3TC and AZdU (azidodeoxyuridine; internal standard added to the extract after enzyme digestion) were extracted by means of a solid phase extraction (SPE) XAD resin column. HPLC separation was performed on an RP column with a mobile phase consisting of methanol and acetonitrile mixture (3:1, v/v) with 0.25% acetic acid. The concentrations of the analytes were determined by using ZDV/AZdU and 3TC/AZdU peak area ratios, and calibration curves from ZDV-TP and 3TC-TP standard solution were prepared every time a series of samples was analysed [22].

The next indirect method was developed for the analysis of intracellular dideoxyadenosine triphosphate (ddATP). Cells were treated with 70% MetOH buffered to pH 7.4 and the samples were incubated on ice for 15 min and stored at −20°C. Before analysis the cell extract was evaporated to dryness and reconstituted in Tris (1 M, pH 7.4). The samples were loaded onto a QMA anion exchange SPE cartridge, MP and DP were eluted by 75 mM KCl, and finally ddATP was eluted with 500 mM KCl. The pH of the eluate was adjusted to 6.0 and it was incubated with acid phosphatase for 30 min at 37°C for dephosphorylation to ddA (dideoxyadenosine). The samples were desalted and purified using C18 SPE cartridges. The ddA

eluted by AcCN was evaporated to dryness and stored at −20°C until analysis. The overall recovery of QMA and C18 SPE was over 95%. The separation was performed on a Purospher-RP-18e column with a mobile phase consisting of MetOH/water (25/75, v/v) containing 1% formic acid. The overall analysis was achieved within 1 min. The LOQ of ddA in the CEM-T4 cells that were analysed was 0.02 ng mL^{-1}. This procedure could be used to perform simultaneous detection of five NRTIs, such as AZT, 3TC, ddA, ddC, and d4T [33].

An indirect method for the determination of the nucleoside analogues MP, DP and TP in an intracellular matrix of red blood cells (RBC) and PBMCs was described by Bushman et al. Cell extracts were loaded onto QMA SPE cartridges and MP, DP and TP fractions were eluted by means of a KCl concentration gradient. The isolated fractions were then treated with acid phosphatase for dephosphorylation to parental nucleoside and the samples were desalted and concentrated with a Strata X-SPE column, and the eluent was dried under nitrogen at 40°C and reconstituted in water. Separation was achieved on a Synergi Polar RP column. The phase for tenofovir (TFV) contained 2% AcCN and 0.1% formic acid in pure water with a run time of 8 min, and for zidovudine (ZDV) it contained 6% 2-propanol and 0.1% acetic acid in pure water with a run time of 12 min, both at an isocratic flow. The method was successfully applied to clinical research generating novel intracellular information for TFV, emtricitabine (FTC), ZDV and 3TC nucleotides [14].

Another indirect method for the determination of adenosine, guanosine and inosine nucleotides was introduced by Jimmerson et al. The analyses were performed on human PBMCs, red blood cells (RBCs) and dry blood spots (DBSs). Methanolic extracts of lysed cells and DBSs were fractionated to MP, DP and TP using an anion exchange cartridge and a potassium chloride salt gradient. The resulting separated fractions were dephosphorylated to the parental nucleosides adenosine, guanosine, and inosine by alkaline phosphatase. Subsequently, the samples were desalted and concentrated on phenylboronic (PBA) SPE cartridges. Analytical separation was performed on an RP column with an aqueous mobile phase containing 4% AcCN and 0.1% formic acid. The detection of nucleosides was performed in positive ESI MRM mode [15]. This group of authors previously described a similar method for the determination of intracellular ribavirin (RBV) MP, DP and TP, in which the particular fractions were isolated from a lysed intracellular matrix using strong anion exchange SPE, dephosphorylated to parent RBV, desalted and concentrated on PBA SPE cartridges and subsequently analysed. Chromatography was performed on a Reversed-Phase-Aqueous column (Develosil C30) with a mobile phase consisting of 2% AcCN and 0.1% formic acid in water at an isocratic flow and with a run time of 4 min. Each injection was followed by strong and weak needle washing. The method was used on human PBMCs and the RBC and DBS of patients taking RBV for the treatment of chronic hepatitis C virus infection [59].

Wang et al. described a method for the determination of creatine phosphate, creatine and 12 nucleotides in rat heart tissue. The extract was separated on a polar endcapped C18 column that was suitable for reversed-phase separations using highly aqueous mobile phases. The mobile phase consisted of 2 mM ammonium acetate in water adjusted with ammonia to pH 10.0 and isocratic elution was applied. The detection was performed by negative electrospray ionization in selection reaction monitoring mode. The study was, however, focused only on group of nucleotides of which the concentration in the tissue is relatively high [45].

The determination of 3′-deoxy-3′-fluorothymidine (FLT) and FLT-MP was used for the monitoring of serum thymidine kinase 1 (TK 1) activity. Separation was achieved on an Aquasil C18 column coupled with a security guard column (Gemini C18) using 0.1% formic acid in water (MF A) and 0.1% formic acid in AcCN (MF B). Elution was carried out under gradient conditions with a total analysis time of 7 min. The applicability of the method for measuring serum TK 1 activity was demonstrated in hepatocellular carcinoma patient serum samples and age-matched control sera [58].

Several methods for the determination of cyclic nucleotides with separation on RP-HPLC columns have been developed. Oeckl et al. described a method for the analysis of cAMP and cGMP in plasma, CSF and the brain tissue of mice. For separation a Varian MetaSil RP column with a mobile phase consisting of 0.1% formic acid in water (A) and acetonitrile (B) was used. The analysis time per sample was 3.5 min [36]. The method was subsequently applied in measuring cAMP and cGMP concentrations in CSF in patients with Creutzfeldt-Jakob disease, Parkinson's disease and amyotrophic lateral sclerosis. It demonstrated that the CSF determination of cAMP and cGMP may be included in the diagnosis of CJD and could be helpful in monitoring the progress of the disease as well as in therapy control [62]. The same separation conditions were used for the determination of cGMP in human plasma in a study by Zhang et al. [37]. In a method for the measurement of 2′,3′-cAMP, 2′,3′-cCMP, 2′,3′-cGMP and 2′,3′-cUMP, separation on a Zorbax eclipse XDB-C18 column connected to a security guard column with MetOH/water (3:97, v/v) as MF A and MetOH/water (97:3, v/v), each containing 5 mM ammonium acetate and 0.1% acetic acid, was achieved. The analysis was applied to the analysis of nucleotides in two different cell lines, Hek293T and HuT-78 [30].

Another use of reversed-phase analytical columns for the determination of nucleotides is possible with the addition of an ion-pairing reagent into the mobile phase [31, 41, 82]. This is described in detail in the chapter 'Ion-pairing chromatography'.

4.2. Ion exchange chromatography

Ion exchange chromatography (IXC) is a separation technique applied to the analysis of charged molecules, including, e.g. ions, polar nucleotides and amino acids, on the basis of their affinity to the ion exchanger. For positively charged analytes, cation exchange chromatography with negatively charged solid support is used and vice versa; negatively charged analytes are attracted to a positively charged solid support in anion exchange chromatography (AX). The elution of bounded negatively charged molecules is performed with an eluent containing anions in a higher concentration or by changing the pH of the column. The elution of strongly charged nucleotides requires a high concentration of competitive ions in the mobile phase and, thus, hyphenation with MS detection cannot be employed.

However, an alternative elution mechanism introduced by Shi et al. based on the application of a pH gradient enabled the direct quantification of intracellular nucleoside triphosphates (NTPs) without any need for high concentrations of non-volatile competing ions for elution. Extracts of human PBMCs were analysed by weak anion exchange (WAX) liquid chromatography coupled to mass spectrometry detection. An inverse ammonium acetate gradient (10–1 mM) enabled separation between MPs, DPs and TPs within 2 min. The method was

validated and used for the determination of the NRTI dexelvucitabine triphosphate metabolite in human PBMC samples from clinical studies [85].

Veltkamp et al. developed a sensitive and specific assay for the quantification of gemcitabine triphosphate (dFdCTP) in human PBMCs. It is based on a WAX LC-MS/MS approach, which makes the method more sensitive [17] than previously published work based on UV detection [70].

Jansen et al. developed and validated a method for the quantitative analysis of cladribine mono-, di- and triphosphates that was applied to a culture medium and MDCKII cell lysate. WAX LC-MS/MS in positive ion mode was applied via a fused-silica electrospray capillary instead of a stainless steel electrospray capillary to minimize the adsorption of analytes and, thus, reduce the variation in the analyte signals [27].

A simultaneous quantification method for 11 relevant nucleotide metabolites of thiopurine drugs (eleven mono-, di- and triphosphates of thioguanosine, methylthioinosine, methylthioguanosine and thioinosine) in RBCs was introduced by Hofmann et al. Ion exchange HPLC on a WAX column using a pH gradient from 6 to 10.5 and a decreasing ammonium acetate concentration from 10 to 1 mM was used for the separation of nucleoside mono-, di- and triphosphates. All eleven metabolites could be determined in RBCs from patients with inflammatory bowel diseases and long-term azathioprine therapy indicating high inter-individual variability of the metabolite levels. Using stable isotope-labelled analogues of the metabolites enabled the reproducible and accurate determination of all the analytes [13].

Anion exchange chromatography was also used for the determination of 2′-C-methylguanosine triphosphate concentration in mouse liver in a study by Rashidzadeh et al. The samples were eluted onto a Luna NH_2 chromatographic column with 1 mM ammonium acetate in water/AcCN (70:30, v/v), pH 8.0 (MP A) and 20 mM ammonium acetate in water/AcCN (70:30, v/v), pH 10. The total run time was 10 min per sample. The assay was linear over a 50–10,000 pmol mL^{-1} concentration range in liver homogenate [42].

In a paper by Derissen et al., the development of an LC-MS/MS assay for the quantification of the widely used chemotherapeutic capecitabine with the active component 5-fluorouracile (FU) and its active metabolites FUTP, FdUTP and FdUMP was described. Because of the low concentrations of the analytes, the optimization of the sample preparation, including cell lysis and nucleotide extraction and subsequent chromatographic separation, was necessary. The samples were loaded onto a BioBasic AX WAX column coupled with a guard column; the mobile phase A and B composition was 10 mM ammonium acetate with pH 6.0 and 1 mM ammonium acetate with pH 10.5, respectively, both in AcCN/water (30:70, v/v). The pH gradient was applied to achieve effective separation of the MP, DP and TP of the nucleoside. The total analysis time was 7 min. The method was validated for the concentration ranges 0.488–19.9, 1.66–67.7 and 0.748–30.7 nM for FUTP, FdUTP and FdUMP, respectively. The assay was successfully applied to quantify 5-FU nucleotides in PBMC samples from patients treated with capecitabine and patients receiving 5-FU intravenously [18]. The method was also used for the quantification of the 5-FU nucleotides in PBMCs in a study exploring the intracellular pharmacokinetics of the 5-FU nucleotides during capecitabine treatment [57].

The WAX principle can also be used for sample preparation by SPE with Wax extraction cartridges followed by separation on RP or PGC columns [81, 83]. This was described previously in the chapter 'Sample preparation'.

4.3. Porous graphitic carbon columns

Another way to achieve the required separation of nucleosides is the use of porous graphitic carbon columns (PGC) because of their unique properties as a stationary phase. Their retention and selectivity for polar and structurally related compounds is different from conventional C18 columns. PGC is very suitable for the analysis of polar and ionic compounds, which are retained on the carbon surface without a need for an IP reagent, and the subsequent elution is not dependent on a high salt concentration. This enables the development of methods compatible with MS detection. PCG columns have the advantage of physical and chemical stability accompanied by toleration of a wide pH range (0–14). Retention increases with increasing analyte hydrophobicity [86]. However, PGC behaves as a strongly retentive alkyl-bonded silica gel for non-polar analytes. Thus, the disadvantage is the difficulty of desorption of non-polar compounds adsorbed on the surface and a general loss of retention on PGC within a run and over a period of time, which can limit their use [87].

A general LC-MS method for the analysis of nucleosides and their mono-, di- and triphosphates using a PGC column was developed by Xing et al. The method was optimized using different organic mobile phases and modifiers. The concentration of ammonium acetate was proved to be a critical step for retention during gradient elution with water/acetonitrile. Diethylamine (DEA) was found to improve the peak shapes of di- and triphosphates for mass spectrometric detection. Finally, the separation of 16 nucleosides and nucleotides was achieved during 15 min under the conditions of a gradient of ACN in water with 50 mM ammonium acetate and 0.1% DEA. In the study, comparison of several silica-based columns for separation of polar compounds was also performed. Hypercarb column provided the best results for separation and quantitation of the nucleotides and their phosphates [88].

Wang et al. described an LC-MS/MS method for the determination of AMP, ADP and ATP in the extract of HepG-2 cells. Chromatographic separation was performed on a PGC analytical column with a basic mobile phase. Negative-ion mode ESI-MS with basic mobile phase condition improved the sensitivity of the MS analysis. The method was successfully applied to determine ATP, ADP and AMP in HepG-2 cells treated with benzo[a]pyrene [25]. This method served as a model for a study focused on the quantification of gemcitabine (2′-2′-difluorodeoxycytidine, dFdC) and its metabolites 2′-2′-difluorodeoxyuridine (dFdU) and 2′-2′-difluorodeoxycytidine-5′ (dFdCTP) in pancreatic ductal adenocarcinoma tumour tissue and plasma from genetically engineered mouse models of pancreatic cancer. The tumour tissue was homogenized in ice-cold 50% AcCN containing tetrahydrouridine. An aliquot of homogenate was mixed with ice-cold 50% AcCN containing IS. After vortex mixing and centrifugation the supernatant was evaporated to dryness and reconstituted in water before analysis. With respect to plasma, it proceeded in the same way as the tumour homogenate by the addition of ice-cold 85% AcCN containing IS. The analytes were separated on a PGC Hypercarb column fitted with a guard column with 10 mM ammonium acetate, pH 10 (MF A) and acetonitrile

(MF B); the total run time was 15 min. In order to minimize carry-over between injections, the needle and injection path were flushed using the external wash procedure with water, 100% AcCN, 50% AcCN and water [46].

Jansen et al. also introduced a method for the separation of 2′-2′-difluorodeoxycytidine (gemcitabine, dFdC), 2′-2′-difluorodeoxyuridine (dFdU) and their mono-, di- and triphosphates using a porous graphitic carbon Hypercarb column. The separation of all the analytes was achieved using an ammonium bicarbonate gradient (0–25 mM) in acetonitrile/water. The rate of pH and redox state of the column had to be controlled in order to maintain the separation conditions within multiple runs [89]. Subsequently, this method was validated for quantification in PBMCs and successfully applied to clinical samples [90].

Another method utilizing PGC-HPLC column separation with MS detection was developed for the quantification of cytarabine triphosphate (araCTP), CTP and dCTP in a human follicular lymphoma cell line. The separation principle is based on an LC-MS/MS ion pair using a PGC analytical column. The mobile phase consisted of 5 mM hexylamine with 0.4% dimethylhexyl amine with a pH of 10 and an ACN/water mixture. The mass spectrometer operated in negative ESI and multiple reaction monitoring mode. The method was able to achieve a low limit of quantification (LLOQ) of 0.1 μg mL^{-1} for araCTP and of 0.01 μg mL^{-1} for both CTP and dCTP. The method was validated and used for the quantification of araCTP, CTP and dCTP formed after the incubation of araC and an araCMP prodrug in the human follicular lymphoma cell line RL [81].

The development and validation of an assay for the quantification of endogenous nucleoside MP and TP by LC-MS/MS in combination with online SPE extraction was introduced by Machon et al. An Oasis®WAX SPE column served for online extraction, whereas PGC Hypercarb® was used as an analytical separation column. The elution solvents were 0.25% NH_4OH adjusted to pH 10 with acetic acid (A), water (B) and acetonitrile (C). The IP reagent was used for the reconstitution of the evaporated samples (5 mM hexylamine—0.5% DEA in water) to prevent peak tailing of nucleoside triphosphates. The total duration of a single run was 37 min. The method also allowed the separation and the detection of other nucleoside MP, DP and TP, deoxyribonucleotides and ribonucleotides. The advantage of the method was that it was based on online SPE, which was less time-consuming. After validation, the method was applied to the evaluation of the effects of gemcitabine and hydroxyurea on nucleotide pools in Messa cells [29].

Kamčeva et al. also introduced a combination of ion-pairing chromatography with PGC column separation. The development of a sensitive LC-MS/MS method for the separation and quantification of eight endogenous nucleotides (ATP, CTP, GTP, UTP, dATP, dCTP, dGTP and dTTP) and 2′, 2′-difluoro-2′-deoxycytidine triphosphate (dFdCTP) in PBMCs was described. The analytes were extracted by simple protein precipitation and chromatographic separation was performed on a Hypercarb column with delivery of a mobile phase containing 5 mM HA, 0.5% DEA, acetonitrile and water in gradient elution adjustment. The total analysis time was 68 min. The method was applied to monitor dFdCTP and changes in endogenous nucleotides in patients who were receiving gemcitabine infusions [60].

http://dx.doi.org/10.5772/68073

Nowadays, methods using PGC column separation represent a good alternative for nucleotide analysis compatible with MS detection in a robust and reproducible manner without the need for an ion-pairing agent or a high salt concentration. The optimization of mobile phase composition and an appropriate elution program facilitating consistent analyte retention remove the need for column regeneration, minimize run times and thus allow PGC columns to be used to their full potential [88].

4.4. Ion-pairing chromatography

Separation by ion-pairing (IP) chromatography (IPC) is based on the interaction between the negatively charged nucleotides and the positively charged IP reagent. The stationary phase is usually the commonly used non-polar C18 or C8 phase. The mobile phase contains cationic reagents such as alkylamines. The previously used tetrabutylammonium salts were effective for the separation of nucleotides by HPLC in combination with UV detection. However, non-volatile tetrabutylammonium salts were incompatible with electrospray-mass spectrometry detection. Thus, a more volatile salt is one of the possible ways to overcome this problem. Triethylamines, tributylamines, dibutylammonium salts, dimethyhexylamine or hexylamine are commonly used. The properties of the mobile phase are optimized for the efficient desorption of analytes using organic modifiers such as methanol or acetonitrile and also by the pH gradient. The concentration of the ion-pairing reagent plays a crucial role in LC separation coupled with MS detection. The amount has to be optimized for successful separation and for minimizing the mass spectrometry ion source contamination. Two of the solutions for reducing the electrospray ion source pollution are to minimize the flow rate of the mobile phase into the MS system or to use trialkylamine with a longer chain, promoting interactions between the IP reagent and a hydrophobic stationary phase, resulting in a reduction in the amount of the IP agent required. Another way is column miniaturization, which provides better chromatographic resolution and sensitivity of the LC-MS system [9].

The first study introducing IP capillary HPLC-MS described the separation of cyclic nucleotides on a C18 reversed-phase column using tetrabutylammonium (TBA) bromide as the IP agent. Different mobile phase compositions were evaluated in the concentration range of 50–500 μM of TBA salt with a combination of low flow rates (5–10 μL min^{-1}) in combination with negative electrospray ionization. Despite the relative non-volatility of TBA salt, the system was able to operate for several days without a reduced signal caused by source pollution being observed. Optimal conditions offered linear detection response in the femtomole to picomole range [91].

Claire et al. introduced the IP-HPLC-MS method for the determination of intracellular emtricitabine triphosphate (FTC-TP) levels in human PBMCs that was also adaptable to all purine- and pyrimidine-based nucleotides. All the nucleotides were extracted by means of aqueous methanol, isolated by IP-SPE and then directly analysed by LC-MS/MS. The mobile phase contained 10 mM ammonium phosphate, pH 6.4, with 2 mM tetrabutylammonium hydroxide and 15% acetonitrile. The method was linear in the range from 0.08 to 80 picomoles on-column. The low amount of TBA, thin column with a 1.0-mm internal diameter, slow flow

rate of 50 μL min^{-1} and continuous flow of 20% methanol through the MS ion source enabled effective separation and detection stability [92]. Hawkins et al. applied the method for the simultaneous determination of the intracellular concentrations and pharmacokinetics of tenofovir diphosphate, carbovir triphosphate and lamivudine triphosphate in samples of patients on a triple-nucleoside regimen [93].

The IP-RP-LC-MS/MS method was developed for the quantitative detection of adefovir and its phosphorylated metabolites in cellular samples by Vela et al. Hep G2 cells were incubated with 10 μM adefovir for 24 h and then extracted using 70% methanol. Chromatographic separation was performed on microbore reversed-phase columns and a mobile phase containing TBA and ammonium phosphate was delivered to the MS system with a low flow of acetonitrile gradient. Further optimization of the method lowered the concentration of TBA and phosphate, reduced the pH and applied a linear gradient of acetonitrile. Thus, the method was found to have sufficient sensitivity, accuracy and precision to be broadly applicable. But despite all the improvements and optimization of the method, using TBA in the injection solvent caused significant ion suppression and phosphate clusters, and their ammoniated adducts also created a number of high-intensity interfering peaks [28]. Finally, TBA in combination with phosphates causes mass spectrometer ion source pollution, ion suppression and background interference that impose some limitations on the determination of nucleotides using IP-LC-MS/MS. Regardless of this, methods using TBA with a limited ion-pair concentration and maintaining low flow rates have been successfully used in many applications.

Trialkylamines are more suitable for MS detection because of their higher volatility than tetraalkylammonium salts. Apffel et al. developed a method for the analysis of oligonucleotides by RP-HPLC-ESI-MS. The mobile phase contained a novel additive, hexafluoropropanol (HFIP), adjusted to pH 7.0 with triethylamine (TEA). This combination resulted in good HPLC separation and efficient negative electrospray ionization. Application was demonstrated for synthetic homopolymers of thymidine, mapping plasmid sequence fragments and phosphorothioate ester antisense oligonucleotides with sensitivity below the 10 pmol level [94].

The IP LC-MS/MS method for the simultaneous determination of intracellular nucleoside triphosphates and other polar metabolites using a TEA-HFIP IP mobile phase was described by Wu et al. Compared to the less volatile ion-pair reagent triethylammonium acetate (100 mM, pH 7.0), the combination of 100 mM HFIP and 8.6 mM TEA increased the MS signal intensity about 50-fold, while retaining comparable chromatographic resolution. A gradient elution program with a total analysis time of 10 min was developed. The method was optimized and validated for the simultaneous and unambiguous determination of eight nucleoside triphosphates (including ATP, CTP, GTP, UTP, dATP, dCTP, dGTP and dTTP) and applied to samples of human lung cancer cell lines. The method can be used for the quantitative profiling of 74 polar metabolites with minor modifications and a prolonged mobile phase gradient [32].

Another widely utilized IP agent is N,N- or 1,5-dimethylhexylamine (DMHA). DMHA served as an ion-pairing agent for the identification and quantification of bisphosphonates, synthetic analogues of pyrophosphate that are used in the treatment of metabolic bone diseases. They can be metabolized intracellularly into non-hydrolyzable nucleotide analogues. The

separation was performed on a C18 reversed-phase LC column with MS detection in negative ESI mode [95, 96].

Tuytten et al. demonstrated the influence of different N,N-DMHA concentrations on the chromatographic and mass spectrometric performance. They developed the IP-LC-MS method using a short capillary column for the separation of 12 nucleotides eluted by a binary gradient of methanol/water/DMHA. Chromatographic performance and MS detection were improved by the addition of ammonium dihydrogen phosphate [97].

Another routine method for the simultaneous determination of the intracellular nucleotides of NRTI stavudine (d4T), as well as the natural corresponding triphosphate in human PBMCs, was developed and validated by Pruvost et al. Separation was performed on a reversed-phase microbore column with an IP reagent coupled to tandem mass spectrometry with negative electrospray ionization and multiple reaction monitoring detection mode. The LOQ for d4T-TP was 138 fmol per 7 mL blood. The method was applied to samples from patients treated with stavudine and could be used on more than 35 samples per day. However, the robustness was poor as a result of column instability because of the application of a high pH [23]. The method was subsequently improved; several HPLC columns were compared in order to enhance the stability of the peak shape over time. The SMT C18 column was replaced with a Supelcogel ODP-50, which is more stable under high-pH conditions. This method was successfully applied to clinical samples of HIV-positive patients receiving antiretroviral therapy containing d4T, ddI (didanosine) and/or 3TC (lamivudine) for the simultaneous determination of its triphosphate metabolites [98]. The problem with interference that occurred in the method was resolved by changing the polarity of the ion source during analysis and looking for another fragmentation pattern of the interfering molecules, resulting in the formation of different product ions without loss of sensitivity. Validation of the improved method for the simultaneous determination of carbovir triphosphate (CBV-TP), lamivudine triphosphate (3TC-TP) and tenofovir diphosphate (TFV-DP) was performed. The composition of the mobile phase was not changed (1,5-DMHA, pH = 10.5). The total run time was 12 min, as opposed to 26 min for NRTI analysis. The positive ESI offered better specificity and slightly better sensitivity than the negative ESI mode for these compounds and resulted in enhanced specificity and more robust assay methods. This assay was applied to PBMC samples from HIV-infected patients with NRTI therapy [16].

The separation of several nucleotides and related phosphate-containing metabolites using IP-LC with DMHA was introduced in the study of Cordell et al. A reversed-phase chromatographic column was loaded with a mobile phase consisting of water and MetOH in various ratio (95:5 for MF A and 20:80 for MF B), with the addition of DMHA in the concentration range 0.5–20 mM and the pH being adjusted by means of acetic acid. The optimized method enabled the simultaneous detection of 24 nucleotides and related phosphorylated compounds in negative ESI mode. The method that had been developed was then applied to profile endogenous levels of intracellular nucleotides in cultured CHO cells [31].

Chen et al. also introduced the IP-LC-MS/MS method for the analysis of intracellular nucleoside triphosphate levels using DMHA as the IP reagent in MF. The analysis was performed on a Supelcogel ODP-50 column coupled to an Xterra MS C18 guard column with a mobile phase

comprising 5 mM DMHA in water buffered to pH 7 by formic acid as MF A and 5 mM DMHA in AcCN (50:50, v/v) as MF B. The method was applied to five different human leukemia cell lines and bone marrow samples of leukemia patients. It enabled the determination of CTP, dCTP, UTP, GTP, dTTP, dGTP/ATP, dATP and 2-chloroadenosine (IS) within a run time of 40 min [26].

An analytical method for 2'-fluoro-5-methyl-beta-L-arabinofuranosyluracil (L-FMAU) triphosphate, a novel L-nucleoside analogue of thymidine known as an inhibitor of the hepatitis B virus, was introduced for the determination of its levels in PBMCs. Ion-pairing chromatography coupled with negative ion electrospray ionization tandem mass spectrometry showed accurate and repeatable detection, the intra- and inter-day precision was lower than 11.2%, and the accuracy was between 97.1 and 106.9%. The method was applied to HBV-infected patients undergoing L-FMAU treatment [99].

Becher et al. developed a method for the direct determination of intracellular levels of zidovudine (AZT) triphosphate in human PBMCs. Mobile phase A consisted of 10 mM DMHA and 3 mM ammonium formate, the pH being approximately 11.5, and mobile phase B contained 20 mM DMHA and 6 mM ammonium formate/acetonitrile (1:1). Separation proceeded on an SMT C18 column and the total analysis time was 26 min. The method was applied to PBMCs from HIV-infected AZT-treated or AZT-free patients [21]. Compain et al. extended the method to ATP monophosphate and the analytical run time was reduced to less than 10 min. The low limits of quantification were at 150 and 300 fmol per sample for AZT-TP and AZT-MP, respectively. The improved method offered the possibility of simultaneous determination of other nucleotide phosphates such as d4T-TP or dTTP [100]. Durand-Gasselin et al. [20] evaluated potential NRTI toxicity in newborns from a human immunodeficiency virus-infected mother with antiretroviral prophylaxis by the determination of zidovudine (AZT) and lamivudine (3TC) metabolites in PBMCs together with the level of the parent drug in plasma. Till then the pharmacological monitoring of these drugs in newborns had been limited to plasma and cord blood. The LC-MS/MS method for PBMC samples was adapted from previously reported assays [21, 100], with minor modifications concerning AZT-MP monitoring [20]. The method was improved by Kinai et al. The extraction of PBMC using a double tube filled with silicon oil completely removed residual plasma phosphates and sodium salts. Together with mobile phase alkalization, using of alkaline-stable HPLC column and tetrabutylammonium hydroxide as the IP reagent resulted in higher sensitivity in comparison with the previous method [19].

Hernandez-Santiago et al. developed a method with gradient elution of decreasing DMHA concentration during analysis. Their MS system operated in negative electrospray mode. The assay was applied predominantly for the determination of β-D-N4-Hydroxycytidine (NHC) triphosphate, a metabolite of a nucleoside analogue with selective anti-hepatitis C virus activity. In pre-clinical studies, the metabolism of the drug was investigated in various liver cells and primary human hepatocytes. Although a decreasing concentration of IP reagent was applied, the MS ion source and the whole LC column had to be regularly cleaned with a water-methanol mixture (50:50, v/v) at the end of each day [101].

Luo et al. focused on the identification and quantification of intracellular metabolites involved in central carbon metabolism, including glycolysis, the pentose phosphate pathway and the

tricarboxylic acid cycle. Separation was performed on an RP C18 column with a mobile phase consisting of 10 mM tributylamine aqueous solution with the pH adjusted to 4.95 with 15 mM acetic acid as eluent A and methanol as eluent B. The total analysis time was 80 min, and before each run, the column was equilibrated for 10 min. The method enabled the determination of 29 negatively charged compounds, including several nucleotides [47].

Hexylamine (HA) as an IP agent was used in the study of Fromentin et al., which was aimed at the determination of several clinically relevant nucleotide analogues and endogenous nucleotides. Separation was optimized for a Hypersil Gold C18 column, which offered the best results compared to other columns that were tested. The mobile phases A and B used in the method for partial validation consisted of 2 mM ammonium phosphate buffer containing 3 mM HA and acetonitrile, respectively. A gradient elution program was applied. The study was applied to human PBMC and macrophages, but it could also be applied for the quantification of other NRTIs with slight modifications [82].

A combination of IPC separation on PGC columns was also introduced in some studies. For a detailed description see the chapter 'Porous graphitic carbon columns' [60, 81].

Thanks to the reduced amount of IP reagent and salts entering the ion source, several robust methods for nucleotide determination with acceptable ion suppression have been developed and applied. However, pollution of the ion source remains the major problem.

4.5. Hydrophilic interaction liquid chromatography

Hydrophilic interaction liquid chromatography (HILIC) is an emerging separation mode of LC. In this variant of normal-phase LC, polar columns with a hydrophilic stationary phase are used in combination with a mobile phase consisting of reversed-phase-type eluents rich in organic solvents. Stationary phases used in HILIC configuration can contain a simple non-polar silica phase or can be modified by amino, anionic, amide, cationic or zwitterionic bonded phases. A typical mobile phase of HILIC mode consists especially of acetonitrile with a small amount of water or also alcohol in a higher concentration than the aprotic solvent to achieve the same retention behaviour. Polar analytes are eluted from the column by increasing the water content of the mobile phase. In HILIC, the analyte is distributed between a water-rich layer on the surface of the polar stationary phase and the organic mobile phase layer, creating a liquid-liquid extraction system. The mechanism of HILIC also includes hydrogen donor interactions between neutral polar species as well as weak electrostatic mechanisms under the high organic solvent conditions used for retention. Hence, this separation mode partly overlaps with ion chromatography and reversed-phase liquid chromatography. The retention behaviour of analytes, peak shape and chromatographic tailing are also controlled by the pH of the mobile phase and the ion strength formed by ionic additives, such as ammonium acetate and ammonium formate. The applied mobile phases are highly volatile, and thus the hyphenation with MS is friendly and favourable. HILIC mode showed very high efficiency for the retention of polar analytes that offered a different selectivity in comparison with the traditionally used RP-HPLC. High throughput of HILIC-MS/MS analysis at a high flow rate was allowed as a result of the very low column backpressure contributed by the high-organic mobile phase. Direct injection of the organic solvent extracts through LLE, SPE and PP onto the HILIC column is possible, in contrast to regular RP-HPLC. HILIC-MS/MS

has been demonstrated to be a very important supplement to the RP-HPLC-MS/MS for the analysis of polar compounds [102, 103].

The HILIC-MS method for the simultaneous determination of 141 endogenous metabolites, including several nucleotides, was introduced by Bajad et al. Separation was performed on an aminopropyl column with an alkaline mobile phase consisting of ammonium acetate and ammonium hydroxide as solvent A with a pH of 9.45 and acetonitrile as solvent B. A gradient elution program was used and the total analysis time was 40 min with five time segments in positive mode and 50 min with four time segments in negative mode. The method was applied to extracts of *E. coli* grown in [12C] vs. [13C] glucose and revealed appropriate 12C- and 13C-peaks of 79 different metabolites [43].

The complex metabolomics method using HILIC separation mode was developed by Karlíková et al. Separation was performed on the Luna NH_2 aminopropyl column with MP A consisted of 20 mM ammonium acetate at pH 9.75 and the mobile phase B consisted of AcCN. Gradient program was used for elution of targeted analytes. The total analysis time was 17 min. The method allowed analysis of 354 compounds as a result of continuous switching of positive and negative mode and detection of analytes using scheduled MRM mode. The method was applied on the metabolite profiling of the plasma and leukocytes of chronic myeloid leukemia patients [104].

Similar separation conditions were used for the determination of 2-methylcytidine triphosphate in a study by Pucci et al. Separation was performed on an aminopropyl column with ammonium acetate, pH 9.45 and acetonitrile. The chromatographic gradient was modified and reduced to 30 min, and the detection of the ions was performed in the negative ESI MRM mode. The calibration curve was linear over the 0.05–50 μM concentration range. The method has been successfully applied for pharmacokinetic studies of 2′-C-methyl-cytidine-triphosphate in rat liver tissue samples [39].

Teleki et al. also introduced alkaline conditions in HILIC mode for the quantitative profiling of more than 50 hydrophilic intracellular key metabolites. Separation was performed on a ZIC-pHILIC column. Optimization was focused on the pH of the mobile phase, buffer concentration, flow rate, column temperature and the gradient slope of the polar eluent. In optimized chromatographic conditions the mobile phase consisted of 10% aqueous buffer solution (10 mM ammonium acetate) and 90% acetonitrile for eluent A and 90% aqueous buffer with 10% acetonitrile for eluent B, both adjusted to a pH of 5.6 with acetic acid or a pH of 9.2 with ammonium hydroxide. The column was kept at 40°C, with a flow rate of 0.2 mL min^{-1}. Under alkaline conditions, 98% of the metabolites showed an absolute time shift of less than 0.04 min, in contrast to 80% under acidic conditions. Significant differences were also observed for the diphosphate and triphosphate metabolites and NADP, as well as for several amino acids with respect to the detection limits under alkaline conditions, which were approximately 20–50 times lower. Moreover, 70% of the metabolites presented more than 1.5-fold higher signal intensities under alkaline mobile phase conditions. The quality of the method was demonstrated by absolute quantification of selected metabolites in intracellular extracts of *E. coli* biomasses using standard-based external calibration, isotope dilution and standard addition as calibration strategies [40].

http://dx.doi.org/10.5772/68073

The HILIC-MS/MS method for the quantification of AMP, GMP, UMP, CMP and IMP in infant formula was developed by Inoue et al. The mobile phase used for the separation consisted of 30 mM ammonium formate in water with a pH of 2.5 and methanol. Data acquisition was achieved by positive ESI MRM; the LOD and LOQ were 5–10 and 10–30 μg mL^{-1} for standard solution, respectively [79].

The HILIC-MS/MS method was developed for simultaneous quantitative analysis of cAMP and ATP for measuring the effect of (partial) agonists on cAMP accumulation *in vitro*. The separation of the analytes proceeded on a ZIC®-pHILIC column with mobile phase A consisting of 10 mM ammonium bicarbonate buffer adjusted to a pH of 9.4 with ammonium hydroxide in 20% AcCN in water and mobile phase B consisting of 100% AcCN. The total run time using pre-sampling was less than 6 min. The method was applied to Chinese hamster ovarian cells cloned and expressing the human dopamine D2L receptor [34].

Pesek et al. developed a method with the use of a silica hydride-based stationary phase for the aqueous normal-phase (ANP) retention of nucleotides. RP columns with a hydride surface underneath, as well as those with an unmodified or a minimally modified hydride material, were tested. The ANP retention of the hydrophilic nucleotides was dependent on mobile phases with a high organic content in combination with an additive to control ionic strength and pH. Both isocratic and gradient elution programs were used for separation optimization, and repeatability in both modes was excellent [105].

A combination of HILIC chromatography and an IP reagent was introduced by Zhang et al. This novel method enabled sensitive and short run-time analysis for adenine nucleotides. The novel aspect of this method is based on the application of DEA-HFIP in the mobile phase in combination with bare silica or NH_2 HILIC columns. This enabled successful separation of isobaric isomers (ATP vs. dGTP, etc.), among others. The highest sensitivity and chromatographic separation capacity was achieved using 100 mM HFIP and 0.5% DEA in MF at a pH of 8.9. The calibration curves showed excellent linear response over the concentration range 10–1000 ng mL^{-1} for AMP and ADP and 2–200 ng mL^{-1} for ATP; the low levels of 10 and 2 ng mL^{-1} represent the LLOQ for individual analytes [12].

Mateos-Vivas et al. also described the HILIC-MS method for the separation of nucleosides and nucleotide mono-, di- and triphosphates in the presence of hydrophilic ion-pairing reagents. During optimization three analytical columns were tested with mobile phases containing a mixture of organic solvent (acetonitrile) and aqueous media at different pH values with different concentrations of salts. HILIC XBridge-Amide was found to be the most suitable column for the separation of 20 nucleosides and nucleotides. The optimized mobile phase consisted of ACN/UHQ water mixtures with 50 mM diethylamine and 100 mM hexafluoro-2-propanol. The total analysis time was 8 min [61].

HILIC mode represents a powerful approach offering highly selective and sensitive separation of a wide range of analytes in complex studies enabling the simultaneous analysis of a large number of compounds in a single run. Using volatile additives in mobile phases enables smooth hyphenation with mass spectrometry detection and this approach is becoming widely used for various analyses today.

5. Matrix-assisted laser desorption/ionization-time of flight (MALDI-TOF)

MALDI is a soft ionization technique used in mass spectrometry commonly applied for the analysis of large molecules (DNA, proteins, peptides, etc.). Analogously to ESI, it offers a soft ionisation to obtain ions in the gas phase. Briefly, the sample is applied to a metal plate together with a suitable matrix such as 3,5-dimethoxy-4-hydroxycinnamic acid (sinapinic acid), α-cyano-4-hydroxycinnamic acid (α-CHCA, alpha-cyano or alpha-matrix) or 2,5-dihydroxybenzoic acid (DHB). The sample is consequently irradiated by means of a pulsed laser, resulting in ablation and desorption of the sample and matrix material. Finally, the analytes are ionized by (de)protonation by laser ionization energy transferred through the matrix molecules and can then be accelerated into the mass spectrometer. The advantage of the method is its higher tolerance to salts and other contaminants from samples in comparison with other MS methods. MALDI-TOF is a sensitive technique that able to detect analytes in very low concentrations, which also result in a small sample amount being required for the analysis and the reduction of the sample preparation time.

Thanks to all of these facts van Kampen et al. developed a MALDI-TOF method for the determination of nucleotide analogue zidovudine (AZT) triphosphate, used as an NRTI for the treatment of HIV infection, and other (deoxy) nucleotide triphosphates. Four different matrices were compared in order to ascertain the sensitivity and reproducibility of the method. Anthranilic acid in combination with nicotinic acid was selected as the most suitable matrix. AZT-TP, ATP and GTP were analysed with LOD of 0.5 fmol per sample. The method was applied for the determination of intracellular levels of AZT-TP and (deoxy) nucleotides in PBMCs [84].

The determination of some endogenous nucleotides was included in a metabolomic study by Edwards and Kennedy. MALDI-TOF was used for the analysis of anionic metabolites, with 9-aminoacridin as the matrix. The detection limits for the standards were from the nM to μM concentration range. The method enabled detection of overall 105 different metabolites in analysis of Langerhans islets extract, direct analysis of single Langerhans islet and *E. coli* extract. It was able to detect different metabolic states depending on environmental conditions such as glucose concentration and the sample type [44].

A shotgun metabolomics approach using MALDI-TOF/TOF mass spectrometry was developed for the rapid analysis of negatively charged water-soluble cellular metabolites by Sun et al. Neutral organic extraction solvents were used to inactivate endogenous enzyme activities. As a result of conjunction with a matrix, that had minimal background noise, identification of 285 peaks corresponding to negatively charged metabolites was possible. The identification of the metabolite peaks was based on mass accuracy and confirmation was performed using tandem mass spectrometry for 90 of the identified metabolite peaks. Assignments of ions from isomeric metabolites and their relative abundance quantitation were achieved through fragmentation ions originating in tandem mass spectrometry (e.g. discrimination of ATP from dGTP). The method is highly sensitive and facilitates the detection of extremely low-abundance metabolites, including signalling molecules such as IP3, cAMP and cGMP. The method was applied to the metabolite profiling of mouse heart extracts [106].

MALDI-TOF is generally less popular for the identification of compounds with low molecular weight because of the presence of a variety of abundant matrix-related ions in the low-mass range of MS spectra and also the non-homogenous co-crystallization of analytes with traditional organic matrices such as 2,5-dihydroxybenzoic and sinapic acid. To overcome the problem, surface-assisted laser desorption/ionization (SALDI) was developed to eliminate matrix ion interferences and improve sample homogeneity. Recently, nanoparticles have been investigated as an effective SALDI matrix. Huang and Chang introduced an analysis for the determination of ATP and glutathione using aptamer-modified gold nanoparticles (Apt-AuNPs) as selective probes and gold nanoparticles (AuNPs) as the SALDI matrices with mass spectrometry detection. In comparison with conventional organic matrices, AuNPs as laser desorption/ionization (LDI) matrices provide a number of advantages, such as ease of preparation, selectivity, sensitivity and repeatability. In combination with Apt-AuNPs as a selective probe for ATP with less efficient LDI compared to AuNPs, the MS approach provided a very good sensitivity for ATP of 0.48 μM. The method was successfully applied to the analysis of ATP and GSH in human cell lysates. This approach demonstrates the practical monitoring of the bioactivity of cells through ATP and GSH levels [35].

Negative MALDI-TOF-MS appears to be a promising tool for nucleotide analysis providing complementary information to the armamentarium of metabolomic techniques. This technique can provide high levels of throughput because of the simple sample preparation, without the need for chromatographic separation and short analysis time, but its usability for low-mass compounds is still limited.

6. Summary

Nowadays, mass spectrometry is very important and widely applied tool in nucleotides analysis. As a result of technological advances in sample purification methods and mass spectrometry detection, the developed methods allow sensitive and selective measurement of polar compounds occurring in low levels in various biological matrices. This enables more potential uses in clinical field. Direct methods require no special sample pre-treatment before analysis in contrast to indirect methods, where fractionation, dephosphorylation and purification are needed. Previously time-consuming chromatographic separation based on the number of phosphate groups was improved as a result of wide spectrum of separation possibilities and settings. The use of IP agent in optimal amount made the methods relatively MS friendly. Alternative approach is the ion exchange chromatography with pH gradient used for elution. High selectivity in separation of closely related nucleotides can be achieved by using porous graphitic carbon columns. HILIC represents a promising approach for analysis of wide spectra of analytes including polar compounds such as nucleotides. High separation efficiency is also achieved with the use of CE with MS detection. Analysis of nucleotides is also described by the means of MALDI-TOF, but poor reproducibility and lack of applications make a limitation for this approach. Selected methods for determination of endogenous nucleotides and nucleotide analogues by mass spectrometry are summarized in **Tables 1** and **2**, respectively.

Analysed nucleotides	Matrix/application	Technique	Nucleotides extraction	Separation	MS polarity	References
cGMP (cAMP, cIMP, AMP, GMP, IMP)	Human plasma	LC-MS/MS	PP (AcCN)	Metasil AQ C18, (RP)	MRM −	[37]
cAMP, cCMP, cGMP, cUMP	Hek293T cells	LC-MS/MS	PP (AcCN:MetOH:H_2O, 2:2:1, v/v)	Zorbax eclipse XDB-C18 (RP)	SRM +	[30]
UXP, CMP, AXP, GXP, TTP, dATP	Mice islet of Langerhans; *E. coli*	MALDI-TOF	PP (MetOH)	-	MS −	[44]
AXP	HepG-2 cells	LC-MS/MS	PP (PCA)	Hypercarb (PGC)	MS −	[25]
AXP, CXP, GXP, IXP, UXP, dAXP, dCXP, dGXP, dTXP, dUXP, cAMP	*E. coli*	LC-MS/MS	PP (80% MetOH)	Luna NH_2 (HILIC)	SRM ±	[43]
CTP, dCTP, UTP, GTP, dTTP, dGTP/ ATP, dATP	human leukemia cells lines (K562, NB4, ML-1, MV4-11, THP-1)	LC-MS/MS	PP (60% MetOH)	Supelcogel ODP-50 (IPC)	MRM −	[26]
TXP, cAMP, cGMP, AXP, GXP, CXP	*E. coli*	CE-MS (LC-MS/MS)	PP + LLE (MetOH + chloroform + H_2O)	Fused-silica 50 μm × 100 cm (Asahipak ODP-50 2D)	MS − (MRM −)	[55]
AXP, CDP, CTP, GDP, GTP, UDP, UTP	Rat kidney tissue	LC/LC-MS	PP (PCA) + online desalting	Zorbax C18 + Synergy Hydro C18, (IPC)	MS +	[41]
AXP, GXP, CXP, UXP, cAMP	*E. coli*	LC-MS/MS	PP (liquid N_2)	ZIC-pHILIC (HILIC)	MRM −	[40]
ATP	MDA-MB-231 cells	SALDI-MS	Sonication, filtration	-	MS −	[35]
CXP, UXP, AXP, GXP, cAMP, cGMP	Chinese hamster ovary cells (CHO)	LC-MS/MS	PP (MetOH) + LLE (hexane)	Symmetry (IPC)	MRM −	[31]
AMP/dGMP, ADP/dGDP, ATP/dGTP	Human blood and plasma	LC-MS/MS	PP (MetOH)	Luna NH_2 (IP-HILIC)	MRM −	[12]
AXP, cGMP	*E. coli*	LC-MS/MS	PP (60% MetOH)	Synergi Hydro-C18 (IPC)	MRM −	[47]
AXP, CTP, GXP, UTP, dATP, dCTP, dGXP, dTXP (CDP, dAMP, dCDP, dUMP, UDP)	H23 cells	LC-MS/MS	PP (60% MetOH) + ultrafiltration	Atlantis T3 (IPC)	MRM −	[32]

Analysed nucleotides	Matrix/application	Technique	Nucleotides extraction	Separation	MS polarity	References
AMP, ATP, dAMP, dATP, UMP, UTP, TMP, TTP, CMP, CTP, dCMP, dCTP, GMP, GTP, dGMP, dGTP	Messa cells	LC-MS/MS	PP (70% MetOH) + online SPE (WAX)	Hypercarb (PGC)	MRM +	[29]
GTP, ATP, UTP, CTP, GDP, ADP, UDP, CDP, GMP, AMP, UMP, CMP	Rat heart tissue	LC-MS/MS	PP (50% MetOH)	Hypersil Gold AQ C18	MRM −	[45]
cAMP, ATP	CHO-K1 cells	LC-MS/MS	Lysis buffer (63% AcCN, 10 mM NH_4HCO_3)	ZIC-pHILIC (HILIC)	MRM −	[34]
cAMP, cGMP	Mice brain tissue, plasma, CSF	LC-MS/MS	PP (PCA)	Varian Metasil AQ C18 (RP)	MRM +	[36]
Adenosine, guanosine, inosine (AMP, ATP, GMP, GTP, IMP, ITP)	PBMC, RBC, DBS	LC-MS/MS Indirect	PP (70% MetOH) + SPE + dephosphorylation + SPE	Develosil C30, RP aqueous	MRM +	[15]

Table 1. Selected methods for determination of endogenous nucleotides using mass spectrometry detection.

Analysed nucleotides	Matrix/application	Technique	Nucleotides extraction	Separation	MS polarity	References
AZT, AZT-XP, 5-methyl-UTP, AZdU	PBMC/plasma	LC-MS/MS	PP (EtOH)	InnertSustain/ InnertSil ODS-30 (IPC)	MRM +	[19]
AZT, AZT-MP, AZT-TP, 3TC, 3TC-TP, dT-TP	PBMC/plasma	LC-MS/MS	PP (Tris-HCl/MetOH)	SMT C18 (IPC)	MRM ±	[20]
Clofarabine-TP	PBMC	LC-MS/MS	PP (AcCN)	CAPCELL PAK CN	MRM −	[24]
d4T, d4T-XP, dT-TP	PBMC	LC-MS/MS	PP (Tris-HCl/MetOH)	SMT C18 (IPC)	MRM −	[23]
AZT-TP	PBMC	LC-MS/MS	PP (TrisHCl/MetOH) + immunoaffinity extraction	Supelcogel ODP-50 (IPC)	MRM −	[21]
FLT, FLT-MP	Human serum	LC-MS/MS	PP (MetOH)	Aquasil C18 (RP)	MRM +	[58]
dFdC, dFdU, dFdC-TP	Mice pancreatic tumour tissue	LC-MS/MS	PP (aqueous AcCN)	Hypercarb (PGC)	MRM ±	[46]
MeGTP	Mouse liver tissue	LC-MS/MS	PP (TCA) + SPE-WAX	Luna NH_2 (IXC)	MRM +	[42]

Analysed nucleotides	Matrix/application	Technique	Nucleotides extraction	Separation	MS polarity	References
MeCTP	Rat liver tissue	LC-MS/MS	PP (70% MetOH)+SPE	Luna NH_2 (HILIC)	MRM −	[39]
2CdA-XP	MDCKII cells	LC-MS/MS	PP (70% MetOH)	Biobasic AX (IXC)	MRM +	[27]
TFV-DP, 3TC-TP, CBV-TP	Human PBMC	LC-MS/MS	PP (Tris-HCl/MetOH)	Supelcogel ODP-50 (IPC)	MRM +	[16]
MeTG-XP, MeTI-XP, TG-XP, TI-MP, TI-TP	RBC	LC-MS/MS	PP (heating, MetOH, $CHCl_3$)	Biobasic AX (IXC)	MRM +	[13]
dFdC-TP	PBMC	LC-MS/MS	PP (PCA)	Biobasic AX (IXC)	MRM −	[17]
FUTP, FdUXP	PBMC	LC-MS/MS	PP (MetOH)	Biobasic AX (IXC)	MRM −	[18]
TFV(XP), ZDV(XP), 3TC(XP), FTC(XP)	RBC, PBMC	LC-MS/MS indirect	PP (70% MetOH), SPE, dephosphorylation, SPE	Synergi Polar RP (RP)	SRM +	[14]
RBV(XP)	RBC, PBMC, DBS	LC-MS/MS Indirect	PP (70% MetOH), SPE, dephosphorylation, SPE	Develosil C30- RP aqueous (RP)	SRM +	[59]
ZDV(TP), 3TC(TP)	PBMC	LC-MS/MS indirect	PP (70% MetOH), SPE, dephosphorylation, SPE	Hypersil C18 (RP)	SRM +	[22]
ddATP	CEM-T4cells	LC-MS/MS indirect	PP (70% MetOH), SPE, dephosphorylation, SPE	Purospher RP-18e (RP)	SRM +	[33]
Adefovir, Adefovir-MP, Adefovir-DP, Tenofovir-DP, dATP	HepG2	LC-MS/MS	PP (70% MetOH)	C18: Xterra/YMC /Luna	MRM +	[28]

Table 2. Selected methods for determination of nucleotide analogues using mass spectrometry detection.

7. Nucleotide profile of cell lines by HILIC chromatography

7.1. Introduction

We adopted and optimized the metabolomics method to cover intermediates in the majority of the metabolic pathways in the cellular metabolome, as well as common metabolites present in urine, plasma and other biofluids, originally published by Bajad in 2006 [43]. It is based on HILIC separation mode, where polar negatively charged metabolites are separated on an aminopropyl column under strongly alkaline conditions (pH > 9). The gradient of the mobile phase, pH and particle size selection (3 μm) in the column was optimized. The list of metabolites was significantly extended by measurement in scheduled MRM mode and applying polarity switching. Under the final conditions, the method allows the separation of 350 metabolites during 17 min of analysis. The method is routinely used in our laboratory [104, 107] and it was applied to the sensitive measurement of selected endogenous

nucleotides and nucleotide analogues in intracellular content [104, 107]. In this chapter, 5-ethynyl-2′-deoxyuridine (EdU) and its mono-, di- and triphosphate analogues resulting from the incubation of cancerous cell lines with EdU and 5-ethynyl-2′-deoxycytidine (EdC), together with endogenous purine and pyrimidine nucleotides, are presented.

7.2. Material and methods

7.2.1. Cell cultures

The cell line 143B PML BK TK [bone, osteosarcoma, contains a herpes simplex virus type 1 thymidine kinase (hsv-1 TK+) plasmid; 143B] was cultivated in DMEM supplemented with 3.7 gL^{-1} of sodium bicarbonate and HAT (0.1 mM hypoxanthine, 400 nM aminopterin and 0.16 mM dT, Sigma Aldrich). The medium was also supplemented with 10% foetal bovine serum (Gibco) and 50 $\mu g\, mL^{-1}$ gentamicin. One week before the experiment, the culture medium was exchanged for a HAT-free medium. For more details see the study by Ligasová et al. [108].

7.2.2. Chemicals

Water, acetonitrile, methanol, acetic acid, ammonium hydroxide (all LC-MS purity grade), DMEM and dimethylsulphoxide (DMSO) were all purchased from Sigma Aldrich (St. Louis, MO, USA). 5-Ethynyl-2′-deoxyuridine (EdU) was purchased from Carbosynth (Compton, Berkshire, United Kingdom) and 5-ethynyl-2′-deoxycytidine (EdC) and EdU triphosphate (EdUTP) from Jena Biosciences (Jena, Germany). EdC monophosphate (EdCMP), EdC diphosphate (EdCDP) and EdC triphosphate (EdCTP) were synthesized by Dr. Liboska from the Institute of Organic Chemistry and Biochemistry, CAS, v.v.vi.

7.2.3. Instrumentation

Analyses of endogenous nucleosides, nucleotides, the nucleoside analogues and their phosphorylated metabolites were performed using the Ultimate 3000 RS high-performance liquid chromatographic system (Dionex, Sunnyvale, CA, USA) coupled with a Triple Quad 6500 tandem mass spectrometer (Sciex, Framingham, MA, USA) equipped with an electrospray IonDrive Turbo V Source. A Luna NH_2 aminopropyl column (2 × 100 mm, 3 μM, Phenomenex) protected by a 4 × 2-mm ID guard column made of the same material (Phenomenex, Torrance, USA) was used for separation.

7.2.4. Sample preparation

The sample preparation of the cells treated with EdU or EdC is described previously in the study by Ligasová et al. [108]. Briefly, cells cultivated in a medium with or without nucleoside analogue for a definite time were immediately vacuum-filtered. The membrane filter with the captured cells was transferred to a pre-cooled Petri dish, extracted with a cold extraction solution (AcCN:MetOH:0.5 M FA/30:10:10), and returned to a −20°C freezer for 30 min. The filter was rinsed with the extraction solution in the dish, the solution was transferred into centrifuge microtubes, and then the filter was re-rinsed with 1 mL of fresh cold extraction

solution, which was thereafter combined with the initial cell extract. After centrifugation, the supernatant was put into the freezer, pellet resuspended in fresh extraction solution, frozen and centrifuged, and the supernatant was combined with the previous one. The extract was neutralized with NH_4HCO_3 and centrifuged and the supernatant was lyophilized and resuspended in 100 μL of water mobile phase before the LC-MS/MS analysis. All the procedures were performed in an ice bath to prevent undesirable metabolic processes in the cells during the sample preparation.

7.2.5. Standard stock solutions

Standard solutions of EdCMP, EdCDP, EdCTP and EdUTP were dissolved in deionized water in concentrations of 1.96, 3.6, 4.7 and 5 μM, respectively. EdU and EdC were dissolved in DMSO to a concentration of a 10-mM stock solution. The working solutions of all standards for mass spectrometry optimization were obtained by serial dilutions to the required concentrations with water of LC-MS purity grade. All the solutions were stored at −80°C.

7.2.6. LC-MS/MS analysis conditions

The separation and mass spectrometry method was previously described by Ligasová et al. [108]. Briefly, mobile phase A consisted of 20 mM ammonium acetate buffer solution, pH = 9.75, and mobile phase B was acetonitrile. The gradient elution program used for the separation started with 95% B and during 7 min was reduced to 10% B and held for the next 7 min. Then, initial conditions were achieved in 1 min and equilibration took 3 min. The column was maintained at 35°C with a flow rate of 0.3 mL min^{-1}. The total analysis time was 17 min. The targeted metabolites were detected in multiple reaction monitoring (MRM) in both positive and negative electrospray ionization mode. The mass spectrometry parameters were optimized using a standard solution of the targeted analytes dissolved in a mixture of mobile phase A and B (50:50, v/v). The final MS conditions are summarized in **Tables 3** and **4** for positive and negative mode, respectively. Both quadrupoles (Q1 and Q3) were set to 'unit' resolution. The ion source parameters were optimized to the following settings: an ionization spray voltage of (−) 4500 V, a curtain gas of 30 psi, a collision gas of 8 psi, a heater gas and turbo ion spray gas of 40 psi, a source temperature of 400°C, and an entrance potential of (−) 10 V. High-purity nitrogen was used as the collision gas. The Analyst 1.6.2 and MultiQuant 3.0 software (Sciex, USA) were used for data acquisition and evaluation. Standards for EdUMP and EdUDP were not available and the mass spectrometry conditions were adopted from the optimization experiments of EdC/EdCMP/EdCDP/EdCTP. For more details, see the previously published study by Ligasová et al. [108].

7.3. Results and discussion

The first step in the mass spectrometry optimization was finding the optimal parameters for targeted metabolite analyses. Selected reaction monitoring (SRM) requires the accurate setting of molecular ion and the most sensitive and selective fragment, the optimal collision energy, declustering potential and entrance and exit potentials. A standard solution of each

ID	Q1	Q3	DP	CE	ID	Q1	Q3	DP	CE	ID	Q1	Q3	DP	CE
A	135.9	118.9	171	31	dHr	252.9	136.9	51	19	GMP	364.0	152.0	36	21
AMP	348.0	135.9	116	27	dUR	228.9	113.0	91	23	Gr	284.0	151.9	51	27
Ar	268.2	136.1	41	29	EdC	252.0	136.1	46	15	Hr	268.9	136.9	81	21
C	111.9	94.8	96	27	EdCDP	412.0	216.1	51	13	HX	136.9	109.9	136	29
CMP	323.8	111.9	46	21	EdCMP	332.0	136.1	36	17	IMP	349.0	136.9	31	19
Cr	244.0	111.9	31	27	EdCTP	491.9	136.1	71	19	T	126.9	109.9	96	23
dAMP	331.9	135.9	41	23	EdU	253.0	137.1	116	17	Tr	242.9	126.8	61	17
dAr	251.9	118.9	36	59	EdUMP	333.0	81.1	36	53	Xr	284.9	152.9	96	15
dCMP	307.9	112.0	56	19	EdUTP	492.9	81.0	111	55					
dGMP	348.1	80.9	10	31	G	152.0	81.9	76	37					

Table 3. MS parameters for targeted analytes in positive mode.

http://dx.doi.org/10.5772/68073

ID	Q1	Q3	DP	CE	ID	Q1	Q3	DP	CE	ID	Q1	Q3	DP	CE
ADP	425.8	133.9	−95	−32	dTDP	400.8	158.8	−60	−34	EdUMP	331.0	135.0	−55	−26
ATP	506.1	159.0	−75	−30	dTMP	320.8	194.9	−35	−24	EdUTP	490.9	158.8	−70	−34
CDP	401.8	158.9	−60	−32	dTTP	480.7	158.8	−70	−46	GDP	441.8	158.8	−95	−36
CTP	481.7	158.9	−70	−44	dUMP	306.8	195.0	−50	−22	GTP	522.0	424.0	−90	−25
dADP	409.8	158.8	−30	−32	dUTP	466.7	158.9	−55	−36	IDP	426.8	134.9	−75	−32
dATP	489.7	158.7	−60	−36	EdC	249.9	136.0	−55	−12	ITP	506.7	158.7	−60	−48
dCDP	385.8	158.9	−30	−30	EdCDP	409.9	274.7	−45	−26	U	111.0	42.1	−35	−22
dCTP	465.7	158.9	−65	−36	EdCMP	329.9	194.8	−55	−22	UDP	402.9	158.8	−70	−34
dGDP	425.8	158.9	−70	−32	EdCTP	489.8	158.8	−5	−34	UMP	322.8	210.9	−65	−22
dGTP	506.1	159.0	−75	−30	EdU	250.9	134.8	−50	−16	UTP	482.7	158.7	−80	−48
dITP	490.7	158.8	−65	−40	EdUDP	411.0	78.9	−70	−102	X	150.9	108.0	−55	−24

Table 4. MS parameters for targeted analytes in negative mode.

http://dx.doi.org/10.5772/68073

nucleotide was directly infused into the mass spectrometer and the parameters were tuned automatically. The most suitable ion for SRM was selected from the fragmentation spectra. The fragmentation spectra of EdU and EdUTP are shown in **Figure 1**. In positive mode, the cleavage of hydroxyl groups from deoxyribose (m/z of 235.0 and 217.2) and whole deoxyribose (137.0, 117.0 and 99.0) and cleavage of the pyrimidine ring (94.0) were typical fragmentation behaviour of EdU. In negative mode, the fragmentation is not so predictable and fragments of whole deoxyriboside (135.0) and the pyrimidine ring (207.8 and 92.0) and deoxyriboside (160.8) were obtained. EdUTP was fragmented in positive mode, similarly to the cleavage of the pyrimidine ring (137.0 and 119.0), whole EdU without hydroxyl groups (217.2) and one terminal phosphate group (81.0), respectively. In negative mode, the fragmentation pattern of EdUTP contained cleavage in six different positions of the triphosphate group (79.0, 97.0/393.0, 159.0, 176.8, 238.8 and 257.0) and the pyrimidine ring (135.0/355.0), respectively.

The fragmentation behaviour of deoxyriboside can be applied to other ribosides/deoxyriboside and their analogues. The cleavage of sugar in both positive and negative ionization modes offers the most intensive product ion of the pyrimidine or purine ring, which is commonly used as a characteristic transition for SRM. Similarly, deoxy/nucleoside di- and triphosphates and their analogues offer the most intensive fragmentation in negative mode, with cleavage of one, two or three phosphates. The situation is different in the case of deoxy/nucleoside

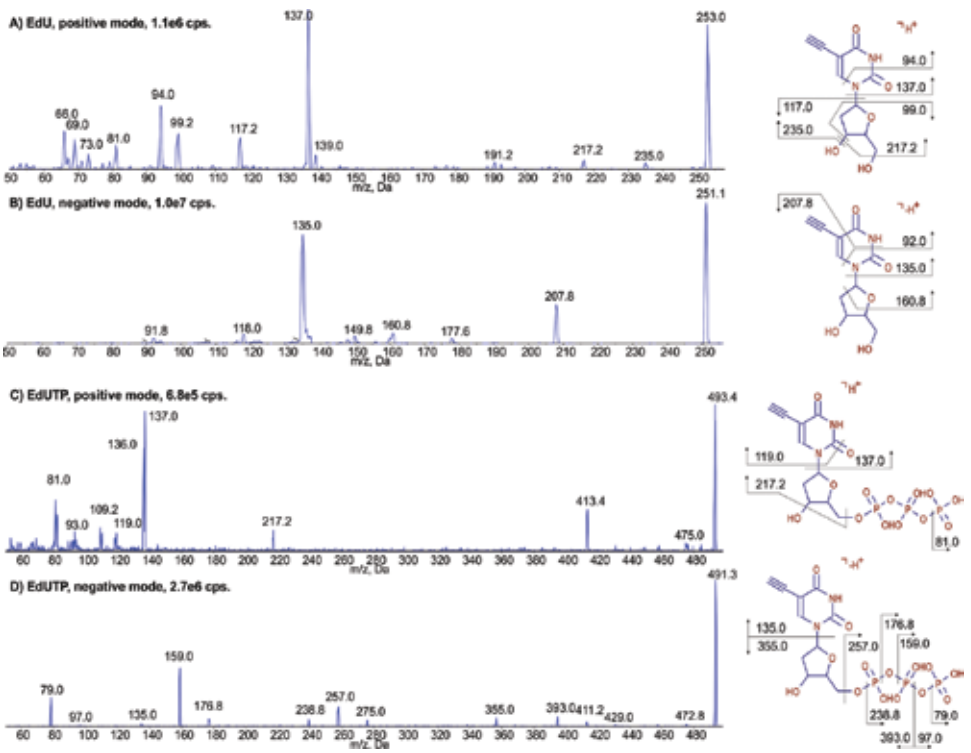

Figure 1. Fragmentation spectra of EdU and EdUTP in positive and negative ESI mode, respectively.

monophosphates, which provide a more intensive signal in positive mode with cleavage of the purine or pyrimidine ring. This approach can be successfully applied for many different nucleosides or nucleotides even when standards are not commercially available. The other crucial parameter is the collision energy, which has to be carefully optimized. Again, it can be adopted from available standards during the compound tuning and optimization procedure. This general phenomenon is documented in **Tables 3** and **4**, which show the SRM transitions and other MS parameters of all the nucleotides included in the method.

For the separation and accurate determination of nucleotides, it is necessary to choose optimal conditions for the stationary and mobile phase, gradient program and flow rate. Nucleotides are very polar analytes, with a hydrophilic-close-to-ionic character. Therefore, the analysis is not successful on common chromatography systems with reversed-phase columns. Using HILIC separation mode based on aminopropyl or amidic stationary phases has advantages in the separation of many polar analytes with negatively charged functional groups, which are commonly present in biofluids or cell extracts. Moreover, analytes with a strong ionic character are retained even more. Typically, purine or pyrimidine analytes from bases up to nucleotide triphosphates can be separated in one analysis (**Figures 2** and **3**). The most important parameter for the separation is a pH with a value above 9.5, where triphosphates are not so strongly retained and the analysis time can be reduced to less than 20 min. The first general issue of using an aminopropyl column is the limited lifetime of the column (<400 analyses), which can be overcome by using an amidic stationary phase (although the separation behaviour is different). A second issue is the presence of significant ion suppression and lower sensitivity for more retained compounds which are eluted by the alkaline buffer in water. This can be overcome by using a thinner column with an inner diameter of 1 mm and by subsequently reducing the flow rate to 50 μL min^{-1} and by increasing the time taken for the analysis to 1 h.

The profiles of adenine, guanine, cytosine and uracil bases, ribosides and nucleotides in the cell line 143B incubated with EdU are shown in **Figures 2** and **3**. Purine bases, ribosides and monophosphates are most sensitive in positive ionization mode compared to di- and triphosphates, which are significantly more ionizable in negative mode. On the contrary, the analysis of uracil and EdU and its nucleotides is more sensitive in negative mode for all the compounds. Three peaks in the range 7–12 min, corresponding to the electrospray fragmentation of nucleotides on bases, can be seen in a chromatogram of adenine SRM transition. Similarly, this phenomenon is also present in other chromatograms (AMP, ADP, GDP …). The new generation of triple quadrupoles brings the dynamic range of intensities up to seven orders, which is very useful for the multicomponent analysis of compounds with a large span of detector responses, such as biofluids. For example, adenosine has an intensity that is three orders higher compared to the uridine in the same sample. The disadvantage of the method is its inability to analyse isobaric compounds with the same separation behaviour: AMP/dGMP, ADP/dGDP and ATP/dGTP.

The cell line 143B was incubated with EdU and the corresponding nucleotides were followed. Because of the toxicity of EdU, the concentration in the incubation mixture was relatively low (10 μmol L^{-1}) and therefore the production of nucleotides was limited to nmol-μmol L^{-1}

http://dx.doi.org/10.5772/68073

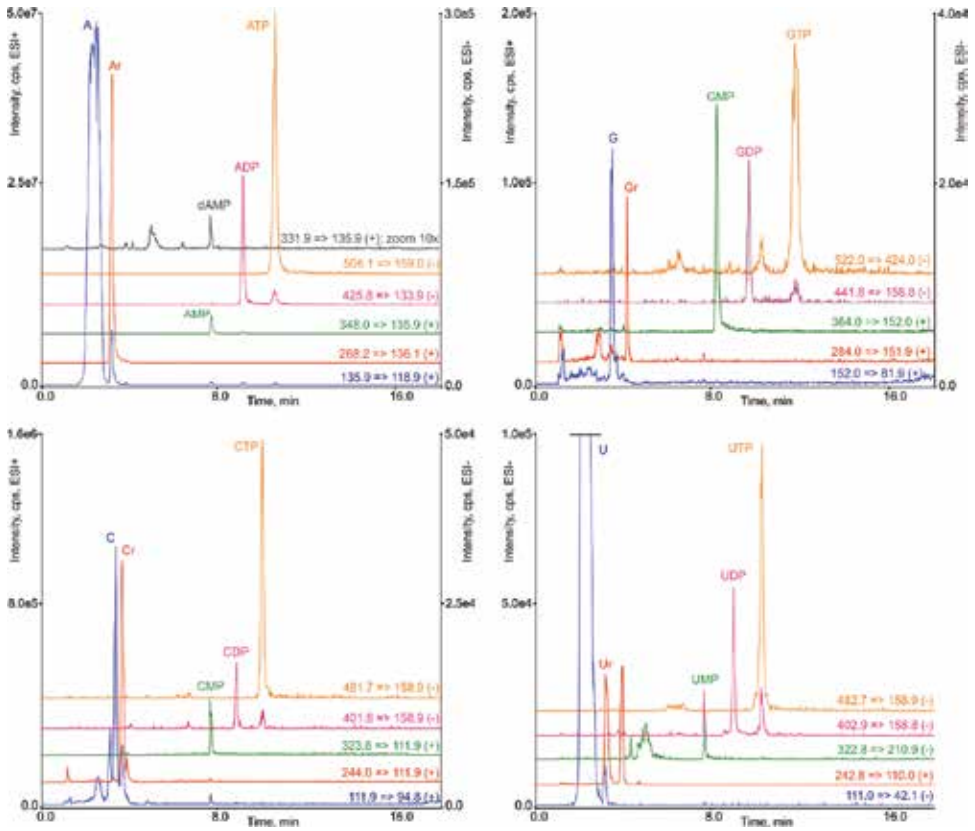

Figure 2. Extracted SRM chromatograms of selected endogenous bases, ribosides and nucleotides in intracellular content of 143B cell line.

concentration levels. **Figure 3** shows chromatograms of EdU and modified nucleotides in the intracellular extract of the incubated cell lines and controls without the addition of EdU. The optimization of the SRM transitions for commercially available EdU and EdUTP was performed. EdUMP and EdUDP were calculated theoretically and SRM transitions with fragments of the pyrimidine base and one phosphate group for EdUMP and EdUDMP offered the most sensitive signal. The approximate concentrations of these two commercially unavailable nucleotides were calculated from the ratio of the analogous SRM of the standards of adenine nucleotides.

7.4. Conclusion

Highly sensitive LC-MS/MS method for determination of intracellular levels of nucleotide analogues EdU and EdC and its phosphorylated metabolites and several endogenous nucleotides was described. The use of aminopropyl column in HILIC adjustment enables efficient separation of polar analytes during 17 min. Despite the limitations of the HILIC separation approach described above, it is very promising and probably the best way to analyse a wide range of

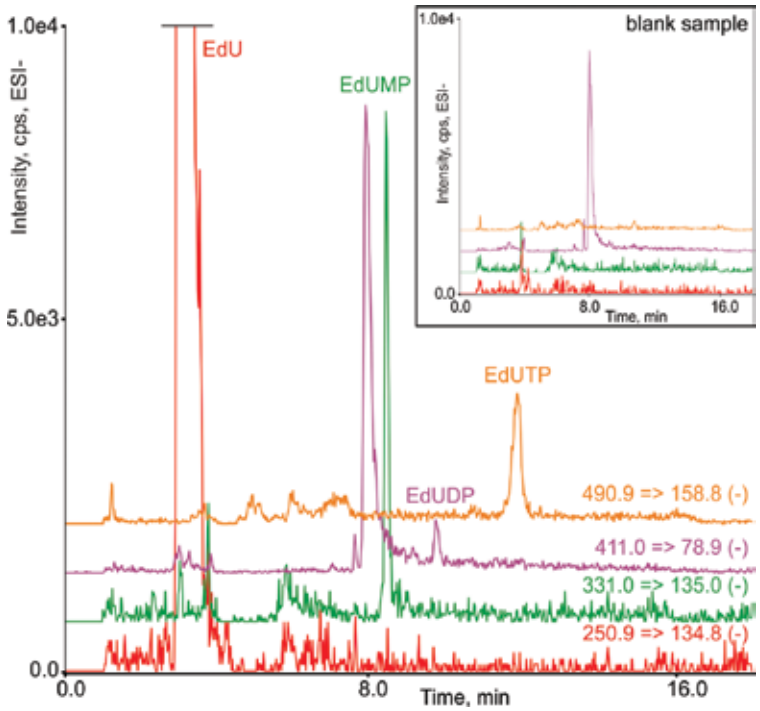

Figure 3. Extracted SRM chromatograms of EdU, EdUMP, EdUDP and EdUTP in intracellular content of 143B cell line treated by EdU.

purine and pyrimidine bases, ribosides and nucleotides within single analysis. Coupled with triple quadrupole mass spectrometry, it offers excellent selectivity and sensitivity, with a high linear response. Sample preparation based on cell lysis and protein precipitation by methanol without a need of SPE extraction allows application of the method on clinical studies. It can be applied on drug monitoring, pharmacokinetics studies and provides an insight into the influence of the nucleotide analogue on intracellular nucleotide pool *in vitro*.

Acknowledgements

This work was supported by the Ministry of Health of the Czech Republic [AZV 15-31604A].

Abbreviations

2cDA	Chlorodeoxyadenosine/cladribine
3TC	Lamivudine
AcCN	Acetonitrile
ADP	Adenosine diphosphate
AICA	5-Aminoimidazole-4-carboxamide

http://dx.doi.org/10.5772/68073

AMP	Adenosine monophosphate
araC	Cytarabine
araCMP	Cytarabine monophosphate
araCTP	Cytarabine triphosphate
ATP	Adenosine triphosphate
AX	Anion exchange
AZdU	Azidodeoxyuridine
AZT	Zidovudine
BrATP	Bromoadenosine triphosphate
cAMP	Cyclic adenosine monophosphate
CBV	Carbovir
cCMP	Cyclic cytidine monophosphate
CDP	Cytidine diphosphate
CE	Capillary electrophoresis
CEC	Capillary electrochromatography
CGE	Capillary gel electrophoresis
cGMP	Cyclic guanosine monophosphate
CIEF	Capillary isoelectric focusing
cIMP	Cyclic inosine monophosphate
CoA	Coenzyme A
CSF	Cerebrospinal fluid
CTP	Cytidine triphosphate
CU	Chlorouracil
cUMP	Cyclic uridine monophosphate
CZE	Capillary zone electrophoresis
d4T	Stavudine
dATP	Deoxyadenosine triphosphate
dCTP	Deoxycytidine triphosphate
ddA	Dideoxyadenosine
ddAMP	Dideoxyadenosine monophosphate
ddATP	Dideoxyadenosine triphosphate
ddI	Didanosine
ddN	Dideoxynucleotides
DEA	Diethylamine
dFdC	Difluorodeoxycytidine/gemcitabine
dFdU	Difluorodeoxyuridine

dGTP	Deoxyguanosine triphosphate
DMHA	Dimethylhexylamine
DNA	Deoxyribonucleic acid
DP	Diphosphate/declustering potential
dTTP	Deoxythymidine triphosphate
EdC	Ethynyldeoxycytidine
EDTA	Ethylenediaminetetraacetic acid
EOF	Electro-osmotic flow
ESI	Electrospray ionization
EtOH	Ethanol
FAD	Flavinadeninedinucleotide
FdUMP	Fluorodeoxyuridine monophosphate
FdUrd	Fluorodeoxyuridine
FdUTP	Fluorodeoxyuridine triphosphate
FLT	3′-Deoxy-3′-fluorothymidine
FTC	Emtricitabine
FU	Fluorouracil
FUrd	Fluorouridine
FUTP	Fluorouridine triphosphate
GMP	Guanosine monophosphate
GDP	Guanosine diphosphate
GTP	Guanosine triphosphate
HA	Hexylamine
HFIP	Hexafluoropropanol
HILIC	Hydrophilic interaction liquid chromatography
HIV	Human immunodeficiency virus
HPLC	High-performance liquid chromatography
CHO	Chinese hamster ovarian
IDP	Inosine diphosphate
IMP	Inosine monophosphate
IP	Ion-pairing
IPC	Ion-pairing chromatography
ITP	Isotachophoresis
IX	Ion exchange
LC	Liquid chromatography

http://dx.doi.org/10.5772/68073

LLE	Liquid-liquid extraction
LLOQ	Lower limit of quantification
MALDI-TOF	Matrix-assisted laser desorption/ionization-time of flight
MeCTP	Methylcytidine triphosphate
MeGTP	Methylguanosine triphosphate
MEKC	Micellar electrokinetic chromatography
MeTI	Methylthioinosine
MetOH	Methanol
MeTG	Methylthioguanosine
MP	Monophosphate
MRM	Multiple reaction monitoring
MS	Mass spectrometry
MS/MS	Tandem mass spectrometry
NAD	Nicotinamide adenine dinucleotide
NADP	Nicotinamide adenine dinucleotide phosphate
NHC	N-hydroxycytidine
NRTI	Nucleotide reverse transcriptase inhibitor
NTPs	Nucleotide triphosphates
PBMC	Peripheral blood mononuclear cells
PBS	Phosphate buffer saline
PCA	Perchloric acid
PGC	Porous graphitic carbon
PP	Protein precipitation
RBC	Red blood cells
RBV	Ribavirin
RNA	Ribonucleotide acid
RP	Reversed phase
SPE	Solid phase extraction
TBA	Tetrabutylammonium
TCA	Trichloroacetic acid
TDP	Thymidine diphosphate
TEA	Triethylamine CTP
TI	Thioinosine
TFV	Tenofovir
TG	Thioguanosine

TK 1	Thymidine kinase 1
TMP	Thymidine monophosphate
TP	Triphosphate
TTP	Thymidine triphosphate
UDP	Uridine diphosphate
UMP	Uridine monophosphate
UTP	Uridine triphosphate
UV/DAD	Ultraviolet/diode array detection
WAX	Weak anion exchange
ZDV	Zidovudine
ZR	5-Amino-4-imidazolecarboxamide riboside

Author details

Kateřina Mičová[1,2], David Friedecký[1,2]* and Tomáš Adam[1,2]

*Address all correspondence to: david.friedecky@gmail.com

1 Faculty of Medicine and Dentistry, Institute of Molecular and Translational Medicine, Palacky University, Olomouc, Czech Republic

2 Department of Clinical Chemistry, University Hospital Olomouc, Olomouc, Czech Republic

References

[1] Korycka A, Lech-Marańda E, Robak T. Novel purine nucleoside analogues for hematological malignancies. Recent Patents on Anti Cancer Drug Discovery. January 2008;**3**(2):123–136

[2] Gesto DS, Cerqueira NMFSA, Fernandes PA, Ramos MJ. Gemcitabine: A critical nucleoside for cancer therapy. Current Medicinal Chemistry. 2012;**19**(7):1076–1087

[3] Robak T, Robak P. Purine nucleoside analogs in the treatment of rarer chronic lymphoid leukemias. Current Pharmaceutical Design. 2012;**18**(23):3373–3388

[4] Jordheim LP, Durantel D, Zoulim F, Dumontet C. Advances in the development of nucleoside and nucleotide analogues for cancer and viral diseases. Nature Reviews Drug Discovery. 31 May 2013;**12**(6):447–464. DOI: 10.1038/nrd4010

[5] Sarvaria A, Topp Z, Saven A. Current therapy and new directions in the treatment of hairy Cell leukemia. JAMA Oncology. 1 January 2016;**2**(1):123. DOI: 10.1001/jamaoncol.2015.4134

[6] Hiramatsu N, Yamada R, Takehara T. The suppressive effect of nucleos(t)ide analogue treatment on the incidence of hepatocellular carcinoma in chronic hepatitis B patients. Journal of Gastroenterology and Hepatology. March 2016;**31**(3):546–552. DOI: 10.1111/jgh.13229.

[7] Galmarini CM, Mackey JR, Dumontet C. Nucleoside analogues and nucleobases in cancer treatment. Lancet Oncology. 2002;**3**(7):415–424. DOI: 10.1016/S1470-2045(02)00788-X

[8] Nyhan WL. Disorders of purine and pyrimidine metabolism. Molecular Genetics and Metabolism. September 2005;**86**(1-2):25–33. DOI: 10.1016/j.ymgme.2005.07.027

[9] Cohen S, Jordheim LP, Megherbi M, Dumontet C, Guitton J. Liquid chromatographic methods for the determination of endogenous nucleotides and nucleotide analogs used in cancer therapy: A review. The Journal of Chromatography B. 2010;**878**(22):1912–1928. DOI: 10.1016/j.jchromb.2010.05.016

[10] Jansen RS, Rosing H, Schellens JHM, Beijnen JH. Mass spectrometry in the quantitative analysis of therapeutic intracellular nucleotide analogs. Mass Spectrometry Reviews. March 2011;**30**(2):321–343. DOI: 10.1002/mas.20280

[11] Dudley E, Bond L. Mass spectrometry analysis of nucleosides and nucleotides. Mass Spectrometry Reviews. 2014;**33**(4):302–331. DOI: 10.1002/mas.21388

[12] Zhang G, Walker AD, Lin Z, Han X, Blatnik M, Steenwyk RC, et al. Strategies for quantitation of endogenous adenine nucleotides in human plasma using novel ion-pair hydrophilic interaction chromatography coupled with tandem mass spectrometry. The Journal of Chromatography A. 2014;**1325**:129–136. DOI: 10.1016/j.chroma.2013.12.017

[13] Hofmann U, Heinkele G, Angelberger S, Schaeffeler E, Lichtenberger C, Jaeger S, et al. Simultaneous quantification of eleven thiopurine nucleotides by liquid chromatography-tandem mass spectrometry. Analytical Chemistry. 2012;**84**(3):1294–1301. DOI: 10.1021/ac2031699

[14] Bushman LR, Kiser JJ, Rower JE, Klein B, Zheng JH, Ray ML, et al. Determination of nucleoside analog mono-, di-, and tri-phosphates in cellular matrix by solid phase extraction and ultra-sensitive LC-MS/MS detection. Journal of Pharmaceutical and Biomedical Analysis. 2011;**56**(2):390–401. DOI: 10.1016/j.jpba.2011.05.039

[15] Jimmerson LC, Bushman LR, Ray ML, Anderson PL, Kiser JJ. A LC-MS/MS method for quantifying adenosine, guanosine and inosine nucleotides in human cells. Pharmaceutical Research. 2017;**34**(1):73–83. DOI: 10.1007/s11095-016-2040-z

[16] Pruvost A, Théodoro F, Agrofoglio L, Negredo E, Bénech H. Specificity enhancement with LC-positive ESI-MS/MS for the measurement of nucleotides: Application to the quantitative determination of carbovir triphosphate, lamivudine triphosphate and tenofovir diphosphate in human peripheral blood mononuclear cells. The Journal of Mass Spectrometry. February 2008;**43**(2):224–233. DOI: 10.1002/jms.1294

[17] Veltkamp SA, Hillebrand MJX, Rosing H, Jansen RS, Wickremsinhe ER, Perkins EJ, et al. Quantitative analysis of gemcitabine triphosphate in human peripheral blood

mononuclear cells using weak anion-exchange liquid chromatography coupled with tandem mass spectrometry. The Journal of Mass Spectrometry. December 2006;**41**(12):1633–1642. DOI: 10.1002/jms.1133

[18] Derissen EJB, Hillebrand MJX, Rosing H, Schellens JHM, Beijnen JH. Development of an LC-MS/MS assay for the quantitative determination of the intracellular 5-fluorouracil nucleotides responsible for the anticancer effect of 5-fluorouracil. Journal of Pharmaceutical and Biomedical Analysis. 2015;**110**:58–66. DOI: 10.1016/j.jpba.2015.02.051

[19] Kinai E, Gatanaga H, Kikuchi Y, Oka S, Kato S. Ultrasensitive method to quantify intracellular zidovudine mono-, di-and triphosphate concentrations in peripheral blood mononuclear cells by liquid chromatography–tandem mass spectrometry. The Journal of Mass Spectrometry. 2015;**50**(6):783–791. DOI: 10.1002/jms.3577

[20] Durand-Gasselin L, Pruvost A, Dehée A, Vaudre G, Tabone M-D, Grassi J, et al. High levels of zidovudine (AZT) and its intracellular phosphate metabolites in AZT- and AZT-lamivudine-treated newborns of human immunodeficiency virus-infected mothers. Antimicrobial Agents and Chemotherapy. July 2008;**52**(7):2555–2563. DOI: 10.1128/AAC.01130-07

[21] Becher F, Schlemmer D, Pruvost A, Nevers M-C, Goujard C, Jorajuria S, et al. Development of a direct assay for measuring intracellular AZT triphosphate in humans peripheral blood mononuclear cells. Analytical Chemistry. 15 August 2002;**74**(16):4220–4227

[22] Rodriguez JF, Rodriguez JL, Santana J, Garcia H, Rosario O. Simultaneous quantitation of intracellular zidovudine and lamivudine triphosphates in human immunodeficiency virus-infected individuals. Antimicrobial Agents and Chemotherapy. 2000;**44**(11):3097–3100. DOI: 10.1128/AAC.44.11.3097-3100.2000

[23] Pruvost A, Becher F, Bardouille P, Guerrero C, Creminon C, Delfraissy JF, et al. Direct determination of phosphorylated intracellular anabolites of stavudine (d4T) by liquid chromatography/tandem mass spectrometry. Rapid Communications in Mass Spectrometry. 2001;**15**(16):1401–1408. DOI: 10.1002/rcm.384

[24] Tu X, Lu Y, Zhong D, Zhang Y, Chen X. A sensitive LC-MS/MS method for quantifying clofarabine triphosphate concentrations in human peripheral blood mononuclear cells. The Journal of Chromatography B. 2014;**964**:202–207. DOI: 10.1016/j.jchromb.2014.01.021

[25] Wang J, Lin T, Lai J, Cai Z, Yang MS. Analysis of adenosine phosphates in HepG-2 cell by a HPLC-ESI-MS system with porous graphitic carbon as stationary phase. Journal of Chromatography B Analytical Technologies in the Biomedical and Life Sciences. 2009;**877**(22):2019–2024. DOI: 10.1016/j.jchromb.2009.05.027

[26] Chen P, Liu Z, Liu S, Xie Z, Aimiuwu J, Pang J, et al. A LC-MS/MS method for the analysis of intracellular nucleoside triphosphate levels. Pharmaceutical Research. June 2009;**26**(6):1504–1515. DOI: 10.1007/s11095-009-9863-9

[27] Jansen RS, Rosing H, De Wolf CJF, Beijnen JH. Development and validation of an assay for the quantitative determination of cladribine nucleotides in MDCKII cells and

culture medium using weak anion-exchange liquid chromatography coupled with tandem mass spectrometry. Rapid Communications in Mass Spectrometry. 30 December 2007;**21**(24):4049–4059. DOI: 10.1002/rcm.3318

[28] Vela JE, Olson LY, Huang A, Fridland A, Ray AS. Simultaneous quantitation of the nucleotide analog adefovir, its phosphorylated anabolites and 2′-deoxyadenosine triphosphate by ion-pairing LC/MS/MS. Journal of Chromatography B Analytical Technologies in the Biomedical and Life Sciences. 2007;**848**(2):335–343. DOI: 10.1016/j.jchromb.2006.10.063

[29] Machon C, Jordheim LP, Puy JY, Lefebvre I, Dumontet C, Guitton J. Fully validated assay for the quantification of endogenous nucleoside mono- and triphosphates using online extraction coupled with liquid chromatography-tandem mass spectrometry. Analytical and Bioanalytical Chemistry. 2014;**406**(12):2925–2941. DOI: 10.1007/s00216-014-7711-1

[30] Bähre H, Kaever V. Measurement of 2′,3′-cyclic nucleotides by liquid chromatography-tandem mass spectrometry in cells. Journal of Chromatography B Analytical Technologies in the Biomedical and Life Sciences. 2014;**964**:208–211. DOI: 10.1016/j.jchromb.2014.02.046

[31] Cordell RL, Hill SJ, Ortori CA, Barrett DA. Quantitative profiling of nucleotides and related phosphate-containing metabolites in cultured mammalian cells by liquid chromatography tandem electrospray mass spectrometry. Journal of Chromatography B Analytical Technologies in the Biomedical and Life Sciences. 2008;**871**(1):115–124. DOI: 10.1016/j.jchromb.2008.07.005

[32] Wu J, Zhang Y, Wiegand R, Wang J, Bepler G, Li J. Quantitative analysis of intracellular nucleoside triphosphates and other polar metabolites using ion pair reversed-phase liquid chromatography coupled with tandem mass spectrometry. Journal of Chromatography B Analytical Technologies in the Biomedical and Life Sciences. 2015;**1006**:167–178. DOI: 10.1016/j.jchromb.2015.10.030

[33] Cahours X, Tran TT, Mesplet N, Kieda C, Morin P, Agrofoglio LA. Analysis of intracellular didanosine triphosphate at sub-ppb level using LC-MS/MS. Journal of Pharmaceutical and Biomedical Analysis. 2001;**26**(5-6):819–827. DOI: 10.1016/S0731-7085(01)00457-5

[34] Goutier W, Spaans PA, van der Neut MAW, McCreary AC, Reinders JH. Development and application of an LC-MS/MS method for measuring the effect of (partial) agonists on cAMP accumulation in vitro. The Journal of Neuroscience Methods. 2010;**188**(1):24–31. DOI: 10.1016/j.jneumeth.2010.01.027

[35] Huang YF, Chang HT. Analysis of adenosine triphosphate and glutathione through gold nanoparticles assisted laser desorption/ionization mass spectrometry. Analytical Chemistry. 2007;**79**(13):4852–4859. DOI: 10.1021/ac070023x

[36] Oeckl P, Ferger B. Simultaneous LC-MS/MS analysis of the biomarkers cAMP and cGMP in plasma, CSF and brain tissue. The Journal of Neuroscience Methods. 2012;**203**(2):338–343. DOI: 10.1016/j.jneumeth.2011.09.032

[37] Zhang Y, Dufield D, Klover J, Li W, Szekely-Klepser G, Lepsy C, et al. Development and validation of an LC-MS/MS method for quantification of cyclic guanosine 3′,5′-monophosphate (cGMP) in clinical applications: A comparison with a EIA method. Journal of Chromatography B Analytical Technologies in the Biomedical and Life Sciences. 2009;**877**(5-6):513–520. DOI: 10.1016/j.jchromb.2008.12.063

[38] Dudley E, El-shakawi S, Games DE, Newton RP. Development of a purification procedure for the isolation of nucleosides from urine prior to mass spectrometric analysis. Nucleosides, Nucleotides and Nucleic Acids. March 2000;**19**(3):545–558. DOI: 10.1080/15257770008035006

[39] Pucci V, Giuliano C, Zhang R, Koeplinger KA, Leone JF, Monteagudo E, et al. HILIC LC-MS for the determination of 2′-C-methyl-cytidine-triphosphate in rat liver. Journal of Separation Science. May 2009;**32**(9):1275–1283. DOI: 10.1002/jssc.200800722

[40] Teleki A, Sánchez-Kopper A, Takors R. Alkaline conditions in hydrophilic interaction liquid chromatography for intracellular metabolite quantification using tandem mass spectrometry. Analytical Biochemistry. 15 April 2015;**475**:4–13. DOI: 10.1016/j.ab.2015.01.002

[41] Klawitter J, Schmitz V, Klawitter J, Leibfritz D, Christians U. Development and validation of an assay for the quantification of 11 nucleotides using LC/LC-electrospray ionization-MS. Analytical Biochemistry. 15 June 2007;**365**(2):230–239. DOI: 10.1016/j.ab.2007.03.018

[42] Rashidzadeh H, Bhadresa S, Good SS, Cohen ML, Gupta KS, Rush WR. Overcoming stability challenges in the quantification of tissue nucleotides: Determination of 2′-C-methylguanosine triphosphate concentration in mouse liver. Biological and Pharmaceutical Bulletin. 2015;**38**(3):380–388. DOI: 10.1248/bpb.b14-00565

[43] Bajad SU, Lu W, Kimball EH, Yuan J, Peterson C, Rabinowitz JD. Separation and quantitation of water soluble cellular metabolites by hydrophilic interaction chromatography-tandem mass spectrometry. The Journal of Chromatography A. 2006;**1125**(1):76–88. DOI: 10.1016/j.chroma.2006.05.019

[44] Edwards JL, Kennedy RT. Metabolomic analysis of eukaryotic tissue and prokaryotes using negative mode MALDI time-of-flight mass spectrometry. Analytical Chemistry. 2005;**77**(7):2201–2209. DOI: 10.1021/ac048323r

[45] Wang JM, Chu Y, Li W, Wang XY, Guo JH, Yan LL, et al. Simultaneous determination of creatine phosphate, creatine and 12 nucleotides in rat heart by LC-MS/MS. Journal of Chromatography B Analytical Technologies in the Biomedical and Life Sciences. 2014;**958**:96–101. DOI: 10.1016/j.jchromb.2014.03.008

[46] Bapiro TE, Richards FM, Goldgraben MA, Olive KP, Madhu B, Frese KK, et al. A novel method for quantification of gemcitabine and its metabolites 2′,2′-difluorodeoxyuridine and gemcitabine triphosphate in tumour tissue by LC-MS/MS: Comparison with 19F NMR spectroscopy. Cancer Chemotherapy Pharmacology. 2011;**68**(5):1243–1253. DOI: 10.1007/s00280-011-1613-0

[47] Luo B, Groenke K, Takors R, Wandrey C, Oldiges M. Simultaneous determination of multiple intracellular metabolites in glycolysis, pentose phosphate pathway and

tricarboxylic acid cycle by liquid chromatography-mass spectrometry. The Journal of Chromatography A. 2007;**1147**(2):153–164. DOI: 10.1016/j.chroma.2007.02.034

[48] Neufeld HA, Towner RD, Pace J. A rapid method for determining ATP by the firefly luciferin-luciferase system. Experientia. 1975;**31**(3):391–392

[49] Aherne GW, Hardcastle A, Raynaud F, Jackman AL. Immunoreactive dUMP and TTP pools as an index of thymidylate synthase inhibition; effect of tomudex (ZD1694) and a nonpolyglutamated quinazoline antifolate (CB30900) in L1210 mouse leukaemia cells. Biochemical Pharmacology. May 1996;**51**(10):1293–1301. DOI: 10.1016/0006-2952(96)00035-4

[50] Piall EM, Aherne GW, Marks V. The quantitative determination of 2′-deoxycytidine-5′-triphosphate in cell extracts by radioimmunoassay. Analytical Biochemistry. April 1986;**154**(1):276–281. DOI: 10.1016/0003-2697(86)90526-9

[51] Ohyama T, Matsubara C, Takamura K. Highly sensitive densitometry for sugarphosphoesters and nucleotides using enzymatic hydrolysis on a TLC plate. Chemical and Pharmaceutical bulletin. 1996;**44**(6):1252–1254

[52] Bezy V, Chaimbault P, Morin P, Unger SE, Bernard M-C, Agrofoglio LA. Analysis and validation of the phosphorylated metabolites of two anti-human immunodeficiency virus nucleotides (stavudine and didanosine) by pressure-assisted CE-ESI-MS/MS in cell extracts: Sensitivity enhancement by the use of perfluorinated acids and al. Electrophoresis. June 2006;**27**(12):2464–2476. DOI: 10.1002/elps.200500850

[53] Cai Z, Fung EN, Sinhababu AK. Capillary electrophoresis-ion trap mass spectrometry analysis of Ziagen and its phosphorylated metabolites. Electrophoresis. September 2003;**24**(18):3160–3164. DOI: 10.1002/elps.200305425

[54] Friedecký D, Tomková J, Maier VV, Janosťáková A, Procházka M, Adam TT, et al. Capillary electrophoretic method for nucleotide analysis in cells: Application on inherited metabolic disorders. Electrophoresis. February 2007;**28**(3):373–380. DOI: 10.1002/elps.200600262

[55] Soga T, Ishikawa T, Igarashi S, Sugawara K, Kakazu Y, Tomita M. Analysis of nucleotides by pressure-assisted capillary electrophoresis-mass spectrometry using silanol mask technique. The Journal of Chromatography A. 2007;**1159**(1-2):125–133. DOI: 10.1016/j.chroma.2007.05.054

[56] Liu CC, Huang JS, Tyrrell DLJ, Dovichi NJ. Capillary electrophoresis-electrospray-mass spectrometry of nucleosides and nucleotides: application to phosphorylation studies of anti-human immunodeficiency virus nucleosides in a human hepatoma cell line. Electrophoresis. April 2005;**26**(7-8):1424–1431. DOI: 10.1002/elps.200410423

[57] Derissen EJB, Jacobs BAW, Huitema ADR, Rosing H, Schellens JHM, Beijnen JH. Exploring the intracellular pharmacokinetics of the 5-fluorouracil nucleotides during capecitabine treatment. British Journal of Clinical Pharmacology. 2016;**81**(5):949–957. DOI: 10.1111/bcp.12877

[58] Faria M, Halquist MS, Kindt E, Li W, Karnes HT, O'Brien PJ. Liquid chromatography–tandem mass spectrometry method for quantification of thymidine kinase activity in human serum by monitoring the conversion of 3′-deoxy-3′-fluorothymidine to 3′-deoxy-3′-fluorothymidine monophosphate. The Journal of Chromatography B. 2012;**907**:13–20. DOI: 10.1016/j.jchromb.2012.08.024

[59] Jimmerson LC, Ray ML, Bushman LR, Anderson PL, Klein B, Rower JE, et al. Measurement of intracellular ribavirin mono-, di- and triphosphate using solid phase extraction and LC-MS/MS quantification. Journal of Chromatography B Analytical Technologies in the Biomedical and Life Sciences. 2015;**978-979**(C):163–172. DOI: 10.1016/j.jchromb.2014.11.032

[60] Kamčeva T, Bjånes T, Svardal A, Riedel B, Schjøtt J, Eide T. Liquid chromatography/tandem mass spectrometry method for simultaneous quantification of eight endogenous nucleotides and the intracellular gemcitabine metabolite dFdCTP in human peripheral blood mononuclear cells. The Journal of Chromatography B. September 2015;**1001**:212–220. DOI: 10.1016/j.jchromb.2015.07.041

[61] Mateos-Vivas M, Rodríguez-Gonzalo E, García-Gómez D, Carabias-Martínez R. Hydrophilic interaction chromatography coupled to tandem mass spectrometry in the presence of hydrophilic ion-pairing reagents for the separation of nucleosides and nucleotide mono-, di- and triphosphates. The Journal of Chromatography A. 2015;**1414**:129–137. DOI: 10.1016/j.chroma.2015.08.040

[62] Oeckl P, Steinacker P, Lehnert S, Jesse S, Kretzschmar HA, Ludolph AC, et al. Csf concentrations of camp and cgmp are lower in patients with creutzfeldt-jakob disease but not Parkinson's disease and amyotrophic lateral sclerosis. PLoS One. 2012;**7**(3):e32664. DOI: 10.1371/journal.pone.0032664

[63] Coolen EJCM, Arts ICW, Swennen ELR, Bast A, Stuart MAC, Dagnelie PC. Simultaneous determination of adenosine triphosphate and its metabolites in human whole blood by RP-HPLC and UV-detection. The Journal of Chromatography B. 15 March 2008;**864**(1-2):43–51. DOI: 10.1016/j.jchromb.2008.01.033

[64] Caruso R, Campolo J, Dellanoce C, Mariele R, Parodi O, Accinni R. Critical study of preanalytical and analytical phases of adenine and pyridine nucleotide assay in human whole blood. Analytical Biochemistry. 1 July 2004;**330**(1):43–51. DOI: 10.1016/j.ab.2004.03.063

[65] Yeung P, Ding L, Casley WL. HPLC assay with UV detection for determination of RBC purine nucleotide concentrations and application for biomarker study in vivo. Journal of Pharmaceutical and Biomedical Analysis. 9 June 2008;**47**(2):377–382. DOI: 10.1016/j.jpba.2008.01.020

[66] Czarnecka J, Cieślak M, Michał K. Application of solid phase extraction and high-performance liquid chromatography to qualitative and quantitative analysis of nucleotides and nucleosides in human cerebrospinal fluid. Journal of Chromatography B Analytical Technologies in the Biomedical and Life Sciences. 5 August 2005;**822**(1-2):85–90. DOI: 10.1016/j.jchromb.2005.05.026

[67] Huang D, Zhang Y, Chen X. Analysis of intracellular nucleoside triphosphate levels in normal and tumor cell lines by high-performance liquid chromatography. Journal of Chromatography B Analytical Technologies in the Biomedical and Life Sciences. 25 January 2003;**784**(1):101–109

[68] Losa R, Sierra M, Gion M, Esteban E, Buesa J. Simultaneous determination of gemcitabine di- and triphosphate in human blood mononuclear and cancer cells by RP-HPLC and UV detection. The Journal of Chromatography B. 7 August 2006;**840**(1):44–49. DOI: 10.1016/j.jchromb.2006.04.036

[69] Nishi R, Yamauchi T, Ueda T. A new, simple method for quantifying gemcitabine triphosphate in cancer cells using isocratic high-performance liquid chromatography. Cancer Science. November 2006;**97**(11):1274–1278. DOI: 10.1111/j.1349-7006.2006.00323.x

[70] Sparidans RW, Crul M, Schellens JH, Beijnen JH. Isocratic ion-exchange chromatographic assay for the nucleotide gemcitabine triphosphate in human white blood cells. The Journal of Chromatography B. 2002;**780**(2):423–430. DOI: 10.1016/S1570-0232(02)00638-4

[71] Yamauchi T, Ueda T. Simple and sensitive method for quantification of fludarabine triphosphate intracellular concentration in leukemic cells using isocratic liquid chromatography. Journal of Chromatography B Analytical Technologies in the Biomedical and Life Sciences. 5 January 2004;**799**(1):81–86

[72] Rodriguez CO, Plunkett W, Paff MT, Du M, Nowak B, Ramakrishna P, et al. High-performance liquid chromatography method for the determination and quantitation of arabinosylguanine triphosphate and fludarabine triphosphate in human cells. Journal of Chromatography B Biomedical Science and Applications. 18 August 2000;**745**(2):421–430. DOI: 10.1128/AAC.44.11.3097-3100.2000

[73] Haink G, Deussen A. Liquid chromatography method for the analysis of adenosine compounds. The Journal of Chromatography B. January 2003;**784**(1):189–193. DOI: 10.1016/S1570-0232(02)00752-3

[74] Andersson C-O, Sørensen P, Stenhagen E, Hartiala K, Veige S, Diczfalusy E. Mass spectrometric studies on amino acid and peptide derivatives. Acta Chemica Scandinavica. 1958;**12**:1353. DOI: 10.3891/acta.chem.scand.12-1353a

[75] Friedecký D, Bednar P, Prochazka M, Adam T. Analysis of intracellular nucleotides by capillary electrophoresis. Mass spectrometry. Nucleosides, Nucleotides and Nucleic Acids. 2006;**25**(9-11):1233–1236. DOI: 10.1080/15257770600894667

[76] Seifar RM, Ras C, van Dam JC, van Gulik WM, Heijnen JJ, van Winden WA. Simultaneous quantification of free nucleotides in complex biological samples using ion pair reversed phase liquid chromatography isotope dilution tandem mass spectrometry. Analytical Biochemistry. May 2009;**388**(2):213–219. DOI: 10.1016/j.ab.2009.02.025

[77] Williams L, Vontungeln L, Beland F, Doerge D. Liquid chromatographic–mass spectrometric determination of the metabolism and disposition of the anti-retroviral nucleoside analogs zidovudine and lamivudine in C57BL/6N and B6C3F1 mice. The Journal of Chromatography B. 5 December 2003;**798**(1):55–62. DOI: 10.1016/j.jchromb.2003.08.051

[78] King T, Bushman L, Anderson PL, Delahunty T, Ray M, Fletcher CV. Quantitation of zidovudine triphosphate concentrations from human peripheral blood mononuclear cells by anion exchange solid phase extraction and liquid chromatography-tandem mass spectroscopy; An indirect quantitation methodology. Journal of Chromatography B Analytical Technologies in the Biomedical and Life Sciences. 2006;**831**(1-2):248–257. DOI: 10.1016/j.jchromb.2005.12.033

[79] Inoue K, Obara R, Hino T, Oka H. Development and application of an HILIC-MS/MS method for the quantitation of nucleotides in infant formula. Journal of Agricultural and Food Chemistry. 22 September 2010;**58**(18):9918–9924. DOI: 10.1021/jf102023p

[80] Gouy M-H, Fabre H, Blanchin MD, Peyrottes S, Périgaud C, Lefebvre I. Quantification of 5′-monophosphate cytosine arabinoside (Ara-CMP) in cell extracts using liquid chromatography–electrospray mass spectrometry. Analytica Chimica Acta. 2006;**566**:178–184. DOI: 10.1016/j.aca.2006.02.058

[81] Crauste C, Lefebvre I, Hovaneissian M, Puy JY, Roy B, Peyrottes S, et al. Development of a sensitive and selective LC/MS/MS method for the simultaneous determination of intracellular 1-beta-d-arabinofuranosylcytosine triphosphate (araCTP), cytidine triphosphate (CTP) and deoxycytidine triphosphate (dCTP) in a human follicular l. Journal of Chromatography B Analytical Technologies in the Biomedical and Life Sciences. 2009;**877**(14-15):1417–1425. DOI: 10.1016/j.jchromb.2009.02.071

[82] Fromentin E, Gavegnano C, Obikhod A, Schinazi RF. Simultaneous quantification of intracellular natural and antiretroviral nucleosides and nucleotides by liquid chromatography-tandem mass spectrometry. Analytical Chemistry. 1 March 2010;**82**(5):1982–1989. DOI: 10.1021/ac902737j

[83] Carli D, Honorat M, Cohen S, Megherbi M, Vignal B, Dumontet C, et al. Simultaneous quantification of 5-FU, 5-FUrd, 5-FdUrd, 5-FdUMP, dUMP and TMP in cultured cell models by LC-MS/MS. Journal of Chromatography B Analytical Technologies in the Biomedical and Life Sciences. 2009;**877**(27):2937–2944. DOI: 10.1016/j.jchromb.2009.07.004

[84] Van Kampen JJA, Fraaij PLA, Hira V, Van Rossum AMC, Hartwig NG, De Groot R, et al. A new method for analysis of AZT-triphosphate and nucleotide-triphosphates. Biochemical and Biophysical Research Communications. 2004;**315**(1):151–159. DOI: 10.1016/j.bbrc.2004.01.032

[85] Shi G, Wu J, Li Y, Geleziunas R, Gallagher K, Emm T, et al. Novel direct detection method for quantitative determination of intracellular nucleoside triphosphates using weak anion exchange liquid chromatography/tandem mass spectrometry. Rapid Communications in Mass Spectrometry. 15 June 2002;**16**(11):1092–1099. DOI: 10.1002/rcm.684

[86] Hanai T. Separation of polar compounds using carbon columns. The Journal of Chromatography A. 14 March 2003;**989**(2):183–196

[87] Bapiro TE, Richards FM, Jodrell DI. Understanding the complexity of porous graphitic carbon (PGC) chromatography: Modulation of mobile-stationary phase interactions overcomes loss of retention and reduces variability. Analytical Chemistry. 21 June 2016;**88**(12):6190–6194. DOI: 10.1021/acs.analchem.6b01167

[88] Xing J, Apedo A, Tymiak A, Zhao N. Liquid chromatographic analysis of nucleosides and their mono-, di- and triphosphates using porous graphitic carbon stationary phase coupled with electrospray mass spectrometry. Rapid Communications in Mass Spectrometry. 30 July 2004;**18**(14):1599–1606. DOI: 10.1002/rcm.1524

[89] Jansen RS, Rosing H, Schellens JHM, Beijnen JH. Retention studies of 2′-2′-difluorodeoxycytidine and 2′-2′-difluorodeoxyuridine nucleosides and nucleotides on porous graphitic carbon: Development of a liquid chromatography-tandem mass spectrometry method. The Journal of Chromatography A. 2009;**1216**(15):3168–3174. DOI: 10.1016/j.chroma.2009.02.002

[90] Jansen RS, Rosing H, Schellens JHM, Beijnen JH. Simultaneous quantification of 2′,2′-difluorodeoxycytidine and 2′,2′-difluorodeoxyuridine nucleosides and nucleotides in white blood cells using porous graphitic carbon chromatography coupled with tandem mass spectrometry. Rapid Communications in Mass Spectrometry. 15 October 2009;**23**(19):3040–3050. DOI: 10.1002/rcm.4212

[91] Witters E, Van Dongen W, Esmans EL, Van Onckelen HA. Ion-pair liquid chromatography-electrospray mass spectrometry for the analysis of cyclic nucleotides. Journal of Chromatography B Biomedical Science and Applications. 20 June 1997;**694**(1):55–63

[92] Claire RL. Positive ion electrospray ionization tandem mass spectrometry coupled to ion-pairing high-performance liquid chromatography with a phosphate buffer for the quantitative analysis of intracellular nucleotides. Rapid Communications in Mass Spectrometry. 15 September 2000;**14**(17):1625–1634. DOI: 10.1002/1097-0231(20000915)14:17<1625:AID-RCM72>3.0.CO;2-0

[93] Hawkins T, Veikley W, St Claire RL, Guyer B, Clark N, Kearney BP. Intracellular pharmacokinetics of tenofovir diphosphate, carbovir triphosphate, and lamivudine triphosphate in patients receiving triple-nucleoside regimens. Journal of Acquired Immune Deficiency Syndromes. 2005;**39**(4):406–411. DOI: 10.1097/01.qai.0000167155.44980.e8

[94] Apffel A, Chakel JA, Fischer S, Lichtenwalter K, Hancock WS. New procedure for the use of high-performance liquid chromatography–electrospray ionization mass spectrometry for the analysis of nucleotides and oligonucleotides. The Journal of Chromatography A. 1997;**777**(7):3–21. DOI: 10.1021/ac960916h

[95] Auriola S, Frith J, Rogers MJ, Koivuniemi A, Mönkkönen J. Identification of adenine nucleotide-containing metabolites of bisphosphonate drugs using ion-pair liquid chromatography-electrospray mass spectrometry. Journal of Chromatography B Biomedical Applications. 1997;**704**(1-2):187–195. DOI: 10.1016/S0378-4347(97)00490-8

[96] Mönkkönen H, Moilanen P, Mönkkönen J, Frith JC, Rogers MJ, Auriola S. Analysis of an adenine nucleotide-containing metabolite of clodronate using ion pair high-performance liquid chromatography-electrospray ionisation mass spectrometry. Journal of Chromatography B Biomedical Science and Applications. 2000;**738**(2):395–403. DOI: 10.1016/S0378-4347(99)00559-9

[97] Tuytten R, Lemière F, Dongen WV, Esmans EL, Slegers H. Short capillary ion-pair high-performance liquid chromatography coupled to electrospray (tandem) mass spectrometry for the simultaneous analysis of nucleoside mono-, di- and triphosphates. Newton RP, editor. Rapid Communications in Mass Spectrometry. 30 June 2002;**16**(12):1205–1215. DOI: 10.1002/rcm.704

[98] Becher F, Pruvost A, Goujard C, Guerreiro C, Delfraissy J-F, Grassi J, et al. Improved method for the simultaneous determination of d4T, 3TC and ddl intracellular phosphorylated anabolites in human peripheral-blood mononuclear cells using high-performance liquid chromatography/tandem mass spectrometry. Rapid Communications in Mass Spectrometry. 30 March 2002;**16**(6):555–565. DOI: 10.1002/rcm.605

[99] Lee J, Yoo B-C, Lee H-S, Yoo H-W, Yoo H-H, Kang MJ, et al. Rapid quantitative determination of L-FMAU-TP from human peripheral-blood mononuclear cells of hepatitis B virus-infected patients treated with L-FMAU by ion-pairing, reverse-phase, liquid chromatography/electrospray tandem mass spectrometry. Therapeutic Drug Monitoring. February 2006;**28**(1):131–137

[100] Compain S, Durand-Gasselin L, Grassi J, Benech H. Improved method to quantify intracellular zidovudine mono- and triphosphate in peripheral blood mononuclear cells by liquid chromatography-tandem mass spectrometry. Journal of Mass Spectrometry. March 2007;**42**(3):389-404. DOI: 10.1002/jms.1176

[101] Hernandez-Santiago BI, Beltran T, Stuyver L, Chu CK, Schinazi RF. Metabolism of the anti-hepatitis C virus nucleoside β-D-N4-hydroxycytidine in different liver cells. Antimicrobial Agents and Chemotherapy. 2004;**48**(12):4636-4642. DOI: 10.1128/AAC.48.12.4636

[102] Tang D-Q, Zou L, Yin X-X, Ong CN. HILIC-MS for metabolomics: An attractive and complementary approach to RPLC-MS. Mass Spectrometry Reviews. September 2016;**35**(5):574-600. DOI: 10.1002/mas.21445

[103] Hsieh Y. Potential of HILIC-MS in quantitative bioanalysis of drugs and drug metabolites. Journal of Separation Science. 2008;**31**(9):1481-1491. DOI: 10.1002/jssc.200700451

[104] Karlíková R, Široká J, Friedecký D, Faber E, Hrdá M, Mičová K, et al. Metabolite profiling of the plasma and leukocytes of chronic myeloid leukemia patients. Journal of Proteome Research. 2 September 2016;**15**(9):3158-3166. DOI: 10.1021/acs.jproteome.6b00356

[105] Pesek JJ, Matyska MT, Hearn MTW, Boysen RI. Aqueous normal-phase retention of nucleotides on silica hydride columns. The Journal of Chromatography A. 2009;**1216**(7):1140-1146. DOI: 10.1016/j.chroma.2008.12.046

[106] Sun G, Yang K, Zhao Z, Guan S, Han X, Gross RW. Shotgun metabolomics approach for the analysis of negatively charged water-soluble cellular metabolites from mouse heart tissue shotgun metabolomics approach for the analysis of negatively charged water-soluble cellular metabolites from mouse heart tissue. Analytical Chemistry. 2007;**79**(17):6629-6640. DOI: 10.1021/ac070843

[107] Karlíková R, Široká J, Jahn P, Friedecký D, Gardlo A, Janečková H, et al. Equine atypical myopathy: A metabolic study. Veterinary Journal. 2016;**216**:125-132. DOI: 10.1016/j.tvjl.2016.07.015

[108] Ligasová A, Liboska R, Friedecký D, Mičová K, Adam T, Oždian T, et al. Dr Jekyll and Mr Hyde: A strange case of 5-ethynyl-2′-deoxyuridine and 5-ethynyl-2′-deoxycytidine. Open Biology. January 2016;**6**(1):150172. DOI: 10.1098/rsob.150172

Chapter 6

LC-HRMS for the Identification of β-Carboline and Canthinone Alkaloids Isolated from Natural Sources

Ana Claudia F. Amaral, Aline de S. Ramos,
José Luiz P. Ferreira, Arith R. dos Santos,
Jefferson D. da Cruz, Adélia Viviane M. De Luna,
Vinicius Vaz C. Nery, Iasmim C. de Lima,
Marcelo Henrique da C. Chaves and
Jefferson Rocha de A. Silva

Additional information is available at the end of the chapter

http://dx.doi.org/10.5772/68075

Abstract

β-carboline and canthinone alkaloids are widely distributed in the Angiosperms. Due to their diverse biological activities, the structures of these alkaloids have been used as important models for the synthesis of novel therapeutic drugs. Combining high-performance liquid chromatography (HPLC) with high-resolution mass spectrometry (HRMS) has provided a valuable tool in the analysis of these alkaloids in, for example, plants, insects, marine creatures, human tissues and body fluids. In this review, we summarized the main β-carboline and canthinone alkaloids studied by liquid chromatography high-resolution mass spectrometry (LC-HRMS) associated with mass analyzers, molecular weight information, mass fragmentation and biological activities, presenting an overview of increasing interest for carboline alkaloids study by LC-HRMS.

Keywords: chromatography, indole, mass analyzer, fragmentogram, biological activity, body samples

1. Introduction

Since ancient times, alkaloids have been used as medicine and in folk medicine for the treatment of different diseases. β-Carboline alkaloids are a group of natural indole alkaloids with different degrees of aromaticity widely distributed in the Angiosperms [1–61]. Canthinones

INTECH
open science | open minds

© 2017 The Author(s). Licensee InTech. This chapter is distributed under the terms of the Creative Commons Attribution License (http://creativecommons.org/licenses/by/3.0), which permits unrestricted use, distribution, and reproduction in any medium, provided the original work is properly cited. CC BY

are β-carboline alkaloids that have an additional ring-fusion. Analysis of these alkaloids may be realized by combination of liquid chromatography-high-resolution mass spectrometry (LC-HRMS/MS) to produce information about metabolites contained in complex natural source samples. The LC-HRMS is commonly used as choice technique to analyze and elucidate β-carboline and canthinone alkaloids of the extract mixture and that fact will be approached in this review together with other topics described below.

2. Source of β-carboline and canthinone alkaloids

In the plant kingdom, β-carboline and canthinone alkaloids are mainly found in Angiosperms, predominantly in Simaroubaceae, Rubiaceae, Rutaceae, Apocynaceae, Amaranthaceae, Annonaceae, Zygophyllaceae and Passifloraceae families [1–61]. **Table 1** shows the alkaloids of these two classes and their natural sources. These alkaloids have been obtained mainly in the studies of isolation of chemical constituents from a natural source, chromatographic LC-HRMS analyses and biological studies.

Alkaloid	Species	Refs.
Annomontine	Annonaceae: *Annona foetida* Mart., *A. montana* Macf., *A. purpurea* Moc & Sessé ex Dunal, *A. reticulata* L.	[1–3]
Brunneins A–C	Cortinariaceae: *Cortinarius brunneus*(Pers.) Fr.	[4]
Canthin-2,6-dione	Simaroubaceae: *Simaba multiflora* A. Juss., *S. polyphylla* (Cavalcante) W.W. Thomas	[5, 6]
Canthin-6-one	Amaranthaceae: *Aerva lanata* (L.) A.L. Juss. ex Schultes; Rutaceae: *Fagara mayu* (Bert.) Engl., *F. viridis* A. Chev., *F. zanthoxyloides* Lam., *Pentaceras australis* Hook. F., *Phellodendron amurense* Rup., *Zanthoxylum belizense* Lundell, *Z. chiloperone* var. *angustifolium* (Engl.), *Z. coreanum* Nakai, *Z. dipetalum* H. Mann, *Z. elephantiasis* Macfad., *Z. flavum* Vahl, *Z. ovalifolium* Tutcher, *Z. suberosum* C.T. White; Simaroubaceae: *Ailanthus altissima* Swingle, *A. excelsa* Roxb., *Brucea antidysenterica* J.F. Mill., *Eurycoma harmandiana* Pierre, *E. longifolia* Jack, *Hannoa chlorantha* Engl. & Gilg., *H. klaineana* Pierre & Engl., *Odyendea gabonensis* (Pierre) Engler, *Picrasma crenata* Engl. in Engl. & Prantl	[6–24]
Canthin-6-one-3-N-oxide	Rutaceae: *Zanthoxylum chiloperone* var. *angustifolium* (Engl.); Simaroubaceae: *Ailanthus altissima* Swingle, *Eurycoma harmandiana* Pierre, *Hannoa chlorantha* Engl. & Gilg., *Simarouba berteroana* Krug & Urban	[6, 8, 11, 13, 14, 17, 25]
Canthin-6-one-9-methoxy-5-*O*-β-D-glucopyranoside	Simaroubaceae: *Simarouba berteroana* Krug & Urban	[25]
β-Carboline-1-propionic acid	Amaranthaceae: *Aerva lanata* (L.) A.L. Juss. ex Schultes; Rutaceae: *Zanthoxylum chiloperone* var. *angustifolium* (Engl.); Simaroubaceae: *Eurycoma harmandiana* Pierre, *Simarouba berteroana* Krug & Urban	[9, 17, 25]
(E)-O-(6′)-Cinnamoyl-4″-hydroxy-3″, 5″-dimethoxy-lyaloside	Rubiaceae: *Psychotria suterella* Müll. Arg., *P. laciniata* Vell.	[26–28]
Deppeaninol	Rubiaceae: *Deppea blumenaviensis* (K. Schum.) Lorence	[29]
4,5-Dihydrocanthin-6-one	Simaroubaceae: *Ailanthus altissima* Swingle	[21]

Alkaloid	Species	Refs.
1,11-Dimethoxycanthin-6-one	Simaroubaceae: *Brucea antidysenterica* J.F. Mill., *Picrasma quassioides* (D. Don) Benn., *Soulamea pancheri* Brongn. & Gris	[21]
4,5-Dimethoxycanthin-6-one	Simaroubaceae: *Odyendea gabonensis* (Pierre) Engler; *Picrasma quassioides* (D. Don) Benn., *Picrolemma granatensis*, *Quassia africana* (Baill.) Baill.	[21, 22, 30–33]
5,9-Dimethoxycanthin-6-one	Simaroubaceae: *Eurycoma longifolia* Jack	[24]
9,10-Dimethoxycanthin-6-one	Simaroubaceae: *Eurycoma harmandiana* Pierre	[17]
Eudistomin G, H, I, P, R, S, T	Polycitoridae: *Eudistoma olivaceum* Van Name	[34]
Eurycomine E	Simaroubaceae: *Picrasma quassioides* (D. Don) Benn.,	[35]
11-O-β-D-Glucopyranosylcanthin-6-one	Simaroubaceae: *Eurycoma longifolia* Jack	[24]
10-O-β-D-Glucopyranosyloxycanthin-6-one	Amaranthaceae: *Aerva lanata* (L.) A.L. Juss. ex Schultes	[9]
1-(2-Guanidinoethyl)-1,2,3,4-tetrahydro-3-(hydroxymethyl)-β-carboline	Nephilidae: *Nephila clavipes* L.	[23]
Harmaline	Malvaceae: *Grewia bicolor* Juss.; Passifloraceae: *Passiflora edulis* f. *flavicarpa* O. Deg., *P. incarnata* L.; Zygophyllaceae: *Peganum harmala* L. *Tribulus terrestris* L.	[36–39]
Harmalol	Zygophyllaceae: *Peganum harmala* L.	[36]
Harmane	Ciidae: *Coriolus maximus* (Mont.) Murrill Malvaceae: *Grewia bicolor* Juss; Passifloraceae: *Passiflora edulis* f. *flavicarpa* O. Deg., *P. incarnata* L.; Tricholomataceae: *Hygrophorus eburneus* (Bull.) Fr.; Zygophyllaceae: *Tribulus terrestris* L.	[4, 37–39]
Harmicine	Apocynaceae: *Kopsia griffithii* King & Gamble	[40, 41]
Harmine	Malpighiaceae: *Banisteriopsis caapi* (Spruce ex Griseb.) Morton; Malvaceae: *Grewia bicolor* Juss.; Passifloraceae: *Passiflora edulis* f. *flavicarpa* O. Deg., *P. incarnata* L.; Zygophyllaceae: *Tribulus terrestris* L.; *Peganum harmala* L.	[36–39]
Harmol	Passifloraceae: *Passiflora edulis* f. *flavicarpa* O. Deg.; Zygophyllaceae: *Peganum harmala* L.	[36, 37]
N-Hydroxyannomontine	Annonaceae: *Annona foetida* Mart.	[1, 2]
10-Hydroxy-antirhine	Apocynaceae: *Ochrosia alyxioidis* Guillaumin; Rubiaceae: *Psychotria prunifolia* (Kunth) Steyerm.	[29]
10-Hydroxy-antirhine N-oxide	Rubiaceae: *Psychotria prunifolia*(Kunth) Steyerm.	[29]
1-Hydroxycanthin-6-one	Simaroubaceae: *Ailanthus altissima* Swingle, *Hannoa chlorantha* Engl. & Gilg.	[8, 11]
11-Hydroxycanthin-6-one	Simaroubaceae: *Ailanthus altissima* Swingle	[18]
8-Hydroxycanthin-6-one	Simaroubaceae: *Hannoa chlorantha* Engl. & Gilg., *Odyendea gabonensis* (Pierre) Engler	[11, 22]
9-Hydroxycanthin-6-one	Simaroubaceae: *Ailanthus altissima* Swingle, *Eurycoma harmandiana* Pierre, *Picrolemma granatensis*, *Simarouba berteroana* Krug & Urban	[17, 18, 25, 31]

Alkaloid	Species	Refs.
10-Hydroxycanthin-6-one (aervine)	Amaranthaceae: *Aerva lanata* (L.) A.L. Juss. ex Schultes; Simaroubaceae: *Ailanthus altissima* Swingle; *Hannoa chlorantha* Engl. & Gilg.	[9, 11, 18]
11-Hydroxycanthin-6-one-N-oxide	Simaroubaceae: *Simarouba berteroana* Krug & Urban	[25]
9-Hydroxycanthin-6-one-N-oxide	Simaroubaceae: *S. berteroana*	[25]
(R)-5-(1-Hydroxyethyl)-canthine-6-one	Simaroubaceae: *Ailanthus altissima* Swingle	[18]
10-hydroxy-iso-deppeaninol	Rubiaceae: *Psychotria prunifolia* (Kunth) Steyerm.	[29]
1-Hydroxy-11-methoxycanthin-6-one	Simaroubaceae: *Eurycoma longifolia* Jack	[24]
10-Hydroxy-9-methoxycanthin-6-one	Simaroubaceae: *E. longifolia*	[21, 24]
11-Hydroxy-1-methoxycanthin-6-one	Simaroubaceae: *E. longifolia*	[21]
11-Hydroxy-10-methoxycanthin-6-one	Simaroubaceae: *E. longifolia*	[24]
5-Hydroxy-4-methoxycanthin-6-one (nigakinone)	Simaroubaceae: *Picrasma excelsa* (SW.) Planch. *Picrasma quassioides* (D. Don) Benn.	[21, 30, 32, 33, 42, 43]
8-Hydroxy-9-methoxycanthin-6-one	Simaroubaceae: *Picrolemma granatensis*, *Simarouba berteroana* Krug & Urban	[25, 31]
8-Hydroxymanzamine A	Petrosiidae: *Acanthostrongylophora ingens* (Thiele); Phloeodictyidae: *Pachypellina* sp.	[44, 45]
6-Hydroxymetatacarbolines A, B, C, D, E, F, G, H, I	Mycenaceae: *Mycena metata* (Fr.) Kumm.	[4]
1-(Hydroxymethyl)-3-(2-hydroxypropan-2-yl)-2-(5-methoxy-9H-β-carbolin-1-yl) cyclopentanol	Rubiaceae: *Galianthe thalictroides* (K. Schum.) E.L. Cabral	[46]
Isovallesiachotamine	Rubiaceae: *Chimarrhis turbinata* DC., *Palicourea rigida* Kunth, *Psychotria bahiensis* DC., *P. suterella* Müll. Arg., *P. laciniata* Vell.	[27]
Lyaloside	Rubiaceae: *Ophiorrhiza japonica* Blume, *Psychotria suterella* Müll. Arg., *P. laciniata* Vell., *Pauridiantha lyalli* (Baker) Bremek., *Uncaria tomentosa* (Willd. ex Schult.) DC., *Palicourea adusta* Standley	[26–28]
Manzamine A	Petrosiidae: *Acanthostrongylophora ingens* (Thiele)	[44]
Metatacarbolines A, B, C, D, E, F, G	Mycenaceae: *Mycena metata* (Fr.) Kumm.	[4]
Methoxyannomontine	Annonaceae: *Annona impressivenia* Safford, *A. Montana* Macf., *A. reticulate* L.; Lauraceae: *Neolitsea Konishii* (H.) Kan & Sas	[2]
3-Methoxycanthin-2,6-dione	Simaroubaceae: *Simaba cuspidata* Spruce ex Engl., S. *multiflora* A. Juss.	[21, 47]
1-Methoxycanthin-6-one	Simaroubaceae: *Ailanthus altissima* Swingle, *Hannoa chlorantha* Engl. & Gilg.	[8, 11]
10-Methoxycanthin-6-one (methylaervine)	Amaranthaceae: *Aerva lanata* (L.) A.L. Juss. ex Schultes	[9]

Alkaloid	Species	Refs.
4-Methoxycanthin-6-one	Amaranthaceae: *Charpentiera obovata* Gaudich.	[6, 48]
5-Methoxycanthin-6-one	Rutaceae: *Zanthoxylum caribaeum* Lam., *Z. chiloperone* var. *angustifolium*(Engl.), Simaroubaceae: *Leitneria floridana* Chapm., *Odyendea gabonensis* (Pierre) Engler	[6, 10, 12–14, 22, 49]
9-Methoxycanthin-6-one	Simaroubaceae: *Eurycoma longifolia* Jack, *Picrolemma granatensis*, *Simaba polyphylla* (Cavalcante) W.W. Thomas, *Simarouba berteroana* Krug & Urban	[5, 17, 25, 31, 50]
9-Methoxycanthin-6-one-3-N-oxide	Simaroubaceae: *Picrolemma granatensis*	[31]
7-Methoxy-β-carboline-1-propionic acid	Simaroubaceae: *Eurycoma harmandiana* Pierre	[17]
1-Methoxycarbonyl-β-carboline	Simaroubaceae: *Picrasma quassioides* (D. Don) Benn.	[42]
9-Methoxy-3-methylcanthin-5,6-dione	Simaroubaceae: *Eurycoma longifolia* Jack	[50]
1-Methoxymethyl-β-carboline	Simaroubaceae: *E. longifolia*	[24]
3-Methylcanthin-2,6-dione	Simaroubaceae: *Picrasma quassioides* (D. Don) Benn.	[30, 42]
N-Methyltetrahydro-β-carboline	Amaranthaceae: *Arthrophytum leptocladum* M. Pop. ex Iljin, *Cyathobasis fruticulosa* (Bunge) Aellen, *Hammada leptoclada* Iljin; Elaeagnaceae: *Elaeagnus angustifolia* L.; Leguminosae: *Acacia simplicifolia* (L.f.) Schinz & Guillaumin, *Anadenanthera peregrina*(L.) Speg.; Malpighiaceae: *Banisteriopsis rusbyana* (Nied.) Morton; Myristicaceae: *Gymnacranthera paniculata* (A.DC.) Warb., *Virola sebifera* Aubl., *Virola theiodora* (Spruce ex Benth. Warb.; Phyllanthaceae: *Flueggea microcarpa* Blume; Poaceae: *Phalaris aquatica* L.; Rubiaceae: *Psychotria carthagenensis* Jacq.; *Psychotria viridis* Ruiz & Pav.; Ochnaceae: *Testulea gabonensis* Pellegr.	[8, 51, 52]
Mitragynine	Rubiaceae: *Mitragyna speciosa* Korth	[53]
Norharmane	Tricholomataceae: *Hygrophorus eburneus* (Bull.) Fr.	[54]
14-Oxoprunifoleine	Rubiaceae: *Psychotria prunifolia* (Kunth) Steyerm.	[29, 55]
Paymantheine	Rubiaceae: *Mitragyna speciosa* Korth	[53]
Picrasidine L (3-methylcanthin-5,6-dione)	Simaroubaceae: *Eurycoma longifólia* Jack, *Picrasma quassioides* (D. Don) Benn., *Quassia amara* L.	[21, 50]
Picrasidine N, M, U, W, X, Y	Simaroubaceae: *Picrasma quassioides* (D. Don) Benn.	[21]
Picrasidine O	Simaroubaceae: *Eurycomma longifólia* Jack, *Picrasma quassioides* (D. Don) Benn.	[21, 35]
Picrasidine P, V	Simaroubaceae: *P. quassioides*	[56]
Picrasidine Q (4-hydroxy-5-methoxycanthin-6-one)	Simaroubaceae: *P. quassioides*	[33]
Psychollatine	Rubiaceae: *Psychotria umbellate* Thonn.	[27]
Reserpine	Apocynaceae: *Rauvolfia hookeri* S.R. Sriniv. & Chithra, *R. micrantha* Hook. f., *R. serpentina* (L.) Benth. ex Kurz, *R.tetraphylla* L., *R. verticillata* (Lour.) Baill., *R. vomitoria* Afzel	[57]
Speciogynine	Rubiaceae: *M. speciosa*	[53]
Strictosamide	Rubiaceae: *Psychotria nuda* (Cham. et Schltdl) Wawra, *P. suterella* Müll. Arg., *P. laciniata* Vell., *P. prunifolia* (Kunth) Steyerm.	[27, 29, 55, 58]

Alkaloid	Species	Refs.
Strictosidinic acid	Rubiaceae: *Psychotria umbellate* Thonn.	[27]
1,2,3,4-Tetrahydro-β-carboline-3-carboxylic acid	Asteraceae: *Cichorium endivia* L.	[60]
Tetrahydroharmine	Malpighiaceae: *Banisteriopsis caapi* (Spruce ex Griseb.) Morton; Zygophyllaceae: *Peganum harmala* L.	[36, 59]
Vallesiachotamine	Rubiaceae: *Chimarrhis turbinata* DC., *Palicourea rigida* Kunth, *Psychotria bahiensis* DC., *P. suterella* Müll. Arg., *P. laciniata* Vell.	[27]
Yohimbine	Apocynaceae: *Aspidosperma discolor*A. DC., *A. excelsum* Benth, *A. eburneum* F. Allem, *A. marcgravianum* Woodson, *A. oblongum*A. DC.	[61]

Table 1. Natural sources of some β-carboline and canthinone alkaloids.

3. Alkaloids and biological activity

Many pharmacological properties attributed to β-carboline alkaloids have been described in the literature, which makes it an important class of natural products. Among them, antimalarial, antileishmanial, trypanocidal, antibacterial and antitumor activities are described [38, 44, 62]. The alkaloids described below have studies of LC-HRMS.

A search for antimalarial drugs describes the activity of the alkaloids (+)-8-hydroxymanzamine A and (+)-manzamine A against chloroquine-sensitive D6 and chloroquine-resistant W2 strains of *Plasmodium falciparum*, with half maximal inhibitory concentration (IC_{50}) of 19.5 and 22.0 ng/mL for (+)-8-hydroxymanzamine A, and selectivity index (SI) of 40 and 35, respectively. For (+)-manzamine A, the IC_{50} values are 20.8 and 25.8 ng/mL, with SI of 47 and 38, respectively [44]. Canthin-6-one and 5-methoxycanthin-6-one, isolated from stem bark of *Zanthoxylum chiloperone* var. *angustifolium*, have IC_{50} values on chloroquine/mefloquine-resistant and sensitive strains of *P. falciparum* of 2.0–5.3 and 5.1–10.4 μg/mL, respectively [10].

The β-carboline alkaloids harmane, harmine and harmaline have been reported to possess antileishmanial activity. Harmane, harmine and harmaline have activity against the amastigote forms of *Leishmania infantum*, with IC_{50} values of 0.27, 0.23 and 1.16 μM, respectively. The harmane and harmaline activities against promastigote forms are less pronounced, with IC_{50} values of 19.2 and 116.8 μM, respectively. Harmine inhibits promastigotes with IC_{50} of 3.7 μM [39]. Strictosamide, alkaloid glycoside isolated from the crude ethanol extracts of roots and branches of *Psychotria prunifolia*, has *in vitro* antiprotozoal activity, especially against promastigotes of *Leishmania amazonensis*, with IC_{50} values of 40.7 μg/mL [29]. The alkaloid (+)-8-hydroxymanzamine A has activity against *Leishmania donovani* with $IC_{50}$of 2.5 mg/mL and $IC_{90}$of 6.1 mg/mL, whereas (+)-manzamine A is less active, with IC_{50} of 11.15 mg/mL and IC_{90} of 31.05 mg/mL [44]. Canthin-6-one, isolated from dichloromethane extract of *Z. chiloperone* stem bark, has antileishmanial activity in BALB/c mice infected with *L. amazonensis*. The intralesional treatment with canthin-6-one is able to decrease by 15.0% a lesion weight and the parasite load by 77.6% when compared with the group of untreated mice [12].

Canthin-6-one also has trypanocidal activity. The alkaloid can provoke 90% of anti-amastigote activity and 79% of trypomastigotes lysis in assays using *Trypanosoma cruzi.* The alkaloid

http://dx.doi.org/10.5772/68075

5-methoxy-canthin-6-one, isolated from the leaves of the same species, is able to cause 66.4% of anti-amastigote activity and 75% of trypomastigotes lysis [14]. Harmine also has trypanocidal effect against *Trypanosoma brucei*, with IC_{50} of 74 μM [13].

The β-carboline alkaloids have antiproliferative effects against many tumor cell lines. The mechanism of action is probably associated with DNA intercalation, inhibition of topoisomerase I and II, cyclin-dependent kinase (CDK), and IkB kinase complex [40, 62]. In cytotoxicity assays with (+)-8-hydroxymanzamine A and (+)-manzamine A, the IC_{50} are, respectively, 0.47 and 1.0 μg/mL against SK-MEL (human malignant melanoma); 0.78 and 1.0 KB μg/mL against KB (human epidermoid carcinoma); 0.75 and 1.1 μg/mL against BT-549 (human breast ductal carcinoma); 0.51 and 4.40 μg/mL against $HepG_2$ (human hepatocellular carcinoma); and 1.25 and 2.15 μg/mL against LLC-PK_{11}(pig kidney epithelial cells) [44]. Canthin-6-one has in vitro cytotoxicity against many cell lines, such as CHO (IC_{50} = 7.529 μM/mL), HepG2 (IC_{50} = 4.551 μM/mL), HeLa (IC_{50} = 14.9 μM/mL), the human epidermoid carcinoma cell line A-431 (IC_{50} = 8.393 μM/mL), the human breast cancer cell line MCF-7 (IC_{50} = 5.541 μM/mL) [9] and MRC5 (fibroblasts) (IC_{50} = 12.1 μg/mL) [10]. The alkaloid 9-methoxy-canthin-6-one has high in vitro cytotoxicity in MCF-7 and A-549 cells (adenocarcinomic human alveolar basal epithelial cells), with IC_{50} of 4.5 and <2.5 μg/mL, respectively [63].

Antimicrobial activity has also been related to this class of compounds. The alkaloids (+)-8-hydroxymanzamine A and (+)-manzamine A are more potent as antimycobacterial than the control ciprofloxacin, with IC_{50} values of 0.13 and 0.36 μg/mL against *Mycobacterium intracellulare* vs. 0.48 μg/mL of ciprofloxacin. However, both substances were inactive against the filamentous fungus *Aspergillus fumigatus* and the Gram-negative bacteria *Escherichia coli* and *Pseudomonas aeruginosa* [44].

Canthin-6-one, 9-hydroxycanthin-6-one and 10-hydroxycanthin-6-one show active in the anti-inflammatory assays involving LPS-induced nitric oxide (NO), a proinflammatory mediator, in RAW 264.7 cells (murine macrophage from blood) with IC_{50} values ranging from 7.73 to 15.09 μM [64].

4. Ionization source and mass analyzers

An analysis of a sample comprises ionization where the ion beam is accelerated by an electric field and then a mass analyzer, a region of the mass spectrometer where the ions are separated according to their mass/charge ratio (m/z) [65].

There are many different ionization methods, such as ESI, APCI, FAB, suitable for different applications. Many types of mass analyzers are used according to the type and objectives of the analysis: e.g., dual focus, quadrupole, ion trap, time-of-flight (TOF), Orbitrap and Fourier transform ion cyclotron resonance (FT-ICR) mass analyzers are the magnetic sectors [66]. According to this review, the most used mass analyzers for the analysis of β-carbonyl and canthinone alkaloids are the quadrupole, ion trap, TOF and Orbitrap. The most articles reported TOF as the most used analyzer followed by Orbitrap. TOF is based on the simple idea that the speed of two ions created at the same instant with the same kinetic energy will vary according to the mass of the ion (the lighter ion will be faster), when traveling against

the mass spectrometer detector. The main characteristics are as follows: simultaneous analysis of all produced ions, high sensitivity and high mass resolution, which requires very fast data acquisition and detection systems. An Orbitrap mass analyzer is an ion trap comprising a barrel type electrode and an inner coaxial electrode similar to a reel holding the ions in an orbital motion inside the trap [66].

Table 2 presents some LC-HRMS data analysis used to identify β-carboline and canthinone alkaloids. These alkaloids are listed in **Table 1** and have publications demonstrating analyses by LC-HRMS.

Name	Ionization source and mode	Mass analyzer	Found mass $[M+H]^+$	Refs.
Brunnein A	ESI+	FT-ICR	245.0919	[54]
Canthin-6-one	ESI+	Triple QTOF	221.0707	[24]
Canthin-6-one-3N-oxide	ESI+	Triple QTOF	237.0658	[24]
β-Carboline-1-propionic acid	ESI+	Triple QTOF	241.0973	[24]
5,9-Dimethoxycanthin-6-one	ESI+	Triple QTOF	281.0913	[24]
9,10-Dimethoxycanthin-6-one	ESI+	Triple QTOF	281.0913	[24]
11-O-β-D-Glucopyranosylcanthin-6-one	ESI+	Triple QTOF	399.1202	[24]
1-(2-Guanidinoethyl)-1,2,3,4-tetrahydro-3-(hydroxymethyl)-β-carboline	ESI+	Triple QTOF	288.1824	[23]
Harmane	ESI+	FT-ICR	183.09152	[54]
11-Hydroxy-10-methoxycanthin-6-one	ESI+	Triple QTOF	267.0752	[24]
1-Hydroxy-11-methoxycanthin-6-one	ESI+	Triple QTOF	267.0752	[24]
5-Hydroxy-4-methoxycanthin-6-one	ESI+	QTOF	267.0758	[43]
10-Hydroxy-9-methoxycanthin-6-one	ESI+	Triple QTOF	267.0752	[24]
10-Hydroxy-antirhine	ESI+	Synapt HDMS	313.1920	[29]
10-Hydroxyantirhine N-oxide derivative	ESI-	Synapt HDMS	327.1712	[29]
11-Hydroxycanthin-6-one	ESI+	Triple QTOF	237.0658	[24]
(*R*)-5-(1-Hydroxyethyl)-canthine-6-one	DART-SVP+	AccuTOF-TLC	265.1006	[18]
10-Hydroxy-iso-deppeaninol	ESI+	Synapt HDMS	327.1693	[29]
(+)-8-Hydroxymanzamine A	ESI+	FT	565.3608	[44]
(+)-8-Hydroxymanzamine A hydrochloride	ESI+	FT	565.3560	[44]

Name	Ionization source and mode	Mass analyzer	Found mass $[M+H]^+$	Refs.
6-Hydroxymetatacarboline A	ESI+	Orbitrap	398.1348	[4]
6-Hydroxymetatacarboline B	ESI+	Orbitrap	526.1934	[4]
6-Hydroxymetatacarboline C	ESI+	Orbitrap	485.1668	[4]
6-Hydroxymetatacarboline D	ESI/MALDI+	Orbitrap	499.1828	[4]
6-Hydroxymetatacarboline E	ESI+	Orbitrap	469.1721	[4]
6-Hydroxymetatacarboline F	ESI+	Orbitrap	497.2032	[4]
6-Hydroxymetatacarboline G	ESI+	Orbitrap	511.2192	[4]
6-Hydroxymetatacarboline H	ESI+	Orbitrap	545.2031	[4]
6-Hydroxymetatacarboline I	ESI+	Orbitrap	511.2192	[4]
7-Hydroxy-β-carboline-1-propionic acid	ESI+	Triple QTOF	257.0915	[24]
Isovallesiachotamine	ESI+	TOF	351.1696	[27]
Lyaloside	ESI+	TOF	527.1982	[27]
(+)-8-Manzamine A	ESI+	FT	549.3592	[44]
(+)-Manzamine A hydrochloride	ESI+	FT	549.3550	[44]
Metatacarboline A	ESI+	Orbitrap	382.1398	[4]
Metatacarboline B	ESI+	Orbitrap	510.1987	[4]
Metatacarboline C	ESI+	Orbitrap	469.1721	[4]
Metatacarboline D	ESI+	Orbitrap	483.1879	[4]
Metatacarboline E	ESI+	Orbitrap	453.1770	[4]
Metatacarboline F	ESI+	Orbitrap	481.2084	[4]
Metatacarboline G	ESI+	Orbitrap	495.2241	[4]
9-Methoxy-3-methylcanthin-5,6-dione	ESI+	Triple QTOF	281.0913	[24]
9-Methoxycanthin-6-one	ESI+	Triple QTOF	251.0817	[24]
9-Methoxycanthin-6-one-3N-oxide	ESI+	Triple QTOF	269.0811	[24]
1-Methoxymethyl-β-carboline	ESI+	Triple QTOF	213.0990	[24]
Norharmane	ESI+	FT-ICR	169.0760	[54]
Speciogynine	ESI+	Orbitrap	399.22766	[53]
Strictosamide	ESI+	TOF	499.2083	[27]
1,2,3,4-Tetrahydro-β-carboline-3-carboxylic acid	ESI+	QTOF	217.0963	[67]
Vallesiachotamine	ESI+	TOF	351.1696	[27]
Yohimbine	ESI+	Quadrupole-Orbitrap	355.2016	[68]

Table 2. LC-HRMS data of β-carboline and canthinone alkaloids.

5. Mass fragmentograms

The observed masses of the fragments in LC-HRMS of the main cited β-carboline and canthinone alkaloids are shown below (**Figure 1**). The principal peaks are shown in the fragmentograms below. The fragments are based on characteristic alkaloid breaks and/or proposals based on mass spectrometry theory.

Figure 1. Fragmentogram of β-carboline and canthinone alkaloids.

http://dx.doi.org/10.5772/68075

6. Advantages and disadvantages of the LC-HRMS as analytical tool

The natural product research requires the development of fast and robust techniques for the difficult identification of substances in samples of plant extracts. Actually, GC-MS and LC-MS/MS are more used techniques than LC-HRMS for the identification of plant metabolites. However, the advantages of LC-HRMS and the chemical complexity of plant extracts can justify the investment in that newer technique.

Compared with gas chromatography (GC), techniques involving liquid chromatography (LC) have the advantage of being applicable to a wider variety of chemical classes of compounds. In GC, the analytes must be in gaseous form, and some substances must be hydrolyzed or derivatized to lower polarity and increase volatility to be analyzed. In LC, the analytes must be soluble in the liquid mobile phase and works well with polar substances. LC-MS/MS also has higher sensitivity than GC-MS [65, 69].

GC-MS has a single quadrupole mass detector, whereas LC-MS/MS has two quadrupole detectors in tandem. In MS/MS, only one ion from the first detector, frequently the molecular ion is fragmented in the second detector. The selected-ion monitoring (SIM) mode can be applied for GC-MS to increase sensibility and consists of the selection of three of the more abundant ions from the mass spectrum to be measured by the spectrometer and the comparison between the abundance relative ratio of these ions with the predetermined ratio for the suspect substance. The presence of contaminants affects the ion ratio hinders the identification. The selected reaction monitoring (SRM) mode is applied for LC-MS/MS and consists of the selection of some ions fragmented in the second detector. Thus, LC-MS/MS has more specificity than GC-MS, because two substances with the same nominal mass will exhibit different fragmentations in the second detector. Therefore, SIM or SRM is suitable only for targeted substances. GC-MS and LC-MS/MS can also be employed for the analyses of unknown compounds, but only in the full-scan MS mode and with lower sensitivity. Both GC-MS and LC-MS/MS have resolution of 1 atomic mass unit (amu) [65].

The LC-HRMS has the characteristics of the accurate mass measurement of the analytes, which confers many advantages as compared to other techniques of analysis traditionally used. The mass resolution is about 2 ppm, which represents an error of 0.0006 amu for substances of 300 amu [65]. The exact molecular ion mass is associated with an exact molecular formula of the analyte, a valuable structural information. The exact mass is a calculated parameter, while other techniques depend on experimental results for comparison. Therefore, the main advantage of LC-HRMS is that it allows the identification of a wider number of analytes, including unexpected substances in the sample, and does not require reference standards or preexisting MS libraries for comparison [70]. Additionally, LC-TOF/MS can be applied to a larger range of molecular masses (up about 20,000 amu), while LC-MS/MS is indicated for substances up to about 3000 amu [65].

Besides the high mass resolution, the LC-HR/MS has other important advantages. A previous chromatographic treatment of the sample is not required, and a robust method for qualitative analysis can be applied for different and unknown samples, even for the identification of minority substances. Thus, analyses are faster than in LC-MS/MS, because the time in the development of the method is saved. It is especially interesting in natural product studies

which frequently are related to complex mixtures, as in metabolomics, extract authentication and screening studies [70–74].

However, given the high complexity of many substances of plant origin, it is important to carry out analyzes using different ionization modes and both polarities. Most alkaloids are detectable in positive mode, either for ESI or APCI, but the matrix interference is more pronounced. The formation of adducts is possible, more specifically, cationization in positive mode may lead to the formation of alkali adducts, with the formation of multimers that add ions to the mass spectrum [73].

The LC-QTOF/MS adds the high mass resolution to mass fragmentation, which provides higher confidence in identification, although with higher cost. Comparing LC-QTOF/MS to LC triple quadrupole linear ion trap (QqLiT), the first leads to fewer false positives, but the latter has slightly lower detection limits in most situations [74].

Besides the high cost, LC-HRMS has the disadvantage of not differentiating structural isomers, which is important in phytochemistry since substances with more than one stereocenter are common. In those cases, it is necessary to complement with other information, such as retention time and spectroscopic data [73]. Another disadvantage is the rapid saturation of the detector, which requires work with more diluted samples [65]. It is expected that these equipments will become less costly, so that the technique will gain wide use.

7. Analysis of alkaloids in body samples by LC-HRMS

Plant species that contain β-carboline alkaloids, including canthinone alkaloids, are widely employed therapeutically or even as a drug of abuse. Given the diversity of the biological activities already described for these alkaloids, including neurological effects, it is necessary to develop techniques for the detection and quantification of these alkaloids and their metabolites in biological fluids and tissues, as a tool for toxicological analysis and pharmacokinetic studies. This knowledge may also be the starting point for the development of new drugs with potential commercialization.

LC-HRMS is promising in toxicological and analytical studies of metabolism, where substances are often unexpected, and the sample is available in small amount. In addition, it provides rapid analysis and the possibility of using a general method for a wide variety of substances [65, 74–76]. To date, there are few studies using LC-HRMS for the analysis of alkaloids, including β-carboline alkaloids in biological samples, possibly because of the still very high equipment prices. Frequently, LC-MS/MS or GC/MS is used previously, and only after the high-resolution mass is obtained for confirmation.

Biological samples, such as blood, bile, urine, milk, feces and pineal dialysates, consist of a complex matrix, which may cause interference in LC-MS analyses of low or high resolution. Therefore, it is common to submit samples to a pretreatment by solid phase extraction (SPE), using HCX cartridge [53, 76] or C18 cartridges [43, 53, 68]. However, in some cases,

http://dx.doi.org/10.5772/68075

the sample is simply extracted with an organic solvent, such as the procedure described by Shi et al. [32] for the analysis of 5-hydroxy-4-methoxycanthin-6-one and its metabolites, that uses ethyl acetate to extract the analytes from plasma and methanol for feces collected from male Sprague-Dawley rats. There are cases that no pretreatment is required, such as in the analysis of β-carbolines (1,2,3,4-tetrahydro-β-carboline, 2-methyl-1,2,3,4-tetrahydro-β-carboline, 6-hydroxy-tetrahydro-β-carboline, and 6-methoxy-tetrahydro-β-carboline), metabolites of dimethyltryptamine and derivatives, in pineal gland microdialysate collected from male Wistar rats [68].

A large variety of phase I metabolites of β-carboline alkaloids, formed by N-decarbonylation, oxidation and methylation, and phase II metabolites, formed by conjugation, such as glucuronides, sulfates and N-acetylcysteine derivatives, are present in body samples. For analysis of phase I metabolites, β-glucuronidase and/or arylsulfatase enzymes can be added to the sample for cleavage of conjugates and to avoid interferences of phase II metabolites [43, 53, 68, 76].

The liquid chromatography step is similar for low and high mass resolution. The separation can occur in TF Hypersil Gold C18 column, 100 mm × 2.1 mm, 1.9 μm [53]; Hedera ODS-2 C18 column, 250 mm × 4.6 mm, 5 μm [43]; C18 BEH column, 100 mm × 2.1 mm, 1.7 μm [67]; Zorbax Eclipse Plus C18, 100 mm × 3.0 mm, 3.5 μm [68]; Superspher 60 RP-8 column, 125 mm × 2 mm, 5 μm [76]; Zorbax Eclipse Plus rapid resolution HT C18 column, 50 mm × 2.1 mm, 1.8 μm [75]. The oven temperature is set at 30°C [43], 35°C [53] or 40°C [75]. After pretreatment, samples are frequently diluted in methanol or in mobile phase before injection in LC systems. The mobile phase is frequently a gradient from formic acid (0.05 or 0.1%) in water to acetonitrile, with or without formic acid [43, 68, 76]. This aqueous phase may be replaced by an aqueous solution containing ammonium formate buffer (2.5 or 10 mM) with 0.1% (v/v) formic acid [53, 75]. The organic phase may be 0.1% formic acid in acetone:acetonitrile 20:80 [67]. The solution B of the method developed by Kolmonen et al. [75] consists of 2.5 mM ammonium formate and 0.1% formic acid in 90% acetonitrile. The flow rate varies from 300 μL/min [68] to 1 mL/min [43]. The total run time varies from 8 min [75] to 67 min [53].

In general, the MS analyzer, TOF or Orbitrap, employs electrospray ion source. For this class of substances, the positive ionization mode is the most applied (ESI+) [43, 53, 67], although it is more appropriate to use both positive and negative ionization modes in screening analyses to cover more substances [68, 75]. Capillary voltage varied from 3 to 4.5 kV, [43, 53, 67, 68, 75] and resolution varies from 7500 to 60,000 [46, 53]. After the analysis, data processing is necessary with suitable software to help in the identification of metabolites.

Although LC-HRMS has been more used to confirm identification, the technique can be used alone successfully in screening, as the methodology proposed by Kolmonen et al. [75]. The methodology uses LCTOFMS for the search of doping agents in human urine. The method is applicable to at least 207 analytes, including the indole alkaloid strychnine, and may even be used for quantitative analyzes for many of this substances. After an SPE sample pretreatment, the analysis run time is 8 min for each ionization mode, with a total time of 16 min.

Some β-carboline alkaloids and their metabolites have been identified in biological tissues and fluids, such as tetrahydro-β-carboline derivatives—present in plant species and also considered

an endogenous alkaloid; [43, 67, 68] speciogynine—isolated from *Mitragyna speciosa*, a plant species used as drug of abuse [53]; 1-methyl-3-carboxy-β-carboline—found in cow milk probably derived from the diet and metabolism [76]. The technique is still expanding, and the few works found in the literature indicate a great potential not yet explored.

8. Summary

An important class of natural products found in Angiosperms, β-carboline and canthinone alkaloids, has various pharmacological properties and toxic effects. Coupled chromatographic and mass spectrometric techniques can be used to identification of these alkaloids. In this chapter, an approach overview of LC-HRMS applied to chemical complexity of plant extracts and forensic samples containing β-carboline and canthinone alkaloids can be a good choice technique to analyze and elucidate this kind of compounds. In addition, the HRMS/MS fragments of some important β-carboline and canthinone alkaloid are shown in mass fragmentograms schemes. Among important advantages of LC-HRMS, the main one is that it allows the identification of a wider number of analytes, including unexpected substances in the sample, and does not require reference standards or preexisting MS libraries for comparison. This technique can be used alone successfully in screening since it provides rapid analysis and the possibility of using a general method for wide variety of substances.

Author details

Ana Claudia F. Amaral[1]*, Aline de S. Ramos[1], José Luiz P. Ferreira[1], Arith R. dos Santos[1], Jefferson D. da Cruz[1], Adélia Viviane M. De Luna[1], Vinicius Vaz C. Nery[2], Iasmim C. de Lima[1], Marcelo Henrique da C. Chaves[3] and Jefferson Rocha de A. Silva[4]

*Address all correspondence to: acamaral@fiocruz.br

1 Laboratório de Plantas Medicinais e Derivados-PN1, Depto de Produtos Naturais, Farmanguinhos – FIOCRUZ, Manguinhos, Brazil

2 Serviços de Métodos Analíticos, Farmanguinhos – FIOCRUZ, Manguinhos, Brazil

3 Divisão de Controle de Qualidade, Farmanguinhos – FIOCRUZ, Brazil

4 Laboratório de Cromatografia – Depto. de Química – UFAM, Japiim, Manaus, Brazil

References

[1] Costa EV, Pinheiro MLB, Xavier CM, Silva JRA, Amaral ACF, Souza ADL, Barison A, Campos FR, Ferreira AG, Machado GMC, Leon LLP. A pyrimidine-β-carboline and other alkaloids from *Annona foetida* with antileishmanial activity. Journal of Natural Products. 2006;**69**:292-294. DOI: 10.1021/np050422s

[2] Costa EV, Pinheiro MLB, Souza ADL, Santos AG, Campos FR, Ferreira AG, Barison A. Mint: Full NMR analysis of annomontine, methoxyannomontine and N-hydroxyannomontine pyrimidine-β-carboline alkaloids. Magnetic Resonance in Chemistry. 2008;**46**:69-74. DOI: 10.1002/mrc.2134

[3] Rejón-Orantes JC, González-Esquinca, La Mora MP, Roldan GR, Cortes D. Mint: Annomontine, an alkaloid isolated from Annona purpurea, has anxiolytic-like effects in the elevated plus-maze. Planta Medica. 2011;77:322-327. DOI: 10.1055/s-0030-1250406

[4] Jaeger RJR, Lamshöft M, Gottfried S, Spiteller M, Spiteller P. Mint: HR-MALDI MS imaging assisted screening of β-carboline alkaloids discovered from *Mycena metata*. Journal of Natural Products. 2013;**76**:127−134. DOI: 10.1021/np300455a

[5] Saraiva RCG, Pinto AC, Nunomura SM, Pohlit AM. Mint: Triterpenos e alcalóide tipo cantinona dos galhos de *Simaba polyphylla* (Cavalcante) W.W. Thomas (Simaroubaceae). Química Nova. 2006;**29**:264-268. DOI: 10.1590/S0100-40422006000200017

[6] Ohmoto T, Tanaka R, Tamotsu N. Mint: Studies on the constituents of *Ailanthus altissima* Swingle on the alkaloidal constituents. Chemical & Pharmaceutical Bulletin. 1976;**24**:1532-1536. DOI: 10.1248/cpb.24.1532

[7] Galih PR, Esyanti RR. Mint: Effect of immobilization on cell growth and alkaloid contents in cell-aggregate culture of *Eurycoma longifolia* Jack. International Journal of Chemical, Environmental and Biological Sciences. 2014;**2**:90-93.

[8] Anderson L, Harris A, Phillipson JD. Mint: Production of cytotoxic canthin-6-one alkaloids by *Ailanthus altissima* plant cell cultures. Journal of Natural Products. 1983;**46**: 374-378. DOI: 10.1021/np50027a014

[9] Bharitkar YP, Hazra A, Poduri NSA, Ash A, Maulik PR, Mondal NB. Mint: Isolation, structural elucidation and cytotoxicity evaluation of a new pentahydroxy-pimarane diterpenoid along with other chemical constituents from *Aerva lanata*. Natural Product Research. 2015;**29**:253-261. DOI: 10.1080/14786419.2014.971794

[10] Cebrián-Torrejón G, Spelman K, Leblanc K, Muñoz-Durango K, Torijano S, Gutiérrez ST, Ferreira ME, Arias AR, Figadère B, Alain Fournet A, Maciuk A, Philippe Grellier P, Nadja B, Cech PN, Poupon E. Mint: The antiplasmodium effects of a traditional South American remedy: *Zanthoxylum chiloperone* var. *angustifolium* against chloroquine resistant and chloroquine sensitive strains of *Plasmodium falciparum*. The Brazilian Journal of Pharmacognosy. 2011;**21**:652-661. DOI: 10.1590/S0102-695X2011005000104

[11] Diakanamwa C, Diallo B, Vanhaelen-Fastré R, Vanhaelen M, Jaziri M, Homès J. Mint: Gas liquid chromatographic determination of canthinone alkaloids in *Hannoa chlorantha* root bark and tissue cultures. Phytochemical Analysis. 1995;**6**:193-195. DOI: 10.1002/pca.2800060403

[12] Ferreira ME, Arias AR, Ortiz ST, Inchausti A, Nakayama H, Thouvenel C, Hocquemiller R, A. Fournet A. Mint: Leishmanicidal activity of two canthin-6-one alkaloids, two major constituents of *Zanthoxylum chiloperone* var. *angustifolium*. Journal of Ethnopharmacology. 2002;**80**:199-202.

[13] Ferreira ME, Nakayama H, de Arias AR, Schinini A, de Bilbao NV, Serna E, Lagoutte D, Soriano-Agatón F, Poupon E, Hocquemiller R, Fournet A. Mint: Effects of canthin-6-one alkaloids from *Zanthoxylum chiloperone* on *Trypanosoma cruzi*-infected mice. Journal of Ethnopharmacology. 2007;**109**:258-263. DOI: 10.1016/j.jep.2006.07.028

[14] Ferreira ME, Cebrián-Torrejón G, Corrales AS, de Bilbao NV, Rolón M, Gomez CV, Leblanc K, Yaluf G, Schinini A, Torresa S, Serna E, de Arias AR, Poupon E, Fournet A. Mint: *Zanthoxylum chiloperone* leaves extract: First sustainable Chagas disease treatment. Journal of Ethnopharmacology. 2011;**133**:986-993. DOI: 10.1016/j.jep.2010.11.032

[15] Haynes HF, Nelson ER, Price JR. Alkaloids of the Australian Rutaceae*: Pentaceras australis* Hook. F. I. Mint: Isolation of the alkaloids and identification of canthin-6-one. Australian Journal of Scientific Research. 1952;**5**:387-400. DOI: 10.1071/CH9520387

[16] Ikuta A, Nakamura T, Urabe H. Mint: Indolopyridoquinazoline, furoquinoline and canthinone type alkaloids from *Phellodendron amurense* callus tissues. Phytochemistry. 1998;**48**:285-291. DOI: 10.1016/S0031-9422(97)01130-8

[17] Kanchanapoom T, Kasai R, Chumsri P, Hiraga Y, Yamasaki K. Mint: Canthin-6-one and b-carboline alkaloids from *Eurycoma harmandiana*. Phytochemistry. 2001;**56**:383-386. DOI: 10.1016/S00319422(00)00363-0

[18] Kim HM, Lee JS, Szirahiga J, Kwon J, Jeong M, Lee D, Choi J-H, Jang DS. Mint: A new canthinone-type alkaloid isolated from *Ailanthus altissima* Swingle. Molecules. 2016;**21**:642. DOI: 10.3390/molecules21050642

[19] Talaprata SK, Dutta S, Talaprata B. Mint: Alkaloids and terpenoids of *Zanthoxylum ovalifolium*. Phytochemistry. 1973;**12**:729-730. DOI: 10.1016/s0031-9422(00)84478-7

[20] Mitscher LA, Showalter HD, Shipchandler MT, Leu RP, Beal JL. Mint: Antimicrobial agents from higher plants. IV. *Zanthoxylum elephantiasis*. Isolation and identification of canthin-6-one. Lloydia. 1972;**35**:177-180.

[21] Ohmoto T, Koike K. Chapter 3: Canthin-6-one alkaloids. In: Brossi A, editor. The Alkaloids: Chemistry and Pharmacology. 1st ed. Elsevier; 1990;**36**:135-170. DOI: 10.1016/s0099-9598(08)60082-6

[22] Forgacs P, Provost J, Touché A. Mint: Alcaloïdes indoliques d'*Odyendea gabonensis*. Planta Medica. 1982;**46**:187-189. DOI: 10.1055/s-2007-971212

[23] Marques MR, Mendes MA, Tormena CF, Souza BM, Cesar LMM, Rittner R, Palma MS. Mint: Structure determination of a tetrahydro-β-carboline of arthropod origin: A novel alkaloid-toxin subclass from the web of spider *Nephila clavipes*. Chemistry & Biodiversity. 2005;**2**:525-534. DOI: 10.1002/cbdv.200590034

[24] Chua LS, Amin NAM, Neo JCH, Lee TH, Lee CT, Sarmidi MR, Aziz RA. Mint: LC-MS/MS based metabolites of *Eurycoma longifolia* (Tongkat Ali) in Malaysia (Perak and Pahang). Journal of Chromatography B. 2011;**879**:3909-3919. DOI: 10.1016/j.jchromb.2011.11.002

[25] Devkota KP, Wilson JA, Henrich CJ, McMahon JB, Reilly KM, Beutler JA. Mint: Compounds from *Simarouba berteroana* which inhibit proliferation of NF1-defective cancer cells. Phytochemistry Letters. 2014;**7**:42-45. DOI: 10.1016/j.phytol.2013.09.007

[26] Aimi N, Seiki H, Sakai S. Mint: Synthesis of lyaloside a prototypal β-carboline gluco indole alkaloid in rubiaceous plants. Mint: Chemical & Pharmaceutical Bulletin. 1992;**40**: 2588-2590. DOI: 10.1248/cpb.40.2588

[27] Passos CS, Soldi TC, Abib RT, Apel MA, Simões-Pires C, Marcourt L, Gottfried C, Henriques AT. Mint: Monoamine oxidase inhibition by monoterpene índole alkaloids and fractions obtained from *Psychotria suterella* and *Psychotria laciniata*. Journal of Enzyme Inhibition and Medicinal Chemistry. 2013;**28**:611-618. DOI: 10.3109/14756366.2012.666536

[28] Valverde J, Tamayo G, Hesse M. Mint: β-carboline monoterpenoid glucosides from *Palicourea adusta*. Phytochemistry. 1999;**52**:1485-1489. DOI: 10.1016/S0031-9422(99)00215-0

[29] Kato L, Oliveira CMA, Faria EO, Ribeiro LC, Carvalho BG, Silva CC, Schuquel ITA, Santin SMO, Nakamura CV, Britta EA, Miranda N, Iglesias AH, Drelprete PG. Mint: Antiprotozoal alkaloids from *Psychotria prunifolia* (Kunth) Steyerm. Journal of the Brazilian Chemical Society. 2012;**23**:355-360. DOI: 10.1590/S0103-50532012000200024

[30] Chen L, Miao X, Peng Z, Wang J, Chen Y.Mint: The pharmacokinetics and bioavailability of three canthinone alkaloids after administration of Kumu injection to rats. Journal of Ethnopharmacology. 2016;**182**:235-241. DOI: 10.1016/j.jep.2016.01.019

[31] Fo EF, Fernandes JB, Vieira PC, da Silva MFGF. Mint: Canthin-6-one alkaloids from *Picrolemma granatensis*. Phytochemistry, 1992;**31**:2499-2501.

[32] Shi Y, Hong C, Xub J, Yang X, Xie N, Feng F, Liu W. Mint: Simultaneous quantification of two canthinone alkaloids of *Picrasma quassioides* in rat plasma by liquid chromatography–tandem mass spectrometry and its application to a rat pharmacokinetic study. Journal of Chromatography B. 2015;**986-987**:100-107. DOI: 10.1016/j.jchromb.2015.02.008

[33] Li H-Y, Koike K, Ohmoto T. Mint: New alkaloids, picrasidines W, X and Y, from *Picrasma quassioides* and X-ray crystallographic analysis of picrasidine Q. Chemical & Pharmaceutical Bulletin. 1993;**41**:1807-1811. DOI: 10.1248/cpb.41.1807

[34] Kinzer KF, Cardellina JH. Mint: Three new β-carbolines from the bermudian tunicate *Eudistoma olivaceum*. Tetrahedron Letters. 1987;**28**:925-926. DOI: 10.1016/S0040-4039(00)95875-1

[35] Sasaki T, Li H, Ohmoto T, Koike K. Mint: Evaluation of canthinone alkaloids as cerebral protective agents. Bioorganic & Medicinal Chemistry Letters. 2016;**26**:4992-4995. DOI: 10.1016/j.bmcl.2016.09.006

[36] Herraiz T, González D, Ancín-Azpilicueta, Arán VJ, Guillén H. Mint: β-carboline alkaloids in *Peganum harmala* and inhibition of human monoamine oxidase (MAO). Food and Chemical Toxicology. 2010;**48**:839-845. DOI: 10.1016/j.fct.2009.12.019

[37] Pereira CAM, Rodrigues TR, Yariwake JH. Mint: Quantification of harman alkaloid in sour passion fruit pulp and seed by a novel dual SBSE-LC/Flu (stir bar sorptive extraction-liquid chromatography with fluorescence detector) method. Journal of the Brazilian Chemical Society. 2014;**25**:1472-1483. DOI: 10.5935/0103-5053.20140130

[38] Manda S, Khan SI, Jain SK, Mohammeda S, Tekwani, BL, Khan IA, Vishwakarma RA, Bharate SB. Mint: Synthesis, antileishmanial and antitrypanosomal activities of N-substituted tetrahydro-β-carbolines. Bioorganic & Medicinal Chemistry Letters. 2014;**24**:3247-3250. DOI: 10.1016/j.bmcl.2014.06.030

[39] Di Giorgio C, Delmas F, Ollivier E, Elias R, Balansard G, Timon-David P. Mint: In vitro activity of the β-carboline alkaloids harmane, harmine, and harmaline towards parasites of the species *Leishmania infantum*. Experimental Parasitology. 2004;**106**:67-74. DOI: 10.1016/j.exppara.2004.04.002

[40] Dighe SU, Khan S, Soni I, Jain P, Shukla S, Yadav R, Sen P, Meeran SM, Batra S. Mint: Synthesis of β-carboline-based N-heterocyclic carbenes and their antiproliferative and antimetastatic activities against human breast cancer cells. Journal of Medicinal Chemistry. 2015;**58**:3485-3499. DOI: 10.1021/acs.jmedchem.5b00016

[41] Lood CS, Koskinen AMP. Mint: Harmicine, a tetracyclic tetrahydro-β-carboline: From the first synthetic precedent to isolation from natural sources to target-oriented synthesis (review). Chemistry of Heterocyclic Compounds. 2015;**50**:1488-1509. DOI: 10.1007/s10593-014-1602-4

[42] Zhao W, He J, Zhang Y, Ito Y, Su Q, Sun W. Mint: Preparative isolation and purification of alkaloids from *Picrasma quassioides* (D. Don) Benn. by high-speed countercurrent chromatography. Journal of Liquid Chromatography & Related Technologies. 2012;**35**:1597-1606. DOI: 10.1080/10826076.2011.621150

[43] Shi Y, Xia Y, Wang J, He J, Feng F, Liu W. Mint: Metabolic profile of 5-hydroxy-4 methoxycanthin-6-one, a typical canthinone alkaloid, in rats determined by liquid chromatography-quadrupole time-of-flight tandem mass spectrometry together with multiple data processing techniques. Journal of Pharmaceutical and Biomedical Analysis. 2016;**129**:60-69. DOI: 10.1016/j.jpba.2016.06.047

[44] Samoylenko V, Khan SI, Jacob MR, Tekwani BL, Walker LA, Hufford CD, Muhammad I. Mint: Bioactive (+)-manzamine A and (+)-8-hydroxymanzamine A tertiary bases and salts from *Acanthostrongylophora ingens* and their preparations. Natural Product Communications. 2009;**4**:185-192.

[45] Ichiba T, Corgiat JM, Scheuer PJ, Kelly-Borges M. Mint: 8-Hydroxymanzamine A, a beta-carboline alkaloid from a sponge, *Pachypellina* sp. 1994:**57**;168-170. DOI: 10.1021/np50103a027

[46] Figueiredo PO, Garcez FR, Matos MFC, Perdomo RT, Queiroz LMM, Pott A, Garcez AJS, Garcez WS. Mint: A new cytotoxic β-carboline alkaloid from *Galianthe thalictroides*. Planta Medica. 2011;**77**:1852-1854. DOI: 10.1055/s-0030-1271154

[47] Giesbrecht AM, Gottlieb HE, Gottlieb OR, Goulart MOF, De Lima RA, Sant'Ana AEG. Mint: Canthinones from *Simaba cuspidata*. Phytochemistry. 1980;**19**:313-315. DOI: 10.1016/S0031-9422(00)81981-0

[48] Scheuer PJ, Pattabhiraman TR. Mint: Hawaiian plants studies XIII isolation of a canthinone from a member of family Amaranthaceae. Lloydia.1965;28:95-100.

[49] Readel KE, Seigler DS, Young DA. Mint: 5-methoxycanthin-6-one from *Leitneria floridana* (Simaroubaceae). Biochemical Systematics and Ecology. 2003;**31**:167-170. DOI: 10.1016/S0305-1978(02)00074-1

[50] Choo C-Y, Cham K-L. Mint: High performance liquid chromatography analysis of canthinone alkaloids from *Eurycoma longifolia*. Planta Medica. 2002;**68**:382-384. DOI: 10.1055/s-2002-26745

[51] Poupat C, Ahondt A, Séveneti T. Mint: Alcaloides de *Acacia simplifolia*. Phytochemistry. 1976;15:2019-2020. DOI: 10.1016/S0031-9422(00)88891-3

[52] Bahçeevli AK, Kurucu S, Kolak U, Topcüu G, Adou E, Kingston DGI. Mint: Alkaloids and aromatics of *Cyathobasis fruticulosa* (Bunge) Aellen. Journal of Natural Products. 2005;**68**:956-958. DOI: 10.1021/np0580006

[53] Philipp AA, Wissenbach DK, Weber AA, Zapp J, Maurer HH. Mint: Phase I and II metabolites of speciogynine, a diastereomer of the main *Kratom* alkaloid mitragynine, identified in rat and human urine by liquid chromatography coupled to low and high-resolution linear ion trap mass spectrometry. Journal of Mass Spectrometry. 2010;**45**:1344-1357. DOI: 10.1002/jms.1848

[54] Teichert A, Lübken T, Schmidt J, Kuhnt C, Huth M, Porzel A, Wessjohann L, Arnold N. Mint: Determination of β-carboline alkaloids in fruiting bodies of *Hygrophorus* spp. by liquid chromatography/electrospray ionization tandem mass spectrometry. Phytochemical Analysis. 2008;**19**:335–341. DOI: 10.1002.pca

[55] Faria EO, Kato L, Oliveira CMA, Carvalho BG, Silva CC, Sales LS, Schuquel ITA, Silveira-Lacerda EP, Delprete PG. Mint: Quaternary β-carboline alkaloids from *Psychotria prunifolia* (Kunth) Steyerm. Phytochemistry Letters. 2010;**3**:113-116. DOI: 10.1016/j.phytol.2010.02.008

[56] Koike K, Ohmoto T, Ikeda K. Mint: β-Carboline alkaloids from *Picrasma quassioides*. Phytochemistry, 1990;**29**:3060-3061. DOI: 10.1016/0031-9422(90)87144-J

[57] Bindu S, Rameshkumar KB, Kumar B, Singh A, Anilkumar C. Mint: Distribution of reserpine in *Rauvolfia* species from India – HPTLC and LC-MS studies. Industrial Crops and Products. 2014;**62**:430-436. DOI: 10.1016/j.indcrop.2014.09.018

[58] Farias FM, Konrath EL, Zuanazzi JA, Henriques AT. Strictosamide from *Psychotria nuda* (Cham. et Schltdl) Wawra (Rubiaceae). Biochemical Systematics and Ecology. 2008;**36**:919-920. DOI: 10.1016/j.bse.2008.10.002

[59] Milen M, Hazai L, Kolonits P, Gomory Á, Szántay CS, Fekete J. Mint: Preparation and separation of 1-methyl-1,2,3,4-tetrahidro-β-carboline enantiomers by HPLC using a new derivatization reagent. Journal of Liquid Chromatography & Related Technologies. 2004;**27**:2921-2933. DOI: 10.1002/hlca.201400035

[60] Wang F-X, Deng A-J, Li M, Wei J-F, Qin H-L, Wang A-P. Mint: (3S)-1,2,3,4-tetrahydro-β-carboline-3-carboxylic acid from *Cichorium endivia*. L. induces apoptosis of human colorectal cancer HCT-8 cells. Molecules. 2013;**18**:418-429. DOI: 10.3390/molecules18010418

[61] Pereira MM, Jácome RLRP, Alcântara AFC, Alves RB, Raslan DS. Mint: Alcalóides indólicos isolados de espécies do gênero *Aspidospema* (Apocynaceae). Química Nova. 2007;**30**:970-983. DOI: 10.1590/S0100-40422007000400037

[62] Kuo PC, Shi LS, Damu AG, Su CR, Huang, CH, Ke CH, Wu JB, Lin AJ, Bastow KF, Lee KH, Wu TS. Cytotoxic and antimalarial β-carboline alkaloids from the roots of *Eurycoma longifolia*. Journal of Natural Products. 2003;**66**:1324-1327. DOI: 10.1021/np030277n

[63] Kim HM, Kim, SJ, Kim HY, Ryu B, Kwak H, Hur J, Choi J-H, Jang DS. Mint: Constituents of the stem barks of *Ailanthus altissima* and their potential to inhibit LPS-induced nitric oxide production. Bioorganic & Medicinal Chemistry Letters. 2015;**25**:1017-1020. DOI: 10.1016/j.bmcl.2015.01.034

[64] Sasaki T, Li W, Higai K, Koike K. Mint: Canthinone alkaloids are novel protein tyrosine phosphatase 1B inhibitors. Bioorganic & Medicinal Chemistry Letters. 2015;**25**:1979-1981. DOI: 10.1016/j.bmcl.2015.03.014

[65] Wu AHB, Gerona R, Armenian P, French D, Petrie M, Lynch KL. Mint: Role pf liquid chromatography–high-resolution mass spectrometry (LC-HR/MS) in clinical toxicology. Clinical Toxicology. 2012;**50**:733-742. DOI: 10.3109/15563650.2012.713108

[66] Pavia DL, Lampman GM, Kriz GS, Vyvyan JR. Introdução à Espectroscopia. Translation of 4th ed. São Paulo: Cengage Learning; 2010. 716 p.

[67] Stanstrup J, Schou SS, Holmer-Jensen J, Kjeld H, Dragsted LO. Mint: Whey protein delays gastric emptying and suppresses plasma fatty acids and their metabolites compared to casein, gluten, and fish protein. Journal of Proteome Research. 2014;**13**:2396-2408. DOI: 10.1021/pr401214w

[68] Steinmann D, Ganzera M. Mint: Recent advances on HPLC/MS in medicinal plant analysis. Journal of Pharmaceutical and Biomedical Analysis. 2011;**55**:744-757. DOI: 10.1016/j.jpba.2010.11.015

[69] Vergeynst L, Van Langenhove H, Demeestere K. Mint: Balancing the false negative and positive rates in suspect screening with high-resolution orbitrap mass spectrometry using multivariate statistics. Analytical Chemistry. 2015;**87**:2170-2177. DOI: 10.1021/ac503426k

[70] Kumari T, Sharma C, Bajpai V, Kumar B, Srivastava M, Arya KR. Mint: Qualitative determination of bioactive metabolites through Q-TOF LC/MS in different parts and undifferentiated cultures of *Ulmus wallichiana* Planchon. Plant Growth Regulation. 2015;**75**:331-340. DOI: 10.1007/s10725-014-9956-2

[71] Kluger B, Bueschl C, Neumann N, Stückler R, Doppler M, Chassy AW, Waterhouse AL, Rechthaler J, Kampleitner N, Thallinger GG, Adam G, Krska R, Schuhmacher R. Mint: Untargeted profiling of tracer-derived metabolites using stable isotopic labeling and fast polarity-switching LC-ESI-HRMS. Analytical Chemistry. 2014;**86**:11533-11537. DOI: 10.1021/ac503290j

[72] Cuthbertson DJ, Johnson SR, Piljac-Žegarac J, Kappel J, Schäfer S, Wüst M, Ketchum REB, Croteau RB, Marques JV, Davin LB, Norman G. Lewis NG, Rolf M, Kutchan TM, Soejarto DD, Lange BM. Mint: Accurate mass - time tag library for LC/MS-based metabolite profiling of medicinal plants. Phytochemistry. 2013;**91**:187-197. DOI: 10.1016/j.phytochem.2013.02.018

[73] Thoren KL, Colby JM, Shugarts SB, Wu AHB, Lynch KL. Mint: Comparison of information-dependent acquisition on a tandem quadrupole TOF vs a triple quadrupole linear ion trap mass spectrometer for broad-spectrum drug screening. Clinical Chemistry. 2016;62:170-178. DOI: 10.1373/clinchem.2015.241315

[74] Kolmonen M, Leinonen A, Kuuranne T, Pelander A, Ojanperä I. Mint: Generic sample preparation and dual polarity liquid chromatography – time-of-flight mass spectrometry for high-throughput screening in doping analysis. Drug Testing and Analysis. 2009;**1**: 250-266. DOI: 10.1002/dta.50

[75] Rouge P, Cornu A, Biesse-Martin A-S, Lyan B, Rochut N, Graulet B. Mint: Identification of quinolone, carboline and glycinamide compounds in cow milk using HRMS and NMR. Food Chemistry. 2013;**141**:1888-1894. DOI: 10.1016/j.foodchem.2013.04.072

[76] Barker SA, Borjigin J, Lomnicka I, Strassman R. Mint: LC/MS/MS analysis of the endogenous dimethyltryptamine hallucinogens, their precursors, and major metabolites in rat pineal gland microdialysate. Biomedical Chromatography. 2013;**27**:1690-1700. DOI: 10.1002/bmc.2981

Chapter 7

Applications of Mass Spectrometric Techniques to the Analysis of Fuels and Lubricants

David W. Johnson

Additional information is available at the end of the chapter

http://dx.doi.org/10.5772/intechopen.68592

Abstract

The application of mass spectrometric techniques for the analysis of the complex mixtures inherent in fuel and lubricant samples will be examined. These samples because they are naturally complex mixtures, typically requires either very high resolution mass spectrometry or one of the hyphenated techniques gas chromatography-mass spectrometry(GC-MS) or liquid chromatography-mass spectrometry (LC-MS). Some fuel problems that can be addressed through mass spectrometry are associated with the changes in composition and degradation of fuels as they age, including the analysis of both major hydrocarbon components non-polar components and minor polar components will be described. The properties and composition of natural and major classes of synthetic lubricants, the presence of additives and the problems that develop as the lubricant is used such as additive depletion, thermal and oxidative degradation and lubricant contamination have also been examined using mass spectrometric techniques.

Keywords: gas chromatography-mass spectrometry, liquid chromatography-mass spectrometry, fuels, lubricants, high resolution mass spectrometry, degradation

1. Introduction

Mass spectrometry has long been an important technique for the identification of materials ranging from pure compounds to complex mixtures [1]. Mass spectrometry can be used to determine molecular weight of compounds; or using different ionization methods, can provide more structural details through the analysis of fragmentation patterns [2]. A wide range of ionization methods and mass analyzers have been developed for the specific problems of complex mixtures like fuels and lubricants [3]. This level of detail can be attained for pure compounds and some mixtures. Mass spectrometry can also be combined with separation

INTECH
open science | open minds

© 2017 The Author(s). Licensee InTech. This chapter is distributed under the terms of the Creative Commons Attribution License (http://creativecommons.org/licenses/by/3.0), which permits unrestricted use, distribution, and reproduction in any medium, provided the original work is properly cited. CC BY

techniques such as gas chromatography [4] or liquid chromatography [5] to allow more complex mixtures to be examined. These hyphenated techniques provide a range of options for the characterization of complex materials. A number of the important developments in mass spectrometry that are important in the analysis of fuels and lubricants are shown in **Figure 1**.

Fuels and lubricants are traditionally derived from the distillation of crude oil providing the base stock [6]. The properties are then modified through the addition of additives to arrive at the final fuel or lubricant. Natural fuels and lubricants are extremely complex mixtures whose composition depends greatly on the source of the crude oil and the processing of material. Fuels are typically characterized by a boiling point range, while lubricants are typically characterized by bulk properties such as viscosity and pour point.

There has been some effort to characterize the fuels based on classes of compounds, for example, but the characterization is not always complete. As the requirement for fuels have increased, there has been increased efforts to determine polar compounds, in particular because they often lead to the formation of deposits in an engine. More recently, there have been efforts made to develop synthetic fuels, based on Fisher-Tropsch catalysts [7] and bio-derived fuels [8]. These fuels present their own challenges in terms of characterization. Mass spectrometry and hyphenated techniques have been used to address a number of different problems in this area, allowing the identification of a number of materials, including additives, impurities and adulterants.

Lubricants derived from crude oil have been used in many applications and have been studied in many ways. The complexity of the samples often requires either hyphenated techniques

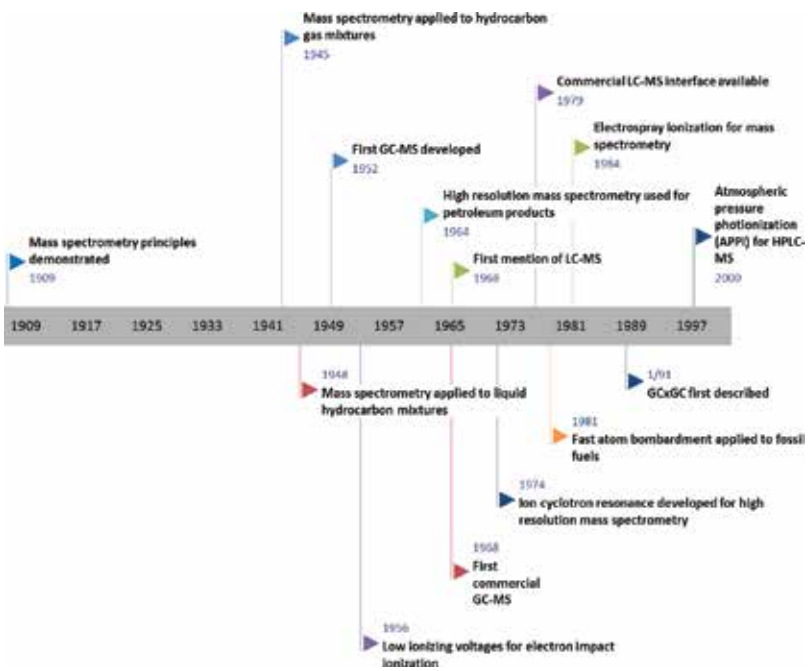

Figure 1. Some of the important advancements in the mass spectrometry of fuels and lubricants.

to identify components in the base stock, additives and also contaminants. Synthetic lubricants have been developed based on alkyl benzenes, poly alkylene glycols and polyol esters in part because of the greater control of the composition and chemistry of the base stock. The synthetic lubricants are simpler in composition and are more amenable to study using mass spectrometry and various hyphenated techniques [9].

In this chapter, the application of mass spectrometry and the various hyphenated techniques to fuels and lubricants is reviewed. A particular emphasis is placed on the examination of some of the problems that mass spectrometry has addressed and how questions about the source, composition and applicability of fuels and lubricants can be addressed. The chapter has sections devoted to mass spectrometric techniques for fuels and lubricants, followed by high resolution mass spectrometry, gas chromatography-mass spectrometry and liquid chromatography-mass spectrometry.

2. Mass spectrometry

The early application of mass spectrometry to fuels and lubricants began in the early 1940s using electron impact ionization [10]. These studies were complicated by the complexity of the mixture and also the extensive fragmentation caused by 70 ev electron impact [11, 12]. The complex mass spectra could yield information about the fuel sample primarily through a complex calibration scheme using ratios of common peaks forum in the mass spectra of different classes of hydrocarbons. The spectra, however gave little information about the average molecular weight of the fuel or lubricant.

Mass spectra at low resolution did not provide enough information to fully characterize many of the petroleum fractions. Some information about compound types could be obtained based on ratios of peaks observed at low mass in the mass spectrum. The low resolution mass spectrum of a mineral oil based lubricant is shown in **Figure 2**. This technique allowed some of the different hydrocarbon types to be identified in the lower boiling (gasoline, for example)

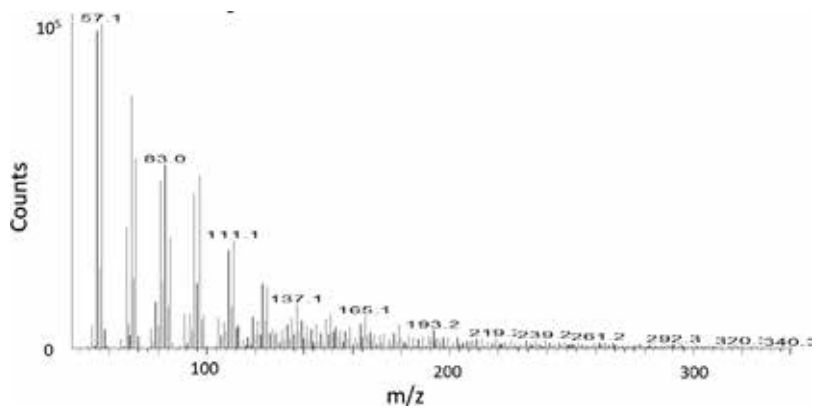

Figure 2. Low resolution mass spectrum of a mineral oil based lubricant (unpublished results).

fractions [13]. Very different compounds have the sample molecular mass at low resolution, so a number of pre-treatment techniques were developed to isolate compounds with certain functional groups for analysis by mass spectrometry. These techniques included preliminary separations by adsorption on silica or alumina [14]. In later work, adsorption chromatography was used as a preliminary treatment prior to mass spectrometric analysis [15].

It was quickly realized that the 70 eV ionization voltage was causing extensive fragmentation and gave no differentiation between different classes of compounds. Low voltage approaches were developed in order to selectively ionize certain classes of hydrocarbons, particularly olefins [16] or aromatics [17]. The lower ionizing voltage significantly reduced fragmentation allowing more high mass ions to be detected.

Success in this area led to the development of other soft ionization techniques some of which are summarized in **Table 1**.

The soft ionization techniques were successful in reducing the fragmentation of the ions formed, however molecular ions were still not always observed and the lack of fragment

Ionization type	Ionizing species	Comment
Electron impact(EI)	Beam of energetic electrons	Induces extensive fragmentation, gas phase technique, masses less than 1000
Chemical ionization(CI)	Ion molecule reactions of a reagent gas such as methane, ammonia or isobutane	Gas phase technique, typically give $[M+H]^+$, fragmentation reduced, limited to masses less than 1000
Field desorption(FD)	Sample deposited on emitter and emitter biased to several kilovolts. As current increases, sample vaporizes, ionization by electron tunneling emitter.	Simple mass spectrum, with a single peak per molecular species, moderate mass range–up to about 3000, sensitive to alkali metal contamination
Field ionization(FI)	Sample is evaporated from probe, GC or gas inlet. Ionization by electron tunneling when sample is near the emitter.	Simple mass spectrum, with a single peak per molecular species, moderate mass range–up to about 3000, sample must be somewhat volatile
Fast atom bombardment(FAB)	Sample is dissolved in a liquid matrix such as glycerol and place on target and bombarded with a fast atom beam	Rapid and simple, strong ion currents, good for high resolution, moderate molecular weights–up to 6000
Electrospray ionization(ESI)	Sample solution is aspirated across a high potential difference, heat and gas flow desolvates clusters	Good for charged, polar or basic compounds, multiply charged species are common, good for LC-MS, mass range to 200 k
Atmospheric pressure chemical ionization(APCI)	Sample solution is aspirated at atmospheric pressure, A corona discharge ionizes the sample	More effective than ESI for non-polar compounds, compatible with LC-MS, Low-moderate mass range up to 2000 AMU
Matrix-assisted laser desorption ionization (MALDI)	Analyte dissolved in a matrix that is UV active, on a Laser target, matrix absorbs laser pulse	Very high mass range–up to 500,000 AMU, requires pulsed mass analyzer, not compatible with LC-MS

Table 1. A summary of ionization techniques [18].

ions made compound identification through the use of libraries impossible. Softer ionization methods do, however give better estimates of molecular weight distributions since more high mass ions are formed. Softer ionization methods also allow differentiation of polar components of fuels or crude oils because they typically are easier to ionize than the hydrocarbon components of the sample. An example is the use of fast atom bombardment for the determination of nitrogen compounds in fossil fuels. The study demonstrated the effectiveness of fast atom bombardment in the analysis of liquid petroleum fractions [19].

3. High resolution mass spectrometry

Advances in mass spectrometry led to the development of instruments capable of much higher resolution than the original mass spectrometers. These high resolution instruments allowed multiple compounds with the same nominal mass to be separated and identified [20]. The introduction of double-focusing instruments and resolutions of 10,000 or more allowed for further reductions in sample preparation and allowed more components to be identified [21]. In many of these samples, the combination of high resolution mass spectrometry with low voltage ionization allowed for only certain major classes of compounds to be observed [22].

More recently, ultra-high resolution mass spectrometry has developed based on Fourier transform ion cyclotron resonance mass spectrometry (ICR-MS) for the determination of ion masses. In ICR-MS the ICR frequency of an ion in a uniform magnetic field depends on the mass and charge of the ion [23]. These instruments have extremely high mass accuracies and resolutions of 10^5–10^6 ($m/\Delta m$) which allows ions with very closely spaced masses to be identified [24]. The availability of ICR-MS has allowed many thousands of peaks in the mass spectrum of a crude oil sample to be identified to a unique molecular formula. The application of ICR-MS to problems in the petroleum field have spanned the range from identifying the source of weathered deposits found on beaches, to examining the types of sulfur compounds present and their susceptibility to removal in the desulfurization process.

The ability to identify several thousand individual compounds in a sample of a petroleum product opens a number of possibilities in the identification and tracking of the source of various products. This area of investigation is often referred to as petroleomics. Oil spills happen with some regularity, however it is not always an oil spill that results in oil fouling of beaches; natural seeps also release oil into the environment. In order to effectively clean up oil spills, it is necessary to know the properties of the oil and how it has weathered before deposition onto the beach. One technique for the identification of a source of an oil is principal component analysis where thousands of heteroatom containing species. The study led to the identification of a number of polar petroleum markers that are environmentally persistent and can identify the source of the oil [25]. In another study, ICR-MS was able to identify many highly oxygenated species that were formed by weathering of crude oil released from the Deepwater Horizon explosion in 2010 [26].

Environmental regulations have mandated a significant reduction in the sulfur content in various fuels in order to reduce sulfur dioxide emissions. Processes have been developed for the desulfurization of various types of fuels; however a portion of the sulfur in the fuel remains

even after aggressive desulfurization. ICR-MS has indicated that a portion of the aromatic sulfur is less able to be removed by the desulfurization process. Based on ICR-MS data, much of the sulfur in the fuel is present as either benzothiophenes or dibenzothiophenes. These compounds are susceptible to desulfurization, but if there are alky groups in certain positions on the aromatic rings (**Figure 3**), the compounds are far less reactive with the desulfurization catalyst [27]. A similar scheme was used in the study of some hexahydrobenzothiophenes [28].

Petroleum based fuels are prepared by the catalytic cracking, reforming and fractional distillation of crude oil. This process leads to a gasoline fraction (C_4–C_{12}), kerosene fraction (C_8–C_{18}) and diesel fraction (C_8–C_{40}). While most components in these fuels are non-polar, there is a wide range of components that have heteroatoms and would be considered to be more polar than the hydrocarbons. It is often the polar compounds that lend themselves to analysis by mass spectrometry due to their ability to be ionized by soft ionization techniques [29]. Nitrogen containing polar compounds are typically observed in positive ion mode using electrospray ionization. Typical classes of nitrogen containing components in fuels are shown in **Figure 4**, below. Nitrogen compounds in fuels have been implicated in a number of fuel

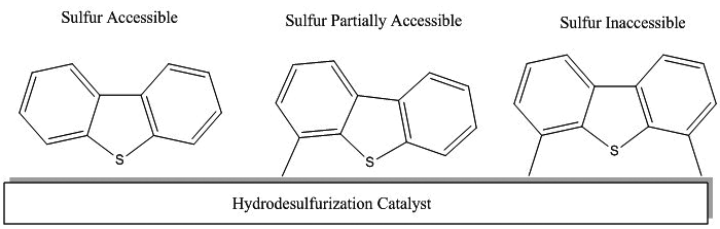

Figure 3. Steric hindrance in the interaction of substituted thiophenes with a dehydrosulfurization catalyst.

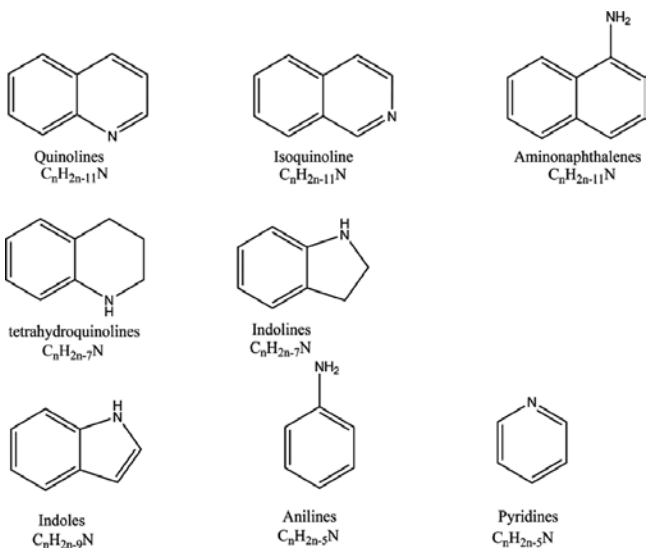

Figure 4. Typical nitrogen containing structures found in fuels.

problems, including fuel instability, sediment and gum formation. Some of the problems can be linked to specific classes of nitrogen compounds, basic nitrogen compounds tended to lead to greater stability, where non-basic compounds with particular substitution patterns are particularly reactive [30].

Negative ion electrospray ionization has also been used to study common types of fuels. Compounds commonly observed in fuels in negative ion mode are substituted phenols and thiophenols. These compounds can easily form either the phenoxide or thiolate ions [31].

On weathering, fuels typically shift in composition to compounds with higher molecular weight, as smaller compounds either evaporate or dissolve. This is primarily observed with kerosene and diesel fractions, as gasoline is too volatile [32].

4. Gas chromatography-mass spectrometry

Early experiments where adsorption chromatography was used to separate classes of compounds, coupled with the development of partition chromatography as a separation tool for use in GC, led to the idea of coupled gas chromatography-mass spectrometry (GC-MS) as an analytical technique. There were numerous problems, including the introduction of even small amounts of gas to the mass spectrometer could stop the mercury diffusion pumps used to maintain the high vacuum, the slow scan speed of magnetic sector instruments and the inability to record data quickly enough to collect all of the data. These problems were eventually solved with a gas separator [33], and then capillary gas chromatography, the development of fast mass analyzers, especially the time of flight [34] and quadrupole mass filter and finally the advent of low cost laboratory computers. The use of GC-MS became truly practical for many laboratories with the introduction of low cost dedicated GC-MS instruments in the early 80's.

The primary advantage of GC-MS as a modern analytical technique is combination of the separating power of capillary gas chromatography with the ability of mass spectroscopy to provide a mass spectrum of the compound being eluted. The technique is especially powerful when combined with libraries of possible compounds allowing a computerized identification of the compounds present in the mixture.

4.1. GC-MS of fuels

Gas chromatography-mass spectrometry has proven to be extremely useful in the analysis and identification of fuels. When operated with electron impact ionization, all compounds of the fuel are ionized, and the total ion chromatogram can give an estimate of the boiling point of the fuel, and an estimate of the molecular weight range. It is also possible to find additives or adulterants by GC-MS, since these materials frequently appear as a single peak in the chromatogram.

The analysis of gasoline is very well suited to GC-MS analysis since the boiling range is relatively low and because of the C4–C12 distribution of the hydrocarbons, the number of isomers is more manageable. A fundamental problem, however, is that fuel properties are not

well predicted based on the distribution of the hydrocarbon species. More important properties include ethanol and aromatic content, which alter octane rating and also vapor pressure, which is important to the environment. Determination of the aromatic content and the identification of the various substituted aromatics is a problem well suited to GC-MS [35], especially when coupled with a good library and search algorithm. Other applications include the identification of adulterants and contamination by higher boiling fuels.

A fuel type that has been heavily studied is the fuel used for aviation. Aviation fuels are highly refined un-leaded kerosene in which the carbon range is between 8 and 16. The demands of aviation require a highly refined fuel in which the flash point is above 38°C and the polar contaminants have been significantly reduces. Additives are typically necessary in order to improve the low temperature and high temperature properties of the fuel [36]. GC-MS has been successfully used to model the properties of a number of military aviation fuels [37]. GC-MS has also been utilized as a method for the quantification of anti-oxidants which are added to reduce autoxidation of the fuels on storage which can lead to the formation of deposits [38]. The GC-MS of two different jet fuels are shown in **Figure 5**. Both samples show a number of major components that are readily identified and other components that would act as a fingerprint for the fuel. A major difficulty, however relates to the observation that the baseline has significant slope, indicating a very large number of minor components present in the sample. The minor components include many components critical to understanding the low temperature reactivity and possible sludge formation in the fuel.

Many of the chemical properties especially autoxidation of fuels can be related to polar components, present at <0.1% in the multicomponent hydrocarbon matrix. These components include phenols, indoles amines, thiophenes and many others. Some of these components can

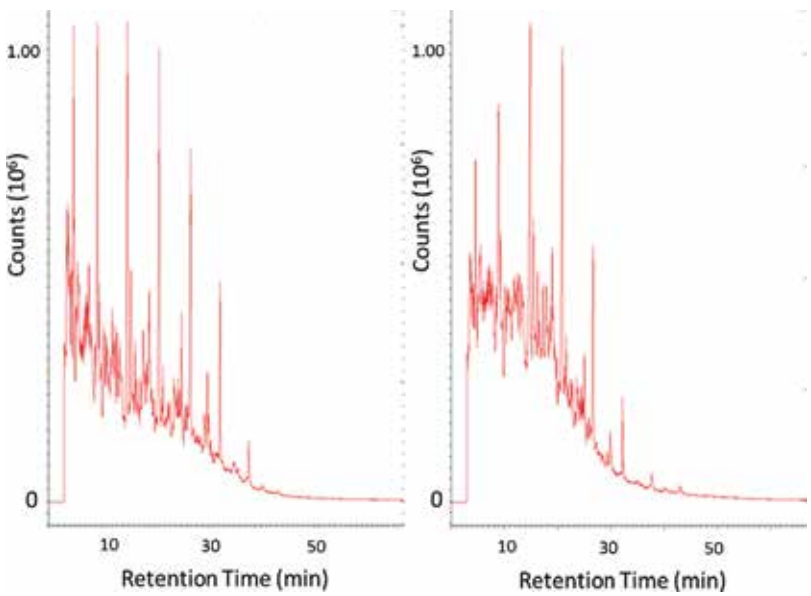

Figure 5. GC-MS total ion chromatograms of two different jet fuel samples.

be determined by chemical pre-treatment using solid phase extraction followed by GC-MS. This technique allowed the more polar compounds to be separated from the hydrocarbons prior to analysis.

The need to determine the trace components of complex mixtures such as jet fuel has encouraged the development of 2 dimensional GC or GCxGC. A sample analyzed by GCxGC is first separated on a non-polar column, which results in a separation primarily based on boiling point. A thermal or valve modulator focused the compound eluted in time slices onto the head of a second column which is typically short (1-2m) with a polar stationary phase [39]. The compounds are then eluted from the second column and detected by mass spectrometry. Two dimensional GC results show the polar compounds having a significantly longer retention time in the second dimension allowing easy identification. Possibly the most important feature of GCxGC data is that similar compounds are grouped at similar retention times in the second dimension.

4.2. GC-MS of lubricants

4.2.1. Mineral oil based lubricants

The GC-MS of mineral oil based lubricants typically results in broad peaks that do not allow individual compounds to be identified. The broad peaks are due to the huge number of isomers possible with hydrocarbons of the C20–C30 range. The compounds are very similar in properties and there are differences depending on the processing and refining methods used for the particular type on mineral oil. The total ion chromatogram for a sample of a yellow mineral oil and a white mineral oil are shown in **Figure 6**. The difference in the distribution of

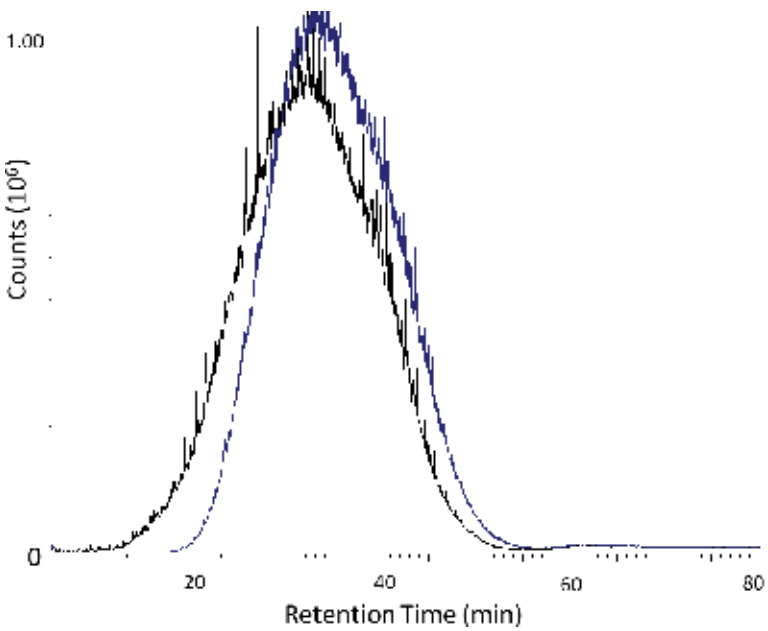

Figure 6. A comparison of the total ion chromatograms of two different mineral oils.

the compounds, which leads to significant differences in properties, can be seen. GC-MS can also be used to examine oil breakdown products, which in the case of mineral oils generally lead to the formation of products that are more polar and frequently have higher molecular weights resulting in longer retention times by GC.

Another important application of GC-MS in the analysis of mineral oils is the identification and quantitation of various additives. Mineral oils typically have a number of additives included in the formulations which improve certain properties of the lubricant, including pour point, oxidative stability and anti-wear properties. In general, the more highly refined the lubricant, the more additives need to be included [40]. This is in part because naturally occurring sulfur compounds are natural anti-oxidants and form hard surfaces on bearings reducing wear. **Figure 7** shows the total ion chromatogram of a formulated mineral oil. The sharp peaks appearing above the distribution are components of the phosphate ester anti-wear additive. Phosphate esters form a surface layer that resists wear under boundary layer lubrication, such as during start-up of the process [41]. GC-MS can indicate additives present and also be an indicator of additive depletion or decomposition. The four sharp peaks at 40–50 minute retention times are the components of the phosphate ester anti-wear additive. The peak at 20 min is due to the anti-oxidant included in the formulation.

4.2.2. Synthetic lubricants

The development of synthetic lubricants has illustrated a need to identify different sources of the lubricant and also identify the different additives needed to improve many of the properties of the lubricants. GC-MS has been shown to be useful in both the identification of the base stock and the quantification of the components of the additive package. Typically, synthetic lubricants fall into categories primarily based on the base stock. Some base stock categories include alkyl benzenes, polyalphaolefins (PAO), polyalkylene glycols and polyol esters. Each of these categories of lubricants has characteristic features which allow them to be identified.

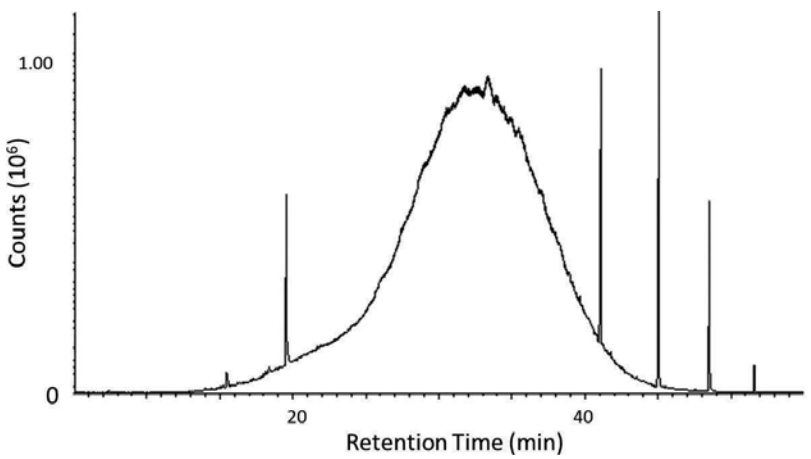

Figure 7. The total ion chromatogram of a blended mineral oil with sharp peaks indicating anti-oxidant and anti-wear additives.

One of the common classes of synthetic lubricant base stocks are the alkyl benzenes. These lubricants have found application in refrigeration systems and heavier alkylbenzenes have been used in automotive applications [42]. The GC-MS of these base stocks are characterized by series of peaks of the same molecular weight corresponding to different attachment points for the alkyl group. The total ion chromatogram for an alkylbenzene refrigeration lubricant is shown in **Figure 8**. The peaks observed at 22–30 min retention time correspond to monoalkyl benzenes with C12–C14 alkyl groups attached. At longer retention times, dialkylbenzenes are observed with similar length alkyl groups.

A second major class of synthetic lubricants are poly alpha olefins. They are available in a wide range of viscosities for applications ranging from compressor lubricants through gear oils and greases, including automotive applications. These lubricants are produced by the polymerization of alpha olefins, with 1-decene used as the main component in lubricants. The oligomeric mixture is the hydrogenated and distilled to give lubricants graded by their viscosity at 100°C [43]. Their GC-MS typically appears as a series of broad peaks indicating different degrees of polymerization. A GC-MS chromatogram of a poly alpha olefin is shown in **Figure 9**.

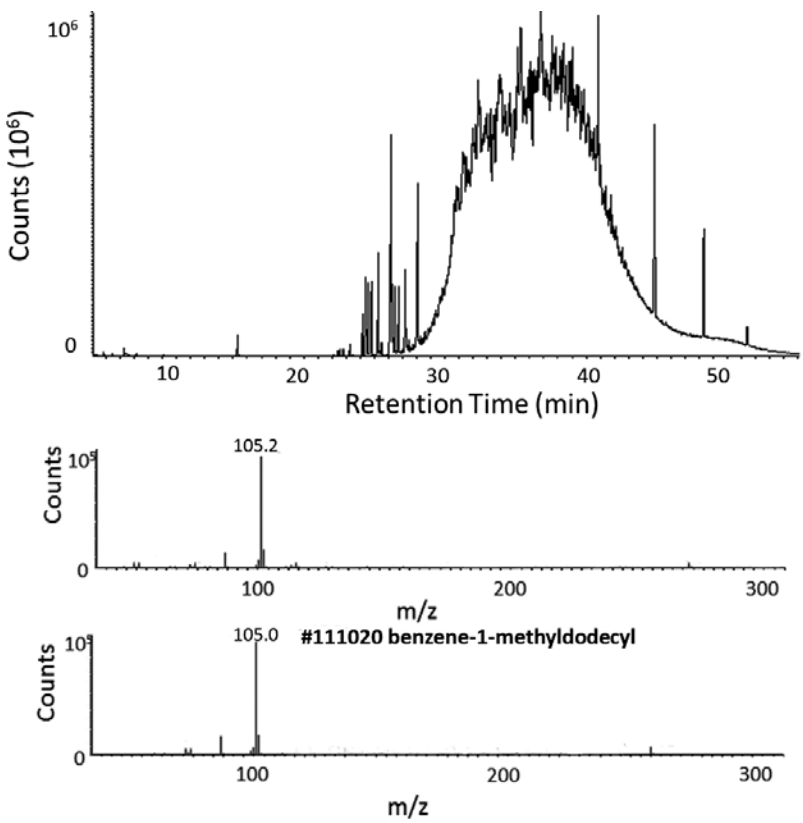

Figure 8. Total ion chromatogram for an alkyl benzene refrigeration lubricant and mass spectrum of peak at 28.034 min (top) and library match (bottom).

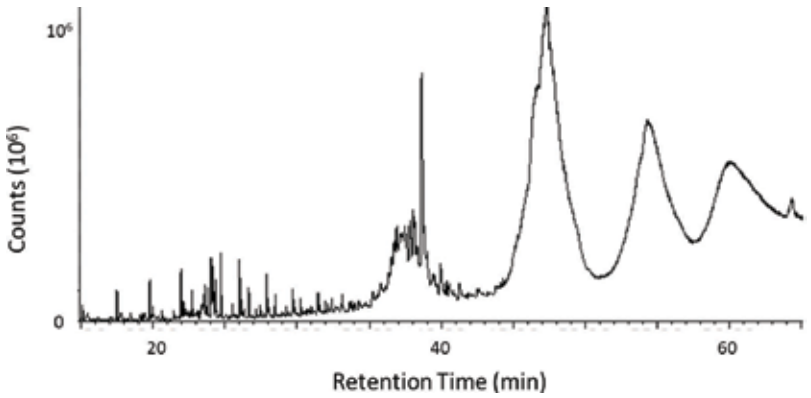

Figure 9. GC-MS chromatogram of a poly alpha olefin lubricant.

Polyalkylene glycol based lubricants were initially developed by the United States Navy as a water soluble, non-flammable hydraulic fluid. As a hydraulic fluid, mixtures of water and glycol had a wide temperature range. Polyalkylene glycol based lubricants that are oil soluble have also found significant application as gear lubricants, particularly for application in wind turbines [44]. The GC-MS chromatograms for several different PAG based oils are shown in **Figure 10**. The chromatograms can be very different depending on the material polymerized, since oils soluble PAGs are typically a mixture of propylene glycol and butylene glycol, where water soluble PAGs are primarily polyethylene glycol based. In many cases, materials of different molecular weights are mixed in order to achieve the correct viscosity and solubility.

Many aerospace lubricants are based on polyol ester base stocks which can be identified based on the polyols and the acids used in the base stock. These lubricants have substantially higher performance than petroleum based lubricants. The lubricants are typically bases on a mixture of polyols and carboxylic acids depending on the desired stability and viscosity. United States military aircraft typically use lubricants with either a MIL-PRF 7808 specification which are based on neopentyl glycol and trimethylolpropane as the alcohol, or MIL-PRF 23699 specification which is based on pentaerythritol esters. The GC-MS total ion chromatogram for two typical polyol

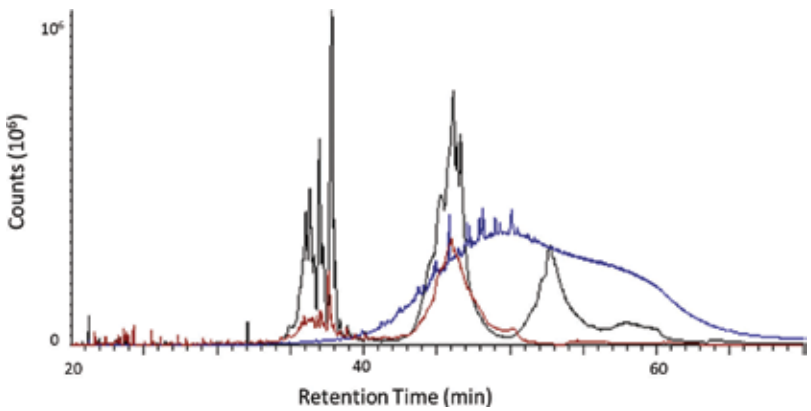

Figure 10. GC-MS chromatograms of three different PAG based lubricants.

ester based lubricants is shown in **Figure 11**. The chromatograms show the effects of a different set of carboxylic acids esterified with pentaerythritol. Using several alcohols and combinations of linear and branched carboxylic acids allows the viscosity and reactivity of the lubricant to be varied considerably.

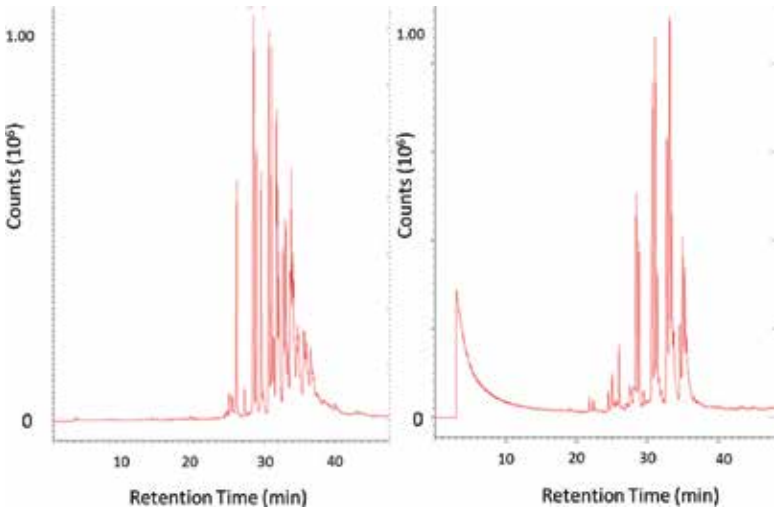

Figure 11. GC-MS total ion chromatogram for two polyol ester based lubricants.

5. Liquid chromatography-mass spectrometry

Gas chromatography-mass spectrometry has seen considerable use in the analysis of fuels and lubricants, but has the primary requirement that all components of the mixture be volatile. High performance liquid chromatography does not suffer from this limitation and can also be used in conjunction with mass spectrometry (LC-MS). LC-MS can be operated in two different separation modes, normal phase in which a polar stationary phase is used and non-polar compounds elute quickly, followed by the polar materials, and reversed phase in which a non-polar stationary phase causes the polar materials to elute first. Both separation modes have been used in the analysis of fuels and lubricants.

LC-MS has been slower to develop than GC-MS, primarily due to the problems associated with the introduction of the sample into the mass spectrometer, without introducing large amounts of the solvent at the same time. This problem has been solved with the development of atmospheric pressure ionization methods. These methods ionize molecules in the sample and allow the majority of the sample to evaporate while drawing charged particles into the mass spectrometer. There are three common atmospheric pressure ionization methods used for the LC-MS of fuels and lubricants; electrospray ionization (ESI), atmospheric pressure chemical ionization (APCI) and atmospheric pressure photoionization (APPI).

Electrospray ionization is an ionization method where a liquid is aspirated into a region where there is a very strong electric field. Ions or clusters of ions are formed in solution and

as the solvent is evaporated by a drying gas, or heated capillary, the analyte forms ions by reaction with ions in solution. The ions are transferred into the mass spectrometer for analysis. Electrospray works well for samples that can gain a proton in positive ion mode or those which can lose a proton in negative ion mode and works well in polar solvents. A major advantage (or disadvantage) is that the hydrocarbons present as the bulk of the fuel or lubricant is not ionized, making the examination of polar species simpler [45].

Atmospheric pressure chemical ionization (APCI) is an ionization method where a corona discharge initially ionizes the nitrogen drying gas, which them ionizes the molecules of interest. APCI does not depend on ionizing the sample while it is still in solution, although recent work has demonstrated that significant ionization does occur in solution [46]. APCI does have the advantage for fuels and lubricants that it can generate ions from neutral species and is useful for low-medium polarity analytes. In many ways APCI is somewhat complementary to ESI for the analysis of polar species in fuels and lubricants.

Atmospheric pressure photoionization (APPI) is a third ionization technique easily available in LC-MS. In APPI, an ultraviolet light source (typically about 10 eV) ionizes a dopant (usually acetone or toluene) added to the mobile phase, which ionizes the analytes. APPI has been show to give higher sensitivity than APCI for certain types of analyte, including polycyclic aromatic compounds and polar aromatic compounds. APPI appears to be an excellent ionization method, especially for polar compounds with low proton affinities [47].

Electrospray ionization has been successfully applied to the identification of nitrogen containing aromatics in crude oil showing a wide range of compound types [48]. Other studies indicated other heteroatom containing compounds could also be ionized and detected using electrospray, including sulfides and aromatics [49]. LC-MS with electrospray ionization has been used to identify several homologous series of nitrogen containing species, including pyridines, anilines, quinolones and carbazoles in several jet fuel samples. **Figure 12** shows the identification of a number of nitrogen containing compounds in a single mass spectrum. It is important to realize that substituted pyridines and substitute anilines can have identical formulas, but very different chemistry.

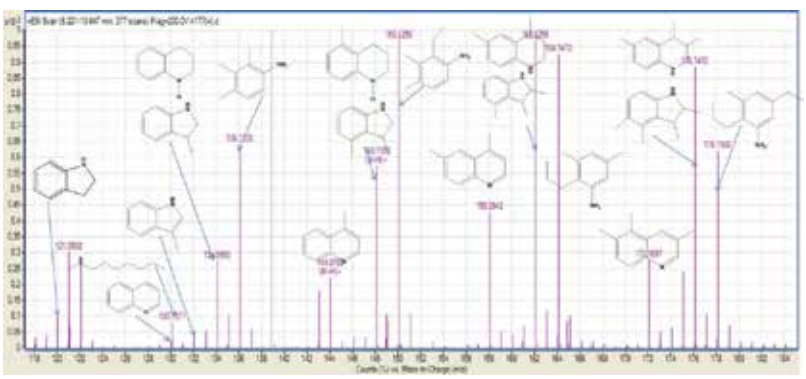

Figure 12. Identification of a number of different nitrogen compounds in the HPLC of a jet fuel sample based on mass spectrometry [50].

Negative ion electrospray has also been used to determine phenols in the same fuels [51]. Phenols are a critical component in low temperature oxidation mechanisms for deposit formation in turbine engines [52]. It has also been shown that fuel additives, especially a corrosion inhibitor/lubricity improver can be determined by LC-MS and ESI ionization in negative ion mode [53]. One of the disadvantages of electrospray ionization is that compound types and functional groups cannot always be identified, even with accurate mass data. In **Figure 13**, the anilines are identified based on the formation of a derivative followed by mass spectrometry. In these cases, a chemical derivatization process may be beneficial in identifying functional groups in conjunction with LC-MS [54].

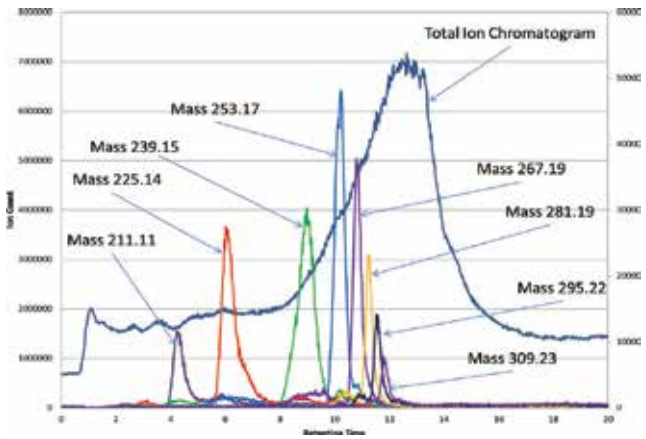

Figure 13. Identification of the anilines based on formation of a derivative with pyridine-2-aldehyde.

6. Conclusions

Mass spectrometry has evolved from a specialist technique for the determination of the bulk characteristics of fuels and lubricants to a general laboratory tool that can be used to answer a wide range of questions. Many of the advances can be traced to advances in technology that have brought about developments in ionization methods, mass separators and ion detectors. Low energy ionization methods allow the trace components with heteroatoms, which are generally more easily ionized to be examined without interference from the major hydrocarbon peaks. The development of high resolution and ultra-high resolution mass spectra has made it possible to determine molecular formulas from each peak in the mass spectrum. This advance has made it clear that petroleum based fuels and lubricants are more complex than was previously thought.

A potentially more important advance mass spectrometry has been the incorporation of separation techniques and library searching procedures which allow complex mixtures to be separated into individual components which can then be identified. Coupling of mass spectrometry with gas chromatography and liquid chromatography has provided tools to

examine complex mixtures without the ultimate in mass resolving power. Coupling of chromatography with mass spectrometry using new ionization methods which reduce the fragmentation have allowed molecular weights of compounds to be determined. While electron impact mass spectra can readily be searched through available libraries to identify individual components in the fuels and lubricants.

Author details

David W. Johnson

Address all correspondence to: djohnson1@udayton.edu

Department of Chemistry, University of Dayton, Dayton, Ohio, USA

References

[1] Williams JD, Burinsky DJ. Mass spectrometric analysis of complex mixtures then and now: The impact of linking liquid chromatography and mass spectrometry. International Journal of Mass Spectrometry. 2001;**212**:111-133. DOI: 10.1016/S1387-3806(01)00460-2

[2] McLafferty FW, Turecek, F. Interpretation of Mass Spectra, 4th ed. Sausalito, California: University Science Books; 1993. ISBN:978-0-935702-25-5

[3] Watson JT, Sparkmen OD. Introduction to Mass Spectrometry: Instrumentation, Applications, and Strategies for Data Interpretation, 4th ed. West Suffix, England: Wiley Books; 2007. ISBN: 978-0-470-51634-8

[4] McMaster MC. GC/MS. A Practical User's Guide 2nd Edition. Hoboken New jersey: John Wiley and Sons; 2008. ISBN: 978-0470101636

[5] McMaster MC. LC/MS. A Practical User's Guide. Hoboken, New Jersey: John Wiley and Sons; 2005. ISBN: 978-0471655312

[6] Rakow MS. Petroleum oil refining. In: Totten GE, Westbrook SR, Shah RJ,editors. Fuels and Lubricants Handbook. West Conshohocken, Pennsylvania: ASTM International; 2003: pp. 3-30

[7] Schulz H: Short history and present trends of Fischer-Tropsch synthesis. Applied Catalysis A. 1999;**186**:3-12. DOI: 10.1016/S0926-860X(99)00160-X

[8] Rye L, Blakey S, Wilson CW. Sustainability of supply or the planet: A review of potential drop-in alternative aviation fuels. Energy and Environmental Science. 2010;**3**:17-27. DOI:10.1039/b918197k

[9] Rizvi SQU. A Comprehensive Review of Lubricant Chemistry, Technology, Selection, and Design. West Conshohocken, Pennsylvania: ASTM International; 2009

[10] Brewer AK, Dibeler VH. Mass spectrometric analyses of hydrocarbon and gas mixtures. Journal of research of the National Bureau of Standards. 1945;**35**:125-139. DOI:10.6028/jres.035.003

[11] Washburn HW, Wiley HF, Rock SM, Berry CE. Mass spectrometry; Industrial and Engineering Chemistry, Analytical Edition. 1945;**12**:74-81. DOI: 10.1021/i560138a003

[12] Brown RA, Taylor RC, Melpolder FW, Young WS. Mass spectrometer analysis of some liquid hydrocarbon mixtures. Analytical Chemistry. 1948;**20**:5-9. DOI: 10.1021/ac60013a002

[13] Brown, RA. Compound types in gasoline by mass spectrometer analysis. Analytical Chemistry. 1951;**23**:430-435; DOI: 10.1021/ac60051a012

[14] Lumpkin, HE, Johnson, BH. Identification of compound types in a heavy petroleum oil. Analytical Chemistry. 1954;**25**:1719-1722. DOI: 10.1021/ac60095a012

[15] Snyder, LR. Routine compound class separation and analysis of heavy petroleum fractions by adsorption chromatography. Analytical Chemistry. 1965;**37**:713-717; DOI: 10.1021/ac60225a022

[16] Field FH, Hastings SH. Determination of unsaturated hydrocarbons by low voltage mass spectrometry. Analytical Chemistry. 1956;**28**:1248-1255. DOI: 10.1021/ac60116a005

[17] Lumpkin HE, Aczel T. Low voltage sensitivities of aromatic hydrocarbons. Analytical Chemistry. 1964;**36**:181-184. DOI: 10.1021/ac60207a057

[18] Ashcroft AE. Ionization methods in organic mass spectrometry, RSC analytical spectroscopy series. In: Barnett NW, editors. Royal Society of Chemistry, 1997, London, 1-186; DOI:10.1039/9781847551191

[19] Grigsby RD, Scheppele SE, Grindstaff QG, Sturm, Jr. GP, Taylor LCE, Tudge H, Wakefield C, Evans S. Evaluation of fast atom bombardment mass spectrometry for the identification of nitrogen-containing compounds in fossil fuels. Analytical Chemistry. 1981;**54**:1108-1113. DOI: 10.1021/ac00244a022

[20] Gallegos EJ, Green JW, Lindeman LP, LeTourneau RL, Teeter RM. Petroleum group type analysis by high resolution mass spectrometry. Analytical Chemistry. 1967;**39**:1833-1838. DOI: 10.1021/ac50157a055

[21] Lumpkin HE. Analysis of a trinuclear aromatic petroleum fraction by high resolution mass spectrometry. Analytical Chemistry. 1964;**36**:2399-2401. DOI:10.1021/ac60219a006

[22] Johnson BH, Aczel T. Analysis of complex mixtures of aromatic compounds by high-resolution mass spectrometry at low ionizing voltages. Analytical Chemistry. 1967;**39**:682-685. DOI: 10.1021/ac60250a035

[23] Marshall AG, Hendrickson CL, Jackson GS. Fourier transform ion cyclotron resonance mass spectrometry: A primer. Mass Spectrometry Reviews. 1998;**17**:1-35. DOI: 10.1002/(SICI)1098-2787(1998)17:1<1::AID-MAS1>3.0.CO;2-K

[24] Hendrickson CL, Quinn JP, Kaiser NK, Smith DF, Blankey GT, Chem T, Marshall AG, Weisbrod CR, Beu SC. 21. Tesla Fourier transform ion cyclotron resonance mass spectrometer: A national resource for ultrahigh resolution mass analysis. Journal of the American Society for Mass Spectrometry. 2015;**26**:1626-1632. DOI: 10.1007/s13361-015-1182-2

[25] Corilo YE, Podgorski DC, McKenna AM, Lemkau KL, Reddy CM, Marshall AG, Rodgers RP. Oil spill source identification by principal component analysis of electrospray ionization Fourier transform ion cyclotron resonance mass spectra. Analytical Chemistry. 2013;**85**:9064-9069. DOI: 10.1021/ac401604u

[26] Ruddy BM, Fuettel M, Kostka JE, Lobodin VV, Bythell BJ, McKenna AM, Aeppli C, Reddy, CM, Nelson RK, Marshall AG, Rodgers RP. Targeted petroleomics: Analytical investigation of Macondo well oil oxidation products from Pensacola Beach. Energy and Fuels. 2014;**28**:4043-4050. DOI: 10.1021/ef500427n

[27] Rodgers RP, White FM, Hendrickson CL, Marshall AG, Andersen KV. Resolution: Elemental composition and simultaneous monitoring by Fourier transform ion cyclotron resonance mass spectrometry of organosulfur species before and after diesel fuel processing. Analytical Chemistry. 1998;**70**:4743-4750. DOI: 10.1021/ac980487i

[28] Japes A, Penassa M, Andersson JTL. Analysis of recalcitrant hexahydrodibenzothiophenes in petroleum products using a simple fractionation process. Energy and Fuels. 2009;**23**:2143-2148. DOI: 10.1021/ef8010228.

[29] Haddad R, Regiani T, Klitzke CF, Sanvido GB, Corilo YE, Augusti DV, pasa VMD, Pereira CC, Romao W, Vas BG, Augusti R, Eberlin MN. Gasoline, kerosene and diesel fingerprinting via polar markers. Energy and Fuels. 2012;**26**: 3542-3547. DOI: 10.1021/ef300277c

[30] Bauserman JW, Mushrush GW, Hardy DR. Organic nitrogen compounds and fuel instability in middle distillate fuels. Industrial & Engineering Chemistry Research. 2008;**47**:2867-2875. DOI: 10.1021/ie071321n

[31] Rostad CE. Differentiation of commercial fuels based on polar components using negative electrospray ionization/mass spectrometry. Environmental Forensics. 2006l;**7**:5-14. DOI: 10.1080/15275920500351684

[32] Rodgers R, Blumer EN, Freitas MA, Marshall AG. Complete compositions from Fourier transform ion cyclotron resonance mass spectrometry. Environmental Science & Technology. 2000;**34**: 1671-1678. DOI:10.1021/es9907991i

[33] Watson JT. A historical perspective and commentary on pioneering developments in gas chromatography/mass spectrometry at MIT. Journal of Mass Spectrometry. 1998;**33**: 103-108. DOI:10.1002/(SICI)1096-9888(199802)33:2<103::AID-JMS633>3.0.CO;2-Z

[34] Gohike RS, McLafferty FW. Early gas chromatography/mass spectrometry. Journal of The American Society for Mass Spectrometry. 1993;**4**:367-371. DOI:10.1016/1044-0305(93)85001-E

[35] Kostecka KS, Rabah A, Palmer Jr: CF.GC/MS analysis of the aromatic composition of gasoline. Journal of Chemical Education. 1995:**72**: 853-854; DOI: 10.1021/ed072p853

[36] Johnson KJ, Morris RE, Rose-Pehrsson. Evaluating the predictive powers of spectroscopy and chromatography for fuel quality assessment. Energy and Fuels. 2006;**20**:727-733. DOI:10.1021/ef050347t

[37] Cramer JA, Hammond MH, Myers, KM, Loegel TN, Morris RE. Novel data abstraction strategy utilizing gas chromatography-mass spectrometry data for fuel property modeling. Energy and Fuels. 2014;**28**:1781-1791. DOI:10.1021/ef4021872

[38] Loegel TN, Morris RE, Myers KM, Katilie CJ. Analysis of phenolic antioxidants in Navy mobility fuels by gas chromatography-mass spectrometry. Energy and Fuels. 2014;**28**: 6267-6274. DOI: 10.1021/ef5013984

[39] Dorman FL, Whiting JJ, Cochran JW, Gardea-Torresdey J. Gas chromatography. Analytical Chemistry. 2010;**82**:4775-4785. DOI:10.1021/ac101156h

[40] Johnson DW. Lubricants for turbine engines. In: Agarwal, RK, editors. Recent Progress in Some Aircraft Technologies. Rijeka, Croatia: InTech;2016. 35-54; DOI: 10.5772/62394

[41] Johnson DW. The tribology and chemistry of phosphorus-containing lubricant additives in Advances. In: Darli PH, editors. Tribology. Rijeka, Croatia: InTech;2016. 175-196; DOI; 10.5772/62208

[42] Semnani A, Langeroodi HS. The application of heavy alkyl benzene in engine oil and hydraulic fluid Formulations. Petroleum Science and Technology. 2014;**32**:2414-2421. DOI:10.1080/10916466.834934

[43] Benda B, Bullen J, Plomer A. Synthetics basics: Polyalphaolefins—base fluids for high performance lubricants. Journal of Synthetic Lubricants. 1996;**13**:41-57. DOI:10.1002/jsl.3000130105

[44] Lawford S. Polyalkylene glycols. In: Synthetics, Mineral Oils and Bio-Based Lubricants: Chemistry and Technology. Rudnick LR, editors. Boca Raton, FL: CRC Press; 2005. DOI:10.1201/9781420027181.ch6

[45] Tamashita M, Fenn JB. Electrospray ion source. Another variation on the free-jet theme. The Journal of Physical Chemistry. 1984;**88**:4451-4459. DOI: 10.1021/j150664a002

[46] Rebane R, Kruve A, Liigand P, Liigang J, Herodes K, Leito I. Establishing atmospheric pressure chemical ionization efficiency scale. Analytical Chemistry. 2016;**88**:3435-3438. DOI:10.1021/acs.analchem.5b04852

[47] Robb DR, Covey TR, Bruins AP. Atmospheric pressure photoionization: An ionization method for liquid chromatography-mass spectrometry. Analytical Chemistry. 2000;**72**: 3653-3659. DOI: 10.1021/ac0001636

[48] Rodgers RP, Hendrickson CL, Emmett MR, Marshall AG. Reading chemical fine print: resolution and identification of 3000 nitrogen-containing aromatic compounds from a single electrospray ionization Fourier transform ion cyclotron resonance mass spectrum of heavy petroleum crude oil. Energy and Fuels. 2001;**15**:492-498. DOI:1021.ef000255y

[49] Qian K, Edwards KE, Diehl JH, Green LA. Fundamentals and applications of electrospray ionization mass spectrometry for petroleum characterization. Energy and Fuels. 2004;**18**:1784-1791.DOI:10.1021/ef049883w

[50] Johnson DW, Adams R, West Z, Striebich RC, Zabarnick S. Identification of Nitrogen Containing Contaminants in Jet Fuel by HPLC-MS and Chemical Derivatization. Pittsburg Conference on Analytical Chemistry and Applied Spectroscopy. Orlando, FL. March 2012

[51] Adams RK, Zabarnick S, West ZJ, Striebich RC, Johnson DW. Chemical analysis of jet fuel polar, heteroatomic species via high performance liquid chromatography with electrospray ionization mass spectrometric detection. Energy and Fuels. 2013;**27**:2390-2398. DOI: 10.1021/ef3015298

[52] Aksoy P, Gul O, Cetiner R, Fonseca DA, Sobkowiak M, Falcone-Miller S, Miller BG, Beaver B. Insight into the mechanism of middle distillate fuel oxidative degradation. Part 2: on the relationship between jet fuel thermal oxidative deposit, soluble macromolecular oxidatively reactive species, and smoke point. Energy and Fuels. 2009;**23**:2047-2051. DOI: 10.1021/ef8007008

[53] Johnson DW, Adams R, Flake M. Determination of corrosion inhibitor-lubricity improver in jet fuels by liquid chromatography-electrospray ionization mass spectrometry. LC-GC, Special Issues 2014;**12**:26-32

[54] Johnson DW, Adams RK, Striebich RC, West ZJ, Zabarnick SS. Analysis of polar components in jet fuel by high performance liquid chromatography/time of flight mass spectrometry with electrospray ionization. Energy and Fuels Division: Preprints, Energy and Fuels Division, American Chemical Society 2012. meeting 248. 403–404. http://pubs.acs.org/cgi-bin/preprints/display?div=fuel&meet=244&page=403.pdf

Chapter 8

Mass Spectrometry for the Detection of Endogenous Steroids and Steroid Abuse in (Race) Horses and Human Athletes

Decloedt Anneleen, Van Landschoot Anita and Vanhaecke Lynn

Additional information is available at the end of the chapter

http://dx.doi.org/10.5772/intechopen.68593

Abstract

The higher the pressure to win, the more athletes are inclined to take steps to improve one's performance through questionable means. To minimize this, strict anti-doping and medication rules are being enforced. All human and equine athletes are regularly subjected to doping analysis to prevent abuse of forbidden substances from affecting their performance. Anabolic-androgenic steroids (AASs) have been part of the forbidden substances list for years, because of their muscle building and performance-enhancing capacities and possible side effects. For most of the AAS, zero-tolerance is held. However, some AASs can be endogenous to the athletes, such as for example testosterone in males. These endogenous steroids can render it very difficult to reveal steroid abuse. Specific mass spectrometric (MS) methods, including ultra-high performance liquid chromatography-MS (UHPLC-MS/MS), high resolution mass spectrometry (HRMS) and gas chromatography–combustion-isotope ratio MS (GC-C-IRMS), have been put forward to overcome these analytical difficulties. Currently, high-tech metabolomic methods are being used to build athlete specific biological passports. In the near future, these passports might allow putting a stop to abuse, by staying ahead of the cheats. These are bright prospects, leading towards clean and fair sports competitions worldwide.

Keywords: steroids, doping, natural, horses, athletes

INTECH
open science | open minds

© 2017 The Author(s). Licensee InTech. This chapter is distributed under the terms of the Creative Commons Attribution License (http://creativecommons.org/licenses/by/3.0), which permits unrestricted use, distribution, and reproduction in any medium, provided the original work is properly cited. CC BY

1. Introduction

1.1. Steroid structures

Steroids are cyclic, organic compounds with basic skeleton 17 carbon atoms (C17) arranged in a four-ring structure: three C6 rings, followed by a C5 ring and a C8 side chain linked to C-17. The four-ring structure is formed after cyclization of a C30 chain, squalene, into lanosterol or cycloartenol [1]. The three cyclohexane rings are designated as rings A, B and C and the cyclopentane ring as ring D. The three cyclohexane rings form the skeleton of a perhydro-derivative of phenanthrene. The D-ring has a cyclopentane structure; hence, though it is uncommon, IUPAC steroids can also be named as various hydro-derivatives of cyclopentaphenanthrene (**Figure 1A**). This 17-carbon compound is also called gonane, the simplest steroid and a substructure present in most steroids. When the two methyl groups (C-10 and C-13) and C8 side chain (at C-17) are present, the steroid is said to have a cholestane framework (5α-cholestane, a common steroid core, e.g. cholesterol, **Figure 1B**). Cholesterol is the precursor of steroids in both humans and animal species [2].

Despite the shared basic steroid skeleton, hundreds of different steroids can be found in animals, plants and even fungi. They include the sex hormones such as 17β-estradiol and testosterone, bile acids, phytosterols, cortisol and drugs such as the anti-inflammatory corticosteroids (e.g. dexamethasone, prednisolone), ergosterols and many more. Individual steroids vary by the oxidation state of the carbon atoms in the rings (single or double bounds) and by the chain and functional groups attached to the four-ring skeleton [3].

Additionally, steroids can vary more markedly via changes to the ring structure (e.g. via ring scissions that produce secosteroids). Secosteroids enhance intestinal absorption of calcium, iron, magnesium, phosphate and zinc. In humans, the most important compounds in this group are vitamin D3 (also known as cholecalciferol) and vitamin D2 (ergocalciferol) [4]. Sterols, including cholesterol and phytosterols, are another particularly important form of steroids, having a cholestane-derived framework and a *hydroxyl group* at the C-3 position (e.g. cholesterol, **Figure 1B**) [5]. These closely related chemical structures of the different steroids already illustrate the challenges faced with steroid detection, identification and quantification methods.

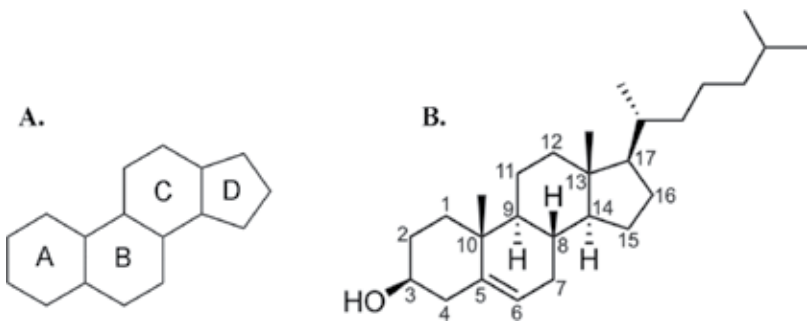

Figure 1. (A) Chemical structure of the basic steroid cyclopentaphenanthrene skeleton including IUPAC-approved ring lettering and (B) chemical structure of cholesterol, including all normally seen branches, atom numbering and stereochemistry.

1.2. Natural steroids and their role in the endocrine system

Hormones are chemical compounds that are naturally produced by both animals and human beings and have a number of important functions in life, such as reproduction and growth. They act as *signalling* molecules between the different parts of the organism and trigger and modulate key reactions to support and promote life [6]. The most well-known hormones are the *steroid hormones*, e.g. 17β-estradiol, progesterone and testosterone, which are involved in endocrine regulation pathways. Next to influencing *reproduction and growth*, these steroids play other important roles as well. Testosterone regulates protein synthesis, 17β-estradiol triggers protein disposition and progesterone has an antagonistic role in oestrogens.

In mammals, including horses and humans, steroid hormones are secreted primarily by the *testicles* of males and the *ovaries* of females, although smaller amounts are also secreted by the *adrenal glands* (**Figure 2**). The adrenal glands are located just in front of the kidneys and consist of two parts, the cortex and the medulla. The *adrenal cortex* consists of three layers, each of which produces a different set of steroid hormones. The *inner layer* produces sex hormones such as oestrogen and progesterone [6, 7].

Next to adrenal and gonadal production of steroids, recent papers implied that *uterine and oviductal tissues* can produce steroids as well [8–10]. Adipose tissue is also no longer considered to be an inert tissue that stores fat. *White adipose tissue (WAT)* is now being recognized as a major endocrine and secretory organ, releasing a wide range of protein factors and signals termed adipokines, in addition to fatty acids and other lipid moieties [11, 12].

In general, steroid hormone biosynthesis involves a battery of oxidative enzymes located in two distinct cell organelles: mitochondria and the endoplasmic reticulum (ER). The transport of free cholesterol from the cytoplasm into mitochondria is the rate-limiting step in this process. CYP11A1, an enzyme bound to the inner membrane of mitochondria, will initiate the biosynthesis by converting cholesterol into pregnenolone. *Pregnenolone* (3β-hydroxypregn-5-en-20-one, also known as P5) undergoes further steroid metabolism in one of three ways, making it the immediate precursor for the synthesis of all of the other steroid hormones, including progestogens, mineralocorticoids, glucocorticoids, androgens and oestrogens, as well as the neuroactive steroids [1].

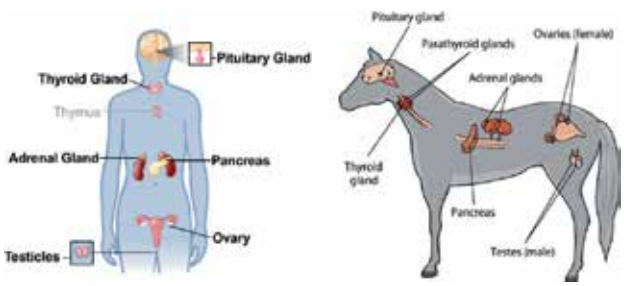

Figure 2. Endocrine system of humans and horses. The adrenal glands and gonads (ovaries in females and testicles in males) are the main organs involved in steroid biosynthesis. Reproduced from https://medlineplus.gov/endocrinesystem.html and the Merck Veterinary Manual (2010).

1.3. Anabolic-androgenic steroids (AAS)

The term anabolic-androgenic steroids (AASs) is used to group the naturally occurring male *sex hormone* testosterone, testosterone precursors and metabolites, and sometimes also (synthetically) produced testosterone variants [13, 14]. 'Anabolic' refers to the muscle-building capacity, 'androgenic' refers to increased male sexual characteristics and 'steroid' refers to the class of these compounds (Section 1.1).

Valid medicinal use of AAS is limited. It is only allowed to use it in the treatment of patients with a negative nitrogen balance, like weakened horses, or to accelerate healing after trauma or surgery. Anabolic steroids can be given by injection, taken orally or used externally. In humans, AASs are classified as controlled substances, due to the possibility of serious adverse effects and a high potential for abuse, as these hormones increase lean muscle mass and can improve athletic performance.

Nevertheless, *non-therapeutic (abuse)* of AAS has been a matter of all times. The first widespread usage of steroids and other forbidden substances in horses dates back to the early 1960s and 1970s (**Figure 3**). In humans, the first documented use of testosterone as a performance-enhancing substance in sport was already reported in the early 1950s. Russian weightlifters out-competed all other athletes and their trainers conceded that they were using testosterone.

Anti-doping policies in horse racing and other horse sports date back to the '1960s. In May 1968, the first horse, Dancer's Image, winner in the Kentucky Derby, was disqualified for using a banned substance. Traces of phenylbutazone, a non-steroidal anti-inflammatory drug (NSAID), were found in his urine post-racing (**Figure 3**).

Figure 3. Jockey Bob Ussery celebrating with Dancer's Image after his fraudulent win at Kentucky Derby in 1968.

http://dx.doi.org/10.5772/intechopen.68593

2. Doping regulations for horses and humans

2.1. Human athletes

In response to the widespread (abuse) of steroids, the American Congress developed the *Anabolic Steroids Control Act in 1990*, placing steroids in the same legal class (class III controlled substances) as amphetamines, methamphetamines, opium and morphine. The World Conference on Doping in Sport held in Lausanne (1999) produced the Lausanne Declaration on Doping in Sport. This document provided for the creation of an independent international anti-doping agency to be fully operational for the Olympic Games in Sydney (2000). Pursuant to these terms set by the Lausanne Declaration, the *World Anti-Doping Agency (WADA)* was established on the 10th of November 1999 (Lausanne, Switzerland). Since then WADA aims to promote and co-ordinate the fight against doping in sport internationally. WADA was founded under the initiative of the International Olympic Committee (IOC), and the IOC still occupies 50% of the positions within the agency. The other 50% of the representatives belong to inter-governmental organizations and governments, public authorities and other public and private bodies that are also involved in the fight against doping in sport [15].

Currently, AASs are still classified as *class III controlled substances (class S1 anabolic agents)*, they are part of the first section of WADA's List of Prohibited Substances and Methods (2017), which discusses substances and methods that are prohibited at all times, both in-competition and out-of-competition, and any athlete can be tested for these substances at any time. The list of anabolic agents is extensive and even if one is not specifically listed, it is still prohibited if it is a metabolite or has a similar chemical structure or similar biological effect(s) to anabolic agents (WADA, 2017 List of Prohibited Substances and Methods). The list includes both exogenous (S1 1.a.) and endogenous anabolic-androgenic steroids (when administered exogenously) (S1 1.b.).

2.2. Race and sport horses

Race and sport horses are, just like human athletes, frequently subjected to doping controls to guarantee a safe and fair competition. *Fédération Equestre Internationale (FEI)*, responsible for all Olympic disciplines including jumping, dressage, endurance and eventing and International Federation of Horseracing Authorities (IFHA) regulations state that '*any use of substances with a potential to affect equine performance, health or welfare and/or with a high potential for misuse is contrary to the integrity of equestrian sport and the welfare of the horses*'.

As strict *zero-tolerance* has been held for many years, anabolic-androgenic steroids might seem to be an issue of the past as new and possibly more effective *'designer' drugs* have been developed over the years (e.g. AICAR, a metabolic modulator and TB-500, a synthetic peptide stimulating muscle development in horses [16, 17]). However, *recent cases* of steroid abuse (FEI equine anti-doping decisions, 2013–2016) prove that, although AAS abuse is better under control than it was some decades ago, it will be of all times. The potential of AAS to improve performance remains too tempting to some trainers and riders, and not only in racing and endurance. If Group VII (Middle-East) countries were excluded from the endurance records,

endurance worldwide even has a cleaner AAS abuse record than *show jumping*. This illustrates that, unfortunately and despite great efforts from the regulatory bodies, AAS abuse is still *rooted deeply* into different equine sport disciplines at both the amateur and professional level.

Additionally, there is no worldwide restriction to the use of AAS as growth promoting and performance-enhancing agents. Boldenone (Bol), androstadienedione (ADD) and Bol esters, for example, are easily available on the (European) *black market* as anabolic preparations, imported from the US [18]. In the *United States,* it also took until 2008 for steroids to be banned from the racing courses. Under this more recent law, a horse may be given steroids only under certain therapeutic conditions, and a horse may not race for at least 60 days afterwards (Press release, Kentucky Horse Racing Commission website, September 5, 2008 and Racing Medication and Testing Consortium (RMTC), 2008). In *Australia,* anabolic steroids were only prohibited on race day, but a new total ban (November 1st 2013 and effective from May 1st 2014, Australian Racing Board, ARB) applies to all thoroughbreds from the age of 6 months, both in- and out-of-competition. These decisions have been welcomed by the IFHA and FEI, to further two of their key objectives, being to co-ordinate and harmonize the rules of all member countries worldwide.

3. How endogenous AAS complicate anti-doping analysis

Steroids can be classified into *three broad classes*: exogenous, designer and endogenous steroids. With the present-day AAS abuse issue in mind, the development of new and better detection techniques is needed to detect and to distinguish between steroids belonging to these different classes. Additionally, not only AAS but also oestrogens, gestagens and androgens (EGAs) as well as thyreostats, corticosteroids and β-agonist compounds, are used alone or in growth promoting *'cocktails'* with low concentrations of several compounds, compromising their detection [6].

Since the first discovery of AAS over 50 years ago, numerous anabolic-androgenic steroids with a variety of functional groups have been produced and/or published. Only a small number of them, the so-called 'known' *exogenous steroids*, have made it to the pharmaceutical market and are still available on the market today. They contain synthetic structures that do not occur in natural steroids (e.g. stanozolol and trenbolone, **Figure 4**). Confirmation of exogenous steroid abuse is relatively straightforward as *qualitative demonstration* of the compound in the sample suffices.

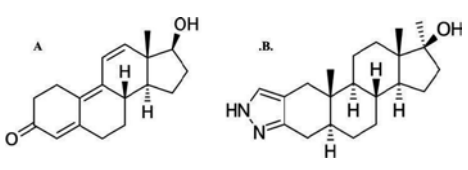

Figure 4. Chemical structures of exogenous steroids: (A) trenbolone (also known as Revalor, Parabolan, Hexabolan, Finaplix, trienolone, trienbolone or Tren), and (B) stanozolol (Winstrol, Winny). Stanozolol and trenbolone both contain a synthetic, conjugated system.

Designer steroids are similar to exogenous steroids, containing synthetic structures that are thought not to occur naturally, but they have not yet been classified as controlled substances and in many cases, like a pro-hormone, require a chemical reaction or enzymatic alteration once in the body to become active [19]. In most cases, they possess additional minor modifications compared to the well-known marketed exogenous steroids. These minor changes render their detection with *targeted mass spectrometry* more difficult, due to the *lack of standards*. An additional worrying feature is that no data are available on the efficacy and safety of the use of these compounds [19].

Endogenous steroids, such as testosterone, are steroids that are known to exist naturally, in one or more animal species (see also **Tables 1** and **2**) [20]. Confirmation of endogenous steroids abuse is difficult, as simple qualitative or quantitative detection of the compound does not suffice. In horses, only testosterone and 17β-boldenone are generally regarded as endogenous (respectively in all horses and in stallions only) (Section 3.1). The classification of a steroid as 'endogenous' is, however, a *grey area*. The 'semi'-endogenous presence of 17β-boldenone and related compounds, for example, in mares and geldings, is a complicating factor in doping control. Proper investigation on the origin of these AASs is required to continue to ensure adequate doping policies in the future [20, 21] (Section 4).

3.1. Reference ranges for AAS in humans and horses

Over the years, multiple studies have measured *excreted concentrations* of testosterone in humans, both in blood plasma and in urine (**Table 1**). On average-levels of testosterone are up to 10 times as great in adult males as in adult females [22]. The reference ranges for blood test of adult males are between 1.8 and 7.5 ng/mL (>50 years old) and 2.90 and 13 ng/mL (<50 years old), while the reference range for adult females is between 0.2 and 0.85 ng/mL [23, 24]. As the metabolic consumption of testosterone in males is greater too, the daily production was estimated to be about *20 times higher in men* [25].

Futterweit et al. were one of the first to set a reference range for testosterone in urine, using thin layer chromatography (TLC) and gas chromatography (GC) [26]. Doberne and New and Tresguerres et al. on the other hand used a, at that time, very new and high-tech isotopically labelled ligand binding assay (Radioimmunoassay, RIA) [27, 28]. Mass spectrometric (MS) methods, coupled to either gas chromatography (GC) or liquid chromatography (LC), were introduced later on in the 1980s and 1990s and used for all types of anti-doping screening and quantitative methods [29–32]. Pesant et al. were an exception, using a competitive immunochemiluminescent assay for the determination of testosterone concentrations [23]. The detailed evolution of analytical methods used for steroid detection will be discussed in detail later on in this chapter (Section 5.1).

Generally, less data are available regarding the normal ranges of excretion of testosterone and its related metabolites in horses. *Testosterone* and its precursors/metabolites are known to be endogenous in males (stallions and geldings) and female horses at varying concentrations [20]. In a recent study, high performance liquid chromatography/mass spectrometry (HPLC-MS) was used to investigate the effect of γ-oryzanol supplementation on endogenous testosterone levels in horses. During that study, urine β-testosterone concentrations were always

Reference	Population	Male		
		n	Mean (ng/mL)	Outliers (ng/mL)
Futterweit et al. [26]	American	10	114*	167*
Doberne et al. [27]	American	10	56*	n.a.
Tresguerres et al. [28]	American	26	100*	231*
Gonzalo-Lumbreras et al. [29]	Spanish	12	125**	191**
Van Renterghem et al. [30]	Caucasian	2027	37	>100
Martinez-Brito et al. [31]	Latin-American	2454	60	>200
Moon et al. [32]	Korean	337	26	>150

*Recalculated based upon an expected average daily urine excretion of 1.5 L/day.
**Samples were collected early in the morning, at the maximum of the excretion curves.
n.a. data non available.

Table 1. Reference ranges for total testosterone in urine of humans (male).

Reference	Population	Female		
		n	Mean (ng/mL)	Outliers (ng/mL)
Futterweit et al. [26]	American	10	4.0*	5.3*
Doberne et al. [27]	American	10	2.8*	n.a.
Tresguerres et al. [28]	American	16	16*	n.a.
Van Renterghem et al. [30]	Caucasian	1004	12	200
Martinez-Brito et al. [31]	Latin-American	1181	13	54

*Recalculated based upon an expected average daily urine excretion of 1.5 L/day.
n.a. data non available.

Table 2. Reference ranges for total testosterone in urine of humans (female).

lower than 1.7 ng/mL for mares and geldings, Mösseler [33]. Both Ho et al. and Popot et al. measured β-Bol, ADD as well as testosterone in urine (and faeces) of (male) horses [34, 35]. Ho et al. used an immunoaffinity column (IAC) purification, followed by liquid chromatography/mass spectrometry (LC-MS/MS) analysis on a quadrupole-time of flight (Q-ToF) instrument while Popot's extraction protocol included diethylether extraction, lipid removal, HPLC purification, derivatization and GC-EI/MS/MS detection. Testosterone levels measured by Popot et al. were between 71 and 214 ng/mL (stallions). If urine samples are being analysed with gas chromatography/mass spectrometry (GC-MS) for the identification of cryptorchidism (presence of an undescended testis in geldings), a cut-off level of 8 ng/mL is held as a marker. Testosterone levels below 8 ng/mL are regarded normal for geldings and, according to these thresholds, no β-Bol should be found in geldings [36]. Bonnaire et al. found that plasma concentrations for cycling mares vary between 20 and 60 pg/mL and can go up to 245–350 pg/mL in bearing mares. Urine concentrations in cycling mares were found to be between 1.4 and 20.1 ng/mL (GC-MS) [37].

β-Boldenone levels measured by Popot et al. (GC-EI/MS/MS) in stallions varied between 1.0 and 2.9 ng/mL urine (n = 7) [35]. The range of free and conjugated (e.g. boldenone sulphate) determined by Ho et al. (LC-MS/MS, Q-ToF) was between 0.1 and 4.34 ng/mL (n = 63, from 37 male horses), and the mean was 1.27 ± 1.03 ng/mL [34]. Boldenone was not detected in geldings (n = 8), in line with the results of Leung et al. (GC-MS) [36]. The mean β-boldenone concentration measured in male horses by Dehennin et al. (GC-MS) was 0.34 ng/mL (minimum 0.02, maximum 1.51 ng/mL) (n = 156) [38].

3.2. Threshold levels for endogenous steroids

Additionally, as sport horses are frequently subjected to doping analysis, normal levels can be derived from anti-doping regulatory bodies *accepted levels*. Very strict zero-tolerance policies are held for most steroids, but exceptions have been made for the naturally occurring androgenic steroids: boldenone and testosterone (and stanozolol and nandrolone, according to a limited number of regulatory organs) (**Table 3**).

Pu et al. were able to directly detect boldenone sulphate and glucuronide conjugates in horse urine by ion trap liquid chromatography-mass spectrometry [39] and Ho et al. [34] and Popot et al. [35] also found endogenous *β-boldenone* in urine and faeces of entire males. Following these results, IFHA (Article 6, 2017), RMTC (Banned Medication List, 2017) and FEI (2017 Equine Prohibited Substances List) abandoned the zero-tolerance policy for entire male horses; a threshold for free and conjugated boldenone of *15 ng/mL* was set. Despite this threshold for *stallions*, the presence of β-Bol in urine from mares or geldings is still prohibited. Nevertheless, occasionally traces of β-Bol or related metabolites have been found in urine of horses that were not treated with AAS [40].

For *testosterone*, thresholds were set for mares and fillies (unless in foal), up to 55 ng/mL free and conjugated testosterone in urine and *20 ng/mL* urine for geldings are allowed. For entire male horses, *amounts in excess of amounts existing naturally in the untreated horse at normal physiological concentrations* are considered to be non-naturally occurring physiological concentrations. The international threshold for testosterone in *plasma* is 100 pg/mL for geldings. Currently, no threshold for mares is set yet, but it is being suggested to introduce the same threshold of *100 pg/mL* (IFHA and FEI, 2017).

For *nandrolone or nortestosterone* (free and conjugated), the RMTC threshold was set at 1 ng/mL in urine (geldings, fillies and mares). In male horses other than geldings, *45 ng/mL* of metabolite, 5σ-estrane-3β,17σ-diol in urine or a ratio in urine of 5σ-estrane-3β,17σ-diol to 5σ-estrene-3β,17σ-diol of > 1:1 is considered to be indicative for abuse. Only a limited number of regulatory organs (e.g. The Canadian Horse Racing Board, CHRB) set a threshold for *stanozolol*, at 1 ng/mL urine. For FEI and IFHA, for example, stanozolol is listed as a banned substance and therefore strictly forbidden. *Estranediol* has also been added to the list of threshold substances. Free and conjugated (5α-estrane-3β,17α-diol), at 45 ng/mL in urine of male horses (other than geldings).

All these thresholds and reference ranges are within the *low ppm or ppb range*, in matrices such as urine, blood and faeces, underlining the need for very sensitive and specific detection methods that are able to determine the exact steroidal status of (race) horses in- and out-of-competition. This explains the extensive use of sensitive, state-of-the-art mass spectrometric methods in this field.

17α-Hydroxyprogesterone	Drostanolone	Methandrostenolone	Normethandrolone
Androstenediol	Epitrenbolone	Methasterone	Oxabolone
Androstenedione (AED)	Estranediol	Methenolone	Oxandrolone
Bolandiol	Ethinylestradiol	Methyldienolone	Oxymesterone
Bolasterone	Ethylestrenol	Methylnortestosterone	Oxymetholone
Boldenone	Fluoxymesterone	Methyltestosterone	Paramethadione
Boldione (ADD)	Formebolone	Methyltrienolone	Prostanozol
Calusterone	Furazabol	Mibolerone	Quinbolone
Clostebol	Gestrinone	Nandrolone/nortestosterone	Stanozolol
Danazol	Hydroxytestosterone	Norandrostenediol	Stenbolone
Dehydrochloromethyltestosterone	Mestanolone	Norandrostenedione	Testosterone
Dehydrochlorotestosterone	Mesterolone	Norbolethone	Tetrahydrogestrinone
Desoxymethyltestosterone	Methandienone	Norclostebol	Tibolone
Dromostanolone	Methandriol	Norethandrolone	Trenbolone

All anabolic steroids listed as banned substances according to the FEI 2017 banned substances list. FEI and IFHA set thresholds for two AAS, boldenone and testosterone, accepting that these compounds can be present as endogenous steroids (black). Other regulatory organs set thresholds for stanozolol and nandrolone (nortestosterone) as well (gray). For *boldenone* a threshold has been set at 15 ng free and conjugated boldenone per millilitre in urine from male horses (other than geldings). Zero-tolerance is held in mares and geldings (FEI, IFHA among others). Δ For *testosterone* 20 ng free and conjugated testosterone per millilitre in urine or 100 ng free testosterone per millilitre in plasma is acceptable for geldings and 55 ng free and conjugated testosterone per millilitre in urine from fillies and mares (unless in foal) (FEI, IFHA and others). For nandrolone (nortestosterone) a threshold of 1 ng/mL urine has been set for mares and geldings. For stallions the threshold is significantly higher, at 45 ng/mL urine (RMTC). Only a limited number of regulatory organs (e.g. The Canadian Horse Racing Board, CHRB) set a threshold for stanozolol, at 1 ng/mL urine. *Estranediol* has also been added to the list of threshold substances. Free and conjugated 5α-estrane-3β,17α-diol) can be tolerated up to 45 ng/mL, in urine of male horses (other than geldings).

Table 3. All anabolic steroids listed as banned substances according to the FEI 2017 banned substances list.

http://dx.doi.org/10.5772/intechopen.68593

4. Analytical instrumentation

4.1. Historical evolution

Both in food residue and sport drug surveillance laboratories, *big progress* has been made over the last few decades regarding the detection of residues and forbidden substances (doping, incl. AAS) in different matrices [18, 41] (**Figure 5**).

In the 1960s and early 1970s, *thin layer chromatography* (TLC) combined with fluorescence detection (TLC-FL) was the most used technique. Later on in the 1970s, immunoassays such as enzyme linked immunosorbent assays (*ELISA)* and enzyme immunoassay (EIA) were developed and widely used. Both EIA and ELISA systems [42] are based on the principle of immunoassay linked to an enzyme rather than radioactivity as the reporter label (radioimmunoassay, RIA) [27, 28].

Mass spectrometry (MS) was introduced in the late 1970s but took until the late 1990s to conquer analytical labs worldwide. MS was first coupled to gas and later on to liquid chromatography (GC-MS and LC-MS) [43, 44]. Modern MS instruments are able to perform *MS in series*. The detection is carried out in the same compartment (MS^n) or in different compartments (MS/MS), on both the precursor ion and fragment ions, allowing to reach higher specificity and sensitivity. Over the years, various methods have been designed as screening tools to detect a large number of compounds in different drug classes, including anabolic steroids.

4.2. GC-MS versus LC-MS

GC-MS has been the *gold standard* for the detection of residues and anabolic steroids (in urine) for many years. In the past decades, however, there has been a general shift from *GC-MS* towards LC-MS/MS for drug residue and in doping control testing [45, 46]. This is mainly attributed to the *rapid improvement* of LC-MS(/MS) in recent years, leading to better sensitivity, faster instrument turnaround time and the ability to handle heat labile and large biomolecules.

Recent work has proven that ultra-high performance liquid chromatography-MS (UHPLC-MS/MS) instrumentation can provide exceptional detection capability of AAS in multiple equine matrices including mane hair [21], plasma [47] and urine [40, 48]. The development of ultra-high performance liquid chromatography (UHPLC), using *sub-2 μm particles* in the column, allowed higher flow rates and improved separation of compounds with similar or identical masses and retention times (e.g. α- and β-isomers of testosterone), while at the same time shortening the run time. LC-MS/MS is *widely used* by anti-doping testing laboratories for this purpose, and several rapid methods have been described to simultaneously detect different classes of compounds [20, 49, 50].

High resolution mass spectrometry (HRMS), on the other hand, operating at higher resolutions of 7500 up to more than 140,000 full width at half maximum (FWHM), is being optimized not as a screening technique only, but also for specific 'omics' biomarker approaches such as metabolomics, proteomics and transcriptomics [51–55].

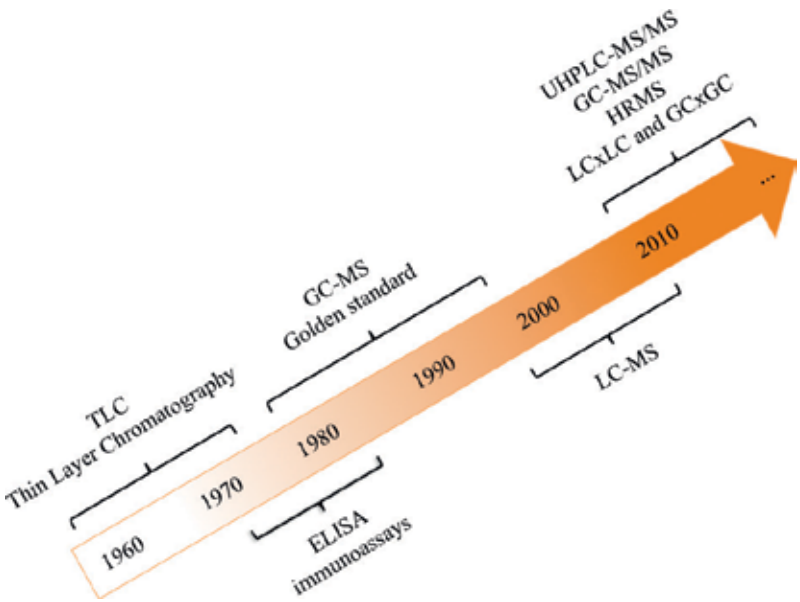

Figure 5. Evolution of analytical techniques used for steroid detection.

Recently, however, this shift to LC has come to a standstill, with even a partial shift back to GC, depending on the type of analysis [45, 46, 56, 57]. As of 2010, GC is again gaining importance as an anti-doping approach, but then coupled to MS/MS, complimentary to LC-MS/MS. GC-MS(/MS) is an important tool for analysing saturated steroid metabolites, as they suffer from *poor ionization* [58]. Alternatively, many urinary screening procedures include hydrolysis of phase-II metabolites, releasing the free compounds for detection, allowing to determine the overall concentration of the compound (free and conjugated), as used to define the thresholds of both the IFHA and FEI (See earlier, **Figure 5**). Additionally, comprehensive two-dimensional separation techniques LC × LC or GC × GC are also being developed [59, 60].

Therefore, at the moment, LC and GC techniques can be considered *complimentary*, as both techniques have their specific advantages and disadvantages, depending on the compound, matrix and goal of the analysis.

4.3. Gas chromatography–combustion-isotope ratio MS (GC-C-IRMS)

As mentioned earlier, the administration of synthetic steroids, especially tackling the *exogenous administration* of steroids of endogenous origin (e.g. testosterone), is an important obstacle for anti-doping regulatory organs. Therefore, doping control laboratories accredited by the WADA require methods of analysis that allow endogenous steroids to be distinguished from their synthetic analogues in urine. To that extend, GC is used in hyphenation with combustion isotope ratio mass spectrometry (*GC-C-IRMS)* a highly specialized instrumental *confirmatory* technique, measuring the *carbon isotope ratio* ($\Delta^{13}C$) of urinary steroids and confirming their synthetic origin based on the abnormal ^{13}C content [18, 61].

The average isotope ratio of each element (e.g. $^{12}C/^{13}C$, $^{1}H/^{2}H$) was fixed around the time of the earth's formation. However, variations can occur based on selective enrichment or depletion of the heavier isotopes (such as ^{13}C), a process known as fractionation. Fractionation can, for example, take place during phase transition; a process also known as equilibrium fractionation. When water vapour condenses, the lighter isotopes (^{16}O and ^{1}H) tend to remain in the vapour phase, while the heavier isotopes (^{18}O and ^{2}H) accumulate in the liquid phase [62]. GC-C-IRMS is capable of measuring these differences in relative ratio of light stable isotopes of carbon ($^{13}C/^{12}C$), hydrogen ($^{2}H/^{1}H$), nitrogen ($^{15}N/^{14}N$) or oxygen ($^{18}O/^{16}O$) in individual compounds, separated from often complex mixtures of components [63, 64].

Already in 1998, Mason et al. showed that when the isotopic composition of 5β-androstane-3α,17α-diol (the main metabolite of *testosterone* in bile) was normalized with respect to that of an endogenous reference compound (ERC, cholesterol) in the same sample, the metabolite could be used to distinguish between animals treated intramuscularly with testosterone and untreated animals [65]. Throughout the last decade, a variety of different methods have been developed and the number of different steroids under investigation by IRMS has grown considerably. Misuse of *norandrosterone, boldenone, corticosteroids or epitestosterone* can now be detected with the aid of carbon isotope ratios as well [66]. However, some limitations of GC-C-IRMS need to be kept in mind (Section 4.4.4).

4.4. Matrix and method of choice

The type of matrix used for steroid detection varies according to the specific goal of the analysis. Traditionally, *urine and blood* samples are being sampled for the detection of forbidden substances in the light of anti-doping controls, but *faeces* and hair are possible matrices as well [21, 35]. The analysis of equine *mane hair,* for example, has the potential to greatly extend the time period over which the detection of anabolic steroid abuse can be monitored. Parent steroids (e.g. testosterone esters) are incorporated into the mane hair and can be detectable for months post-treatment. Additionally, the use of segmental analysis can potentially provide additional information on the timing of administration [21]. In residue analysis, *meat* samples and *skin swabs* are also used [20, 41, 67].

4.4.1. Direct detection and the use of thresholds or zero-tolerance policy

Depending on the context and the specific class of steroids (endogenous, exogenous or synthetic, Section 3), the method and matrix of choice can be different. Most methods are based upon the direct mass spectrometric detection of the steroid of interest and/or its metabolites in biological matrices, merely urine and/or blood samples. This direct detection is coupled to two different approaches: a threshold concentration and *zero-tolerance* policy.

For most anabolic steroids in horses (**Table 3**), zero-tolerance is held: neither the compound itself nor its direct metabolites should be detected to consider the sample as clean. For some (endogenous) steroids, a threshold concentration has been determined. For boldenone, for example, a *threshold concentration* has been set for stallions (15 ng/mL), while zero-tolerance is held for mares and geldings. For testosterone, a threshold concentration of 20 ng/mL for

geldings and 55 ng/mL for mares is held. For stallions, no threshold has been set as the natural testosterone concentration is under the influence of age, seasonal variations and whether or not the stallion is a breeding stallion [68]. The idea of a threshold concentration relies on the *statistical likelihood* that a certain concentration can be detected in an *untreated horse*. The threshold must be based upon populations' studies and relevant to the concentrations measured post-treatment [49]. If the threshold concentration is set too high, concentrations measured post-treatment could be inadvertently listed as endogenous. If the threshold is set too low, non-treated horses could be unjustly banned from competitions and their owners/trainers sanctioned.

4.4.2. Measuring biological effect

As an *alternative* to the direct measurement of steroids, a range of assays have been developed *measuring the biological effect* of the steroids rather than the responsible compounds themselves. Two categories of assays can be distinguished: biosensors and biomarkers.

Biosensors utilize biological techniques to detect steroidal activity in a sample *ex vivo*, whereas biomarker techniques aim to monitor perturbation of 'normal' *in vivo* physiological parameters. With the rise of high resolution non-targeted approaches, the latter use of *specific qualitative biomarkers* has gained popularity over the last few years. Biomarkers or biological markers are metabolites that are measurable indicators of some biological state or condition, e.g. (illegal) treatment with a certain compound or compound cocktail. Biomarker monitoring can already be considered a new era in human anti-doping [69] and different biomarker approaches are being developed for equine purposes at the moment. As such, longitudinal monitoring of biomarkers can reveal non-physiological responses independently of the used doping technique or substance and may cause sanctioning of illicit practices [70].

An example hereof is an efficient strategy that has been developed to screen for *abuse of nandrolone*, a 'semi'-endogenous steroid in stallions (**Table 3**), monitoring the endogenous steroid profile disruption in urine and blood upon nandrolone administration [70]. A panel of (endogenous) steroids of interest was extracted from equine urine and plasma samples and quantified by GC-MS/MS. Statistical processing of the collected data permitted to establish statistical models capable of discriminating control samples from those collected post-administration. These *statistical models* succeeded in predicting the compliance status of routine samples collected from racing horses.

4.4.3. Phase I and II metabolites

A typical problem associated with the direct detection of boldenone and other (related) AAS is that they often do not result in a measurable excretion of the parent steroid in urine and faeces. Instead, these AAS are *metabolized*, by the liver, and excreted as their more hydrophilic phase I and II metabolites [39]. Phase I metabolites are merely formed through classical *oxidative and reductive* reactions. Phase-II metabolites arise from the conjugation of these hydroxyl groups as either *sulphates* or *ß-glucuronides*. These conjugates account for up to 90% of the excreted metabolites, making them an important class for screening [71].

http://dx.doi.org/10.5772/intechopen.68593

In the case of boldenone metabolism, the 1,4-diene-3-one structure of the A-ring appears to stabilize the steroid for reductive metabolism and boldenone-17ß-sulphate is the major (phase II) metabolite [72]. Therefore, *extraction* of urine and faeces samples includes *hydrolysis* of both metabolites, releasing the free compounds for detection. Hydrolysing conjugates allow determining the overall concentration (free and conjugated) of the compound, as used to define the thresholds of both the IFHA and FEI (Section 3.2). Ho et al., for example, identified intact boldenone sulphoconjugates as a direct evidence for the endogenous nature of boldenone in entire male horses.

These conjugates can, however, also be used as biomarker in equine anti-doping. They have been used is the detection of *boldenone misuse*. Exogenous boldenone is known to be extensively conjugated in phase-II metabolism. Gomez et al. found that after boldenone treatment, boldenone sulphate and in some cases α-Bol sulphate were present in urine samples, together with low concentrations of exogenous boldenone (the original, active drug) and *BM1* (the main boldenone metabolite, 5β-androst-1-en-17β-ol-3-one) [73]. Thus, according to Gomez et al., *BM1, β-Bol and α-Bol sulphates* may be used as markers for the exogenous administration of boldenone, and they can be used to reduce the number of samples to be analysed by GC-IRMS. In samples where boldenone and BM1 are detected at low concentrations and these concentrations thus might be of endogenous origin, further analysis by GC-IRMS will only be needed if boldenone sulphates and α-Bol sulphates are also present. GC-IRMS will then be used to confirm exogenous administration.

4.4.4. Limitations of GC-C-IRMS

As described earlier, GC-C-IRMS can be used as a confirmatory tool. However, the limitations of the IRMS approach need to be kept in mind. In equine, anti-doping establishing IRMS as a *confirmatory tool* is not that straightforward, as one of the factors influencing fractionation is genetic. Monocotyledonous plants (C4 plants), such as corn and desert or marine plants, typically have $\Delta^{13}C$ values varying from −8 to −20%. Most dicotyledons (C3 plants, including up to 95% of the plants on earth) have $\Delta^{13}C$ values varying from −22 to −35%. Because animals can only incorporate carbon through the ingestion of plant (or animal matter), the carbon isotope ratios in an animal will reflect the isotope ratios of the food source: *'you are what you eat'* [63]. For horses, this implies that $\Delta^{13}C$ values are very close to the ones of exogenous substances, hampering the ability to differentiate between endogenous and exogenously administered compounds (steroids).

Another problem associated with the use of IRMS in horses is the *'third sex': geldings*. If tests are performed to determine if an atypical steroid profile in humans is due to administration of an endogenous steroid androsterone (Andro), etiocholanolone (Etio) and/or the androstanediols (5α- and 5β-androstane-3α,17β-diol) are typically analysed by IRMS to determine the $\Delta^{13}C$ values. The ratios of these target compounds are compared to the $\Delta^{13}C$ ratio of an endogenous reference compound (ERC) such as 5β-pregnane-3α,20α-diol (Pdiol) [74]. For geldings, it is very difficult to obtain such a *reliable endogenous reference compound (ERC).* It is possible to find a reliable ERC for stallions and mares, but this ERC is not consistent with geldings (personal communication, Laboratoire des Courses Hippiques, L.C.H.). In this context, Piper et

al. and Cawley and Flenker also described some of the complexities that can be encountered to obtain valid $\Delta^{13}C$ measurements from GC-C-IRMS and the need for *careful interpretation* of all relevant information concerning an individual's metabolism in order to make an informed decision with respect to a doping violation [66, 75].

Overall, this illustrates that the direct detection approach (relying on threshold concentrations), the biosensor/biomarker approaches and GC-C-IRMS have their *limitations*, including for requiring large population studies for validation and the fact that statistical outliers can be present at any time. These limitations are a part of the reason that *zero-tolerance* is still the preferred method to deal with 'semi'-endogenous steroids, unless irrefutable evidence has been gathered proving the endogenous prevalence of a certain compound, in mares, geldings and/or stallions.

5. (Equine) biological passport

To conquer the latter limitations, WADA introduced the athlete biological passport (ABP) for human athletes in 2009. An APB is *an individual, electronic record for professional athletes in which profiles of biological markers of doping and results of doping tests are collated over a period of time*. The ABP is considered to be an effective tool in the fight against doping as monitoring selected biological variables over time can indirectly reveal the effects of doping, rather than attempting to detect the doping substance or method itself (Section 4.4.2) [76].

The *concept* of launching a similar equine biological passport (EBP) is not new, the earlier discussions started back in 2010, but the tone and urgency of these discussion among veterinary and regulatory authorities are changing in the wake of recent doping scandals (e.g. cobalt scandal in Australia, 2015). This sudden public focus might spur funding that helps turn complicated concepts, such as introduction of EBPs as a means to curtail doping, into reality.

With the *metabolomics technology* invested in the equine passport, the industry can be proactive in identifying those who are engaging in doping practices, without necessarily knowing what the specific substance is, eliminating the strict reliance on targeted analysis of post-racing urine and blood samples. Every horse has a *unique metabolic signature* that can be identified by monitoring metabolites or markers. This individualized approach facilitates a better understanding of the specific traits of each horse, providing more precise measurement of the *biological effect of training, stress and/or drugs* (controlled medication or doping) than is available with current technologies. Metabolomics is already recognized as a cutting-edge science in human medicine and anti-doping.

Additionally, the EBP can include monitoring the genes of racehorses, identifying changes throughout their careers, to combat *gene doping*. Gene doping is defined by the World Anti-Doping Agency (WADA) as '*the non-therapeutic use of cells, genes, genetic elements or of the modulation of gene expression, having the capacity to improve athletic performance*'. Suspected targets for gene doping are erythropoietin (EPO), myostatin and the insulin-like growth factor (ILGF).

Unfortunately, the use of biological passports will be a *logistic and analytical challenge* to all but the top-flight racing analytical labs around the world. The EBP is a whole-of-organization

initiative requiring high-tech equipment and the co-operation of analysts (scientists), stewards, anti-doping investigators and veterinarians to ensure all of the available information concerning prohibited practices to be integrated in real time. Racing New South Wales (Racings N.S.W., Australia) and leading French racing authorities (including L.C.H.) are currently working together on the development of EBPs.

In the past, doping sinners have always been a step or two ahead of the authorities, but with these new spectrometric techniques changing the way of handling drug abuse—not by finding the drugs but finding changes in the physiology of the horse created by the drugs—the gap may be about to close. A *cheerful outlook* for the fight against doping abuse.

Author details

Decloedt Anneleen[1,2]*, Van Landschoot Anita[1,2] and Vanhaecke Lynn[1]

*Address all correspondence to: anneleen.decloedt@ugent.be

1 Laboratory of Chemical Analysis, Department of Public Health and Food Safety, Faculty of Veterinary Medicine, Ghent University, Merelbeke, Belgium

2 Faculty of Bioscience Engineering, Ghent University, Ghent, Belgium

References

[1] Hanukoglu I. Steroidogenic enzymes: Structure, function, and role in regulation of steroid hormone biosynthesis. The Journal of Steroid Biochemistry and Molecular Biology. 1992;**43**:779–804

[2] Hu J, Zhang Z, Shen WJ, Azhar S. Cellular cholesterol delivery, intracellular processing and utilization for biosynthesis of steroid hormones. Nutrition and Metabolism (London). 2010;**7**:47

[3] Shoppee CW. Chemistry of the Steroids. London: Butterworths Scientific Publications; 1958

[4] Holick MF. High prevalence of vitamin D inadequacy and implications for health. Mayo Clinic Proceedings. 2006;**81**:353–373

[5] Norman AW, Henry HL. Hormones. 3rd ed. Academic Press; China by Elsevier, ISBN: 978-0-12-369444-7

[6] Regal P, Cepeda A, Fente CA. Natural Hormones in Food-Producing Animals: Legal Measurements and Analytical Implications. InTech; 2012. ISBN: 978-953-307-887-8, http://www.intechopen.com/books/food-production-approaches-challenges-and-tasks/natural-hormones-infood-producing-animals-legal-measurements-and-analytical-implications

[7] Becker KL. Principles of Practice of Endocrinology and Metabolism. Lippincott Williams & Wilkins; 2001. p 2477. ISBN 0781717507, 9780781717502

[8] Nelis H, Vanden Bussche J, Wojciechowicz B, Franczak A, Vanhaecke L, Leemans B, Cornillie P, Peelman L, Van Soom A, Smits K. Steroids in the equine oviduct: Synthesis, local concentrations and receptor expression. Reproduction Fertility and Development. **28**(9):1390–1404 https://doi.org/10.1071/RD14483

[9] Franczak A, Kotwica G. Secretion of estradiol-17beta by porcine endometrium and myometrium during early pregnancy and luteolysis. Theriogenology. 2008;**69**:283–289

[10] Franczak A, Kotwica G. Androgens and estradiol-17beta production by porcine uterine cells: In vitro study. Theriogenology. 2010;**73**:232–241

[11] Trayhurn P. Endocrine and signalling role of adipose tissue: New perspectives on fat. Acta Physiologica Scandinavica. 2005;**184**:285–293

[12] Coelho M, Oliveira T, Fernandes R. Biochemistry of adipose tissue: An endocrine organ. Archives of Medical Science. 2013;**9**:191–200

[13] Hoberman JM, Yesalis CE. The history of synthetic testosterone. Scientific American. 1995;**272**:76–81

[14] Dotson JL, Brown RT. The history of the development of anabolic-androgenic steroids. Pediatric Clinics of North America. 2007;**54**:761–769

[15] W.A.-D.A. WADA [Internet]. 2017. Available from: https://www.wada-ama.org/en/who-we-are

[16] de Laat MA, Robinson MA, Gruntmeir KJ, Liu Y, Soma LR, Lacombe VA. AICAR administration affects glucose metabolism by upregulating the novel glucose transporter, GLUT8, in equine skeletal muscle. Veterinary Journal. 2015;**205**:381–386

[17] Ho EN, Kwok WH, Lau MY, Wong AS, Wan TS, Lam KK, Schiff PJ, Stewart BD. Doping control analysis of TB-500, a synthetic version of an active region of thymosin beta(4), in equine urine and plasma by liquid chromatography-mass spectrometry. Journal of Chromatography A. 2012;**1265**:57–69

[18] McKinney AR. Modern techniques for the determination of anabolic-androgenic steroid doping in the horse. Bioanalysis. 2009;**1**:785–803

[19] Kazlauskas R. Designer steroids. Handbook of Experimental Pharmacology. 2010;(195): 155–85. doi: 10.1007/978-3-540-79088-4_7.

[20] Scarth J, Akre C, van Ginkel L, Le Bizec B, De Brabander H, Korth W, Points J, Teale P, Kay J. Presence and metabolism of endogenous androgenic-anabolic steroid hormones in meat-producing animals: A review. Food Additives & Contaminants. Part A, Chemistry, Analysis, Control, Exposure & Risk Assessment. 2009;**26**:640–671

[21] Gray BP, Viljanto M, Bright J, Pearce C, Maynard S. Investigations into the feasibility of routine ultra high performance liquid chromatography-tandem mass spectrometry

analysis of equine hair samples for detecting the misuse of anabolic steroids, anabolic steroid esters and related compounds. Analytica Chimica Acta. 2013;**787**:163–172

[22] Mooradian AD, Morley JE, Korenman SG. Biological actions of androgens. Endocrine Reviews. 1987;**8**:1–28

[23] Pesant MH, Desmarais G, Fink GD, Baillargeon JP. Reference ranges for total and calculated free and bioavailable testosterone in a young healthy women population with normal menstrual cycles or using oral contraception. Clinical Biochemistry. 2012;**45**:148–150

[24] MedlinePlus.gov. National Library of Medicine Reference Values; 2016

[25] Southren AL, Gordon GG, Tochimoto S, Pinzon G, Lane DR, Stypulkowski W. Mean plasma concentration, metabolic clearance and basal plasma production rates of testosterone in normal young men and women using a constant infusion procedure: effect of time of day and plasma concentration on the metabolic clearance rate of testosterone. The Journal of Clinical Endocrinology and Metabolism. 1967;**27**:686–694

[26] Futterweit W, Mcniven NL, Guerragarcia R, Gibree N, Drosdowsky M, Siegel GL, Soffer LJ, Rosenthal I.M, Dorfman RI. Testosterone in human urine. Steroids. 1964;**4**:137–145.

[27] Doberne Y, Levine MS, New MI. Elevated urinary testosterone and androstanediol in precocious adrenarche. Pediatric Research. 1975;**9**:794–797

[28] Tresguerres JAF, Lisboa BP, Tamm J. Simple radioimmunoassay for measurement of testosterone glucosiduronate in unextracted urine. Steroids. 1976;**28**:13–23

[29] Gonzalo-Lumbreras R, Pimentel-Trapero D, Izquierdo-Hornillos R. Development and method validation for testosterone and epitestosterone in human urine samples by liquid chromatography applications. Journal of Chromatographic Science. 2003;**41**:261–265

[30] Van Renterghem P, Van Eenoo P, Geyer H, Schanzer W, Delbeke FT. Reference ranges for urinary concentrations and ratios of endogenous steroids, which can be used as markers for steroid misuse, in a Caucasian population of athletes. Steroids. 2010;**75**:154–163

[31] Martinez-Brito D, Correa Vidal MT, de la Torre X, Garcia-Mir V, Ledea Lozano O, Granda Fraga M. Reference ranges for the urinary steroid profile in a Latin-American population. Drug Testing and Analysis. 2013;**5**:619–626

[32] Moon JY, Kwon W, Suh S, Cheong JC, In MK, Chung BC, Kim JY, Choi MH. Reference ranges for urinary levels of testosterone and epitestosterone, which may reveal gonadal function, in a Korean male population. The Journal of Steroid Biochemistry and Molecular Biology. 2014;**140**:100–105

[33] Mösseler A, Licht S, Wilhelm L. Kamphues J. Can oral intake of gamma-oryzanol (experimentally given orally as pure substance) result in doping relevant testosterone levels in the urine of mares and geldings? 5th European Workshop on Equine Nutrition; 2010; Cirencester

[34] Ho EN, Yiu KC, Tang FP, Dehennin L, Plou P, Bonnaire Y, Wan TS. Detection of endogenous boldenone in the entire male horses. Journal of Chromatography B, Analytical Technologies in the Biomedical and Life Sciences. 2004;**808**:287–294.

[35] Popot MA, Boyer S, Menaut L, Garcia P, Bonnaire Y, Lesage D. Boldenone, testosterone and 1,4-androstadiene-3,17-dione determination in faeces from horses, untreated and after administration of androsta-1,4-diene-3,17-dione (boldione). Biomedical Chromatography. 2008;**22**:662–670.

[36] Leung DKK, Tang FPW, Wan TSM, Wong JKY. Identification of cryptorchidism in horses by analysing urine samples with gas chromatography/mass spectrometry. Veterinary Journal. 2011;**187**:60–64

[37] Bonnaire Y, Dehennin L, Plou P, Toutain PL. Testosterone administration to mares: Criteria for detection of testosterone abuse by analysis of metabolites in plasma and urine. Journal of Analytical Toxicology. 1995;**19**:175–181

[38] Dehennin L, Bonnaire Y, Plou P, Ho ENM, Yiu KCH, Wan TSM. Urinary excretion of endogenous boldenone by entire male horses: Identification and quantification by gas chromatography–mass spectRometry. In: Proceedings of the 14th International Conference Racing Analysts Veterinarians; 2002; Orlando, Florida, USA. Newmarket, England; R & W Publications; 2003. pp. 58–64

[39] Pu F, McKinney AR, Stenhouse AM, Suann CJ, McLeod MD. Direct detection of boldenone sulfate and glucuronide conjugates in horse urine by ion trap liquid chromatography-mass spectrometry. Journal of Chromatography B, Analytical Technologies in the Biomedical and Life Sciences. 2004;**813**:241–246.

[40] Decloedt A, Bailly-Chouriberry L, Vanden Bussche J, Garcia P, Popot MA, Bonnaire Y, Vanhaecke L. A validated UHPLC-MS/MS method to quantify low levels of anabolic-androgenic steroids naturally present in urine of untreated horses. Analytical and Bioanalytical Chemistry. 2015 Jun;**407**(15):4385–96. doi: 10.1007/s00216-014-8428-x. Epub 2015 Jan 17.

[41] De Brabander HF, Poelmans S, Schilt R, Stephany RW, Le Bizec B, Draisci R, Sterk SS, van Ginkel LA, Courtheyn D, Van Hoof N, Macri A, De Wasch K. Presence and metabolism of the anabolic steroid boldenone in various animal species: A review. Food Additives and Contaminants. 2004;**21**:515–525

[42] Lequin RM. Enzyme immunoassay (EIA)/enzyme-linked immunosorbent assay (ELISA). Clinical Chemistry. 2005;**51**:2415–2418.

[43] Erni F. Liquid chromatography-mass spectrometry in the pharmaceutical industry: Objectives and needs. Journal of Chromatography. 1982;**251**:141–151

[44] Gohlke RS, McLafferty FW. Early gas chromatography/mass spectrometry. Journal of the American Society for Mass Spectrometry. 1993;**4**:367–371

[45] Thevis M, Thomas A, Schanzer W. Current role of LC-MS(/MS) in doping control. Analytical and Bioanalytical Chemistry. 2011;**401**:405–420

[46] Ahrens BD, Starcevic B, Butch AW. Detection of prohibited substances by liquid chromatography tandem mass spectrometry for sports doping control. Methods in Molecular Biology. 2012;**902**:115–128

[47] Guan F, Uboh CE, Soma LR, Luo Y, Rudy J, Tobin T. Detection, quantification and confirmation of anabolic steroids in equine plasma by liquid chromatography and tandem mass spectrometry. Journal of Chromatography B: Analytical Technologies in the Biomedical and Life Sciences. 2005;**829**:56–68

[48] Wong CH, Leung DK, Tang FP, Wong JK, Yu NH, Wan TS. Rapid screening of anabolic steroids in horse urine with ultra-high-performance liquid chromatography/tandem mass spectrometry after chemical derivatisation. Journal of Chromatography A. 2012;**1232**:257–265

[49] Scarth J. Approaches to the Detection of Steroid Abuse in Veterinary Species. Ghent: Faculty Veterinary Medicine, Public Health and Food Safety, Ghent University; 2011. p. 331

[50] Scarth JP, Teale P, Kuuranne T. Drug metabolism in the horse: A review. Drug Testing and Analysis. 2011;**3**:19–53.

[51] Van Meulebroek L, Bussche JV, Steppe K, Vanhaecke L. Ultra-high performance liquid chromatography coupled to high resolution Orbitrap mass spectrometry for metabolomic profiling of the endogenous phytohormonal status of the tomato plant. Journal of Chromatography A. 2012;**1260**:67–80.

[52] Cho K, Evans BS, Wood BM, Kumar R, Erb TJ, Warlick BP, Gerlt JA, Sweedler JV. Integration of untargeted metabolomics with transcriptomics reveals active metabolic pathways. Metabolomics: Official Journal of the Metabolomic Society. 2015;**11**(3): 503–517 doi: 10.1007/s11306-014-0713-3

[53] Giron AJ, Deventer K, Roels K, Van Eenoo P. Development and validation of an open screening method for diuretics, stimulants and selected compounds in human urine by UHPLC-HRMS for doping control. Analytica Chimica Acta. 2012;**721**:137–146

[54] Scarth JP. Modulation of the growth hormone-insulin-like growth factor (GH-IGF) axis by pharmaceutical, nutraceutical and environmental xenobiotics: an emerging role for xenobiotic-metabolizing enzymes and the transcription factors regulating their expression. A review. Xenobiotica; The Fate of Foreign Compounds in Biological Systems. 2006;**36**:119–218

[55] Granger JH, Baker A, Plumb RS, Perez JC, Wilson ID. Ultra performance liquid chromatography-MS(TOF): New separations technology for high throughput metabonomics. Drug Metabolism Reviews. 2004;**36**:252

[56] Van Eenoo P, Van Gansbeke W, De Brabanter N, Deventer K, Delbeke FT. A fast, comprehensive screening method for doping agents in urine by gas chromatography-triple quadrupole mass spectrometry. Journal of Chromatography A. 2011;**1218**:3306–3316

[57] Revelsky AI, Samokhin AS, Virus ED, Rodchenkov GM, Revelsky IA. High sensitive analysis of steroids in doping control using gas chromatography/time-of-flight mass-spectrometry. Drug Testing and Analysis. 2011;**3**:263–267

[58] Le Bizec B, Pinel G, Antignac JP. Options for veterinary drug analysis using mass spectrometry. Journal of Chromatography A. 2009;**1216**:8016–8034

[59] Stoll DR, Li XP, Wang XO, Carr PW, Porter SEG, Rutan SC. Fast, comprehensive two-dimensional liquid chromatography. Journal of Chromatography A. 2007;**1168**:3–43

[60] Dalluge J, Beens J, Brinkman UAT. Comprehensive two-dimensional gas chromatography: A powerful and versatile analytical tool. Journal of Chromatography A. 2003; **1000**:69–108

[61] Teale P, Houghton E. Metabolism of anabolic steroids and their relevance to drug detection in horseracing. Bioanalysis. 2010;**2**:1085–1107

[62] Faure G, Mensing TM. Isotopes: Principles and Applications. Hoboken N.J. 3rd ed. 2004 ISBN: 978-0-471-38437-3

[63] Muccio Z, Jackson GP. Isotope ratio mass spectrometry. Analyst. 2009;**134**:213–222

[64] Piper T, Thevis M, Flenker U, Schanzer W. Determination of the deuterium/hydrogen ratio of endogenous urinary steroids for doping control purposes. Rapid Communications in Mass Spectrometry: RCM. 2009;**23**:1917–1926

[65] Mason PM, Hall SE, Gilmour I, Houghton E, Pillinger C, Seymour MA. The use of stable carbon isotope analysis to detect the abuse of testosterone in cattle. Analyst. 1998;**123**:2405–2408

[66] Piper T, Emery C, Saugy M. Recent developments in the use of isotope ratio mass spectrometry in sports drug testing. Analytical and Bioanalytical Chemistry. 2011;**401**:433–447

[67] Bussche JV, Decloedt A, Van Meulebroek L, De Clercq N, Lock S, Stahl-Zeng J, Vanhaecke L. A novel approach to the quantitative detection of anabolic steroids in bovine muscle tissue by means of a hybrid quadrupole time-of-flight-mass spectrometry instrument. Journal of Chromatography. A. 2014;**1360**:229–239

[68] Irvine CHG, Alexander SL, Turner JE. Seasonal-variation in the feedback of sex steroid-hormones on serum LH concentrations in the male horse. Journal of Reproduction and Fertility. 1986;**76**:221–230

[69] Pottgiesser T, Schumacher YO. Biomarker monitoring in sports doping control. Bioanalysis. 2012;**4**:1245–1253

[70] Kaabia Z, Dervilly-Pinel G, Popot MA, Bailly-Chouriberry L, Plou P, Bonnaire Y, Le Bizec B. Monitoring the endogenous steroid profile disruption in urine and blood upon nandrolone administration: An efficient and innovative strategy to screen for nandrolone abuse in entire male horses. Drug Testing and Analysis. 2014;**6**:376–388

[71] Dumasia MC, Houghton E, Bradley CV, Williams DH. Studies related to the metabolism of anabolic steroids in the horse: The metabolism of 1-dehydrotestosterone and the use of fast atom bombardment mass spectrometry in the identification of steroid conjugates. Biomedical Mass Spectrometry. 1983;**10**:434–440.

[72] Houghton E, Maynard S. Some aspects of doping and medication control in equine sports. Handbook of Experimental Pharmacology; 2010;(195):369-409. doi: 10.1007/978-3-540-79088-4_17.

[73] Gomez C, Pozo OJ, Geyer H, Marcos J, Thevis M, Schanzer W, Segura J, Ventura R. New potential markers for the detection of boldenone misuse. Journal of Steroid Biochemistry and Molecular Biology. 2012;**132**:239–246

[74] Van Renterghem P, Polet M, Brooker L, Van Gansbeke W, Van Eenoo P. Development of a GC/C/IRMS method-confirmation of a novel steroid profiling approach in doping control. Steroids. 2012;**77**:1050–1060

[75] Cawley AT, Flenker U. The application of carbon isotope ratio mass spectrometry to doping control. Journal of Mass Spectrometry. 2008;**43**:854–864.

[76] Saugy M, Lundby C, Robinson N. Monitoring of biological markers indicative of doping: The athlete biological passport. British Journal of Sports Medicine. 2014;**48**:827–832

Chapter 9

Use of Mass Spectrometry for the Determination of Formaldehyde in Samples Potentially Toxic to Humans: A Brief Review

Aline de Souza, Isabela Cristina Matos Cunha,
Júnior Olair Chagas,
Elisandra Bárbara Pontes Carlos,
Luana Lacerda Santos,
Thamires Ráfaga Campos e Figueredo,
Lucília Alves Linhares Machado,
Vanessa Moreira Osório, Karla Moreira Vieira and
Fabiana Aparecida Lobo

Additional information is available at the end of the chapter

http://dx.doi.org/10.5772/intechopen.68922

Abstract

The chemical characteristics of formaldehyde make it widely used and important in the global economy. It has applications in the health area and in various industrial sectors. However, formaldehyde is considered toxic substance and is classifed as a persistent organic pollutant. Direct and prolonged contact with formaldehyde can cause serious damage to the body and may even lead to death. It is classifed by several agencies as a human carcinogen and may exhibit mutagenic/teratogenic efects and/or damage the endocrine system. Various matrices have been found to contain formaldehyde at concentrations higher than those permited by global health regulatory agencies. To this end, mass spectrometry can provide a very useful tool, enabling the identifcation and quantifcation of formaldehyde. Although various analytical techniques can be used for the determination and quantifcation of volatile organic compounds, chromatography is one of the most widely used methods due to its precision. Coupled to a detection system such as mass spectrometry, it can be employed for the determination of compounds potentially toxic to humans, including formaldehyde. The purpose of this chapter is to summarize some recent and important studies concerning the quantifcation of formaldehyde using mass spectrometry as a powerful analytical tool.

Keywords: Formaldehyde, mass spectrometry, toxicology, chromatography

INTECH
open science | open minds

© 2017 The Author(s). Licensee InTech. This chapter is distributed under the terms of the Creative Commons Attribution License (http://creativecommons.org/licenses/by/3.0), which permits unrestricted use, distribution, and reproduction in any medium, provided the original work is properly cited. CC BY

1. Introduction

Formaldehyde (FA), the simplest aldehyde, is a carbonyl compound with the molecular formula H_2CO, density of 1.081 g.cm^{-3}, and molecular mass of 30.03 g mol^{-1}. At standard temperature and pressure (STP), it is found in the gaseous state and is colourless and inflammable [1, 2]. It has an irritating odour, is soluble in most organic solvents, and is fairly soluble in water [1]. Formaldehyde is globally one of the top 25 most widely produced chemical substances, due mainly to its high reactivity, absence of colour, commercial purity, and low cost [3].

Commercially available in the solid phase (paraformaldehyde) and as the trioxide [$(CH_2O)_3$], formaldehyde is typically used and stored in 30–50% v/v aqueous solutions, which usually contain methanol as a stabilizing agent (to avoid polymerization) at concentrations that may exceed 15% v/v. Formaldehyde is known by several names, depending on the area of activity where it is used, including formaldehyde, formic aldehyde, formalin, methanal, and methylene oxide, among others [4].

The chemical characteristics of this compound, especially its germicidal activity, make it a product of widespread applicability and important for the global economy [5]. It has uses in the health area (in medical laboratories and hospitals) and in various industrial sectors including civil construction, timber, and paper manufacturing and is employed as a preservative in foods and cosmetics, among other uses [5, 6].

In hospital pathology and anatomical laboratories, formaldehyde is used as a fixative or preservative, in which the biological material is dipped in order to conserve it, and it is also considered a good disinfectant that does not cause excessive hardening of the tissues. Formaldehyde is an excellent medium for the preservation and storage of biopsy and surgical specimens [7].

In civil construction, formaldehyde is employed in the form of urea-methanal coating foams, which are among the most widely used systems for coating buildings [4, 7].

In the timber industry, formaldehyde is used in the production of agglomerates, plywood, laminates, furniture, and adhesives [8]. In the textile finishing industry, it is a constituent of most of the resins used to provide the degree of stiffness and elasticity required to maintain permanent folds while helping to avoid the formation of wrinkles during washing and use of garments [8].

In agriculture, formaldehyde is used as a seed preservative and in the preservation of tubers and fruits. It is employed in the form of disinfectants to eliminate or limit microbiological degradation in the sugar, beer, and leather industries [9].

In the perfume and cosmetics sector, formaldehyde is employed in shampoos, hair creams, deodorants, bath products, creams, and lotions for the skin and can also be found in masks and as makeup for the eyes, in mouth refreshers, cuticle removers, nail polish, and nail hardener, among other products [10, 11].

At the same time, formaldehyde is considered a highly toxic substance and can be characterized as a persistent organic pollutant causing human carcinogenicity and toxicity to aerobic

and anaerobic microorganisms [4]. Exposure to this substance increases the risk of cancers of the pharynx, nasopharynx, and brain, as well as dermatitis and allergic reactions. Formaldehyde is absorbed through the skin and mucous membranes and is rapidly metabolized by reaction with hydrochloric acid or other inorganic chlorides present in the body, forming bis(chloromethyl)ether, a substance that has carcinogenic effects in humans [12]. Therefore, direct and prolonged contact with formaldehyde causes serious damage to the body and can even lead to death [4, 13].

For these reasons, several agencies have classified this compound as a human carcinogen that may be mutagenic/teratogenic to the endocrine system of humans [1, 4, 10]. These organizations include the Brazilian National Health Surveillance Agency (ANVISA) [14], the International Agency for Research on Cancer (IARC) [12], the National Cancer Institute José Alencar Gomes da Silva (INCA) [6], the United States Occupational Safety and Health Administration (OSHA) [15], and the National Toxicology Program (NTP) [16].

Given the problems caused by the presence of formaldehyde in the human body, it is necessary to develop procedures for the determination of this compound in different sample types, since many matrices can contain formaldehyde at concentrations higher than the levels permitted by global health regulatory agencies. To this end, the mass spectrometry (MS) technique is a very useful tool that enables the detection and quantification of formaldehyde in a wide range of sample types.

Mass spectrometry is an analytical technique that can be used for the structural characterization and quantification of a wide range of molecules [17]. The technique is extensively used by chemists for the analysis of small and volatile organic compounds. It is highly sensitive and can be used to determine substances present at low concentrations, as in the case of doping, food control, environmental contamination, and many other areas of application [18, 19].

In the early stages of the development of mass spectrometry, the sample was introduced into the system by direct vaporization, but with the evolution of chromatographic techniques, the use of a chromatograph to introduce the sample into the mass spectrometer became commonplace (showed in **Figure 1**). In these techniques, the components of the sample are separated and individually introduced into the MS ionization source, generating ions that are then transferred to the analyser for detection and quantification [20]. In the mass spectrometer, the gas phase ions are separated according to their mass to charge ratio (m/z). These ratios are presented in the form of a mass spectrum, which is a graph showing the relative abundance (intensity) of each ion appearing in the form of a peak with defined m/z [21].

This detection technique, when coupled to a chromatograph, enables the construction of a chromatogram of the most important ion fragments, with the elimination of interfering ions, hence increasing the reliability of identification of the components of a sample. Gas chromatography coupled with mass spectrometry (GC-MS) is a powerful analytical tool that is usually used in the analysis of complex gas phase mixtures. However, this limits the technique to the analysis of volatile and semi-volatile compounds of low polarity and low molecular weight. In the case of compounds of higher molecular weight and/or greater polarity and

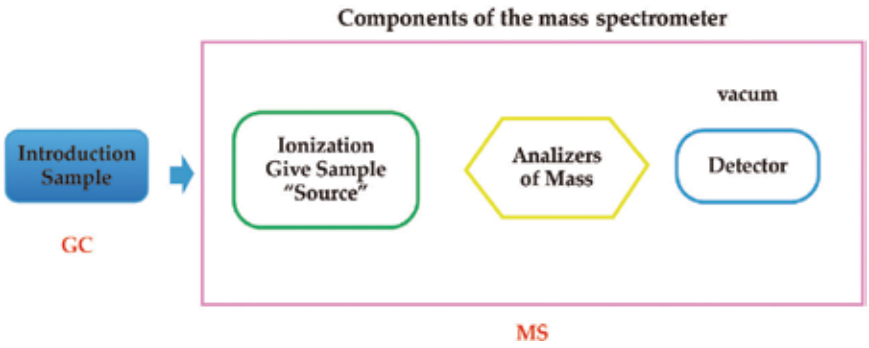

Figure 1. An illustrative figure for mass spectrometer components. Source: Own authors.

lower volatility, the most suitable technique is the coupling of high-performance liquid chromatography and mass spectrometry (HPLC-MS) [20].

Mass spectrometry used as a detection method coupled with gas chromatography offers advantages for the analysis of formaldehyde in different types of samples. These advantages lie in the fact that this technique not only considers the retention time of this compound but also the mass of each of the main fragments generated and the ratio between their intensities, which ensure that the signal is related to the analyte [22].

One of the crucial steps in the analysis of formaldehyde using the mass spectrometry technique involves the use of derivatization reactions. These reactions modify the functional groups of the compound, improving its stability and enabling its detection [9, 10]. The main derivatization agents currently employed in aldehyde analyses include 2,4-dinitrophenylhydrazine (2,4-DNPH) (**Figure 2a**), O-(2,3,4,5,6-pentafluorobenzyl)-hydroxylamine (PFBHA) (**Figure 2b**), and pentafluorophenyl hydrazine (PFPH) (**Figure 2c**) [23–29].

In the particular case of formaldehyde, preference has been given to the use of 2,4-DNPH as the derivatization reagent, followed by analysis of the resulting hydrazones (FA-DNPHo) by mass spectrometry [30]. This procedure increases the sensitivity and selectivity of the method. In most DNPH derivatization methods, analysis by HPLC-MS is generally preferred rather than GC-MS. However, in the analysis of FA-DNPHo, the GC-MS system provides greater sensitivity and selectivity, compared to HPLC-MS [30], with gas chromatography providing the benefits of precision and operational simplicity. **Figure 3** shows an illustrative scheme of the identification of formaldehyde in possible sources of contamination and the mass spectral for its identification in the form of Fo-DNPH, using GC-MS, and **Table 1** summarizes some important derivatization studies using mass spectrometry.

The following discussion describes some of the techniques involving chromatography coupled to MS employed for the analysis (detection and quantification) of formaldehyde in different types of samples.

http://dx.doi.org/10.5772/intechopen.68922

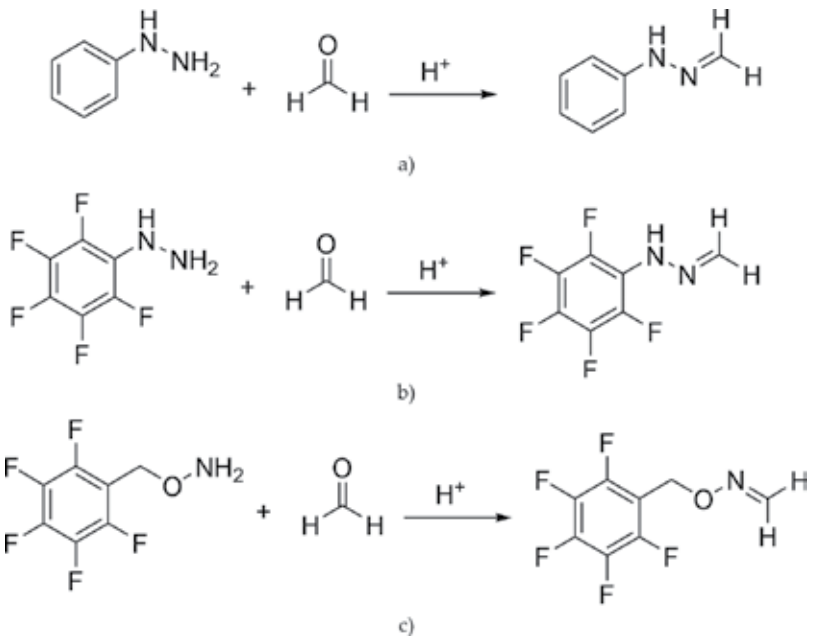

Figure 2. (a) A reaction of formaldehyde with 2,4-dinitrophenylhydrazine to form 2,4 dinitrophenylhydrazone. (b) A reaction of formaldehyde with O-(2,3,4,5,6-pentafluorobenzyl)-hydroxylamine to form the oxime. (c) A reaction of formaldehyde with pentafluorophenyl hydrazine to form pentafluorophenyl hydrazone. Source: Own authors, 2017.

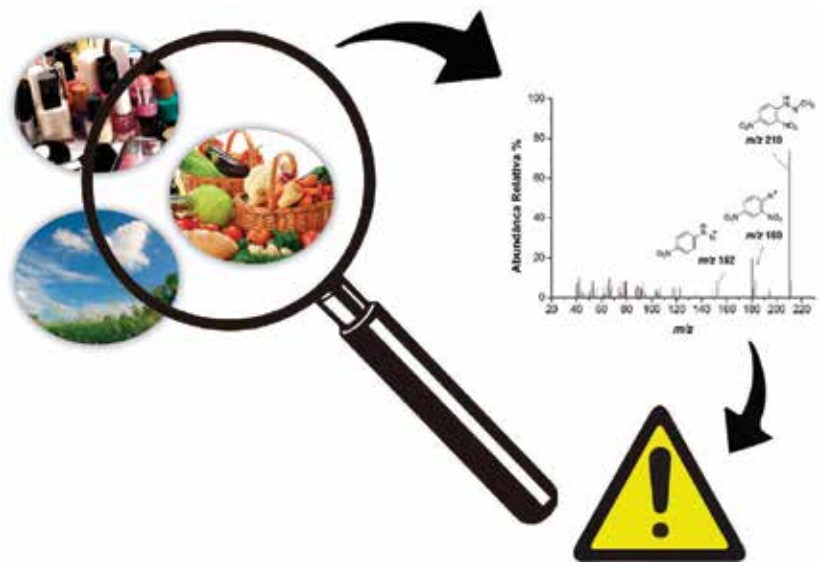

Figure 3. An example mass spectrum for FA-DNPHo [spectrum obtained using a gas chromatograph with mass spectrometric detection (CGMS-QP2010 Plus, Shimadzu)]. Source: Own authors, 2017. Google Images [31].

Sample type	Sample analysis	Main results	References
Hair creams	Solubilisation of straightener cream samples, addition of 2,4-dinitrophenylhydrazine in acetonitrile, and direct injection of the prepared samples	All samples had formaldehyde levels above the concentration permitted by Brazilian law.	[32]
Foods	Derivatization with 2,4-dinitrophenylhydrazine	Analysis of free and reversibly bound formaldehyde in 10 squid and squid products.	[33]
Foods	Derivatization with 2,2,2-trifluoroethylene hydrazine	All food samples analysed contained formaldehyde.	[34]
Bio-oil	Derivatization with (2,3,4,5,6-pentafluorobenzyl) hydroxylamine hydrochloride	Contained ~2% formaldehyde	[35]
Terpenes α- and β-pinene/limonene/ Δ3–carene	Derivatization with 2,4-dinitrophenylhydrazine and subsequent analysis by high-performance liquid chromatography	Low limits of detection and quantification improved the technique	[36]
Air affected by incense burning	Derivatization on a solid sorbent containing O-(2,3,4,5,6-pentafluorobenzyl)-hydroxylamine	The concentration of formaldehyde in a closed room was higher than the concentration in an open place	[37]
Blood	Gas chromatography with mass spectrometry following derivatization with pentafluorophenyl hydrazine	Detection of formaldehyde in rat blood samples	[12]

Table 1. Studies reported in the literature on the analysis of formaldehyde in various types of matrices, using derivatization procedures.

2. Overview of analytical techniques for formaldehyde determination

2.1. Formaldehyde in environmental samples

Several studies have investigated the levels of formaldehyde in samples of air, diesel, water, and other media. The monitoring of formaldehyde in these sample types is very important, due to the likelihood of exposure to part of the population.

Tessini et al. [35] determined aldehydes in bio-oil using HPLC-UV and GC-MS techniques. For analysis using HPLC-UV, the aldehydes were derivatized with 2,4-DNPH in solution, followed by headspace analysis. For analysis by GC-MS, the aldehydes were extracted using

a solid-phase microextraction (SPME) fibre, and the following derivatization in solution with pentafluorobenzyl)hydroxylamine hydrochloride (PFBHA) was analysed. Optimization was performed of the reaction between low molecular mass aldehydes and 2,4-DNPH, forming hydrazones, as well as the HPLC-UV analysis. The best condition found was use of 0.15 μmol of DNPH at 40°C for 30 min. The separation of formaldehyde-DNPH was achieved under the optimized separation conditions, although the presence of interferences was observed. Optimization of the derivatization in solution with PFBHA and analysis by GC-MS resulted in the best conditions being derivatized at 85°C for 60 min, with agitation at 350 rpm. The formation of isomers was observed, except in the case of the derivatization reaction producing the formaldehyde-PFBHA oxime. The selectivity was evaluated by comparison of the mass spectra obtained for the bio-oil sample chromatographic signals with those for a standard solution.

In the study of aldehydes derivatization and extraction on an SPME fibre, evaluation was required of the fibre coating and the optimal HS-SPME conditions for the on-fibre modification. The use of a selective fibre was necessary due to the complexity of the bio-oil matrix, which contains a large quantity of volatile compounds that could interfere in the aldehyde analysis by HS-SPME. The fibres studied were polyacrylate (PA), carboxen/polydimethylsiloxane (CAR/PDMS), and divinylbenzene/polydimethylsiloxane (DVB/PDMS), used for 30 min at temperatures of 30, 40, and 60°C of the aqueous fraction of bio-oil. The best option was found to be DVB/PDMS because at all the temperatures tested, the extraction efficiency was lower for interfering aromatic compounds. The optimization of aldehyde extraction from bio-oil samples, with on-fibre derivatization, was studied using five extraction parameters: PFBHA concentration ($mg.L^{-1}$), temperature for sorption of PFBHA by the fibre (°C), agitation time for sorption of PFBHA by the fibre (min), agitation time for the derivatization reaction (min), and temperature for the derivatization reaction (°C). The best conditions for the extraction of formaldehyde were 1.0 mg L^{-1}, 27°C, 10 min, 20 min, and 35°C, respectively.

No statistical significant difference was observed between the concentrations of formaldehyde, acetaldehyde, and propionaldehyde found in bio-oil samples (n = 5) using either on-fibre derivatization and analysis by GC-MS or derivatization in solution and analysis by GC-MS. The concentration of formaldehyde found in bio-oil is of interest, considering its possible use in industrial production of phenol/formaldehyde resin.

The most commonly used methods for the analysis of airborne carbonyls involve the collection of analytes on solid sorbents coated with a suitable derivatization agent, typically 2,4-DNPH, followed by desorption using solvents.

Pang et al. [25] studied the determination of formaldehyde in airborne samples by GC-MS in comparison with an HPLC method. A novel GC-MS method was described for the analysis of airborne carbonyls based on their PFPH derivatives. The method involved sampling using simple tubes packed with PFPH-coated Tenax TA, followed by GC-MS analysis with liquid injection. The method was considered appropriate for the determination of 23 carbonyl compounds in the range C1–C9 and was applied for the determination of these carbonyls in ambient air and from a strong emission source (cigarette smoke). The technique was subsequently compared with the HPLC-MS method.

In this study, one brand of cigarettes consumed in the UK was tested, with the smoke drawn into a Tedlar bag and diluted to 100 L with nitrogen. The carbonyls in the cigarette smoke were identified and their diluted concentrations in the Tedlar bag were determined. The concentrations of formaldehyde obtained by PFPH-GC-MS were significantly different from those found using DNPH-HPLC-MS, with a mean difference of 2.6% between the two methods. The concentrations of formaldehyde (in ppb) in the diluted cigarette smoke sample were 42.3 ± 2.5 and 45.7 ± 4.3 for the PFPH and DNPH methods, respectively, considering three sampling periods. The mean weight of each cigarette was 0.82 ± 0.02 g, with combustion producing 10 mg of tar, 0.9 mg of nicotine, and 10 mg of carbon monoxide. Only formaldehyde, acetaldehyde, butyraldehyde and valeraldehyde were detected in the ambient air samples, using both PFPH and DNPH methods. In comparative field tests with the classical DNPH–HPLC method, it was concluded that there were similarities between the two methods for the same carbonyls, although more carbonyl species were detected by the PFPH-GC-MS method. The PFPH-GC-MS method provides better separation for carbonyls with similar molecular structures, is highly sensitive, and provides mass spectrometric identity confirmation by the acquisition of structural information.

In recent years, there has been increasing attention given to the presence of aldehydes as disinfection and oxidation by-products formed during drinking water treatment processes. Studies show that formaldehyde, acetaldehyde, glyoxal and methylglyoxal are the major organic by-products produced during the ozonation of natural water.

Tsai and Chang [28] analysed aldehydes in three different types of samples (double distilled water, well water, and chlorinated tap water) using the SPME technique with on-fibre derivatization. Poly(dimethylsiloxane)/divinylbenzene fibres were used, with O-2,3,4,5,6-(pentafluorobenzyl)hydroxylamine hydrochloride being first loaded onto the fibre. The aldehydes present in the samples were transferred into the headspace by agitation and extracted (the extraction was conducted for 10 min) by SPME with on-fibre derivatization. GC-MS was used for analysis of the oximes formed and the adsorption-time profiles were examined. It was observed that the equilibrium times (10 min) were similar for most of the oximes formed on the fibre, with the exception of the formaldehyde oxime. The reason for the different adsorption time profile of formaldehyde was not clear. It was also observed that there were syn- and anti-isomers of the oximes because aldehydes are asymmetrical carbonyl compounds (except formaldehyde). Investigation was made of the effects of salt additions (0, 10, and 20% NaCl) to samples of double distilled water, with only formaldehyde showing increased extraction as the concentration of salt added was increased. Similar results were observed for the addition of salt to well water and chlorinated tap water. The influence of different extraction temperatures (without heating, 40 and 60°C) was also investigated. The formaldehyde peak area increased in line with the temperature. It was concluded that the analysis of aldehydes in water by SPME with on-fibre derivatization provided acceptable precision and sensitivity, with simple and fast procedures. The proposed method was suitable for the routine analysis of water samples.

Ho and Yu [37] determined formaldehyde and other carbonyl compounds in environments affected by incense burning in Chinese homes and temples. The sample air was trapped on a solid sorbent containing O-(2,3,4,5,6-pentafluorobenzyl)-hydroxylamine for

the derivatization of formaldehyde and other compounds, followed by thermal desorption and GC/MS analysis. The concentration of formaldehyde in a worship room (at a range of 340–346 ppbv) was higher that the concentrations in a temple yard (at a range of 154–247 ppbv) and outside the temple (11.1 ppbv). These results were correlated with the intensity of incense burning in the environment. The lowest concentration outside the temple could be explained by faster dispersion in the air of this environment. In the home, the sample was collected during and after incense burning (1 and 2 h). The level of formaldehyde decreased once the burning ended, proving that burning incense emits carbonyl species. In this work, formaldehyde was the most abundant carbonyl compound emitted from incense burning. The study showed that it is necessary to quantify the emission rates of toxic aldehyde species from various brands of incense.

Figure 4 illustrates environmental samples as sources of formaldehyde.

2.2. Formaldehyde in food samples

Chemical contamination is one of the leading causes of foodborne illnesses. Research involving food safety is necessary to preserve the health of the human population and ensure safe food production, distribution, and preparation. The development of new methods of risk analysis needs to include consideration of potentially susceptible populations as well as the combined low-level exposure to several different chemicals. The US Environmental Protection Agency [40] has established an acceptable daily intake (ADI) for formaldehyde of 0.2 $mg.kg^{-1}$ body weight, with the potential adverse health effects increasing at intakes higher than the ADI.

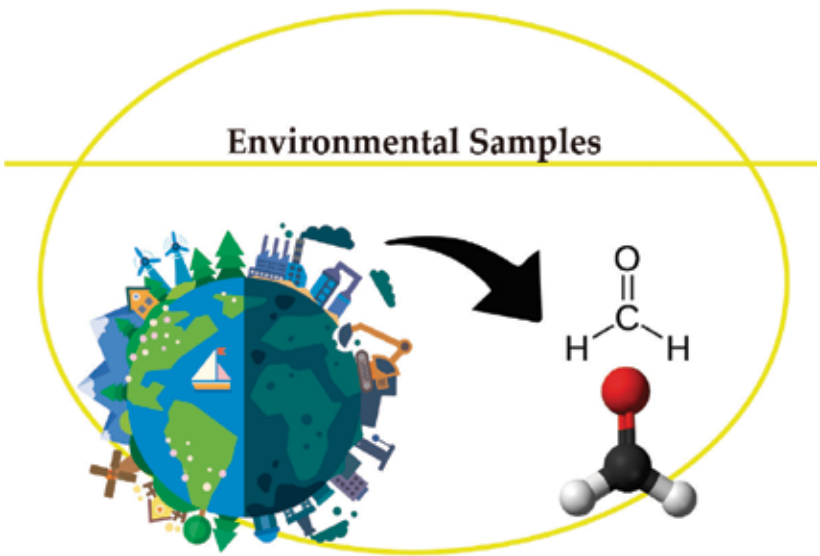

Figure 4. Environmental samples as sources of formaldehyde. Own authors, 2017, Deposit Photos [38], and Info Escola [39].

In 2012, Shin and Lim [34] developed a headspace solid-phase micro-extraction gas chromatography-mass spectrometry (HS-SPME GC-MS) method for the detection of formaldehyde in traditional Korean fermented foods and applied the new method to real sample analysis. The focus of the research was the validation of a robotic sample preparation and detection methodology. Derivatization was performed by the reaction of FA with TFEH (2,2,2-trifluoroethylhydrazine), a highly volatile hydrazine, using food samples contained in headspace vials. The volatile formaldehyde-TFEH formed was vaporized, simultaneously adsorbed on a fibre, and then desorbed into the GC-MS system. The limits of detection (LOD) and quantification (LOQ) for FA were 0.1 and 0.3 $\mu g.kg^{-1}$, respectively. The accuracy and precision of this method were very good, with relative standard deviation less than 10%. The standard curve obtained by computing a least squares regression between the FA concentration and the peak area ratio of FA-TFEH to acetone-d6-TFEH (as internal standard) demonstrated a linear relationship, with a correlation coefficient value of 0.999. The developed method was employed to analyse the concentrations of formaldehyde in 20 samples of traditional Korean foods including kimchi, water radish kimchi, soya bean paste, red pepper paste, soya sauce, and bean-paste soup. All the samples presented detectable levels of formaldehyde in the range from 0.104 to 13.048 $mg.kg^{-1}$. The Korean traditional fermented foods generally contained low levels of formaldehyde, although a red pepper paste sample exceeded the 10 $mg.kg^{-1}$ limit for crustaceans established by the Italian Ministry of Health.

Bianchi et al. [26] determined the formaldehyde contents of different fish and shellfish maintained under different conditions. Validation was performed of an SPME-GC–selective ion monitoring (SIM)-MS method using a CAR-PDMS fibre, based on in-situ on-fibre derivatization with PFBHA, and 12 species of fresh, frozen, stored-on-ice, boiled, roasted, and canned fish were analysed. The fibre was exposed to the headspace of a vial containing an aqueous solution of PFBHA. Fish and fish products fulfil an important role in human nutrition as a source of biologically-valuable proteins, fats, and fat-soluble vitamins, with frozen and fresh fish being the most widely sold products. In fish and crustaceans, formaldehyde is known to form post mortem from the enzymatic reduction of trimethylamine-N-oxide (TMAO) to formaldehyde and dimethylamine [41, 42]. It accumulates during frozen storage, reacts with proteins, and consequently causes protein denaturation and muscle toughness [41].

The performance of the SPME-GC-MS method developed by Bianchi et al. [26] was demonstrated in the determination of formaldehyde at trace levels, with LOD and LOQ values at 17 and 28 $\mu g.kg^{-1}$, respectively, obtained using a blank trout sample. The precision of the method was evaluated in terms of repeatability and between-day precision, with CV% values lower than 3.2% and 9.7% obtained, respectively. No significant differences, at the 95% confidence interval, were found among the mean values for data obtained over 3 days ($p = 0.127$). An extraction recovery of 94.8 ± 1.7% ($n = 3$) was obtained after spiking blank fish samples with formaldehyde at 2.5 $mg.kg^{-1}$. The data obtained for the various samples generally indicated that no adverse effects on human health would be expected due to consumption of the fish and shellfish. However, higher formaldehyde levels were found in species belonging to the Gadidae family, while the freshwater fish and crustaceans generally presented lower values. Evaluation was also made in the influence of cooking, which acted to reduce the formaldehyde contents of the samples analysed.

Wang and co-authors [24] applied HS-SPME analysis of low molecular mass (C1–C10) aldehydes to aqueous solutions of dry white wine, fish, and particle board samples, using PFPH and PFBHA for on-fibre derivatization using fibres coated with PDMS-DVB. Background contamination peaks were observed, most notably for formaldehyde, as found previously in a number of other studies. Using PFBHA, typical formaldehyde concentrations observed were in the region of 25 $\mu g.L^{-1}$. The concentrations obtained using PFPH were significantly higher, at approximately 65 $\mu g.L^{-1}$, indicating a higher level of impurity in the derivatization reagent. Further precautions would be necessary in order to improve the sensitivity and accuracy of the methods for the determination of formaldehyde at low concentrations. Of all the aldehydes studied, formaldehyde showed a steadier increase in derivative formation with extraction time, in the range tested, using both derivatization reagents. This could be explained by the greater affinity of formaldehyde towards the aqueous phase, compared to the other aldehydes studied. Another observation was that formaldehyde presented by far the lowest extraction efficiency, compared to the other aldehydes, with approximately 50% remaining for the second extraction. This was also probably linked to the affinity of this substance for the aqueous phase, which reduced the rate at which it was transferred from the sample to the fibre. The detection limit, linear range, and reproducibility for formaldehyde using the PFPH method were 65, 65–250 $\mu g.L^{-1}$ ($R^2 = 0.9910$), and 10.7%, respectively. The corresponding values for the PFBHA method were 25, 25–250 $\mu g.L^{-1}$ ($R^2 = 0.9955$), and 10.5%, respectively.

The developed PFBHA method was applied to the three different sample matrices (particle board, white wine, and fish). In the case of the particle board sample, it was no surprise to find that the predominant aldehyde was formaldehyde, due to its use as an adhesive in the material. The formaldehyde could not be quantified because the concentration was significantly above the linear range of the method. No formaldehyde was detected in the wine samples. In the raw fish sample, the formaldehyde concentration was again too high for quantification.

The authors concluded that in aldehyde headspace analysis by SPME-GC-FID, use of the PFBHA reagent provided superior on-fibre derivatization, compared to PFPH, under the conditions employed, with detection limits from the low- to sub-microgram level per litre. The automated method was successfully applied to a variety of sample types and could handle samples containing elevated levels (10,000 $\mu g.L^{-1}$) of formaldehyde. GC-MS analyses were performed and compound identifications were made using spectral libraries supplied with the software.

Formaldehyde can occur naturally (endogenously) in many foods and is sometimes used illegally as a food preservative in aquatic products. Due to this, many countries have investigated the form and content of formaldehyde, especially in seafood [34]. For example, the European Commission released an alert notification after finding that shiitake mushrooms from China contained 300 mg/kg of formaldehyde and suggested the possibility that the aldehyde had been added deliberately [33 apud 43]. Yeh and co-authors [33] analysed free and bound formaldehyde in squid and squid products by GC-MS and performed comparative studies with HPC-UV. A comparison was made of free formaldehyde with free and reversibly bound formaldehyde, and similar results were obtained using HPLC-UV and GC-MS.

The GC-MS method provides additional information on the structure of the compound, for example, using mass fragmentation data for identity confirmation. The HPLC-UV method is not

specific to the compound studied and is more liable to matrix effects. In the study by Yeh et al. [33], exposure to formaldehyde due to the consumption of squid and squid products was found to be less than 0.2 mg/kg/d, which is the oral reference dose suggested by the United States EPA.

Figure 5 illustrates foods as source of formaldehyde.

2.3. Formaldehyde in pharmaceutical and related samples

Excipients are substances added to pharmaceuticals in order to ensure the stability and biopharmaceutical properties of the products as well as to improve the organoleptic characteristics and hence increase the patients' acceptance of the formulations. Excipients can be variously classified as follows: preservatives, colourants, flavourings, sweeteners, thickeners, emulsifiers, stabilizers, antioxidants, diluents, humectants, solvents, absorption promoters, and extended release matrices [43].

In 2004, Riveiro and Topiwala [45] developed and optimized an analytical methodology for the extraction of formaldehyde present in cosmetics (shampoos and liquid soaps), using in situ derivatization followed by solid-phase headspace microextraction. The headspace derivatization process was carried out on a PDMS-DVB-coated fibre, followed by extraction for 15 min at 35°C, resulting in an efficiency of around 80%. Sodium chloride was identified as the best salt for the salting-out process. The best analyte desorption time was 5 min, giving an efficiency of 99.8%. The precision, recovery, and detection limit were determined for all the samples. The relative standard deviations were less than 10% for all the cosmetics samples, with recoveries between 89.00 and 101.23%, and the limit of detection was 0.39 $\mu g.L^{-1}$. The proposed method was considered suitable for use in the routine analysis of cosmetics products, offering the advantages of speed and no requirements for the use of large volumes of solvents.

Figure 5. Foods as sources of formaldehyde. Source: Own authors, 2017, Sabor Saudável [44], Info Escola [39].

Del Barrio et al. [46] reported that formaldehyde is a common impurity in many excipients, such as polysorbate, povidone, and polyethylene glycol 300 and that it can form crosslinks with gelatin, leading to incomplete capsule shell dissolution and subsequent drug release problems. Due to oxidation on contact with air, formaldehyde is partially converted to formic acid. Hence, these impurities can coexist in many excipients and can react with active drugs, affecting their stability, so for this reason, it is very important to develop rapid, sensitive, and reliable analytical methods to simultaneously determine formaldehyde, formic acid, and formic acid esters.

Del Barrio et al. [47] developed and validated a GC-MS method for the simultaneous determination of formic acid and formaldehyde in pharmaceutical excipients. An alcohol was selected as the reagent, because both formic acid and formaldehyde can readily react with alcohols, in the presence of an acidic catalyst, to give the corresponding ester and acetyl compounds, respectively, which are volatile and suitable for GC determination. Besides that, the alcohol was used as a solvent to dissolve or disperse the excipients and assist completion of the derivatization reactions. Following evaluation trials, ethanol was selected as the derivatization reagent and solvent, while p-toluenesulfonic acid was used as the catalyst.

Using the SIM mode, the performance of the GC-MS method was evaluated in terms of linearity, range, detection limit, precision, and accuracy, and this mode was subsequently used in the screening of pharmaceutical excipients. Using this method, it was found that almost all the excipients contained varying levels of formic acid and formaldehyde. The good recoveries of both analytes (within the range of 80–120%) indicated that matrix effects were insignificant for the excipients tested. A total of 28 excipients were screened, covering a range of formulations varying in grade, batch, and/or vendor.

Hair products are among the most widely used cosmetics, and the market is growing in Brazil. With an average annual growth of 11% over the last 10 years, Brazil has achieved third place in the world ranking for consumption of cosmetics. Formaldehyde is the chemical compound most widely used in hair products to alter the protein structure of the hair and provide smoothing. In 2001, the National Health Surveillance Agency, which is a branch of the Brazilian Ministry of Health, issued a decree to control the use of formaldehyde, restricting it to a maximum concentration of 0.2% in cosmetics.

Lobo et al. [32] developed a method for the quantification of formaldehyde in hair straightening creams collected at various salons of a city in Brazil, using 2,4-DNPH as a derivatization reagent and analysis by GC-MS. The pH is an important factor in this reaction, due to competition between the nucleophilicity and basicity of 2,4-DNPH. The compound formed is formaldehyde-2,4-dinitrophenylhydrazone, and the mass spectrum for a well-defined peak identified in the chromatogram corresponded to the reference spectrum available in the National Institute of Standards and Technology (NIST) database. Identification of formaldehyde-DNPH was confirmed by the presence of the molecular ion ($m/z = 210$) and its characteristic fragmentation pattern.

In this work, the optimization studies included comparison of the sensitivities of two different procedures, with either external calibration or the use of standard additions. Significant interference from the sample matrix was observed (with decreased sensitivity) so the standard additions method was selected for quantification of formaldehyde in the hair cream samples. As expected, the sensitivity values were significantly different for the two calibration procedures adopted.

The LOD and LOQ values were calculated for each analytical curve of each sample. The values obtained were less than or equal to 0.0165 and 0.055 mg.L^{-1}, respectively. The standard deviation and relative standard deviation obtained were lower than or equal to 81.36 and 18.67%, respectively. The recoveries of known amounts of standards from blank cream samples were in the range from 88 to 115%. Satisfactory results were obtained for formaldehyde-2,4 DNPH standard solutions, enabling the determination of formaldehyde in the real samples. The levels of formaldehyde found in some hair cream samples exceeded the limit permitted according to Brazilian law, giving rise to health concerns, especially for users of these products in hair salons.

Use of dental prostheses on a daily basis can, in some individuals, lead to allergies associated with certain chemicals used in the production of the devices, including methyl methacrylate, ethylene glycol dimethacrylate, hydroquinone, and especially formaldehyde. Mikai and Fuji (2006) [47] carried out a study to evaluate the presence of these substances in several types of denture samples. The materials were prepared by washing, using appropriate agents, and were then sliced into 10-mm-wide portions that were completely immersed in 10 mL of methanol in borosilicate tubes. The tubes were shaken 80 times for 1 min. The procedure was repeated over 4 weeks, with the samples kept in the dark at 37°C. Finally, the eluate was removed, filtered through a 0.2-μm pore size membrane and analysed using GC-MS and HPLC. The results showed that all the samples contained formaldehyde in their compositions, and it was concluded that this substance was a strong candidate for causing allergies.

Figure 6 illustrates cosmetics as source of formaldehyde.

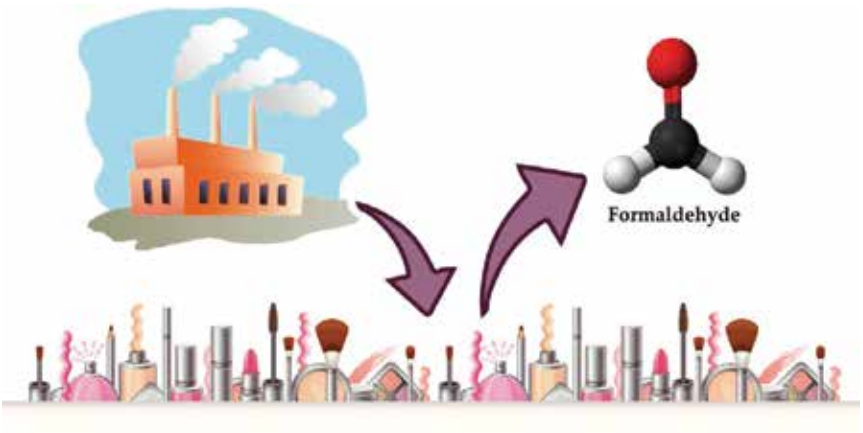

Figure 6. Cosmetics as source of formaldehyde Source: Own authors, 2017; Dreamstime, 2017 [48], Clip Art, 2017 [49], and Info Escola, 2017 [39].

3. Conclusion

Formaldehyde is a substance widely used for many purposes worldwide. However, it is considered carcinogenic by international agencies. The present chapter describes some important work on the determination of formaldehyde in different sample types using

mass spectrometry. This brief discussion demonstrates that mass spectrometry can make a valuable contribution to the determination of commonly encountered toxic compounds such as formaldehyde.

Acknowledgements

An acknowledgement is given to the Brazilian National Council for Scientific and Technological Development [Conselho Nacional de Desenvolvimento Científico e Tecnológico (CNPq) (projects 479273/2013-8 and 420266/2013-5)], the Research Support Foundation of Minas Gerais [Fundação de Amparo à Pesquisa de Minas Gerais (FAPEMIG) (projects CEX-APQ-01850-14 and SICONV 793988/2013)], the Minas Gerais Chemical Network [Rede Mineira de Química (RQ-MG) (FAPEMIG CEX-RED-00010-14)], and the Pro-Vice Chancellor's Office for Research and Graduate Studies [Pró-Reitoria de Pesquisa e Pós-Graduação (PROPP)] of the Federal University of Ouro Preto [Universidade Federal de Ouro Preto (UFOP)] for their scholarships and financial support.

Author details

Aline de Souza[1], Isabela Cristina Matos Cunha[1,2], Júnior Olair Chagas[1], Elisandra Bárbara Pontes Carlos[3], Luana Lacerda Santos[4], Thamires Ráfaga Campos e Figueredo[2], Lucília Alves Linhares Machado[2], Vanessa Moreira Osório[5], Karla Moreira Vieira[2] and Fabiana Aparecida Lobo[1]*

*Address all correspondence to: fabs_lobo@yahoo.com.br

1 Department of Chemistry, Institute of Exact and Biological Sciences, Federal University of Ouro Preto, Ouro Preto, MG, Brazil

2 Department of Exact and Applied Sciences, Institute of Exact and Applied Sciences, Federal University of Ouro Preto, João Monlevade, MG, Brazil

3 Federal University of Juiz de Fora, Juiz de Fora, MG, Brazil

4 Federal University of Itajubá, Itabira, MG, Brazil

5 Department of Chemistry and Physics, Center of Exact Sciences, Natural and Health, Federal University of Espírito Santo, Alto Universitário, Alegre, ES, Brazil

References

[1] Cetesb. Toxicological Information Sheet. Formaldehyde [Internet]. Available from: http://www.cetesb.sp.gov.br/userfiles/file/laboratorios/fit/formaldeido.pdf [Accessed: 2 June 2016]

[2] Portal Educação. Formol or Formaldehyde [Internet]. Available from: https://www.portaleducacao.com.br/farmacia/artigos/357/formol-ou-formaldeido [Accessed: 9 October 2016]

[3] Vieira IIF, Dantas BPA, Ferreira FCP, Carvalho RBAC, Freire IB, Neto EJS. Efeitos da utilização do formaldeído em laboratório de anatomia. Rev. Ciênc. Saúde Nova Esperança. 2013;**11**(1):97-105

[4] Viegas SPC. Estudo da exposição profissional a formaldeído em laboratórios hospitalares de anatomia patológica [PhD thesis]. Lisbon: Universidade Nova de Lisboa; 2010

[5] Alves CA, Acile SDG. Formaldeído em escolas: uma revisão. Química Nova. 2010;**25**(10): 2025-2029

[6] Instituto Nacional do Câncer (INCA). Formol or Formaldehyde [Internet]. Available from: http://www.inca.gov.br/conteudo_view.asp?id=795#topo [Accessed: 6 August 2016]

[7] Belo CAVF. Avaliação da exposição profissional ao formaldeído e xileno no serviço de anatomia patológica dos hospitais da Universidade de Coimbra [Master's thesis]. Portugal: Universidade de Coimbra, Portugal; 2011

[8] Carvalho MZ. Abordagem multivariada do comportamento das propriedades físico-químicas e caracterização de adesivos naturais à base de taninos. Lavras [PhD thesis]. Brazil: Universidade Federal de Lavras; 2016

[9] Rossi F. O uso de formaldeído na alimentação de cães e gatos. Curitiba. Brazil: Universidade Federal de Tuiuti do Paraná; 2014

[10] Lonta LMP. Efeitos tóxicos do formaldeído em escova progressiva: 10° Congresso de Pós-Graduação: Qualificação e expansão da educação superior no contexto do Plano nacional da educação. 2012. UNIMEP (Universidade Metodista de Piracicaba).

[11] Lorenzini, S. Efeito adverso da exposição ao formaldeído em cabelereiros. 2012. 77 pp. PhD thesis, Rio Grande do Sul, Programa de pós-graduação em ciências pneumológicas, Universidade do Rio Grande do Sul, Brazil.

[12] Iarc M. Analytical methods for formaldehyde. Chemical and Physical Data. 1995;**88:**39-93

[13] Abreu VM, Azevendo MGB, Falcao JSA. Cosmetovigilância em alisantes capilares: Determinação do teor de formaldeído por espectrofotometria e avaliação do rótulo. Rev. Ciênc. Farm. Básica Apl. 2015;**36**(1):51–58

[14] Agência Nacional de Vigilância Sanitária (ANVISA). Resolução – RDC N° 15, de 26 de março de 2013. Available from: http://www.cosmeticsonline.com.br/ct/painel/fotos/assets/uploads/regulatorios/ae972-Rdc-15.pdf [Accessed: 9 October 2016]

[15] Occupational safety and health administration (OSHA). 2011. Hair smoothing products that could release formaldehyde [Internet]. Available from: https://www.osha.gov/SLTC/formaldehyde/hazard_alert.html [Accessed: 10 October 2016]

[16] Report on carcinogens background document for formaldehyde. 2009. National Toxicology Program (NTP) [Internet]. Available from: http://ntp.niehs.nih.gov/ntp/roc/2009/november/background/formaldehydedraftbackgrounddocument.pdf [Accessed: 10 October 2016]

[17] Cunha MM, Rodrigues CR, Ferreira VS, Rodrigues AR, Lemes SR, Chaves DA, Mesquita MM, Araujo LA, Junior NJS, Melo-Reis PR. Eficiência do método de espectrometria de massas em drogas de abuso. Estudos. 2015;**42**:409-423

[18] Colnago LA, Almeid FCL, Valente AP. Espectrometria de massas RMN multidimensional e multinuclear: Revolução no estudo de macromoléculas biológicas. Química Nova na Escola. 2002;**16**:9-14

[19] Cunha RB, Castro MS, Fontes W. Espectrometria de massas de proteínas. Biotecnologia Ciência & Desenvolvimento Ano IX. 2006;**16**:40-46

[20] Lancas FMA. Cromatografia líquida moderna e a espectrometria de massas: finalmente "compatíveis"? Scientia Chromatographica. 2009;**1:**35-61

[21] Wilson K, Walker J. Principles and Techniques of Biochemistry and Molecular Biology. Cambridge University Press; 2009. p. 352

[22] Silva TO. Estudo de emissão de aldeídos e outros COV por óleos de dendê e soja em diferentes condições, sob aquecimento a temperatura de processos de fritura [Master's thesis]. Salvador: Universidade Federal da Bahia; 2017

[23] Sowinski P, Wardencki W, Partyka M. Development and evaluation of headspace gas chromatography method for the analysis of carbonyl compounds in spirits and vodkas. Analytica Chimica Acta. 2005;**539:**17-22

[24] Wang Q, O'Reilly J, Pawliszyn J. Determination of low-molecular mass aldehydes by automated headspace solid-phase microextraction with in-fibre derivatisation. Journal of Chromatography A. 2005;**1071:**147-154

[25] Pang X, Lewis AC, Hamilton JF. Determination of airborne carbonyls via pentafluorophenylhydrazine derivatisation by GC-MS and its comparison with HPLC method. Talanta. 2011;**85:**406-414

[26] Bianchi F, Careri M, Musci M, Mangia A. Fish and food safety: Determination of formaldehyde in 12 fish species by SPME extraction and GC-MS analysis. Food Chemistry. 2007;**100**:1049-1053

[27] Dong JZ, Moldoveanu SC. Gas chromatography–mass spectrometry of carbonyl compounds in cigarette mainstream smoke after derivatization with 2,4-dinitrophenylhydrazine. Journal of Chromatography A. 2004;**1027**:25-35

[28] Tsai SW, Chang CM. Analysis of aldehydes in water by solid-phase microextraction with on-fiber derivatization. Journal of Chromatography A. 2003;**1015**:143-150.

[29] Chi Y, Feng Y, Wen S, Lu H, Yu Z, Zhang W, Sheng G, Fu J. Determination of carbonyl compounds in the atmosphere by DNPH derivatization and LC-ESI-MS/MS detection. Talanta. 2007;**72**:539-545

[30] Jeong HS, Chung H, Song SH, Kim CII, Lee JG, Kim YS Validation and determination of the contents of acetaldehyde and formaldehyde in foods. Toxicology Research. 2015;**31**(3):273-278

[31] Google Images. 2017 [Internet]. Available from: https://www.google.com.br/imghp [Accessed: 24 March 2017]

[32] Lobo FA, Santos TM, Vieira KM, Osorio VM, Taylor JG Determination of formaldehyde in hair creams by gas chromatography-mass spectrometry. Drug Testing and Analysis. 2015;**7**:848-852

[33] Yeh TS, Lin TC, Chen CC, Wen HM. Analysis of free and bound formaldehyde in squid and squid products by gas chromatography-mass spectrometry. Journal of Food and Drug Analysis. 2013;21:190-197

[34] Shin HS, Lim HH. Simple determination of formaldehyde in fermented foods by HS-SPME-GC/MS. International Journal of Food Science and Technology. 2012;**47**:350-356

[35] Tessini C, Muller N, Mardones C, Meier D, Berg A, Von Baer D. Chromatographic approaches for determination of low-molecular mass aldehydes in bio-oil. Journal of Chromatography A. 2012;**1219**:154-160

[36] Bergh VV, Coeckelberghs H, Vankerckoven H, Compernolle F, Vinckier C. Study of the carbonyl products of terpene/OH radical reactions: Detection of the 2,4-DNPH derivatives by HPLC-MS. Analytical and Bioanalytical Chemistry. 2004;**379**:484-494

[37] Ho SSH, Yu JCZ. Concentrations of formaldehyde and other carbonyls in environments affected by incense burning. Journal of Environmental Monitoring. 2002;**4**:728-733

[38] Deposit Photos. [Internet] 2017. Available from: <http://br.depositphotos.com/> [Accessed 24 March 2017]

[39] Info Escola. [Internet] 2017. Available from: http://www.infoescola.com/ [Accessed: 24 March 2017]

[40] US Environmental Protection Agency (EPA). Integrated Risk Information System (IRIS) on Formaldeyde. Washington, DC: National Center for Environmental Assessment, Office of Research and Development; 1999

[41] Sotelo CG, Pineiro C, Perez-Martin RI. Denaturation of fish proteins during frozen storage: Role of formaldehyde. Lebensmittel Untersuchung und Forschung. 1995;**200**:14-23

[42] Badii F, Howell NK. Changes in the texture and structure of cod and haddock fillets during frozen storage. Food Hydrocolloids. 2002;**16**:313-319

[43] Rapid alert system for food and feed (RASFF). Alert notification 2001/106, presence of formalin in fresh mushrooms from China (EC) [Internet]. Available from: https://webgate.ec.europa.eu/rasff-window/portal/index.cfm? [Accessed: 24 March 2017.

[44] Sabor Saudável, 2017. Available At: <Https://Saborsaudavelalimentos.Wordpress.Com/>. Accessed On: March 24, 2017.

[45] Riveiro R. T., Topiwala V. Quantitative Determination Of Formaldehyde In Cosmetics Using A Combined Solid-Phase Microextraction–Isotope Dilution Mass Spectrometry Method. Journal Of Chromatography A 1029 (2004) 217–222.

[46] Del Barrio M. A., Hu J. Zhou P., Cauchon N. Simultaneous Determination Of Formic Acid And Formaldehyde In Pharmaceutical Excipients Using Headspace Gc-Ms. Journal Of Pharmaceutical And Biomedical Analysis 41 (2006) 738–743.

[47] Mikai M., Koike M., Fuji H. Quantitative Analysis Of Allergenic Ingredients In Eluate Extracted From Used Denture Base Resin. Journal Of Oral Rehabilitation 33 (2006) 216-220.

[48] Dreamstime, 2017. Available from: ttps://Pt.Dreamstime.Com/ [Accessed: 24 March 2017]

[49] Clip Art, 2017. Available from: http://Pt.Clipartlogo.Com/ [Accessed: 24 March 2017].

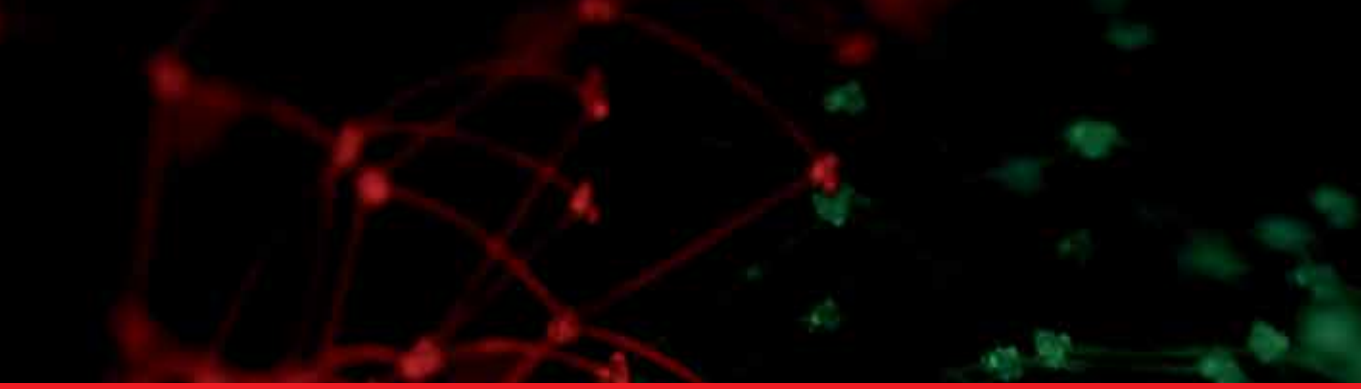

Edited by Mahmood Aliofkhazraei

Mass spectrometry is an analytical technique that can be used for the structural characterization and quantification of a wide range of molecules. The technique is extensively used by chemists for the analysis of small and volatile organic compounds. Mass spectrometry has long been an important technique for the identification of materials ranging from pure compounds to complex mixtures. Mass spectrometry can be used to determine molecular weight of compounds or using different ionization conditions, can provide more structural details through the analysis of fragmentation patterns. This level of detail can be attained for pure compounds and some mixtures. Mass spectrometry can also be combined with separation techniques such as gas chromatography or liquid chromatography to allow more complex mixtures to be examined. These hyphenated techniques provide a range of options for the characterization of complex materials.

ISBN 978-953-51-4805-0

Photo by Pietro Jeng / unsplash

IntechOpen